

22300575

THESIS



This is to certify that the

dissertation entitled

A DIENCEPHALIC CONTRIBUTION TO SYMPATHETIC NERVE DISCHARGE IN THE ANESTHETIZED CAT

presented by

Kurt James Varner

has been accepted towards fulfillment of the requirements for

Doctoral degree in Pharmacology/
Toxicology



RETURNING MATERIALS: Place in book drop to remove this checkout from your record. FINES will be charged if book is returned after the date stamped below.

A DIENCEPHALIC CONTRIBUTION TO SYMPATHETIC NERVE DISCHARGE IN THE ANESTHETIZED CAT

By

KURT JAMES VARNER

A DISSERTATION

Submitted to
Michigan State University
in partial fulfillment of the requirements
for the degree

DOCTOR OF PHILOSOPHY

Department of Pharmacology and Toxicology

1987

ABSTRACT

A DIENCEPHALIC CONTRIBUTION TO SYMPATHETIC NERVE DISCHARGE IN THE ANESTHETIZED CAT

By

Kurt James Varner

The purpose of this thesis was to study the role of diencephalic structures in the control of sympathetic nerve discharge (SND) in the anesthetized cat. This laboratory (Huang et al., Am. J. Physiol. 252: R645-R652, 1987) previously showed that the forebrain is responsible for a significant component of inferior cardiac SND in cats anesthetized with alpha-chloralose. My research assessed the contribution of various diencephalic regions to the forebrain-dependent component of SND in this preparation. The reductions in inferior cardiac SND and blood pressure produced by midbrain transection in nonlesioned control cats were compared with those in cats in which diencephalic lesions were made with radio-frequency current. Lesions of the lateral hypothalamus, posterior medial hypothalamus, attenuated the effects of midbrain transection. These results suggest that the medial hypothalamus and medial thalamus contribute to SND in the anesthetized cat.

Tungsten microelectrodes were used to record the spontaneous discharges of individual neurons in the medial thalamus and hypothalamus to determine whether these regions contained the cell bodies of neurons that influence basal SND. Spike-triggered averaging of SND revealed the existence of two types of

hypothalamic and medial thalamic neurons with sympathetic nerve-related activity in baroreceptor-innervated cats. The activity of type 1 neurons was synchronized to an aperiodic spike-like component in SND whereas that of type 2 neurons was synchronized to a 2-to 6-Hz rhythmic component. Microstimulation at type 1 and type 2 unit recording sites increased SND. These results are consistent with the possibility that diencephalic neurons contribute to the rhythmic and aperiodic components of SND in the anesthetized cat.

Spike-triggered averaging of frontal-parietal cortical activity (EEG) revealed that all medial thalamic and most hypothalamic neurons with activity related to SND also had EEG-related activity. Thus I considered whether the frontal-parietal cortex contributed to the forebrain-dependent component of SND. Electrical stimulation of the cortex evoked excitatory sympathetic nerve responses and activated some type 1 and type 2 diencephalic neurons. However, frontal lobotomy failed to attenuate the decreases in SND and blood pressure produced by midbrain transection suggesting that these cortical regions do not contribute to basal SND in the anesthetized cat.

To my grandmother, Margret Varner whose spirit of scholarship is embodied in this work and to Laurie whose support and understanding were invaluable.

ACKNOWLEDGEMENTS

I would like to offer my sincere thanks to my advisors Dr. Gerard Gebber and Dr. Susan Barman, whose guidance, advice, patience and friendship have allowed me to grow as both a scientist and a person.

I would also like to thank the members of my thesis committee, Dr. Glenn Hatton, Dr. Gregory Fink, Dr. Irena Grofova and Dr. Robert McCall whose advice and critiques have been very helpful in the preparation of this dissertation. I would also like to thank Dr. Zhong-Sun Huang, for his advice and assistance in performing the lesion and decerebration studies.

Finally, I would like to thank Diane Hummel for her secretarial assistance, and William Cook and Ronald Winters for their technical help.

TABLE OF CONTENTS

			Page
LIST	OF TA	BLES	viii
LIST	OF FI	GURES	ix
LIST	OF AE	BEREVIATIONS	xii
INTR	ODUC	TION	1
L	cardic A.	ement of the cerebral cortex and limbic system in autonomic ovascular function Early evidence of autonomic regulation by the cortex Cardiovascular responses elicited from the infralimbic cortex	3 3 7
II.	A.	ovascular responses evoked from the thalamus Cardiovascular responses elicited by electrical stimulation of the thalamus	8
		Cardiovascular responses evoked by chemical stimulation of the thalamus	10
ш.	A. (halamic regulation of the cardiovascular system Cardiovascular responses elicited by electrical stimulation of the hypothalamus	11 11
	B. C.	Chemical stimulation of the hypothalamus The defense arousal system: possible source of sympathetic tone	14
	D.	Models of hypertension involving diencephalic systems 1. Renin-dependent renal hypertension 2. Nonrenin-dependent renal hypertension 3. Neurogenic hypertension 4. Mineralocorticoid-salt hypertension 5. Spontaneous hypertension	23 23 26 28 29 30
IV.	A. 1	Ation of rhythmic activity by the diencephalon and brain stem The generation of basal SND L. Early views on the origin of basal SND L. Evidence that the brain stem is intrinsically capable of rhythm generation L. Proposed mechanisms of SND generation in the brain stem L. Possible brain stem regions involved in the generation of SND	31 31 31 32 34

TABLE OF CONTENTS (continued)

			Page
	B.	Thalamic mechanisms for the generation of electrocortical	
		rhythms	38
		1. Early models of thalamic generation of EEG rhythms	38
		 Mechanisms for the generation of alpha spindle activity The thalamic reticular nucleus as a generator of tha- 	40
		lamic spindle sequences	43
		4. Origin of the cortical delta and theta rhythms	47
ME	THODS	S AND PROCEDURES	50
A.	Gene	eral procedures	50
	1.	Baroreceptor denervation	50
	2.	Nerve recordings	51
	3.	Electrical stimulation of the diencephalon and cortex	52
	4.	Histology	52
в.	Data	analysis	53
	1.	Quantification of SND and blood pressure	53
	2.	Crosscorrelation and autocorrelation analysis	54
	3.	Post-R wave interval analysis	54
	4.	Post-stimulus analysis	55
	5.	Power spectral density analysis	55
	6.	Peri-spike-trigger averaging	55
	7.	Interspike interval analysis	56
	8.	Statistical analysis	56
c.	Proje	ect A: Midbrain transection and radio-frequency lesions	56
••	1.	Decerebration procedures	56
	2.	Radio-frequency diencephalic lesions	57
	3.	Data analysis	57
	4.	Histology	57
D.	Proje	ect B: Multiunit diencephalic activity	58
	1.	Multiunit diencephalic recordings	58
	2.	Electrical and chemical stimulation of the diencephalon	58
	3.	Data analysis	59
E.	Doolo	of Co. Characterization of dispersability common with summer	
e.		ect C: Characterization of diencephalic neurons with sympa-	59
		c nerve-related activity	
	1.	Diencephalic unit recordings	59
	Z.	Electrical stimulation	60
	3.	Efffect of baroreceptor reflex activation	60
	4.	Data analysis	60

TABLE OF CONTENTS (continued)

				Page
F.	1.	Electrical sti	thetic responses elicited by cortical stimulation imulation of the cortex	60
	2.	Diencephalic	unit recordings	61
	3.	Frontal lobot	omy and decerebration	61
G.	Dru	s used		62
RES	ULTS			63
L	Iden	ification of di	encephalic regions contributing to SND	63
	A.		section in nonlesioned cats	64
	B.	Anterior med	ial hypothalamic lesions	. 64
	C.		hypothalamic lesions	73
	D.		chalamic lesions	78
	E.	Medial thalan		78
II.	Sync	ronization of	SND to diencephalic multiunit activity	87
_	A.		t recordings of diencephalic activity	87
	B.	Patterns of re	elationship between SND and diencephalic activity	92
		1. SND rel	lated only to medial thalamic activity	92
		2. SND rel	lated to medial and lateral thalamic activity	95
		3. SND rel	lated to hypothalamic activity	100
		4. SND uni	related to thalamic activity	100
	c.	Electrical and	i chemical stimulation of the diencephalon	105
		1. Sympat! stimulat	hetic nerve responses elicited by electrical	105
			tion Llamic injection of picrotoxin	112
		o muaina	Mainte injection of pictotoxia	
Ш.		fication of o	diencephalic neurons with sympathetic nerve-	118
	A.		of diencephalic neurons with sympathetic nerve	110
	***	related activi		118
			halic unit discharge patterns	119
			nization of diencephalic unit activity to inferior	/
		cardiac	•	119
			ison of unit firing times	125
	В.	Detailed anal	lysis of diencephalic neurons with sympathetic	
	٠.	nerve-related		130
			l analysis of type 1 neurons	130
			l analysis of type 2 neurons	130
			al stimulation	142
			eptor reflex activation	147

TABLE OF CONTENTS (continued)

			Page
IV.	Sym	pathetic nerve responses elicited by cortical stimulation	150
	A.	Sympathetic nerve responses elicited by cortical stimulation	150
	B.	Synaptic activation of type 1 and type 2 neurons by cortical stimulation	157
	C.	Effects of frontal lobotomy on the forebrain-dependent component of SND	161
DISC	cussi	ON	165
SUM	MAR	Y	181
BIBL	JOGE	LAPHY	186

LIST OF TABLES

Table	<u>1</u>	Page
1	Mean onset latencies of inferior cardiac sympathetic nerve excitation produced by diencephalic stimulation with 10-ms trains of three pulses of supramaximal intensity (1 mA)	107
2	Mean onset latencies of inferior cardiac sympathetic nerve responses produced by cortical stimulation with 10-ms trains of three pusles or 1-ms single shocks of supramaximal intensity (1 mA)	156

LIST OF FIGURES

Figure		Page
1	Representative histological sections showing lesions of lateral hypothalamus (A), posterior hypothalamus (B) and medial thalamus (C)	
2	Comparison of effects of midbrain transection on inferior cardiac sympathetic nerve discharge (SND) and mean blood pressure (BP) in nonlesioned control cats with those in cats with anterior medial hypothalamic or large medial hypothalamic lesions	
3	Effect of midbrain transection on inferior cardiac (ICN) and renal (RN) sympathetic nerve discharge (SND), and mean blood pressure (BP) in nonlesioned baroreceptordenervated cat anesthetized with chloralose	
4	Effects of midbrain transection at stereotaxic plane A3 (A) and ganglionic blockade (B) on blood pressure (BP), inferior cardiac (ICN) and renal (RN) sympathetic nerve discharge in a nonlesioned baroreceptor-denervated cat anesthetized with chloralose	71
5	Representative lesion in anterior medial hypothalamus	74
6	Representative large lesion in medial hypothalamus	76
7	Comparison of effects of midbrain transection on inferior cardiac sympathetic nerve discharge (SND) and mean blood pressure (BP) in nonlesioned control cats with those in cats with lateral hypothalamic lesions	79
8	Representative lateral hypothalamic lesion	81
9	Comparison of effects of midbrain transection on inferior cardiac sympathetic nerve discharge (SND) and mean blood pressure (BP) in nonlesioned contol cats with those in cats with medial thalamic lesions	83
10	Representative medial thalamic lesion	85
11	Thalamic activity and sympathetic nerve discharge (SND) in a baroreceptor-denervated cat	88

LIST OF FIGURES (continued)

Figure		Page
12	Power spectra of arterial pulse wave (AP), sympathetic nerve discharge (SND) and thalamic activity in two experiments	90
13	Selective relationship between medial thalamic activity and sympathetic nerve discharge (SND)	93
14	Relationship between medial thalamic activity and sympathetic nerve discharge (SND) in a decorticate and baroreceptor-denervated cat	
15	Distribution of diencephalic recording sites in experiments in which sympathetic nerve discharge (SND) was related to activity in medial but not in lateral thalamic nuclei	
16	Nonselective relationship between thalamic activity and sympathetic nerve discharge (SND)	101
17	Crosscorrelograms showing relationships of sympathetic nerve discharge (SND) and activity recorded from thalamus and hypothalamus	103
18	Sympathetic nerve responses elicited by diencepablic stimulation (10-ms trains of three 1-mA pulses applied once every 2 s) in a CNS-intact (A) and decorticate (B) cat	108
19	Depth-threshold curves for sympathetic nerve responses elicited by medial thalamic, hypothalamic and midbrain stimulation with 10-ms trains of three pulses	110
20	Changes in sympathetic nerve discharge (SND) produced by injection of picrotoxin into the medial thalamus	113
21	Changes in sympathetic nerve discharge (SND) and frontal- parietal cortical activity (EEG) produced by the intravenous administration of a convulsive dose of picrotoxin	116
22	Representative recordings of action potentials of diencepablic neurons with sympathetic nerve-related activity	120
23	Peri-spike-triggered averages of inferior cardiac sympathetic nerve discharge (SND) for a type 1 hypothalamic and a type 2 hypothalamic neuron in the same cat	123
24	Anatomical distribution of diencephalic neurons with sympathetic nerve-related activity	126

LIST OF FIGURES (continued)

Figure		Page
25	Firing times of type 1 (A,B) and type 2 (C, D) hypothalamic and medial thalamic neurons relative to inferior cardiac sympathetic nerve discharge (SND)	128
26	Type 1 medial thalamic neuron	131
27	Type 2 medial thalamic neuron with cardiac-related activity	133
28	Type 2 hypothalamic neuron with cardiac-related activity	135
29	Type 2 medial thalamic neuron without cardiac-related acti- vity	138
30	Activity of a type 2 medial thalamic neuron synchronized to a noncardiac-related component of SND	140
31	Comparison of changes in inferior cardiac sympathetic nerve discharge (SND) accompanying diencephalic unit spike occurrence and an electrical stimulus applied at site of unit recording	143
32	Peri-spike-triggered and peri-stimulus averages of inferior cardiac sympathetic nerve discharge (SND)	145
33	Effect of baroreceptor reflex activation produced by a ortic obstruction on firing rate of two type 2 hypothalamic neurons (I, II)	148
34	Increases and decreases in inferior cardiac sympathetic nerve discharge (SND) elicited by stimulation (10-ms trains of three pulses applied once every two s) of the motor cortex	151
35	Sympathetic nerve responses elicited by stimulation (10-ms trians of three 1-mA pulses applied once every 2 s) of prefrontal, frontal (A) and infralimbic (B) cortex	154
36	Synaptic activation of a type 1 hypothalamic neuron by single shock stimulation (1 mA; 1-ms duration delivered once every 2 s) of the motor cortex	159
37	Effect of bilateral frontal lobotomy (panels A and B) and midbrain transection (panels C and D) on inferior cardiac sympathetic nerve discharge (SND) and mean blood pressure (BP) in seven baroreceptor-denervated cats anesthetized with chloralose	162

LIST OF ABBREVIATIONS

Diencephalic structures:

aHd area hypothalamica dorsallis Am N. anterior medialis AV N. anterior ventralis CA commissura anterior CC corpus callosum Cd N. caudatus CI capsula interna Ch chiasma optica CL N. centralis lateralis CM N. centrum medianum En N. entopedumcularis Fil N. filiformis Fx fornix Ha hypothalamus anterior HbL N. habenularis lateralis HL hypothalamus lateralis

Hvm hypothalamus ventromedialis H1.H2 Forel's fields IAM N. interanteriormedialis LD N. lateralis dorsalis LP N. lateralis posterior MD N. medialis dorsalis MFB medial forebrain bundle Mm corpus mammillare NCM N. centralis medialis NHvm N. hypothalami ventromedialis

hypothalamus posterior

NR N. ruber

Hp

Pc N. paracentralis Ped pedunculus cerebralis Pf N. parafascularis

PVH N. paraventricularis hypothalami

R N. reticularis thalami

RE N. reuniens Rh N. rhomboidens RPO Regio preoptica TO tractus opticus VA N. ventralis anterior VL. N. ventralis lateralis W.V N. ventralis medialis

VPL N. ventralis posterolateralis VPM N.ventralis posteromedialis

ZI zona incerta

Cortical abbreviations

A.S. ansate sulcus **ASC** association cortex C.G. coronal gyrus Co.S. coronal sulcus Cr.S. cruciate sulcus E.S.G. ectosylvian gyrus F.G. fornicatus gyrus L infralimbic cortex MI primary motor cortex marginal gyrus

M.G. O.B. olfactory bulb 0.G. orbital gyrus

SI primary sensory cortex SII secondary sensory cortex

S.G. sigmoid gyrus S.S.G. suprasylvian sulcus

LIST OF ABBREVIATIONS (continued):

Other abbreviations:

EPSP	excitatory post synaptic potentia
IPSP	inhibitory post synaptic potential
IML	intermediolateral nucleus
ISI	interspike interval
LTF	medullary lateral tegmental field
VLM	ventrolateral medulla
SHR	spontaneuosly hypertensive rat
SND	sympathetic nerve discharge
EEG	electroencephalogram

INTRODUCTION

In the anesthetized animal the sympathetic nervous system maintains a level of basal activity. The first studies to characterize sympathetic activity were performed by Adrian et al. (1932) and Bronk et al. (1936) who demonstrated that in most cases the activity in sympathetic nerve bundles is synchronized into bursts which are locked in a 1:1 relationship to the cardiac cycle. In addition, SND contains a respiratory-related periodicity since the amplitude of these cardiac-related bursts waxes and wanes in relation to the respiratory cycle.

That supraspinal networks generate basal sympathetic tone to the heart and vasculature was recognized when Bernard (1863) produced a sustained decrease in blood pressure by transecting the cervical spinal cord. Subsequent studies by Owsjannikow (1871) and Dittmar (1873) attempted to localize the brain regions responsible for generating sympathetic tone by monitoring changes in blood pressure in response to serial transection of the neuraxis in rabbits. In these experiments, blood pressure was not affected until the level of transection was at a point 1-2 mm behind the caudal border of the inferior colliculi. On this basis it was concluded that, at least in the anesthetized animal, the forebrain is not involved in maintaining the level of resting blood pressure. Transections made more caudally produced further decreases in blood pressure. When the level of transection was 4-5 mm above the calamus scriptorius, blood pressure fell to a level similar to that produced by transection of the cervical spinal cord. Thus it appeared that the region of the neuraxis responsible for the generation of basal sympathetic tone lies between the caudal one third of the pons and the rostral two

thirds of the medulla. Alexander (1946) confirmed this by monitoring the effects of brain stem transection on the level of tonic activity in the cervical and inferior cardiac sympathetic nerves of cats.

Although it is widely accepted that sympathetic nerve discharge (SND) is generated in the brain stem of the anesthetized animal, there are several (often ignored) observations which support the view that the forebrain contributes to SND in this preparation. First, SND can be locked to a rhythmic 2- to 6-Hz component of frontal-parietal cortical activity (EEG) in chloralose- (Barman and Gebber, 1980) or dially lbarbiturate-urethane- (Gebber and Barman, 1981) anesthetized cats and chloralose-anesthetized dogs (Camerer et al., 1977). Furthermore, the spontaneous discharges of individual medullary neurons in the cat (Gebber and Barman, 1981) are temporally related to rhythmic 2- to 6-Hz components in both SND and cortical activity. Langhorst et al. (1975) identified medullary neurons whose activity is related to a 2- to 6-Hz rhythm in cortical activity and to the arterial pulse. Second, several laboratories have reported that midcollicular decerebration in anesthetized animals produces a 30-40 mmHg decrease in blood pressure (Wang and Chai, 1962; Reis and Cuenod, 1964; Peiss, 1965; Huang et al., 1987) and a 38+7% reduction in postganglionic inferior cardiac SND (Huang et al., Taken together these data raise the possibility that the forebrain participates to a significant extent in setting the level of SND in the anesthetized animal. Moreover, Huang et al. (1987) demonstrated that the effects of decerebration on blood pressure and SND are prevented by removal of the medial diencephalon prior to transection. Therefore, the purpose of this thesis was to examine the role of the diencephalon in the control of basal SND in the anesthetized cat.

To place this study in the proper perspective, I will first review classic and current literature related to the involvement of forebrain structures in sympathetic function with special emphasis on their role in cardiovascular regulation. Moreover, since a distinguishing feature of basal SND is its rhythmicity, I will also review the proposed mechanisms by which SND is thought to be generated in the brain stem, as well as mechanisms by which the forebrain is thought to generate rhythmic activity patterns. These reviews are not intended to be global in scope. Rather their intent is to orient the reader in terms of the rationale and conclusions of this study.

- L Involvement of the Cerebral Cortex and Limbic System in Autonomic Cardiovascular Function
 - A. Early evidence of autonomic regulation by the cortex

An extensive review of the early literature regarding cortical regulation of autonomic function has been provided by Hoff et al. (1963). In 1869 Hughlings Jackson first proposed that the "cortex controls not only voluntary movements of the body, but the movements of the arteries and viscera as well." Jackson based his conclusions not on experimental evidence, but on the clinical observation that somatic and visceral responses accompany epileptic seizures. Early experimental studies of cortical involvement in cardiovascular function used electrical stimulation to elicit changes in heart rate and/or blood pressure. In the mid 1870's, Schiff, Danilewsky and Bochfeontain working independently, reported that stimulation of the suprasylvian sulcus and the anterior and posterior sigmoid gyri elicits primarily increases in blood pressure. Changes in heart rate (increases and decreases) often accompanied the blood pressure responses; however, no consistent relationship between the direction of the blood pressure response and the heart rate changes was observed. In 1866, Fechterew and Mislawski reported that stimulation of the globus pallidus and internal capsule elicits increases in

blood pressure which persist after the elimination of descending motor fibers by lesioning the motor cortex. These results suggest that motor and autonomic responses are mediated over separate pathways.

Hoff and Green (1936) used electrical stimulation to map cortical pressor and depressor sites in ether-anesthetized cats and monkeys. In cats, pressor responses are consistently elicited from the posterior and anterior sigmoid gyrus and gyrus proreus (motor and premotor areas). In most cases, a 5 to 10% increase in heart rate accompanied pressor responses; however, decreases in heart rate are observed in some cats in which the stellate ganglion and adrenal glands were removed suggesting that these effects are vagally mediated. Depressor responses are consistently elicited from the lateral median, medial suprasylvian, ectosylvian and sylvian gyri. In the monkey, pressor responses are produced by stimulating areas adjacent to the superior paracentral sulcus (motor and premotor areas). Depressor responses are occasionally produced by stimulating the marginal gyrus and the anterior tip of the superior paracentral sulcus. No vasoreactive sites were found in the parietal or occipital cortex. In cats and monkeys pressor and depressor responses are not the result of current spread to subcortical structures, since they are abolished by either undercutting or applying local anesthetic to the cortex. In addition, pressor and depressor responses are obtained from sites separated by 2-4 mm. Vasomotor responses could often be elicited in the absence of skeletal muscle movement.

In a subsequent paper, Green and Hoff (1937) compared the vasomotor responses and changes in blood flow evoked by cortical stimulation in cats and monkeys anesthetized with ether or diallylbarbiturate. In contrast to the pressor responses that are elicited by stimulating the motor and premotor cortex in cats and monkeys anesthetized with ether, stimulation of these same cortical areas in Dial-anesthetized animals elicits depressor responses or no change in pressure.

Pressor responses elicited from the motor and premotor areas are associated with an increase in blood flow to the limbs and a decrease in kidney blood flow. This was true for both cats and monkeys regardless of the anesthetic used. Depressor responses were often accompanied by a decrease in limb blood flow and an increase in renal blood flow. Blood flow changes are considered to be active rather that passive for several reasons. 1) Dilation of the limbs occurs in the absence of a pressor response. 2) Changes in blood flow persist after removal of the adrenal glands. 3) The changes in limb blood flow are abolished by denervation of the limb. 4) Changes in blood flow are observed in the absence of muscles movement. It was concluded that a mechanism exists whereby the motor and premotor cortical areas influence the distribution of blood to various body regions to favor circulation in active muscles.

The possibility that the variability of cardiovascular responses was due to experimental variables such as type and depth of anesthesia was examined by Delgado (1960) who studied cortically-evoked cardiovascular responses in conscious unrestrained cats, monkeys and humans. In the cat, stimulation of the motor cortex including the hidden motor cortex usually increases blood pressure, although depressor responses are sometimes observed. Pressor and depressor sites are randomly distributed in the motor cortex. Stimulation produces variable effects on heart rate. Cardiovascular responses occur in the absence of cortical seizures and seizure activity is seen without accompanying cardiovascular effects, indicating that the cardiovascular effects are not due to generalized seizure activity.

Eliasson et al. (1952) elicited atropine-sensitive vasodilator responses from the cruciate sulcus in dogs. Associated with the vasodilator response is either an increase or a decrease in blood pressure. By using electrical stimulation Eliasson et al. traced a pathway from the cortex to a region in the hypothalamus

located near the midline 1-2 mm above the optic chiasma. Vasodilator responses elicited from this hypothalamic area are also atropine-sensitive and are observed in hind limbs denervated except for their sympathetic innervation. These results are in agreement with those of Hsu et al. (1942) who also reported that active vasodilation is elicited by stimulation of the motor cortex in chloralose-anesthetized dogs.

Clark et al. (1968) examined the blood flow changes elicited by stimulation of the motor cortex in chloralose-anesthetized monkeys and baboons. They located sites in area 4 from which discrete movement and an increase in blood flow are elicited in the contralateral limb. Stimulation produced small (5-10 mmHg) or no change in blood pressure. Blood flow responses are not altered after preventing muscle movement by administering decamethonium bromide or surgically transecting the spinal cord at the third or fourth lumbar segment. Similar responses are also observed in skinned limbs, suggesting that the changes in blood flow involve changes in muscle perfusion. Stimulus-induced increases in blood flow are not affected by atropine, suggesting that the changes in flow result not from the activation of a sympathetic cholinergic vasodilator system, but rather from the inhibition of sympathetic vasoconstrictor tone. Alternatively, these effects may reflect the activation of a noncholinergic vasodilator system. From these results Clarke et al. suggested that somatomotor and vasomotor representation of the limbs in the cortex are topographically co-localized.

Hilton et al. (1979), working in althesin (alphaxalone-alphadalone)anesthetized cats contradicted the conclusions of Clarke et al. Although muscle
contraction and vasodilation in the contralateral hind limb accompanied stimulation of the motor cortex in the cat, they noted parallel reductions in muscle
contraction and vasodilation after lesioning the contralateral pyramidal tract or
administering gallamine. During recovery from gallamine contractile and blood

flow responses increase in parallel. Vasodilation and muscle contraction (as verified by electromyographic recordings) are prevented by lumbar cordectomy. The lack of vasodilation after lumbar cordectomy is not due to disruption of the sympathetic outflow since an atropine-sensitive vasodilation of the hind limb muscles is elicited by stimulation of the hypothalamic defense region. They concluded that the vasodilation elicited by stimulation of the motor cortex is due to a post-contraction hyperemia, rather than the activation of a cortical sympathetic vasodilator system.

B. Cardiovascular responses elicited from the infralimbic cortex

The infralimbic cortex (including the anterior cingulate gyrus and subcallosal cortex) is thought to control autonomic and behavioral variables such as respiration, gastric motility, blood pressure, pupillary size, attention and searching. (cf. Kaada, 1960; Lofving, 1961).

Smith (1945) was the first to demonstrate that cardiovascular responses can be elicited by stimulating the anterior portions of the cingulate gyrus in monkeys anesthetized with ether. Three types of cardiovascular responses are observed: 1) a marked increase in blood pressure (20-30 mmHg) without a change in heart rate, 2) a decrease in arterial pressure and heart rate, 3) a fall in blood pressure and skipping of cardiac beats. The bradycardia was presumed to be vagally mediated since it is accentuated by administering the anticholinesterase eserine. Similar cardiovascular responses are observed in conscious cats and monkeys (Anand and Dua, 1956).

Lofving (1961), in a very detailed study in the cat, identified pressor and depressor sites in the medial portions of the rostral cingulate gyrus. The strongest responses occur upon stimulation of the area around the genu of the corpus callosum. While some overlap is noted, vasoactive sites are topographically arranged with depressor sites in the dorsal and pressor sites in the ventral

portions of this region. The pressor responses are associated with a pronounced decrease in blood flow to skeletal muscles and a moderate decrease in flow to the intestines. No change in renal blood flow is observed. These responses are mediated via the activation of vasoconstrictor fibers since they are abolished by sectioning the white rami (i.e., preganglionic sympathetic fibers). Stimulation of depressor sites in atropinized, curarized-cats elicits increases in blood flow to skeletal muscles (most pronounced), skin and intestines with no change in renal perfusion. Stimulation of depressor sites in animals having intact vagi reduces heart rate by up to 40%. However, after sectioning the vagi, heart rate is still reduced by up to 10% suggesting that the bradycardic response is in part due to inhibition of sympathetic tone. Electrolytic lesions of the anterior hypothalamic depressor area abolish the depressor responses suggesting that the subcallosal depressor area mediates its effects via the anterior hypothalamic depressor area.

II. Cardiovascular Responses Evoked from the Thalamus

A. Cardiovascular responses elicited by electrical stimulation of the thalamus

Early investigations of thalamic influences on cardiovascular function monitored blood pressure responses elicited by electrical stimulation (cf. Kabat et al., 1935). In 1911 Sachs used the Horsley-Clark stereotaxic instrument and found that electrical stimulation of the n. reuniens and n. ventralis increases blood pressure, whereas stimulation of the anterior thalamic nuclei occasionally elicits depressor responses. In contrast, Kabat et al. (1935) reported that electrical stimulation of the thalamus in pentobarbital-anesthetized cats fails to change blood pressure. The only exception is an area along the course of the periventricular fiber tract medial to the habenulopeduncular tract from which pressor and depressor responses are occasionally elicited.

Stimulation of the medial and intralaminar thalamic nuclei increases blood pressure and decreases renal blood flow in chloralose-anesthetized dogs (Takeuchi et al., 1960; 1962) and nembutal-anesthetized rabbits (Jurf and Blake, 1972). The increase in renal vascular resistance was both neural and humoral in origin as determined in cross perfusion studies (removing humoral influences) and via direct measurement of adrenal catecholamine release. Pressor responses are accompanied by a reflex vagal bradycardia. Depressor responses are obtained from n. ventralis pars medilais and n. lateralis posterior and are most often accompanied by decreases in renal blood flow with no change in heart rate. Stimulation of sites in ventral and lateral thalamic nuclei usually produce no change in either blood pressure or renal blood flow.

Angyan (1978) examined the cardiovascular effects associated with stimulation of rewarding sites the mediodorsal and anteromedial thalamic nuclei in chronically instrumented cats. Stimulation at these sites was associated with increases in blood pressure, respiratory rate, heart rate and a decrease in pulse pressure. Contrary to studies mentioned above, no depressor sites were located in the thalamus. Interestingly, stimulation of nonrewarding thalamic sites failed to evoke cardiovascular responses.

lar responses elicited by electrically stimulating the anteromedial and medio-dorsal thalamic nuclei in conscious rabbits. Stimulation of the anteromedial nucleus evoked an increase in blood pressure and a biphasic cardiac response (a brief acceleration followed by a larger deceleration). Phentolamine abolished both the bradycardia and pressor responses suggesting that the bradycardia results secondarily from baroreceptor reflex activation. Administration of atropine abolished the bradycardia suggesting that it is vagally mediated. Stimulation of the mediodorsal nucleus elicited pressor responses and bradycardia. Phentolamine

administration prevents the pressor response but does not affect the bradycardia. Propranolol attenuates the decrease in heart rate and in combination with atropine abolishes it, suggesting that the bradycardia is in part vagally mediated and in part due to sympathoinhibition. Like Angyan (1978), these authors failed to locate depressor points in the medial thalamic nuclei. No cardiovascular responses were produced by stimulating the lateral thalamic nuclei.

B. Cardiovascular responses evoked by chemical stimulation of the thalamus

An inherent problem in the use of electrical stimulation is its nonselective activation of cell bodies and axons of passage. For this reason many investigators have used chemical substances to activate selectively cell bodies and/or synaptic networks.

Rockhold et al. (1985) reported that heart rate and blood pressure increase after the injection of the excitatory neurotoxins kainic acid and N-methyl-D-aspartic acid into the n. reuniens of the thalamus in urethane anesthetized rats. On this basis, it was concluded that the n. reuniens contains cell bodies having excitatory efferent projections to areas regulating cardiovascular functions. Due to the proximity of the n. reuniens to the ventricular system and hypothalamus the possibility must be considered that these cardiovascular effects reflect the activation of other diencephalic structures. In this regard, these authors have reported similar cardiovascular responses following the injection of these substances into the hypothalamus (Rockhold et al., 1987).

A similar study was performed in conscious rabbits by Powell and Buchanan (1986). Small volumes of glutamate, Gamma aminobutyric acid (GABA) and carbachol were injected into the n. medialis dorsalis via indwelling cannulae. Glutamate and carbachol, but not GABA, produced dose related (nmol to mmol range) increases in heart rate and blood pressure. They noted similar responses during electrical stimulation of the same region (Buchanan and Powell, in press).

Injections into the anteroventral thalamus or reticular nucleus were without effect. Injection of equal concentrations of glutamate and carbachol into the lateral ventricles decreases heart rate and blood pressure, suggesting that the effects of the intrathalamic injection of these substances are not the result of the spread of the drugs to the ventricular system.

III. Hypothalamic Regulation of the Cardiovascular System

Traditionally the hypothalamus is thought to be involved in the integration of a wide variety of autonomic and behavioral responses. Several investigators have even raised the possibility that this area is tonically involved in the control of the cardiovascular system.

A. Cardiovascular responses elicited by electrical stimulation of the hypothalamus

Karplus and Kreidl in a series of papers from 1907-1927 first demonstrated that a variety of autonomic responses are elicited by electrical stimulation of the hypothalamus (Kabat et al., 1935). These investigators showed that electrical stimulation of the ventral surface of the hypothalamus produces increases in blood pressure, bladder contraction, rate and depth of respiration and alterations in gastrointestinal motility. Also observed are increases in the secretion of sweat, tears and saliva. Cardiovascular responses are not altered by administering curare, by adrenalectomy or by hypophysectomy; however, sectioning the renal nerves does attenuate the pressor response.

In the mid 1930's Ranson, Magoun and coworkers (Ranson et al., 1935; Kabat et al., 1935) used the Horsley-Clark stereotaxic instrument to systematically explore the hypothalamus for vasoactive sites in curarized nembutal-anesthetized cats. Pressor responses resulted from stimulation of the lateral hypothalamus, medial forebrain bundle, anterior commissures, periventricular fibers, posterior hypothalamic nucleus, H1, H2 Forel's fields or the perifornical

stimulating regions rostral or dorsal to the hypothalamus and therefore concluded that the hypothalamic pressor responses do not involve the activation of pressor fibers entering the hypothalamus from the cerebral cortex, corpus striatum or thalamus. A few depressor sites were found in more caudal and lateral hypothalamic regions. Stimulation of the region surrounding the anterior commissure decreases the rate and depth of respiration, increases bladder contraction and often decreases blood pressure (10-20 mmHg). Evidence that the anterior hypothalamus contains a parasympathetic system was provided by Korteweg et al. (1959) who showed that vagotomy prevents the decreases in heart rate and blood pressure produced by stimulating the anterior hypothalamus.

Wang and Ranson (1941) reported that decreases in heart rate (6-19%) and depressor responses (18-30 mmHg) are elicited by stimulating the preoptic area in chloralose-anesthetized cats. Vagotomy does not alter the depressor response and only partially attenuates the bradycardia. Both vagal and sympatho-inhibitory mechanisms were postulated to account for these responses.

Morison and Rioch (1937) elicited pressor responses from the hypothalamus in chronic decorticate cats (lacking corticofugal fibers). Pressor responses are elicited by stimulating the anterior hypothalamus, rostral periventricular system, caudal septum and the olfactory tubercule. The strongest pressor responses are elicited from the posterior hypothalamus. In contrast, depressor responses are elicited from the rostral pole of the amygdala, rostrobasal septum and rostral wall of the third ventricle. On the basis of evidence from ablation experiments, it was concluded that a sympathoinhibitory mechanism is located in the anterior hypothalamus. In contrast to others (Ranson et al., 1935; Kortweg et al., 1959), Morison and Rioch did not find evidence of a parasympathetic system in the anterior hypothalamus.

The presence of a sympathoinhibitory system in the anterior hypothalamus of the anesthetized cat was confirmed by Folkow et al. (1959). Stimulation of a circumscribed area located just caudal and ventral to the anterior commissure decreases blood pressure (105 mmHg) and heart rate (20%) and increases blood flow to skeletal muscle, skin and visceral beds. The depressor response is not blocked by atropine, but is prevented by adrenergic antagonists. After regional sympathectomy, stimulation of this area elicits parallel decreases in blood pressure and blood flow to skin, muscle and the viscera. The bradycardia likely reflects the inhibition of cardio-accelerator fibers in these vagotomized animals. The authors concluded that stimulation of this anterior hypothalamic site may produce a generalized inhibition of sympathetic tone by activating a relay center for cortical sympathoinhibitory systems.

Hilton and Spyer (1971) reported that lesioning the anterior hypothalamus in cats attenuates the cardiovascular responses produced by baroreceptor afferent stimulation, leading them to suggest that the anterior hypothalamus is involved in integrating the cardiovascular response to baroreceptor reflex activation. Furthermore, stimulation of this hypothalamic region located ventral and caudal to the anterior commissure and extending in the dorsal hypothalamus dorsal to the fornix, elicits a pattern of cardiovascular effects resembling that produced by baroreceptor reflex activation. These effects consisted of decreases in blood pressure (30-50 mmHg), heart rate (25%) and vascular resistance. Respiratory rate was also decreased. The depressor response is due to sympathoinhibition, since it is potentiated by carotid artery occlusion and abolished by administering guanethedine. The bradycardic response is prevented by sectioning the vagi.

Reis and Nathan (1973) showed that bilateral electrolytic lesion in the anterior hypothalamus of the rat increases arterial pressure. Within five to seven hours the rats died from pulmonary edema. The hypertension is associated with a 50% decrease in cardiac output and is abolished by administering phentolamine. The lesion-induced hypertension apparently results from a sympathetically-mediated increase in total peripheral resistance.

Manning and Peiss (1960) examined the cardiac effects produced by stimulating pressor areas in the lateral and posterior hypothalamus in vagotomized cats. Three basic types of short latency (1-4 s) cardiac and vascular responses are observed: 1) an essentially pure sympathetic cardioaccelerator response without an increase in blood pressure, 2) a vasoconstrictor responses with equal increases in systolic and diastolic pressure, 3) an augmentor response represented primarily as an increase in systolic pressure due to an increase in myocardial contractile force. Augmentor responses are observed without an accompanying increase in heart rate. These three types of cardiac responses are observed alone or more commonly in combination. These responses are presumed to be sympathetically mediated owing to their short latency and abolition by stellate ganglionectomy. Cardiac augmentor and accelerator responses are generally concentrated into two zones, one in the periventricular areas and nuclei bounding the ventricular walls and the other located more lateral, extending into the area of the medial forebrain bundle, the H1 and H2 Forel's fields and extending into the subthalamic nuclei.

B. Chemical stimulation of the hypothalamus

Masserman (1937) compared the cardiovascular effects elicited by electrical and chemical stimulation of the anterior hypothalamus in etheranesthetized cats. In contrast to studies discussed above, a 10-60 mmHz rise in blood pressure and reductions in heart and respiratory rates were produced by

electrically stimulating the anterior hypothalamus. The intrahypothalamic injection of sodium amytal produces a 25-60 mmHg decrease in blood pressure and increases in heart rate, pulse pressure and respiratory rate. In contrast, the injection of coramine elicits a slight increase in blood pressure and respiratory rate.

More recently, Redgate and Gellhorn in a series of papers (Gellhorn and Redgate, 1955; Redgate and Gellhorn, 1956a; 1956b;) examined the cardiovascular effects occurring after the intrahypothalamic injection of barbiturates or local anesthetics in chloralose-anesthetized cats. The injection of pentothal, nembutal or procaine into the posterior hypothalamus produces a 10-80 mmHg fall in blood pressure. The fall in blood pressure is usually accompanied by a decrease in heart rate. In addition, the action of hypotensive drugs such as acetylcholine or histamine are potentiated following the injection of barbiturates into the posterior hypothalamus. On this basis they concluded that the posterior hypothalamus exerts a strong tonic excitatory sympathetic drive. Injection of pentothal or nembutal into the anterior hypothalamus between the optic chiasma and the anterior commissure increases blood pressure and heart rate. These responses are smaller in magnitude than those produced by posterior hypothalamic injections. The injection of barbiturates into the anterior hypothalamus reduces the reflexlyinduced bradycardia occurring after the intravenous injection of norepinephrine. In addition, the magnitude of the pressor response to a given dose of norepinephrine is greater following the injection of barbiturate into the anterior hypothalamus. They suggested that the anterior hypothalamus exerts a tonic parasympathetic influence. The results and conclusions of Redgate and Gellhorn must be viewed with a degree of caution in view of the fact that they used injection volumes of up to 40 ul/dose in these experiments.

In 1964, Gellhorn demonstrated that electrolytic lesions of the posterior hypothalamus produce decreases in blood pressure and heart rate similar to those occurring after the intrahypothalamic injection of barbiturates into these same regions. These posterior hypothalamic lesions destroyed n. mammillaris, n. ventrolateralis, n. lateralis and n. posterior. In contrast, the injection of metrazol or strychine into the posterior hypothalamus increases blood pressure and heart rate. Lesion of the anterior hypothalamus produces even greater increases in blood pressure and heart rate than does the injection of barbiturates into the anterior hypothalamus. The anterior lesions destroyed n. preopticus, n. supraopticus, n. superchiasmaticus, and n. hypothalamus anterior.

Lee et al. (1972) studied the cardiovascular effects elicited by the intrahypothalamic injection of the GABA antagonist picrotoxin in the cat. The injection of picrotoxin (30-40 µg) into either the lateral or posterior hypothalamus increases blood pressure (64 mmHg) and heart rate (30 beats/min) and produces cardiac arrhythmias similar to those seen during electrical stimulation of the same sites. Unlike intravenous administration, the intrahypothalamic injection of picrotoxin does not produce a reflex bradycardia even though blood pressure often rises above 250 mmHg. These effects are similar to those elicited by the injection of picrotoxin into medullary pressor sites and are thought to reflect a hypothalamic-mediated inhibition of the vagal reflex. The ability of picrotoxin injections to increase blood pressure indicates that sympathoexcitatory systems in the lateral and posterior hypothalamus are under tonic GABAergic inhibitory influences. Unfortunately, no attempt was made to determine whether these sympathoexcitatory systems are tonically active by injecting a GABA agonist. The injection of picrotoxin into depressor sites (as determined by electrical stimulation) in the anterior hypothalamus produces only slight increases in blood pressure (14 mmHg) and heart rate.

Dimicco and colleagues (Williford et al., 1980; Schmidt and Dimicco, 1984) identified a sympathoexcitatory system in the periventricular hypothalamus of the cat which is under GABAergic control. Bicuculline (8-32 µg in 100 nl) injected into the left lateral cerebral ventricle was confined to the lateral and third ventricles by cannulating the aqueduct of Sylvius. Within one minute of bicuculline injection, blood pressure, heart rate and hind limb vascular resistance increase. The vagally-induced bradycardia normally accompanying the pressor response is prevented. The intraventricular injection of muscimol (10 µg in 100 nl) during the peak bicuculline-induced cardiovascular response abruptly reverses these effects. Following muscimol, heart rate and blood pressure are at slightly less than control levels. These findings support the suggestion of Redgate and Gellhorn that the hypothalamus exerts a tonic sympathoexcitatory drive. However, this is not directly tested by administering muscimol alone. These authors also failed to consider the possibility that these effects reflect an action of bicuculline in the thalamus or other diencephalic structures.

A pattern of cardiovascular effects similar to that reported by Dimicco and colleagues was seen after injecting bicuculline or the GABA synthesis inhibitors isoniazid and 3-mercaptopropionic acid into the posterior hypothalamus of the rat (Finch and Hicks, 1977). The increases in arterial pressure, respiratory rate and tachycardia produced by the GABA antagonist and synthesis inhibitors are reversed by intrahypothalamic muscimol. The injection of muscimol alone fails to change baseline blood pressure or heart rate. It is concluded that unlike in the cat, the GABAergic mechanism in the anesthetized rat is sufficiently active to suppress tonic activity in the sympathoexcitatory hypothalamic system activated by GABA antagonists.

Histamine (0.01-10 µg/µl) injected into the posterior or anterior hypothalamus in urethane anesthetized rats also increases blood pressure and

heart rate (Finch and Hicks, 1977). These effects are thought to be mediated by H1 receptors since they are attenuated by the H1 antagonist mepyramine. Similar volumes of histamine injected into the ventromedial hypothalamus, lateral hypothalamus, preoptic area or medial thalamus fails to elicit changes in heart rate or blood pressure suggesting that the cardiovascular effects elicited by histamine involve the activation of systems in the posterior and anterior hypothalamus.

Rockhold et al. (1987) showed that the injection of kainic acid and N-methyl-D-aspartic acid (30-1000 ng dissolved in 100 nl saline) into the area of the paraventricular nucleus (PVH) in rats increases heart rate and blood pressure and causes mydriasis, exopthalmos and increases in respiratory rate. Injection of these agents into the lateral hypothalamus and lateral cerebral ventricle produced cardiovascular effects of similar magnitude when 1000 ng but not 30 ng was administered. Pressor and tachycardic responses are reversed by phentolamine and propranolol, respectively, suggesting sympathetic mediation of the cardiovascular responses. In contrast, injections of L-glutamate into this region produces only minimal cardiovascular effects. No attempt was made to determine whether these regions tonically influence sympathetic tone.

Sum and Guyenet (1986) elicited increases in arterial pressure and a reflex bradycardia by injecting L-glutamate into the lateral hypothalamus of the rat. In addition, the injection of glutamate increases the discharge rate of medullospinal sympathoexcitatory neurons in the rostral ventrolateral medulla. This hypothalamic projection to the ventrolateral medulla is thought to be glutamatergic since the activation of the medullospinal neurons and pressor response to hypothalamic stimulation were blocked by injecting the glutamate antagonist, kynurenate into the ventrolateral medulla.

C. The defense arousal system: Possible source of sympathetic tone

Fear and rage reactions are associated with stereotypic behavioral and visceral responses which prepare the organism for flight or attack. Cannon in the 1920's suggested that sympathetic activation during these reactions mimics the effects of epinephrine (Hilton, 1982). That is, sympathetic activation increases skeletal muscle blood flow, while reducing flow to visceral structures, thus driving blood out of the viscera and into skeletal muscles to prepare for the exertion of attack or escape.

Hess and collaborators in the 1940's (cf. Hilton, 1982) used electrical stimulation to map the regions from which the patterns of behavior characteristic of alerting and ultimately attack or flight (increased stimulus intensity) are elicited. Behavioral responses which completely mimic those elicited by natural stimuli are evoked in conscious cats from the tuberal region of the hypothalamus just medial, ventral and lateral to the fornix. Hess, collectively termed these responses the defense reaction.

Abrahams et al. (1960) used electrical stimulation to map those regions of the hypothalamus and midbrain from which the cardiovascular components of the defense reaction are elicited in anesthetized cats. Stimulation of reactive sites in the hypothalamus elicit a stereotypic pattern of cardiovascular responses including increases in skeletal muscle blood flow, blood pressure and heart rate. Also observed are vasoconstriction in the skin and intestine, pupillary dilation, retraction of the nictating membrane, piloerection along the back and tail and an increase in respiratory rate. Small doses of atropine abolish the increase in skeletal muscle blood flow. The responsive zone consists of a narrow strip running bilaterally along the length of the hypothalamus. In the tuberal region the reactive area extends laterally giving rise to a highly reactive site just dorsal to the cerebral peduncle. Stimulation identified three mesencephalic

regions giving similar patterns of responses: 1) in the tegmentum ventral to the superior colliculus, 2) in the dorsolateral part of the central gray and 3) dorsal to the cerebral peduncle. The pattern of responses elicited from the central gray most resembles that occurring during hypothalamic stimulation. The regions that produce active muscle vasodilation are identical to those identified by Hess and others as producing the behavioral defense reaction in unanesthetized animals (see Abrahams et al., 1960). This fact was confirmed by Abrahams et al. (1960) who elicited alerting and defense behaviors in conscious cats by stimulating sites which elicit muscle vasodilation in anesthetized preparations.

In a subsequent study, Coote et al. (1973) showed that the region producing defense-like cardiovascular responses, including active muscle vasodilation extends caudally into the medulla. This region consists of a narrow strip 2.5 mm on either side of the midline, starting ventral to the inferior colliculus and ending close to the floor of the fourth ventricle. This region is anatomically distinct from the bilateral hypothalamic cholinergic vasodilator pathway coursing near the ventral surface of the medulla. Stimulation of the medullary defense area in conscious animals produces defense-like behaviors; however, these responses are not as vigorously expressed as those occurring during stimulation of the hypothalamic or midbrain defense areas. The skeletal muscle dilation elicited by stimulation of the caudal defense area is only partially reversed by atropine, suggesting that the vasodilation is due to the activation of both a cholinergic vasodilator system and the inhibition of sympathetic vasoconstrictor tone.

Hilton et al. (1983) used electrical stimulation to trace an efferent pathway from the hypothalamic and midbrain defense areas through the ventral medulla. This pathway courses as a narrow strip ventral to the superior olive and nucleus of the trapezoid body to the level of the rostral inferior olive where it lies ventral to the facial nucleus. Guetzenstein et al. (1978) and Hilton et al. (1983)

demonstrated that bilateral application of glycine to the ventral surface of the medulla overlying the caudal end of the efferent pathway decreases blood pressure (20-60%), heart rate and cardiac output and stops respiration. Also total peripheral resistance decreases primarily due to an increase in splanchnic conductance. Moreover, after applying glycine, stimulation of the hypothalamic or mesencephalic defense areas fails to elicit a defense response. From these results Hilton et al. (1983) concluded that glycine blocks a synaptic relay in the efferent pathway from the defense regions to preganglionic sympathetic neurons. Furthermore, they suggested that the neurons in the ventral medulla receiving inputs from the defense area provide a tonic excitatory drive to preganglionic sympathetic neurons and that the tonic drive originates in the hypothalamic and mesencephalic defense regions. Thus these authors concluded that the defense regions are responsible for the maintaining basal sympathetic tone. On the basis of the data presented, this suggestion is tenuous at best. The authors present no evidence that the defense regions are indeed tonically active. In addition, no attempt was made to determine whether other brain regions provide input to the glycine-sensitive area. For example, Barman and Gebber (1987) showed that the ventral lateral medulla (which may correspond to the glycine sensitive area) receives sympathoexcitatory input from the lateral tegmental field of the dorsal medulla. In addition, it is well known that sympathetic tone is maintained in the decerebrate animal.

Lovick et al. (1984) identified neurons in the glycine sensitive area of the ventral medulla which are antidromically activated by stimulating the ventrolateral funiculus of the cat thoracolumbar spinal cord. Approximately half of these neurons are excited by stimulating the hypothalamic or midbrain defense regions. In addition, other neurons in the ventral medulla respond to stimulation of either or both defense regions; however, whether these neurons have spinally

projecting axons is not known. They did not address the question of whether the efferent pathway from the defense regions to these medullary neurons is tonically active.

Hilton and Redfern (1986) compared the responses produced by chemical and electrical stimulation of sites in the classical defense regions in order to locate the cell bodies of neurons responsible for these responses. In conscious and anesthetized rats, sites from which the defense reaction can be elicited by electrical stimulation correspond to those identified by Abrahams et al. (1960) in the cat. In contrast, chemical stimulation via the microinjection of the excitatory amino acid, D,L-homocysteic acid identified four discrete sites within the electrically-defined defense region from which the defense reaction is elicited. These four sites were the dorsomedial periaqueductal gray matter, an area overlying the lateral optic chiasma, the medial tuberal hypothalamus and a region medial to the lateral lemniscus in the pons. Of these regions the full pattern of visceral, respiratory and behavioral responses is only elicited by chemically stimulating the periaqueductal gray. In the remaining three regions, chemical stimulation elicits decreases rather than increases blood pressure. In addition, chemical stimulation of the tuberal hypothalamus fails to elicit renal vasoconstriction. Thus it is concluded that the components of the defense reaction are generated in many areas of the brain and integrated in the periaqueductal gray. The rather wide distribution of areas from which the defense response is elicited by electrical stimulation is thought to reflect the activation of fibers of passage.

Indirect evidence that the defense region is tonically active and may generate a component of SND is provided by studies examining the cardiovascular changes accompanying transitions between awake and sleep states. Mancia et al. (1970) showed that as cats pass from wakefulness to synchronized and then into

desynchronized sleep, they display a characteristic pattern of cardiovascular responses. During synchronized sleep there are slight reductions in heart rate and blood pressure without much change in total peripheral resistance. During desynchronized sleep there are greater reductions in cardiac output, total peripheral resistance and blood pressure. In addition, there is a distinct pattern of vascular responses, including increased conductance in the skin, mesenteric and renal vascular beds and a decrease in skeletal muscle conductance. The changes in vascular resistance are apparently centrally mediated, since, during periods of desynchronized-like sleep resulting from the administration of physostigmine, the level of activity on cardiac, renal, splanchnic and lumbar sympathetic nerves decreases, while activity in vasoconstrictor nerves to skeletal muscles increases (cf. Coote, 1982). Similar neural responses are reported to occur in other species during desynchronized sleep (cf. Coote, 1982). Interestingly, the pattern of cardiovascular responses observed during the transition from the awake state to desynchronized sleep are the opposite of those resulting from the activation of the defense reaction. Conversely, the pattern of cardiovascular responses during awakening from desynchronized sleep mimics that during the defense reaction. Thus the defense areas appear to be tonically active, with the level of activity in the system being governed by the behavioral state of the animal.

D. Models of hypertension involving diencephalic systems

Further evidence that the diencephalon can influence cardiovascular function comes from studies which demonstrate the involvement of diencephalic structures in several models of experimental hypertension.

1. Renin-dependent renal hypertension

Renal hypertension is produced experimentally by renal artery stenosis, perinephritis, renal compression or aortic ligation in animals having one or two kidneys. The initial rise in blood pressure and increase in peripheral

resistance in these hypertensive models is associated with increases in plasma renin and circulating angiotensin IL. This early phase of hypertension is known as renin-dependent renal hypertension. As reviewed by Brody et al. (1984) angiotensin II has both peripheral and central sympathomimetic actions. The pressor response to intravenous administration of angiotensin II is prevented by cooling or lesioning the area postrema in dogs, rabbits and cats. In the rat, the region mediating the central pressor response to intracerebroventricular (icv) angiotensin II is not the area postrema, but the anteroventral region of the third ventricle This region incorporating the organum vasculosum of the lamina terminalis is accessible to both blood-borne and cerebrospinal fluid angiotensin IL. The central action of angiotensin was demonstrated by Fink et al. (1980), who compared the pressor responses produced by the intracarotid and intra-aortic administration of angiotensin II. Since the pressor response to intracarotid angiotensin is larger, their difference is used as an index of angiotensin's central pressor effect. The injection of the angiotensin antagonist saralasin into the third ventricle significantly reduces the central pressor effect of angiotensin IL. Furthermore, the central pressor effect is also abolished by electrolytically lesioning the AV3V region, suggesting that this region is responsible for mediating the pressor effect of circulating angiotensin II.

In a similar study, Lappe and Brody (1984) compared the pressor and regional vascular responses to intracarotid and abdominal aortic infusions of angiotensin II in conscious rats. Both the intracarotid and intra-aortic infusion of angiotensin II produce pressor responses and increases in resistance in the renal, mesenteric and hindquarter vascular beds. However, these changes are uniformly greater after intracarotid, than after intra-aortic administration. Ganglionic blockade with hexamethonium abolishes both the central pressor and mesenteric vascular responses; however, renal vasoconstriction is only slightly reduced, while

no difference in the hindquarter vasoconstriction is observed. Similarly, the injection of saralasin into the lateral cerebral ventricle eliminates the pressor response and significantly attenuates the vasoconstriction in the renal and mesenteric vasculature. These results indicate that angiotensin acts centrally to induce vasoconstriction of the hindquarters, renal and mesenteric vasculature.

Haywood et al. (1983) showed that the sustained renin-dependent hypertension produced by unilateral clipping of a renal artery is prevented by electrolytically lesioning the AV3V region. In both AV3V lesioned and nonlesioned rats, clipping of one renal artery produces an initial increase in blood pressure; however, the level of hypertension is lower in lesioned animals. After five days, blood pressure in the lesioned animals begins to decrease reaching levels similar to those in sham-operated, sham-clipped controls within two weeks. In addition, the hypertensive rats (sham-lesioned, clipped artery) show a tendency to increase water intake and urine volume, presumably due to the dipsogenic effect of increasing angiotensin II levels. The AV3V lesioned animals do not show an increase in water turnover.

The ability of centrally administered angiotensin II to elicit increases in sympathetic nerve activity was directly demonstrated by Tobey et al. (1983). These authors showed that the intra-aortic injection of angiotensin II increases splenic and renal sympathetic nerve activity and blood pressure. The increase in activity is greater on the splenic than on the renal nerve. In contrast, the icv injection of angiotensin II (20 µg) increases splenic but not renal sympathetic nerve activity, indicating that central angiotensin II can differentially affect sympathetic nerve activity. The ability of angiotensin II to increase sympathetic nerve activity is confirmed by Keim and Sigy (1971) who reported that the intravertebral infusion of angiotensin II increases the level of activity on preganglionic cervical sympathetic nerves in unanesthetized cats.

Hartle et al. (1982) mapped the pathway from the AV3V region believed to mediate the pressor response to icv administered angiotensin IL. By examining the central angiotensin pressor response after a series of electrolytic lesions, it was determined that the pathway mediating the pressor response originates in the AV3V region from where it ascends along the lamina terminalis to the level of the anterior commissure. The pathway then descends medially through the anterior hypothalamus. A series of horizontal knife cuts showed the pathway descends anterior to the PVH and then passes ventral to this nucleus. The authors concluded that lesions of the AV3V regions which prevent remindependent hypertension most likely interrupt part of this pathway.

2. Nonrenin-dependent renal hypertension

A chronic level of hypertension is produced by removing one kidney and then either constricting the renal artery (one kidney Goldblatt) or wrapping the contralateral kidney (one kidney Grollman). Most authors feel that this form of hypertension is not renin-dependent (Brody et al. 1984). For example, Bumpus et al. (1973) showed that the angiotensin II antagonists [Le 3]-and [Sar 1, He 8] reverse the initial rise in blood pressure resulting from the ligation of the renal artery in both one- and two-kidney models of hypertension. However, these antagonists do not lower blood pressure in chronically hypertensive one-kidney Goldblatt animals.

Buggy et al. (1977) reported that lesions of the AV3V region prevent the hypertension and increase in drinking normally occurring following the one-kidney Grollman procedure. Lesion of the AV3V region alone produced a temporary adipsia in one half of the rats, and a transient (1 week) hypertension. The failure of lesioned animals to develop hypertension is not the result of decreases in water intake since restricting the water intake of sham-lesioned animals with renal wrapping does not prevent them from reaching hypertensive

levels similar to those of sham-lesioned animals which were allowed to increase their water intake.

Buggy et al. (1978) demonstrated that lesion of the AV3V region six weeks after the initiation of one-kidney Grollman hypertension returns blood pressure to normotensive levels. Lesion of the AV3V region two weeks after the development of two-kidney Goldblatt hypertension reduces, but does not completely return blood pressure to normotensive levels. These results indicate that the AV3V region is also involved in the nonrenin-dependent maintenance phase of renal hypertension.

Katholi et al. (1981) studied the contribution of renal afferent nerve activity to the maintenance phase of hypertension in the one-kidney Grollman rat. Denervation of the remaining kidney by stripping the adventitia and painting the renal artery with phenol significantly decreases the chronically elevated blood pressure in these animals. Denervated animals experience no change in sodium excretion, urine volume, water or sodium intake, or renal function compared to sham-operated controls. Since renal denervation failed to alter water or electrolyte balance, it is suggested that renal-denervation disinhibits a central sympathoinhibitory mechanism.

Hartle and Brody (1982) identified two separate vasoconstrictor pathways emanating from the AV3V region in the rat. These pathways were identified by determining which of a series of lesions and knife cuts would block the pressor response to icv angiotensin II, hypertonic saline or carbachol. The first, pathway is the periventricular pathway described above (see Hartle et al., 1982). This pathway mediates the pressor responses to icv angiotensin II, hypertonic saline and carbachol. Furthermore, lesion of this pathway prevents the development of renin-dependent but not renin-independent forms of hypertension, and does not block the hemodynamic effects produced by electrically stimulating

the AV3V region. Instead, the hemodynamic effects evoked by stimulating the AV3V are conducted along a laterally directed pathway which eventually joins the medial forebrain bundle. Although not directly tested, the authors speculate that the lateral pathway is involved in nonrenin-dependent forms of hypertension which are prevented by AV3V lesion.

3. Neurogenic hypertension

Hypertension which results from removal of baroreceptor inhibitory input to the central nervous system is called neurogenic hypertension. This form of hypertension is marked by persistent fluctuations (lability) in blood pressure. It remains controversial as to whether blood pressure remains elevated over long periods of time in these animals (see Brody et al., 1984).

Bing et al. (1945) examined the development of neurogenic hypertension in unanesthetized dogs occurring after sectioning the carotid sinus and aortic depressor nerves. Denervation produced tachycardia, sustained increases in blood pressure, cardiac output, renal vascular resistance and blood flow through the forelimb. The authors concluded that these cardiovascular changes are consistent with an increase in sympathetic tone, however, this was not demonstrated directly.

Doba and Reis (1973) produced neurogenic hypertension in rats by electrolytically lesioning the middle third of the n. tractus solitarii (NTS), an area in which the integration of baroreceptor afferent activity is thought to occur. The acute effects of NTS lesion include abolition of the baroreceptor reflexes, an increase in blood pressure without a change in heart rate and a decrease in respiratory rate. These effects are only present after discontinuation of the halothane anesthesia. Also observed was a 255% increase in total peripheral resistance and a 62% reduction in cardiac output. These effects are attenuated by administering the alpha adrenergic antagonist phentolamine and are

baroreceptor mediated inhibition. The hypertension is prevented or reversed by midcollicular decerebration indicating that the forebrain is essential for the development and maintenance of neurogenic hypertension. All rats developing neurogenic hypertension died within 5 hours as a result of pulmonary edema.

Zhang and Ciriello (1985a,b) reported increases in blood pressure and heart rate after sectioning the aortic depressor nerves in rats. Both electrolytic and more selective kainic acid lesions of the PVH before or after aortic baroreceptor denervation prevents or reverses, respectively, the hypertension and tachycardia occurring after denervation. Lesion of the PVH had no effect on heart rate or blood pressure in rats with intact buffer nerves. Kainic acid lesions destroyed the parvocellular but not the magnocellular neurons in the PVH.

The possibility that the increases in arterial pressure and heart rate after sinoaortic denervation are the result of humoral factors was explored by Alexander and Morris (1982). These investigators measured arginine vasopressin, osmolality and sodium levels in rats up to 7 days after sinoaortic denervation. While no changes in osmolality or sodium are noted, vasopressin levels are elevated 15 min and 7 days after denervation, suggesting that an increase in vasopressin contributes to the neurogenic hypertension. This conclusion was challenged by Brody et al. (1984), who reported that administering vasopressin antagonists fails to prevent the development of neurogenic hypertension occurring after sinoaortic denervation.

4. Mineralocorticoid-salt hypertension

A combination of dietary salt and repeated administration of mineralocorticoids such as deoxycorticosterone acetate (DOCA) produces a non-remin-dependent hypertension. Several causal factors such as elevated vasopressin

and sympathetic hyperactivity have been implicated in this model of hypertension.

Berecek et al. (1982) reported that lesion of the AV3V region prevents the development of DOCA-salt hypertension. The systemic administration of vaso-pressin to lesioned animals elicits only small increases in blood pressure indicating that the protective effects of AV3V lesion apparently involve more than the prevention of vasopressin release.

Takeda and Bunag (1980) compared the level of sympathetic nerve activity and the magnitude of pressor responses in DOCA-salt hypertensive and normotensive rats. Under urethane anesthesia, blood pressure and the frequency of sympathetic nerve firing are significantly higher in DOCA-salt hypertensive rats than in normotensive rats. Electrical stimulation of the posterior hypothalamus in both groups increases sympathetic nerve activity and blood pressure; however, the magnitude of the increases is significantly greater in the hypertensive rats. Ganglionic blockade by pentolinium reduces blood pressure and sympathetic nerve activity to similar levels in both groups. Thus it was concluded that DOCA-salt hypertension is associated with sympathetic hyperactivity.

5. Spontaneous hypertension

The spontaneously hypertensive rat (SHR) was isolated from an inbred strain of Wistar rats. These rats are characterized by a pronounced hypertension which develops with age. The hypertension in SHR is thought to involve a central mechanism.

Judy et al. (1976) demonstrated that hypertension in SHR's is associated with an increase in activity on the splanchnic, cervical, renal and splenic sympathetic nerves in both anesthetized and conscious SHR's. Sympathetic nerve activity and blood pressure increase in parallel with increasing age in the SHR. This conclusion is disputed by Touw et al. (1980) who, by comparing the

effects of hexamethonium sympathectomy in conscious adult and juvenile SHR and normotensive rats, concluded that neurogenic vasoconstrictor tone is not elevated in SHR's and is thus not directly responsible for the higher blood pressure.

Although AV3V lesions fail to prevent the development or maintenance of hypertension in SHR's (Gordon et al., 1982; Buggy et al., 1978) several other forebrain mechanisms and structures are thought to be involved in the development or maintenance of hypertension in the SHR. These include hyperactivity of sympathetic systems in the posterior hypothalamus (Bunag and Eferakeya, 1976), exaggerated cardiovascular responsiveness to environmental stress resembling the alerting-defense reaction (Hallback and Folkow, 1974; Galeno et al., 1984) and the amygdala (Galeno et al., 1982).

IV. Generation of Rhythmic Activity by the Diencephalon and Brain Stem

A. The generation of basal SND

1. Early views on the origin of basal SND

As first demonstrated by Adrian et al. (1932) basal sympathetic nerve discharge contains cardiac- and respiratory-related rhythms. Historically there have been two main theories concerning the manner in which the rhythmic patterns in SND are generated by networks of supraspinal neurons.

The classical theory of how patterns of sympathetic activity are generated held that sympathetic tone was randomly generated within a diffusely organized brain stem reticular network. The presence of rhythms in the outflow of this system was thought to arise as a consequence of periodic activity in afferents to the generating network. For example the cardiac-related rhythm in SND was believed by Adrian et al. (1932) and others (Green and Heffron, 1967; Cohen and Gootman, 1970) to arise from the pulse synchronous activity in

baroreceptor afferent nerves. That is, increases in baroreceptor nerve discharge during systole cause a delayed inhibition of SND, whereas, removal of inhibition during diastole reflexly increases SND. Similarly, the slower respiratory-related rhythm in SND was thought to arise from the synchronous activity in vagal pulmonary lung inflation afferents.

This view of sympathetic rhythm generation is no longer held. It is now well established that central sympathetic networks in the brain stem are inherently capable of generating complex output patterns in the absence of periodic afferent input (cf. Gebber, 1982; 1984).

2. Evidence that the brain stem is intrinsically capable of rhythm generation

Evidence that the brain stem is inherently capable of rhythm generation was first presented by Green and Heffron (1967) and Cohen and Gootman (1969). These authors found that SND in baroreceptor-innervated cats can contain a noncardiac-related 10 Hz rhythm.

Recently, Barman and Gebber and collaborators have advanced the theory that the 2- to 6-Hz rhythm in SND which is normally cardiac-locked is generated in the brain stem and then entrained to the cardiac cycle by the baroreceptor reflexes. Several lines of evidence support this view. First, although no longer cardiac-locked, the 2- to 6-Hz rhythm in SND persists after complete baroreceptor denervation (Taylor and Gebber, 1975; Barman and Gebber, 1980). Therefore, the occurrence of rhythmic bursts in SND (recorded as slow waves using a band pass of 1 to 1000 Hz) at frequencies between 2 and 6 Hz is not the result of pulse synchronous baroreceptor nerve activity. The 2- to 6Hz rhythm in SND is apparently generated in the brain stem since it persists after midcollicular decerebration (Barman and Gebber, 1980), but not after acute transection of the spinal cord at the first cervical segment (McCall and Gebber; 1975). Second, slowing of the heart rate by cardiac pacing or vagal stimulation

produces dramatic shifts in phase between sympathetic nerve slow waves and the arterial pulse (Gebber, 1976, Morrison and Gebber, 1982). If the cardiac-related rhythm in SND is the result of pulse synchronous baroreceptor discharge then the phase relation between SND and the arterial pulse should be independent of the heart rate. Third, when the heart rate is slowed to less than 2.5 beats/s, the declining phase of the sympathetic nerve slow wave begins before the onset of pulse synchronous baroreceptor afferent nerve activity, thus the decline of the sympathetic slow wave cycle can not be attributed to baroreceptor-mediated inhibition of SND. The termination of the slow wave must involve a central mechanism. Gebber (1976) proposed that an inhibitory phasing mechanism is responsible for the baroreceptor reflex entrainment of centrally generated sympathetic slow waves to the cardiac cycle. In this model, the rising phase of the sympathetic nerve slow wave begins only when baroreceptor inhibition falls to some minimum level.

The respiratory-related component of SND is observed following vagotomy indicating that it, at least in part, is of central origin (Cohen and Gootman, 1970; Preiss et al., 1975; Barman and Gebber, 1976; Bachoo and Polosa, 1987). However, the origin of the respiratory-related rhythm in SND is controversial. Several authors (Cohen and Gootman, 1970; Preiss et al. 1975; Bachoo and Polosa, 1987) have proposed that this slow rhythm in SND is extrinsically imposed on sympathetic networks by elements of the brain stem respiratory oscillator. In contrast, Koepchen and Thurau (1959) and Barman and Gebber (1976), proposed that the slow component in SND is generated by a sympathetic oscillator which is normally, but not always, coupled to the respiratory oscillator. Three observations led to this conclusion: 1) changes in respiratory rate were accompanied by dramatic shifts in phase relations between sympathetic and phrenic nerve discharge, 2) slow oscillations of sympathetic and phrenic nerve

discharge were not always locked in a 1:1 relation, 3) the sympathetic nerve slow wave activity persists when respiratory rhythmicity ceases during periods of hyperventilation.

3. Proposed mechanisms of SND generation in the brain stem

In the baroreceptor-denervated cat, the rhythm in SND is characterized by irregularly occurring 2- to 6-Hz slow waves (i.e. variable interslow wave intervals (Taylor and Gebber, 1975; Barman and Gebber, 1980). Barman et al. (1984) tested the possibility that the irregular 2- to 6-Hz activity pattern of SND in baroreceptor-denervated cats arises from multiple brain stem generating networks. By using crosscorrelation and power density spectral analysis, they found that the frequency components of activity simultaneously recorded from different postganglionic sympathetic nerves can be markedly different. Moreover, by using peri-spike-triggered averaging (a method of crosscorrelation) they found that the activity of some ventrolateral and raphe medullary neurons is more strongly correlated to the activity on one sympathetic nerve than another. Evidence that the sympathetic generating circuits are coupled is provided by the fact that although more strongly correlated to activity in one nerve, the medullary units with sympathetic nerve-related activity are correlated to activity in both nerves. Furthermore, considerable overlap is observed in the frequency spectra of SND recorded from two sympathetic nerves.

Langhorst and collaborators (1975; 1980; 1984) argue against the notion that there are discrete pools of sympathetic reticular neurons capable of selective sympathetic control. Rather, they believe that rhythmic activity in a variety of effector systems including SND is generated by a "common brain stem system". Effector systems under the simultaneous control of this common brain stem system include the cardiovascular, respiratory, and general activating systems plus afferent sensory inputs. The output onto the effector system is

determined by the integration of convergent afferent inputs from somatic and vegetative receptors. Individual reticular neurons receiving the convergent inputs then influence more than one effector system. Support for this hypothesis comes from correlation and spectral analysis which showed that on a long time scale the rhythmic discharge patterns of all reticular neurons display a common rhythmic component having a period of 4 to 10 seconds. While often not the predominant rhythm, a similar slow 0.1- to 0.25-Hz rhythm is usually observed in the activity patterns of the effector systems. In addition, power spectral analysis revealed that there are common rhythmic components in the discharge patterns of some reticular neurons and the activity patterns in several effector systems. The authors provided this as evidence that individual reticular neurons influence more than one effector system.

There are several problems with the common brain stem model. First, the authors fail to prove that the common slow rhythm in reticular activity is even generated in the brain stem reticular formation. Second, the discharges of most reticular neurons are not related to the activity patterns in several effector systems. This is true in their work and in the work of others (Barman and Gebber, 1981; 1982; 1984). Barman and Gebber demonstrated that most reticular neurons do not have sympathetic nerve-related activity and those that do often do not have cardiac-activity and/or EEG-related activity. Third, Langhorst et al. failed to address the possibility that the discharges of reticular neurons are related to activity in more than one effector system because there is coupling between functionally distinct reticular systems controlling specific effector systems. In this case the temporal relationship between the discharges of these neurons and the activity in effector systems may not reflect a role of these neurons in controlling all effector systems.

4. Possible brain stem regions involved in the generation of SND

In recent years electrophysiological and pharmacological investigations have revealed three areas of the medulla which may be involved in the control of basal SND in the anesthetized animal. The first of these regions is the rostral ventrolateral medulla (VLM) located caudal to the facial nucleus. Ross et al. (1984) and McAllen et al. (1982) showed that both electrical stimulation and the application of excitatory amino acids in the VLM elicits dramatic increases in arterial blood pressure and heart rate. Furthermore, bilateral lesions of this area lower arterial blood pressure to levels resembling those occurring after acute transection of the cervical spinal cord (Dampney and Moon, 1980). By using spike-triggered averaging, Barman and Gebber (1983; 1985) showed that the spontaneous discharges of some VLM neurons are temporally related to SND in baroreceptor-denervated and -intact cats. The axons of many of these neurons project to the intermediolateral nucleus (IML) of the thoracolumbar spinal cord (Barman and Gebber, 1985). These neurons are thought to be sympathoexcitatory since their firing rate decreases during baroreceptor reflex activation.

The second area is the lateral tegmental field (LTF) of the dorsolateral medulla, including the reticularis parvocellularis and reticularis ventralis nuclei. Like the VLM, electrical stimulation of the LTF elicits increases in blood pressure and SND (Dampney and Moon, 1980; Gebber and Barman, 1985). The injection of excitatory amino acids into the rostral portions of n. reticularis parvocellularis increases blood pressure in the rabbit (Goodchild and Dampney, 1985). Lesion of this region also produces a profound decrease in blood pressure (Kumada et al., 1979). The spontaneous discharges of some neurons in the LTF are temporally related to SND (Barman and Gebber, 1981; Gebber and Barman, 1985). Some LTF neurons with sympathetic nerve-related activity respond to baroreceptor reflex activation with a decrease in firing rate whereas others show

an increase. The axons of LTF neurons with sympathetic nerve-related activity do not project to the thoracic spinal cord. However, as demonstrated by antidromic activation sympathoexcitatory LTF neurons project to the region of the VLM containing sympathoexcitatory neurons which project to the IML (Barman and Gebber, 1987).

The third area believed to be involved in the control of SND is the medullary raphe nuclei (raphe magnus, pallidus and obscurus). These nuclei are contained in the medial medullary depressor region of Wang and Ranson (1939). Electrical stimulation of this area elicits either decreases or increases in blood pressure and SND (Adair et al., 1977; Morrison and Gebber, 1982; McCall and Humphrey, 1985). Lesion of the medial medulla including the medullary raphe nuclei increases SND (Barman and Gebber, 1978). By using spike-triggered averaging Morrison and Gebber (1982; 1984; 1985) showed that some neurons in the medullary raphe nuclei have spontaneous activity temporally related to SND. The majority (75%) of these neurons are sympathoinhibitory with the rest being sympathoexcitatory. As with the VLM sympathetic neurons, the axons of some raphe neurons with activity related to SND also project to the thoracic spinal cord, however, only sympathoinhibitory raphe neurons terminate in the PAL.

Gebber and Barman (1985) compared the firing times of neurons in the LTF, VLM and raphe nuclei relative to the peak of the first slow wave to the right of time zero in the spike-triggered averages of SND. The rationale behind this comparison is that the neurons which are closer to the origin of SND should fire earlier in the sympathetic cycle. That is, the interval between unit spike occurrence and the peak of SND in the spike-triggered averages should be longer for these neurons. Gebber and Barman found that sympathoexcitatory neurons in the LTF fire on the average, 35 and 43 ms before their counterparts in the VLM and raphe, respectively. Interestingly, the modal onset latency of

synaptic activation of sympathoexcitatory VLM neurons to electrical stimulation of the LTF (26±3 ms) is very similar to the difference in the mean firing times between LTF and VLM sympathoexcitatory neurons (Barman and Gebber, 1987). A comparison of sympathoinhibitory neurons showed that LTF neurons fire before their counterparts in the raphe. A direct connection between these two regions has yet to be demonstrated. Based on these findings it is concluded that the sympathetic neurons in the LTF are closer to the origin of SND. Whether the LTF neurons comprise a sympathetic oscillator which outputs through the VLM and raphe remains to be determined. Alternatively the LTF may receive input from some as of yet undefined generator of SND located in the brain stem or the forebrain.

B. Thalamic mechanisms for the generation of electrocortical rhythms

Under a variety of experimental and behavioral conditions the electrical activity in the cerebral cortex is rhythmic in nature (EEG, electroencephalogram). It is widely accepted that much of this cortical activity originates in the thalamus (cf. Dempsey and Morison, 1942b). A number of mechanisms by which these cortical rhythms are generated have been proposed.

1. Early models of thalamic generation of EEG rhythms

Dusser de Barenne and McCollock (1938a, 1938b) used the local application of strychnine to the cortex and thalamus to demonstrate the functional reciprocity between the thalamic relay nuclei and that portion of the cerebral cortex to which they project. Undercutting of the projection cortex abolishes or greatly alters the normal pattern of EEG activity. On this basis, it is proposed that the reverberating activity in thalamocortical-thalamic circuits is the source of normal EEG activity.

An alternative model of cortical rhythm generation was proposed by Morison and Dempsey in the early 1940's (Dempsey and Morison, 1942a,b;

Morison and Dempsey, 1942). These authors showed that stimulation of the thalamus elicits two types of cortical responses. Stimulation of sensory relay thalamic nuclei elicits a "primary" or augmenting response in their projection cortices. These responses with onset latencies of less than 4 ms are characterized as a positive/negative wave form capable of following stimulus frequencies up to 120 Hz. Stimulation of the nonspecific medial thalamic nuclei at frequencies of 2- to 15-Hz evokes the recruiting response in wide regions of the cortex. The recruiting response has a long onset latency (20-35 ms) and is characterized by a monophasic surface negative waveform which waxes and wanes in amplitude with successive stimuli. The recruiting responses closely resemble, in both contour and frequency (8-12 Hz), the spontaneous bursts of cortical spindle activity (alpha spindles) seen in barbiturate-anesthetized or sleeping animals. The recruiting response and spontaneous cortical spindles are recorded in cortical areas isolated except for their thalamic connections indicating that the generalized nature of the recruiting response reflects the activity of a widely distributed system and is not the result of the intracortical spread of activity from discrete cortical regions. Based on the similarities, it is concluded that the spontaneous spindle burst and recruiting responses are identical. Dempsey and Morison concluded that the spontaneous cortical alpha rhythm is generated in the medial thalamus and transmitted to wide spread cortical areas via a diffuse thalamic projection system separate from that relaying sensory information to the the cortex. mechanism is proposed in spite of the fact that at this time cortical projections from many of the medial thalamic nuclei have not been demonstrated.

In a series of papers in the early 1950's, Jasper and colleagues modified the original hypothesis of Morison and Dempsey (cf. Andersen and Andersson, 1968). These authors believed that the midline and intralaminar thalamic nuclei in conjunction with n. reticularis thalami and n. ventralis anterior

constitute a rostral extension of the generalized reticular activating system proposed by Magoun and Ranson in 1949. They proposed that the pacemaker activity of the medial thalamic nuclei is relayed to the cortex via n. reticularis and n. ventrais anterior where this activity "acts upon the cortex, controlling the form and rhythm of the background of cortical activity upon which afferent impulses must act, and regulating the generalized excitatory states of the cortex as a whole" (Jasper, 1949). This theory had to be discounted when it became clear that the n. reticularis does not project to the cortex (Scheibel and Scheibel, 1966; Jones, 1985).

2. Mechanisms for the generation of alpha spindle activity

Purpura and coworkers (Purpura and Cohen, 1962; Purpura and Shofer, 1963; Purpura et al., 1965) proposed that the nonspecific medial thalamic nuclei are the major source of synchronizing input to the thalamus. These authors examined the synaptic events occurring in thalamic neurons during the recruiting response elicited by stimulation of the nonspecific medial thalamic nuclei. Intracellular recordings from thalamic neurons during the recruiting response revealed that the synchronization of neuronal firing is produced by a recurring sequence of a short-latency (4-15 ms) excitatory postsynaptic potential (EPSP), followed by a long-latency (15-40 ms), prolonged (80-200 ms) inhibitory postsynaptic potential (IPSP). The prolonged IPSP is thought to be the major feature of the synchronization process since neither spontaneous nor evoked neuronal discharges of the thalamocortical neuron occur during the IPSP. Rather, the discharges of thalamocortical neurons are restricted to the short periods between IPSPs. This EPSP-IPSP sequence is observed in over 70% of the neurons recorded in widely separated regions of the n. ventralis anterior, n. ventralis medialis, n. ventralis lateralis and from the intralaminar and midline thalamic nuclei. Thalamic focal potentials recorded during the recruiting response reveal long-latency (15-40 ms),

long-duration (40-80 ms) positive waves presumably reflecting the summation of EPSP-IPSP sequences throughout the thalamus. These positive thalamic waves are temporally related to the negative waves in the cortical recruiting response. Similar EPSP-IPSP sequences are recorded in cells in the ventrobasal complex during spontaneous alpha spindle activity in the sensory cortex (Maekawa and Purpura, 1967). High frequency (20 Hz) stimulation of the medial thalamic nuclei which blocks the recruiting response in the cortex also prevents the development of prolonged IPSPs in thalamic cells (Purpura and Shofer, 1963). Instead, an increase in neuronal discharge associated with a steady depolarization or no change in membrane potential is observed.

Like Purpura and coworkers, Andersen and Eccles (1962) observed that the rhythmic bursting discharge of thalamic neurons is associated with a recurring sequence of EPSPs and IPSPs. Andersen and Eccles also demonstrated that rhythmic burst discharges in thalamic relay cells occurs during stimulation of peripheral afferents or the antidromic activation of thalamocortical neurons, suggesting that the generation of rhythmic activity is an inherent property of all thalamic neurons. From these data Andersen and Eccles proposed the facultative pacemaker theory for the generation of rhythmic burst discharges in thalamic neurons. This model was later expanded upon by Andersen and Andersson in 1968. Briefly, this model proposes that the thalamocortical cells excited by afferent inputs emit excitatory recurrent axon collaterals onto local interneurons. The interneurons in turn inhibit the thalamocortical neuron. Furthermore, it is proposed that during the declining phase of the interneuron-induced inhibition, the thalamocortical neuron becomes hyperexcitable (post anodal exaltation) and discharges again, thus initiating a repeating cycle of excitation and inhibition. The post anodal exaltation is thought to be an intrinsic property of the membrane, thus endowing the neuron with pacemaker properties. The possibility that

excitatory interneurons help to trigger subsequent neuronal discharges and recruit other relay neurons is also proposed.

Andersen and Sears (1964) demonstrated that spindle bursts and 8- to 12-Hz focal waves can be recorded in midline and relay thalamic nuclei in acute and chronically decorticate cats. Spindle activity is also present in relay nuclei after section of all connections with the nonspecific medial thalamic nuclei. On this basis, it is concluded that all regions of the thalamus are inherently capable of generating rhythmic spindle activity via facultative pacemaker circuits. In contrast to Purpura and coworkers, the medial thalamic nuclei are not believed to be the major source of spindling activity in the thalamus, although these regions may exert control over these rhythms. Andersson and Manson (1971) later demonstrated that rhythmic activity occurring simultaneously from different thalamic regions in unanesthetized decorticate cats can be quite different. These data further suggest that the rhythmic activity in the cortex and thalamus is not generated by or in one specific thalamic region.

Although attractive, the faculatative pacemaker theory is seriously flawed. For example Purpura and colleagues pointed out that the long latency and duration of the IPSP in the thalamocortical cells is hard to reconcile on the basis of a simple feedback inhibitory synapse. These authors also pointed out that brief periods of stimulation (7 Hz) of the midline thalamic nuclei elicits EPSP-IPSP sequences in thalamic neurons and spindle waves in the cortex which persist (in the absence of neuronal spikes) following termination of the stimulus (Purpura et al., 1966). According to the facultative pacemaker model, the thalamocortical neuron must discharge in order to observe the IPSPs in thalamic neurons. Perhaps the strongest evidence against this model comes from anatomical studies of thalamic nuclei using the Golgi method. These studies failed to support the facultative pacemaker theory since only 15-20% of thalamocortical

neurons have recurrent axon collaterals (Scheibel et al., 1973). In Scheibel's words the small number of collaterals was deemed to be "an insignificant substrate for the powerful recursive effects ascribed to them."

 The thalamic reticular nucleus as a generator of thalamic spindle sequences

The n. reticularis thalami is a sheet-like structure encompassing the rostral and lateral borders of the thalamus. The structure and connections of this nucleus have been well characterized (see Scheibel and Scheibel, 1966; Steriade et al., 1984; Jones, 1985). The axons of most thalamocortical neurons emit collaterals in the n. reticularis in a topographical fashion. The axons of these thalamic reticular neurons project back to those thalamic regions from which the collateral input arises. Corticothalamic neurons also collateralize in the reticular nucleus; however, the reticular nucleus does not have cortical projections.

The early development of the hypothesis that the n. reticularis is involved in the generation of the 8- to 12-Hz spindle rhythms is reviewed by Steriade and Hobson (1976). On the basis of mostly anatomical data, the Scheibels proposed that the rhythmic bursting discharge of the thalamic relay cells is due to direct feedback inhibition from n. reticularis. Physiological evidence in support of this hypothesis was provided by Schlag and Waszak who showed that a reciprocal relationship exists between the burst discharges of n. reticularis and thalamocortical neurons. During episodes of EEG spindling or high amplitude cortical slow waves, the discharge rates of neurons in n. reticularis increase while those of thalamocortical neurons decrease. Moreover, the burst discharges of the reticularis neurons often spanned the spindle sequence and are thus thought to be responsible for the spindle-related hyperpolarization (IPSP) of the thalamocortical neurons. During EEG desynchronization elicited by stimulating the mesencephalic reticular formation, the discharge rates of neurons in n. reticularis decrease while

those of thalamocortical neurons increase. Additional support for this proposal comes from the work of Houser et al. (1980) who demonstrated that many of the projections from n. reticularis to thalamic relay nuclei are GABAergic.

Further evidence that the n. reticularis is involved in generating the alpha spindles is provided by the observation that neurons in the anterior thalamic nuclei (anterior ventral, anterior medial and anterior dorsal) which do not receive afferents from n. reticularis do not display spontaneous or evoked spindle-like discharges (Mulle et al., 1985). This is the case even though these neurons have intrinsic membrane properties similar to those of thalamic neurons displaying spindling activity. Furthermore, EEG recorded from the parasplenial projection cortex of these nuclei also fails to display spindle activity.

Although it is generally accepted that the n. reticularis is involved in generating the alpha rhythm, Steriade and colleagues (Steriade and Deschenes, 1984; Steriade et al., 1985; 1986; 1987) have questioned whether the regulation of activity in thalamocortical neurons is due solely to a direct feedback inhibition from n. reticularis. That a more complex mechanism is involved is suggested by Steriade et al. (1986) who recorded the activity of neurons in thalamic relay nuclei and n. reticularis during various sleep and awake states in cats. As in earlier studies, during EEG synchronization n. reticularis neurons fire in long bursts (increasing then decreasing interspike intervals) which often span the spindle sequence of the thalamocortical cells. In contrast, during arousal and awake states (EEG desynchronized) n. reticularis and thalamocortical neurons both cease spindling and significantly increase their firing rates in parallel. Such parallelism is not consistent with a direct inhibitory action of reticularis neurons on thalamocortical neurons.

To account for the state-dependent relationships between the activity of thalamocortical and n. reticularis neurons, Steriade and colleagues

(Steriade et al., 1985; 1986; 1987) proposed a model whereby n. reticularis controls the activity in thalamocortical circuits. Moreover, these authors propose that the n. reticularis functions as a pacemaker to generate alpha spindling. In this model, neurons in n. reticularis have direct GABAergic projections to thalamocortical neurons and to GABAergic interneurons located near the thalamocortical neurons. These inhibitory interneurons in turn contact the thalamocortical neurons. The presence of GABAergic interneurons was reported by Montero and Singer (1985). A central feature of this model is the notion that the projections from n. reticularis exert differential inhibitory effects on the thalamocortical and GABAergic interneurons, with the more powerful inhibitory effects being exerted on the interneurons. Thus state-dependent changes in the amount of GABA released by the n. reticularis neurons changes the activity pattern in thalamocortical circuits by changing the ratio of inhibition of the interneurons and thalamocortical neurons. For example during EEG-desynchronization, the n. reticularis cells cease bursting and fire tonically as single spikes at an increased rate. The GABA released by the n. reticularis neurons inhibits the more sensitive interneurons. As a consequence, the thalamocortical neurons become more excitable due to the disinhibition and fire at a higher frequency. This proposal is supported by the observation that reticularis-disconnected thalamocortical neurons have a lower average firing rate than do their counterparts in reticularis-intact cats during EEG-desynchronization. Conversely, during EEGsynchronized states, the n. reticularis neurons begin to discharge in prolonged bursts. During these bursts the intraburst frequencies are higher than the fastest tonic discharge rates occurring during desynchronized states and as a consequence, more GABA is released. The increased in GABA release via direct reticularis inputs is now sufficient to hyperpolarize the thalamocortical neurons. The hyperpolarization of the thalamocortical neuron triggers the deinactivation of

a calcium (Ca⁺⁺) conductance, eventually leading to the spindle burst discharge of the neuron. At the same time an overabundance of GABA released by the bursting n. reticularis neuron saturates the more GABA-sensitive interneurons, completely inhibiting their firing.

Evidence in support of this model is presented by Steriade et al. (1985) who examined the discharges of thalamocortical neurons after removing inputs from the n. reticularis by using either knife cuts or kainic acid lesions. Removing inputs from the n. reticularis abolished spindle-related rhythms (sequences of 7-12 Hz waves recurring at 0.1-0.2 Hz) in the thalamus and ipsilateral EEG. In addition, n. reticularis-disconnected thalamocortical neurons no longer display spindle-related sequences of prolonged IPSPs. Instead short duration IPSPs are recorded. Thalamocortical cells exhibit high frequency spike bursts whose parameters (number of spikes, intraburst frequency, duration of consecutive intervals) are the same as those in relay and intralaminar cells having intact reticularis connections. However, the characteristic pattern of spindle-related sequences of spike bursts and irregularly occurring single-spike discharges during non-spindling periods is replaced by solitary bursts occurring with remarkable regularity at 1- to 2-Hz. This regular 1- to 2-Hz burst pattern is thought to be mediated by the GABAergic interneurons which are disinhibited by removing inputs from n. reticularis. The increased activity in the interneurons produces a series of short duration IPSPs in the thalamocortical neurons. The rapidly occurring IPSPs summate and hyperpolarize the thalamocortical neuron deinactivating a low threshold, long duration Ca++ conductance whose activation leads to the burst response. This conclusion is based on the finding that a subconvulsive dose of bicuculline administered intravenously changes the discharge pattern of reticularis-disconnected thalamocortical neurons from rhythmic bursting to irregularly occurring single spikes.

Evidence that the n. reticularis functions as a pacemaker in the generation of spindle rhythmicity during EEG-synchronization is provided by Steriade et al. (1987). In this study extracellular recordings of unit discharges and focal potentials were made in the rostral pole of n. reticularis after surgically disconnecting it from all other thalamic nuclei. As previously discussed disconnection of n. reticularis abolishes spindle activity in the ipsilateral cortex and thalamic nuclei (Steriade et al., 1986). However, neurons in the disconnected n. reticularis discharge in the biphasic (acceleration-deceleration) pattern of spike bursts characteristic of neurons in the intact n. reticularis during EEG synchronization. The spike bursts were of long duration (50 ms-1.5 s) and recurred with a frequency of 0.1- to 0.3-Hz. Simultaneous recordings of focal potentials through the recording microelectrode reveal spindle sequences (grouped 7-16 Hz slow waves recurring at 0.1-0.3 Hz) temporally related to the spike bursts of the n. reticularis neurons. The authors suggest that the synchronization of the burst discharge of the reticularis neurons involves dendrodendritic interactions between the GABAergic reticularis neurons. The presence of dendrodendritic connections between reticularis neurons has been demonstrated with the electron microscope (Deschenes et al., 1985). In addition, the intravenous administration of bicuculline greatly reduces spike bursts in the deafferentated n. reticularis.

4. Origin of the cortical delta and theta rhythms

Although it is fairly well established that the cortical alpharhythm (8-12 Hz) is generated in the thalamus there is some controversy as to whether the slower delta and theta rhythms in the EEG are generated in the thalamus.

Villablanca (1974) examined sleep and behavioral patterns in chronic athalamic and decorticate cats. During the first 10 days after removing the thalamus, irregular high voltage slow waves occurring at frequencies of 2- to

4-Hz dominate the EEG. Initially, the synchronized EEG pattern is unchanged during behavioral arousal, however, after 15 to 25 days, periods of desynchronized-like EEG activity accompany arousal. At no time after thalamic ablation are 8- to 12-Hz alpha spindles observed in the EEG, nor can they be induced by administering pentothal. In acute (3-5 days postoperative) decorticate cats, rhythmic 8- to 12-Hz waves which wax and wane in amplitude are recorded in the electrothalamogram (EThG). After six postoperative days, the spindle-like rhythms diminish. During waking irregular, low voltage waves occurring at frequencies of over 10 Hz are recorded in the EThG. During nonREM sleep the irregular waves in the EThG increase in voltage and became slower (2- to 6-Hz). Thus it was suggested that the thalamus is capable of generating at least some of the slow wave activity in the EEG.

Steriade et al. (1987) confirmed Villablanca's (1974) observation that slow wave activity in the EEG persists after removing thalamic influences. Knife cuts of the corona radiata, which severed corticothalamic connections, abolish cortical spindle bursts; however, synchronous 0.5- to 4-Hz slow waves persist in the EEG.

Andersson and Manson (1971) identified three patterns of synchronized thalamic slow wave activity in acute unanesthetized decorticate and decerebrate cats. The first pattern of activity recorded primarily from the ventrobasal complex, is characterized by 10- to 14-Hz spindles. The second pattern is characterized by long lasting irregular slow waves occurring at a frequency of 4- to 8-Hz. This pattern of activity is recorded primarily in the dorsolateral thalamus. The third pattern is most often recorded from the medial thalamic nuclei and consists of 8- to 12-Hz spindle bursts separated by periods of slower frequency (4- to 6-Hz) slow waves. These findings indicate that the

thalamus is capable of generating spindles as well as synchronized slow wave activity.

Jahnsen and Llinas (1984), by using a guinea-pig thalamic slice preparation, demonstrated that most thalamic neurons are endowed with intrinsic membrane properties which allow them to oscillate at frequencies of 9- to 10-Hz or 5- to 6-Hz. Thus each thalamic neuron is capable of operating as a single cell oscillator. The central feature of the proposed mechanism for the 5- to 6-Hz rhythmic discharge is the prolonged afterhyperpolarization following the spike burst. Increasing the level of hyperpolarization by synaptically generated IPSPs or by current injection de-inactivates a transient potassium (K⁺) current and a Ca⁺⁺-dependent K⁺ conductance, thus increasing the duration of the afterhyperpolarization. This in turn de-inactivates a low threshold Ca⁺⁺ conductance triggering a rebound low threshold spike burst which begins the cycle again. The time course (170 ms) of these events is responsible for the 5- to 6-Hz frequency oscillations.

METHODS AND PROCEDURES

A. General Procedures

Cats of either sex, weighing between 2.0 and 4.5 kg were used in these studies. The animals were initially anesthetized with ketamine hydrochloride (10 mg/kg, im) followed by intravenous alpha-chloralose (40 mg/kg, initial dose). The animals were paralyzed with gallamine triethiodide (4 mg/kg, iv) and artificially ventilated. The rate (12-20 strokes/min) and stroke volume (50-75 ml/stroke) of the respirator (Harvard model 607) were adjusted to mimic natural respiration. A bilateral pneumothoracotomy reduced respirator pump-related movements. Supplemental doses of chloralose and neuromuscular blocking agent were administered as required. Rectal temperature was maintained at 37+1°C by using a heat lamp. Blood pressure was monitored from either the femoral or brachial artery with a Statham transducer (Model P23AC) and displayed on a Grass polygraph (model 7D). Standard techniques were used to record lead II of the electrocardiogram (ECG). Drugs were administered through a cannula inserted in the femoral vein. In approximately 60% of the experiments, a solution of dextran (6% in saline) and norepinephrine (20 µg/ml) was infused through a femoral vein cannula to maintain mean arterial blood pressure at or above 100 mmHg. The cats were placed in a David Kopf Instruments stereotaxic apparatus and spinal investigation unit.

1. Baroreceptor denervation

In some experiments the baroreceptor nerves (carotid sinus, aortic depressor and cervical vagus nerves) were sectioned bilaterally. These nerves

were isolated from a ventral approach after reflecting the trachea and esophagus. The carotid sinus nerve was identified on both sides at its junction with the hypoglossal nerve. The cervical, vagus and aortic depressor nerves were isolated at a midcervical level. Denervation was deemed complete if 1) a sudden rise in blood pressure failed to inhibit reflexly inferior cardiac SND and 2) sympathetic slow wave activity was no longer locked in a 1:1 fashion to the cardiac cycle.

2. Nerve recordings

The left postganglionic inferior cardiac sympathetic nerve was isolated retropleurally at its exit from the stellate ganglion after removing the head of the first rib. The nerve was tied distal to the ganglion with saline-soaked silk thread. A loop was then tied in the thread and the nerve cut distal to the tie. Nerve activity was recorded monophasically after placing the silk loop on the indifferent pole and the proximal portion of the nerve on the central pole of a bipolar platinum electrode. To prevent drying, the nerve and ganglion were covered with an emulsion of silicone release agent (Dow Corning 7 Compound) and paraffin oil (Fischer Scientific Co.).

The left postganglionic renal sympathetic nerve was isolated retroperitoneally through an incision in the left flank. One of the branches was tied
with saline-soaked silk thread and cut between the tie and the nerve's junction
with the renal artery. A loop was then tied in the thread. Monophasic recordings
were made as just described. The abdominal skin flaps were secured to a frame in
order to form a pool which was filled with warm paraffin oil to cover the nerve.

Nerve activity was amplified by using a capacity-coupled preamplifier at a band pass of 1 to 1,000 Hz. This allowed the synchronous discharges of the sympathetic nerves to be viewed as slow waves (i.e. envelopes of spikes) on the polygraph and oscilloscope (see RESULTS; Figure 11).

Electrical cortical activity (electroencephalogram, EEG) was recorded monophasically between a gold plated electrode (Grass Instruments, Model E4G) affixed to the frontal bone and a indifferent electrode (an alligator clip) attached to reflected scalp muscle. Cortical activity was preamplified using a band pass of 1 to 1,000 Hz and displayed on a polygraph and oscilloscope.

3. Electrical stimulation of the diencephalon and cortex

Square wave pulses (10-ms trains of three pulses or single shocks) were delivered to selected sites in the diencephalon and frontal-parietal cortex by using a Grass S88 stimulator connected to a Grass PSIU-6 constant current unit. Stimuli were passed through either concentric bipolar electrodes, 0.25 mm exposed tip (Rhodes Medical Instruments, Model NE-100) or etched monopolar tungsten microelectrodes (10-30 kilo ohm tip impedance). In the latter case, the anode (an alligator clip) was attached to reflected scalp muscle. Stimulus current was measured by monitoring the voltage drop across a 100 ohm resistor in series with the anode. Potentials evoked on sympathetic nerves by stimulation of the diencephalon and cortex were computer averaged (Nicolet, Model 1070; see section B.4), displayed on an oscilloscope and photographed.

4. Histology

The diencephalon and in some cases the brain stem were removed and placed in 10% buffered formalin for a period of at least 7 days. In decerebration studies the completeness and level of midbrain transection was verified by gross inspection of the brain stem and microscopic evaluation of frontal sections of 30- µm thickness stained with cresyl violet. Transection at stereotaxic plane A3 was at a level approximately midway between the rostral and caudal borders of the superior colliculus. Transection at stereotaxic plane A0 was near the midcollicular level. Only those experiments in which the transections were complete and the planes of transection were within +0.5 mm of the A3 and APO planes of Jasper

and Ajmone-Marsan (1954) are included in the RESULTS. To identify unit (or multiunit) recording sites and stimulation sties, frontal sections (30-µm thickness) of the diencephalon were cut on a cryostat microtome and stained with cresyl violet. Diencephalic lesions were reconstructed by projecting serially arranged frontal sections onto the stereotaxic planes of Jasper and Ajmone-Marsan (1954). Sites of stimulation and unit recording in the diencephalon were also reconstructed from stained frontal sections. Since I recorded the depth of all stimulation and recording sites for each electrode penetration, these sites were reconstructed using the end of the tracks as reference points. Shrinkage during fixing was taken into account.

B. Data Analysis

Data were analyzed either on- or off-line. On-line analysis used a Nicolet MED-80 computer. Off-line analysis from magnetic tape was performed by using either a Nicolet MED-80 computer or an RC Electronics Computerscope System. For this purpose arterial pressure, neural activity and pulses derived from the R wave of the ECG or stimuli applied to the neuraxis were stored on magnetic tape. The data from tape were analyzed after passing SND, EEG and diencephalic multiunit activity through an A.P. Circuit Corp. variable filter with the low pass cut-off frequency set at 50 Hz. The following methods of analysis were used.

1. Quantification of SND and blood pressure

In Projects A and D, after preamplification the sympathetic nerve signal was led to a Grass 7P10 cumulative integrator. Raw and integrated SND were displayed on a polygraph (see RESULTS; Figure 4). Changes in integrated SND were quantified by comparing mean epoch length (integrated records). Corrections were made for the integration of noise. The noise level was measured following ganglionic blockade with hexamethonium chloride (5 mg/kg, iv). Mean

blood pressure was calculated from pulsatile records of blood pressure recorded on the polygraph. The mean blood pressure (BP) was calculated using the formula:

$$BP = Pd + 1/3 (Ps - Pd)$$

where Pd is the diastolic pressure and Ps is the systolic pressure.

2. Crosscorrelation and autocorrelation analysis

Autocorrelation was used to extract the rhythmic components in inferior cardiac SND, EEG, and thalamic and hypothalamic multiunit activity. Forty seconds of data were analyzed. Crosscorrelation analysis was used to determine whether SND, multiunit diencephalic activity and the EEG contained common components that were temporally correlated. Normalized crosscorrelation functions [Rxy(T)] N were calculated by using the formula:

$$[Rxy(T)]N = \frac{Rxy(T)}{\{Rxx(O)Ryy(O)\}}$$
 {} = square root

where Rxy(T) is the nonnormalized crosscorrelation function in watts (voltage squared); x and y are the input signals; T is the lag in the crosscorrelation function; Rxx(0) and Ryy(0) are values (in watts) at zero lag in the nonnormalized autocorrelograms. The resolution was 20 ms and 10 ms for the crosscorrelation and autocorrelation analysis.

3. Post-R wave interval analysis

Trigger pulses coincident with the R wave of the ECG were used to construct normalized averages (minimum of 500 trials) of the arterial pulse wave, inferior cardiac SND, EEG and diencephalic multiunit activity. Post-R wave interval histograms of unit discharge were also constructed. These analyses revealed whether SND, EEG, multiunit diencephalic activity and diencephalic unit discharges were temporally related to the cardiac cycle.

4. Post-stimulus analysis

Trigger pulses coincident with stimuli delivered through metal electrodes in the diencephalon or cortex were used to construct normalized averages of evoked responses in the inferior cardiac nerve and histograms of unit responses. From these averages the modal onset latency of synaptic activation or inhibition of the neuron and onset latency and time to peak of the evoked sympathetic nerve response were calculated.

5. Power spectral density analysis

This analysis, performed by fast Fourier transform (Bendat and Piersol, 1971), was used to examine the frequency components and relative power (in watts) of each frequency band in SND, EEG and diencephalic activity. Power is plotted against frequency. Aliasing of high frequency components into the 0- to 15-Hz frequency bands was prevented by filtering the signals (15 Hz low pass cutoff) prior to analysis. Spectra were constructed by averaging six 20-s data blocks. The resolution of the analysis was 0.1 Hz.

6. Peri-spike-trigger averaging

Normalized averages (minimum of 500 trials) of SND and EEG activity were acquired before and after the spike trigger (a naturally occurring unit spike). For this purpose, the unit discharge was passed through a window discriminator. A standardized pulse coincident with unit spike occurrence was used to trigger computer sweeps. The portion of the average to the left of time zero was computed from data that preceded the spike trigger, while the second half (right 0 lag) represents data that followed the spike. Thus it was possible to determine whether the activity of the neuron was temporally related to changes in SND or EEG which preceded or followed its discharge. A random pulse train with about the same frequency as the neuronal spike train was used to trigger a "dummy" average of SND and EEG. Neurons were considered to have sympathetic nerve-

related and/or EEG-related activity if the amplitude of the first peak to the right of time zero in the spike-triggered averages of SND and EEG exceeded by at least a factor of three that of the largest deflection in the "dummy" averages.

7. Interspike interval analysis

This routine constructs a histogram of the distribution of the intervals between consecutive spontaneously occurring neuronal spikes. A minimum of 500 spikes are used. This method was used to calculate the mean frequency of discharge of the individual diencephalic units as well as to gain information on the periodic components in the spike train.

8. Statistical analysis

Data are expressed as mean \pm S.E. The Student's t-test was used to compare changes in mean blood pressure between lesioned and nonlesioned groups. Changes in mean SND between lesioned and nonlesioned groups were compared using the Students's t-test after transforming the data using arcsin square root transformation. A random block design analysis of variance (ANOVA) was used to analyze the effect of time on mean blood pressure after midbrain transection. The least significant difference test (LSD) was used for individual comparisons. Regression analysis was used to compare the intervals between the spontaneous unit spike to peak SND and stimulus to peak SND intervals in the spike-triggered averages of diencephalic neurons with activity related to SND. In all cases, a 95% confidence level was used as a criteria for significance.

C. <u>Project A: Experiments Involving Midbrain Transection and Radio-frequency Lesions</u>

1. Decerebration procedures

Following removal of the appropriate portions of the parietal bone and dura mater, serial transections at stereotaxic planes A3 and AP0 were made with spatulas constructed so that their diameters and contours corresponded with those

of the left and right halves of the midbrain. The spatulas were held in a stereotaxic electrode manipulator. Left and right hemisections were performed sequentially at each stereotaxic plane. The two-stage transection was completed within 90 s without excessive bleeding or subsequent swelling of the brain stem. The experiment was terminated on those rare occasions when transection caused excessive bleeding or swelling of the brain.

2. Radio-frequency diencephalic lesions

Diencephalic lesions were made bilaterally with a radio-frequency generator (Radionics Inc., Model RFG-4). An unmodulated sine wave (500 Hz) was passed through an electrode (0.7 mm tip diam; 1.5 mm uninsulated tip length) stereotaxically placed into the diencephalon. Current was adjusted to maintain the temperature of the tissue contacting the thermal sensing electrode tip at 75°C for 1 min. A lesion of 1-2 mm in diameter was produced at each site of current application.

3. Data analysis

Changes in SND and blood pressure were quantified as described in section B.1. The level of activity during the 5-min period before midbrain transection was compared with that during the first 2-min period, the following 3-min period and then during subsequent 5-min periods after midbrain transection. Either mean blood pressure or change in mean blood pressure was plotted at these specified intervals following midbrain transection.

4. Histology

The completeness and level of transection were verified and lesions reconstructed as described in section A.4.

D. Project B: Multiunit Diencephalic Activity

CNS-intact or decorticate cats with intact or sectioned baroreceptor nerves were used in this study. Portions of the parietal bone and underlying dura were removed bilaterally providing access to the diencephalon. The exposed neural tissue was covered with paraffin oil to prevent drying. In those instances in which decortication was performed, the skull was removed from the coronal suture to the lambdoidal suture in a rostral caudal direction and bilaterally as close to the squamosal suture as possible. Decortication was performed in two steps. First, a bilateral frontal lobotomy was performed 1 mm caudal to the ansate sulcus. Second, the cortex, hippocampus, corpus callosum and fornix surrounding the diencephalon and basal ganglia were removed by suction under visual observation with 6X magnification. The completeness of decortication was evaluated by gross inspection and subsequent examination of histological sections. In two cases there was damage to the anterior portions of the caudate and in all cases a small portion of the pyriform cortex remained connected to the diencephalon.

1. Multiunit diencephalic recordings

Multiunit activity in the thalamus and hypothalamus was recorded (capacity-coupled preamplifier band pass, 1 to 1,000 Hz) by using concentric bipolar stainless steel electrodes (Rhodes Medical Instruments, Model NE-100) with exposed leads (0.5 mm) separated by 0.5 mm. The electrodes were placed stereotaxically into the diencephalon according to the coordinates of Jasper and Amjone-Marsan (1954). The multiunit thalamic and hypothalamic activity was displayed on the polygraph and oscilloscope.

2. Electrical and chemical stimulation of the diencephalon

The diencephalon was electrically stimulated and sympathetic potentials averaged as described in section B.4. In a series of experiments, chemical stimulation was accomplished by microinjecting the GABA antagonist picrotoxin (5 µg in 0.5 µl saline) bilaterally over a 2 minute period into selected thalamic sites by using a 26 gauge needle attached to a 10 µl Hamilton syringe. The needle was placed stereotaxically according to the coordinates of Jasper and Amjone-Marsan (1954).

3. Data analysis

The following methods of computer analysis were used: 1) crosscorrelation and autocorrelation analysis. 2) Post-R wave interval averaging. 3) Power spectral density analysis. 4) Post-stimulus averaging. The methodology and application of these analyses are described in section B.

E. <u>Project C</u>: Characterization of Diencephalic Neurons with Sympathetic Nerve-related Activity

1. Diencephalic unit recordings

Metal microelectrodes (Frederick Haer, 2-µm tip diam, 2-3 mega ohm tip impedance, 0.5 mm exposed tip length) were used to record extracellularly the action potentials of thalamic and hypothalamic neurons from the left side of the diencephalon in baroreceptor-innervated cats. The indifferent electrode was a gold-plated disc affixed to the frontal bone. Capacity coupled preamplification with a band pass of 0.3-3 KHz was used. The position of the recording electrode was controlled by using a David Kopf Instruments stepping hydraulic microdrive. Stereotaxic placement of the electrodes was made according to the coordinates of Jasper and Ajmone-Marsan (1954). The unitary nature of the recordings was judged on the basis of the constancy of action potential shape, amplitude and duration. For units which discharged as high frequency bursts, the comparison was made for the first spike in successive bursts. The majority (60%) of unit recordings were from the soma-dendritic region of the neurons. This was indicated by the presence of an inflection on the rising phase of the action

potential (see RESULTS; Figure 22B2, C2). These inflections likely reflect separation of the action potentials of the axon hillock and the soma dendritic region (Coombs et al., 1957).

2. Electrical stimulation

A Grass S88 stimulator and a PSTU-6 stimulus isolation unit were used to deliver square wave pulses (90-800 µA, 1.0 ms duration) to selected recording sites in the thalamus and hypothalamus. Stimuli were passed through the recording microelectrode. The strength of the stimulus was measured as described in section A.3.

3. Effect of baroreceptor reflex activation

Baroreceptor reflex activation was produced by either the bolus injection of norepinephrine bitartrate (1-2 µg/kg, iv) or by inflating the balloon-tipped end of a catheter (Fogerty embolectomy catheter, Model 12 A-100-4F) placed into the abdominal agree via the femoral artery. The firing rate of selected thalamic and hypothalamic neurons was assessed during baroreceptor-induced reflex inhibition of SND. These procedures do not affect unit activity or SND in baroreceptor-denervated cats (Barman and Gebber, 1987).

4. Data analysis

The following methods of computer analysis were used: 1) Peri-spike-triggered averaging. 2) Interspike interval analysis. 3) Post-R wave interval analysis. 4) Post-stimulus averaging and histogram construction. 5) Autocorrelation analysis. The methodology and applications of these analyses are discussed in section B.

F. Project D: Sympathetic Responses Elicited by Cortical Stimulation

Experiments were performed on baroreceptor-intact and -denervated cats.

Baroreceptor denervation was performed as described in section A.1. In four

animals the meninges on the left cerebral hemisphere were deafferentated by sectioning the left trigeminal nerve at a point between the medulla and the sensory ganglion. The trigeminal nerve was exposed by removing portions of the occipital and basisphenoid bones and the tympanic bulla. EEG activity was recorded using either a plate electrode (as described in section A.3) or a wick electrode. Wick electrodes consisted of a small (2x6 mm) piece of cotton wrapped with silver wire. The electrode was then soaked in saline and placed directly on the cortical surface. The indifferent lead was an alligator clip placed on crushed scalp muscle.

1. Electrical stimulation of the cortex

The prefrontal and sensorimotor cortex was exposed bilaterally by removing the appropriate portions of the frontal and parietal bones and dura mater as described in section C.1. The exposed cortex was covered with warm paraffin oil. Electrical stimuli were applied to the cortex using procedures described in section A.3.

2. Diencephalic unit recordings

In some experiments the action potentials of medial thalamic neurons with sympathetic nerve-related activity were recorded. The responses of these neurons to cortical stimulation were recorded on magnetic tape for later off-line construction of post-stimulus histograms (see section B.4).

3. Data analysis

Computer-aided analyses and changes in blood pressure and inferior cardiac SND before and after lobotomy and A3 transection were quantified as described in sections B and C.3.

G. Drugs Used

The following drugs were used in this study. alpha-chloralose (Sigma), gallamine triethiodide (Lederle), hexamethonium chloride (Mann Research Laboratories), atenolol (Sigma) and picrotoxin (Sigma).

RESULTS

L Identification of diencephalic regions contributing to SND

Huang et al. (1987) reported that decerebration in the anesthetized cat produces transient (<30 min) decreases in inferior cardiac postganglionic SND (reduced to 62±7% of control) and blood pressure (33±4 mmHg). Three observations led Huang et al. to conclude that the transient effects of midbrain transection (i.e., decerebration) reflect the loss of a forebrain-dependent component of SND in the anesthetized cat rather than a nonspecific phenomenon such as generalized trauma or the mechanical stimulation of a descending sympathoinhibitory system. First, following recovery from the effects of decerebration, a second transection more caudally in the midbrain (APO) fails to affect SND and blood pressure. Second, crosscorrelation analysis revealed that a component of SND is synchronized to frontal-parietal cortical activity only in those experiments in which subsequent midbrain transection reduces SND > 30%. Third, the effects of the initial transection are prevented by prior removal of the hypothalamus and those medial thalamic nuclei located 0 to 4 mm lateral to the midline.

The diencephalic lesions made by Huang et al. were extensive. Thus, the purpose of my first set of experiments was to localize those regions of the hypothalamus and/or medial thalamus responsible for the forebrain-dependent component of SND. For this purpose, the effects of midbrain transection on SND and blood pressure in nonlesioned control cats were compared with those in cats in which selective diencephalic lesions were made with radio-frequency current.

Figure 1 shows examples of histological sections used to reconstruct the diencephalic lesions made in these experiments. The lesions in panels A, B, and C were
in the lateral hypothalamic region, the posterior hypothalamic region and the
medial thalamus, respectively.

A. Midbrain transection in nonlesioned cats

The effects of midbrain transection on inferior cardiac SND and mean blood pressure in 23 nonlesioned baroreceptor-denervated cats are summarized in Figure 2A and B, respectively. SND was reduced to 65±5% of control and mean blood pressure was reduced 35±3 mmHg in the first 2 min after midbrain transection at A3. These changes were statistically significant. There was a tendency for recovery toward control levels, however, in contrast to the results of Huang et al. (1987) SND and blood pressure were still significantly reduced at the end of the 30 min observation period.

In six of the 23 nonlesioned cats, renal as well as inferior cardiac SND were recorded. As shown in Figure 3, A3 midbrain transection produced parallel changes in renal and inferior cardiac SND. Figure 4 shows the polygraph records of raw and integrated SND and blood pressure from one of the six experiments in this series. The reductions in SND and blood pressure produced by A3 transection are shown in panel A. Subsequently, hexamethonium (5 mg/kg, iv) was used to produce ganglionic blockade (panel B).

B. Anterior medial hypothalamic lesions

Lesions placed in the anterior medial hypothalamus failed to attenuate significantly the decreases in inferior cardiac SND and blood pressure produced by midbrain transection (Figure 2). A3 transection was performed one hour after completion of the lesions. Mean blood pressure (111+4 mmHg) just prior to midbrain transection in these six experiments was not different from that (109+4 mmHg) in the 23 nonlesioned control cats.

Figure 1. Representative histological sections showing lesions of lateral hypothalamus (A), posterior hypothalamus (B) and medial thalamus (C). Each section is from a different cat. Calibration is 2 mm.

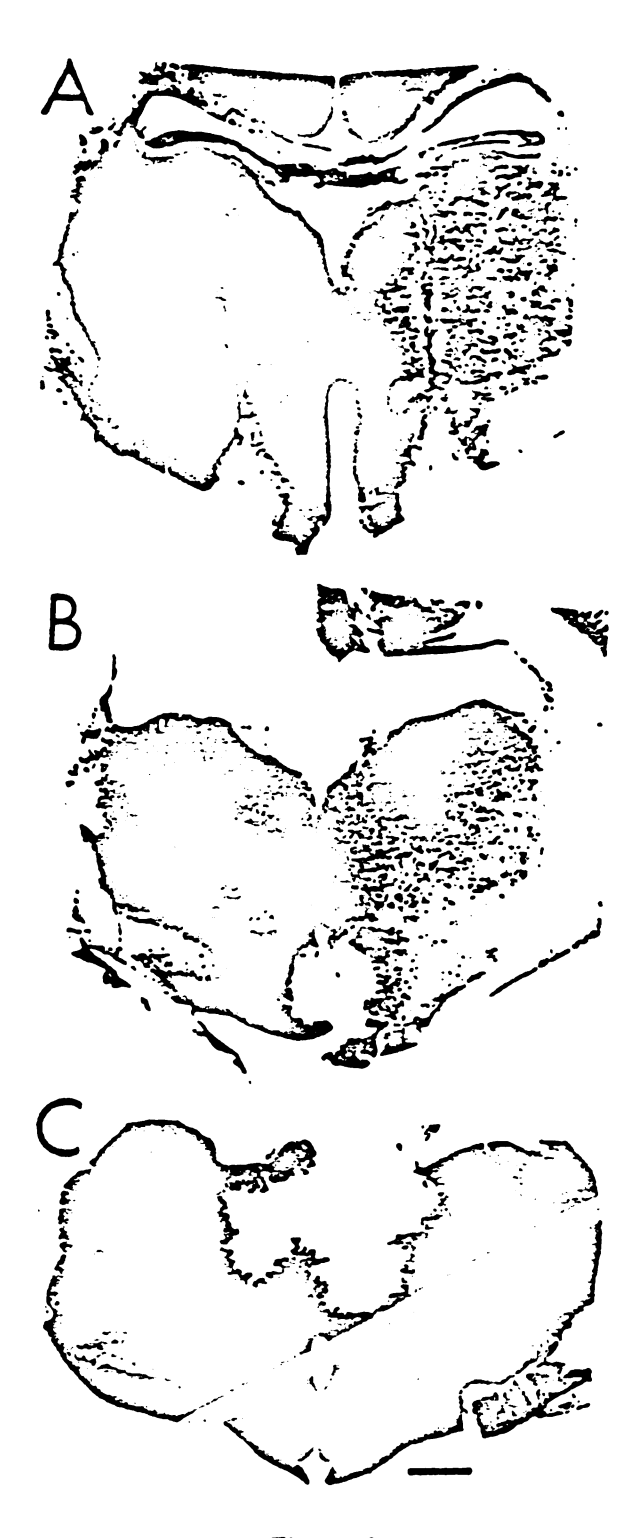


Figure 1

Figure 2. Comparison of effects of midbrain transection on inferior cardiac sympathetic nerve discharge (SND) and mean blood pressure (BP) in nonlesioned control cats (n=23) with those in cats with anterior medial hypothalamic (n=6) or large medial hypothalamic (n=7) lesions. All cats were baroreceptor-denervated and anesthetized with alphachloralose. Changes in SND (% of control) in panel A were quantified by comparing mean epoch length (integrated records) during 5-min period before transection with that during the first 2-min period, the following 3-min period, and then during subsequent 5-min periods after midbrain transection. Change in BP (mmHg) is shown. *Denotes a statistically significant difference from corresponding data point on control curve. Values are means ± SE.

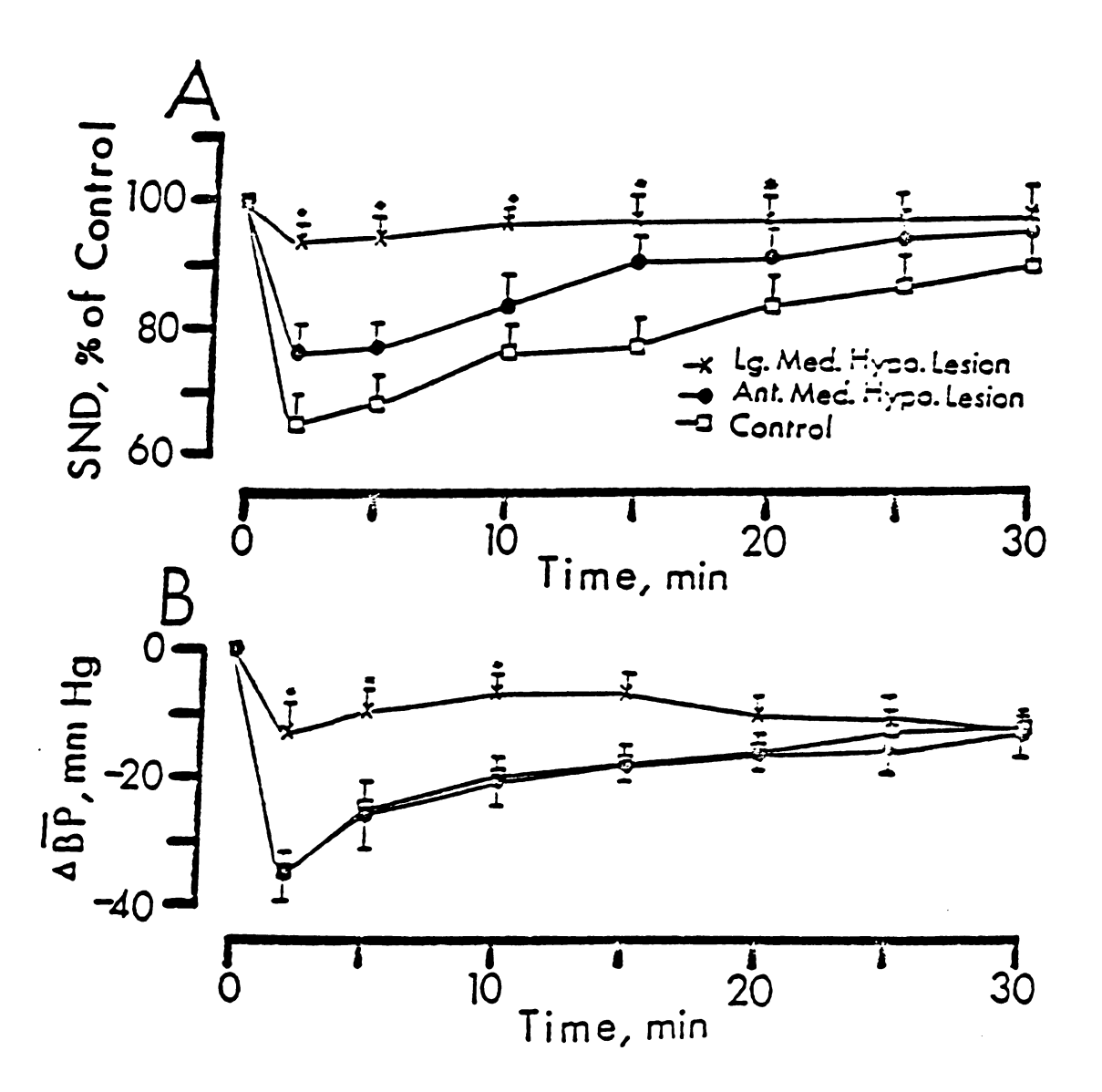


Figure 2

Figure 3. Effect of midbrain transection on inferior cardiac (ICN) and renal (RN) sympathetic nerve discharge (SND), and mean blood pressure (BP) in 6 nonlesioned baroreceptor-denervated cats anesthetized with chloralose. SND was quantified as described for Figure 2. BP (mmHg) is plotted against time after transection (panel B). Values are means + SE. *Denotes a statistically significant difference from pretransection level.

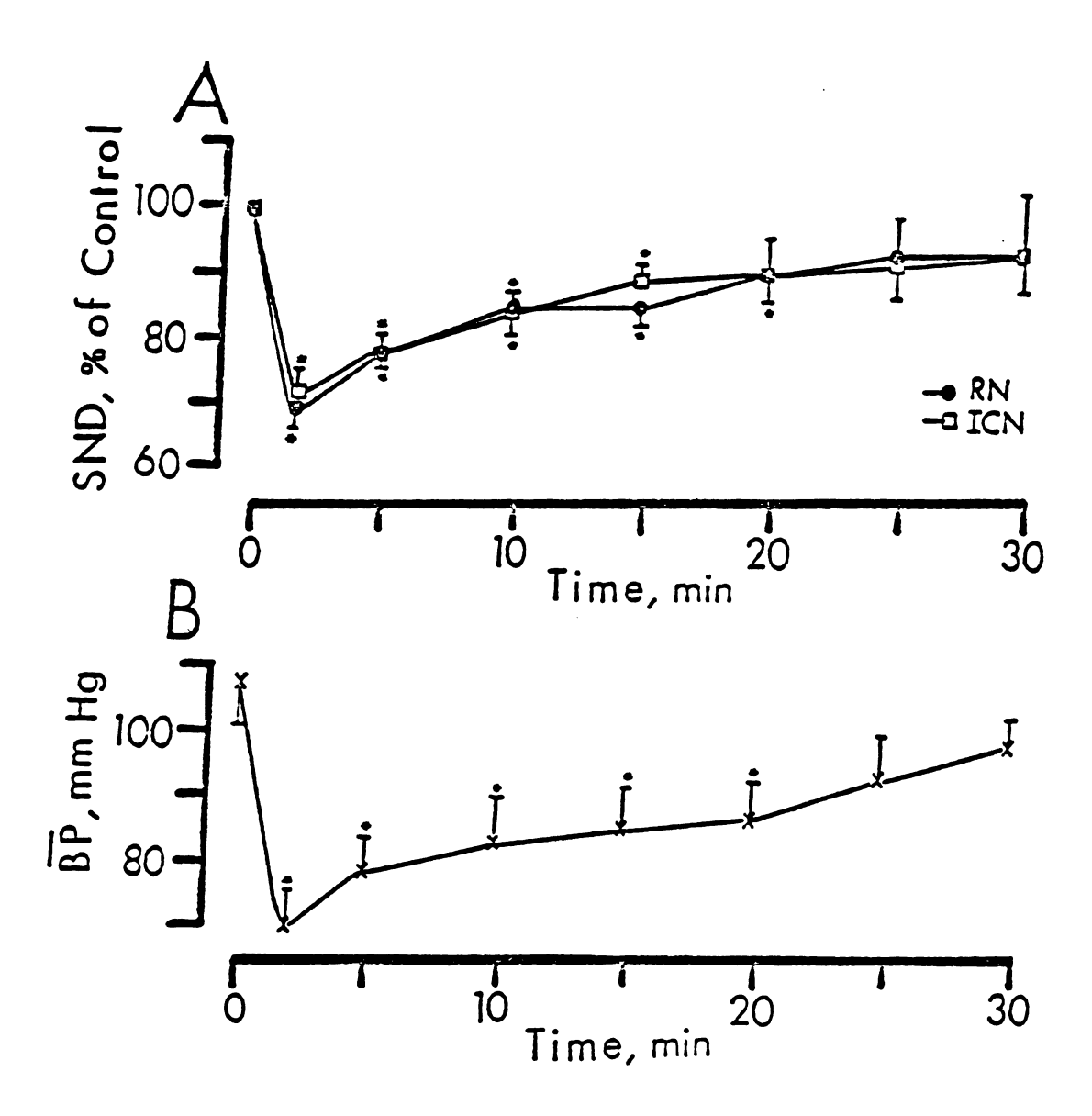
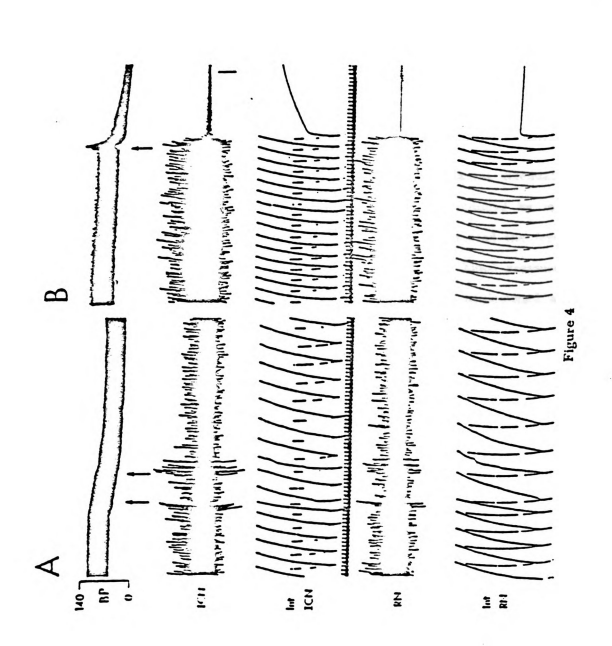


Figure 3

cat ancethetized with chloraloso. Raw and integrated records of sympathetic nervo activity are shown. Arrows in panel A mark left then right hemisection. Arrow in B marks injection of hexamethonium chloride (5 mg/kg, iv) 1 hr after midbrain transection. Vertical calibration is 75 µV for ICN and 125 µV for RN. Time base is 5 s per division. Figure 4. Effects of midbrain transection at stereotaxic plane A3 (A) and ganglionic blockade (B) on blood pressure (BP), inferior cardiac (ICN) and renal (RN) sympathetic nerve discharge in a nonlesioned baroreceptor-denervated



The extent of the anterior medial hypothalamic lesion shown in Figure 5 is typical for this series of experiments. This lesion destroyed most of the paraventricular hypothalamic nucleus (PVH) and n. filiformis (Fil), and a small portion of the dorsal hypothalamic area (aHd) between stereotaxic planes All and Al3. There was minimal involvement of the posterior hypothalamic (Hp) and anterior hypothalamic (Ha) nuclei. A small portion of the fornix (Fx) on the right side was destroyed in this particular experiment.

C. Large medial hypothalamic lesions

More extensive lesions of the medial hypothalamus attenuated the decreases in inferior cardiac SND and blood pressure produced by midbrain transection. Thus large medial hypothalamic lesions attenuated the forebrain-dependent component of SND. The reductions in SND and blood pressure were significantly smaller in these seven experiments than in nonlesioned animals during the first 20 min and 10 min, respectively, after midbrain transection (Figure 2). The absence of significant differences beyond 20 min reflects the rapid, although partial recovery of SND and blood pressure towards control levels following midbrain transection in nonlesioned cats. Mean blood pressure (107±5 mmHg) just prior to midbrain transection in this series of experiments was not different from that in nonlesioned cats. Thus, it appears that between 30 and 60 min were required for complete recovery from the loss of the forebrain-dependent component of SND produced by either midbrain transection or diencephalic lesions.

The extent of the large medial hypothalamic lesion shown in Figure 6 is typical for this series of experiments. In addition to PVH and Fil in the anterior medial hypothalamus, large portions of aHd, posterior hypothalamic (Hp) and the ventromedial hypothalamic (NHvm) nuclei were destroyed at more posterior

Stereotaxic planes and abbreviations (top) are as defined by Jasper and Ajmone-Marsan (1954). aHd, area hypothalamica dorsalis; AM, N. anterior medialis; AV, N. anterior ventralis; CC, corpus callosum; Cd. N. caudatus; CI, capsula interna; CL, N. centralis lateralis; En, N. entopeduncularis; Fil., N. filiformis; Fx, fornix; Ha, hypothalamus anterior; HL, hypothalamus lateralis; Hp, hypothalamus posterior; Hvm, hypothalamus ventromediaventromedialis; PVII, N. paraventricularis hypothalami; R, N. reticularis; RE, N. reuniens; Ru, N. rhomboldens; TO, tractus opticus; VA, N. ventralis anterior; VL, N. ventralis lateralis; VM, N. ventralis medialis; VPL, N. Figure 5. Representative lesion in anterior medial hypothalamus. Extent of lesion is shown in black on bottom lis; IAM, N. interanteriormedialis; MD, N. medialis dorsalis; MFB, medial forebrain bundle; NIIvm, N. hypothalami ventralis posterolateralis. Calibration is 2 mm. traces.

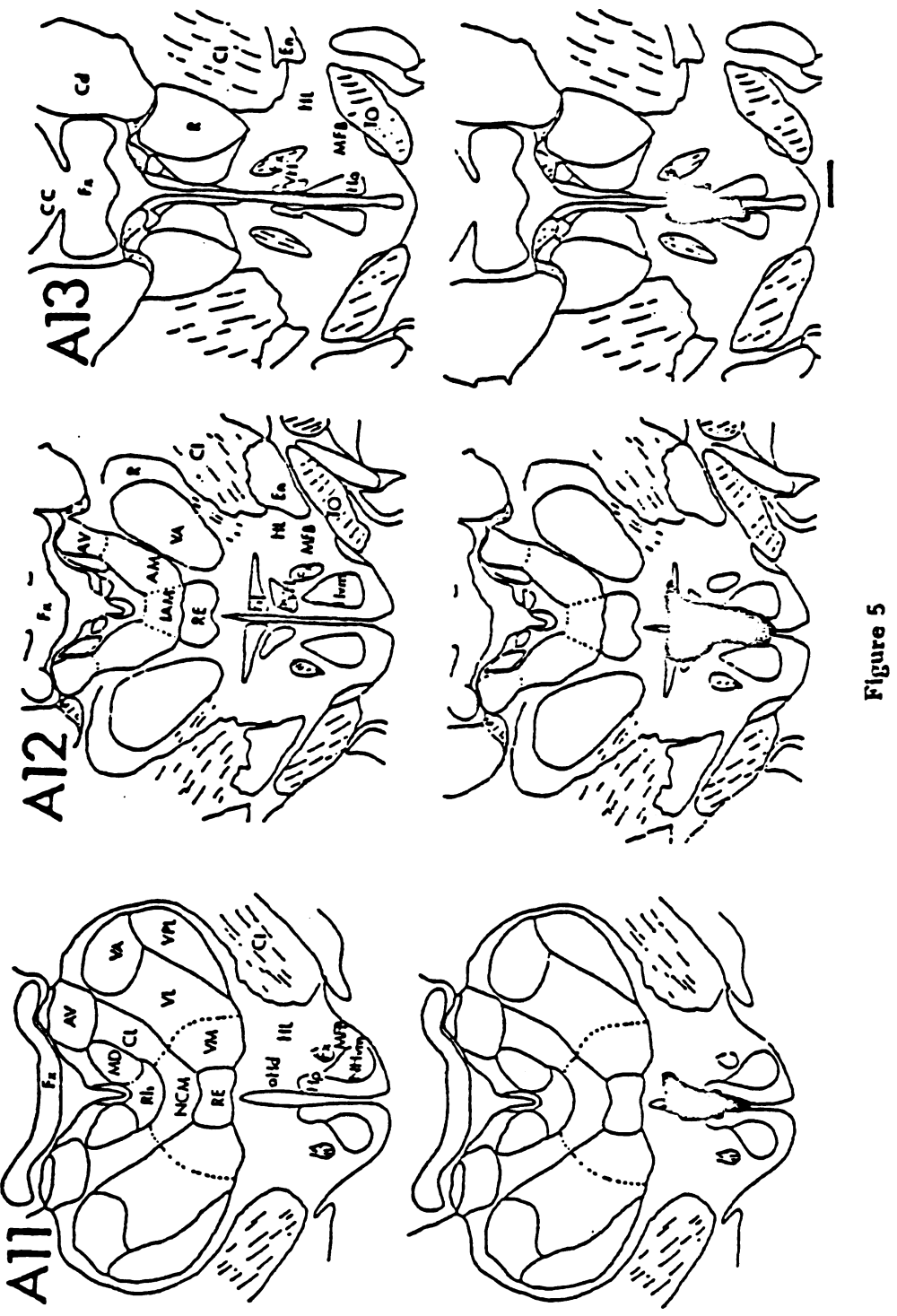


Figure 6. Representative large lesion in medial hypothalamus. Abbreviations are as in Figure 5 with the addition of H1, H2, Forel's fields; LD, N. lateralis dorsalls; LP, N. lateralis posterior; Mm, Corpus mammillare; NCM, N. centralis medialis, Pc paracentralis; Ped, Pedunculus cerebralis; VPM, N. ventralis posteromedialis; ZI, zona incerta. Calibration is 2 mm.

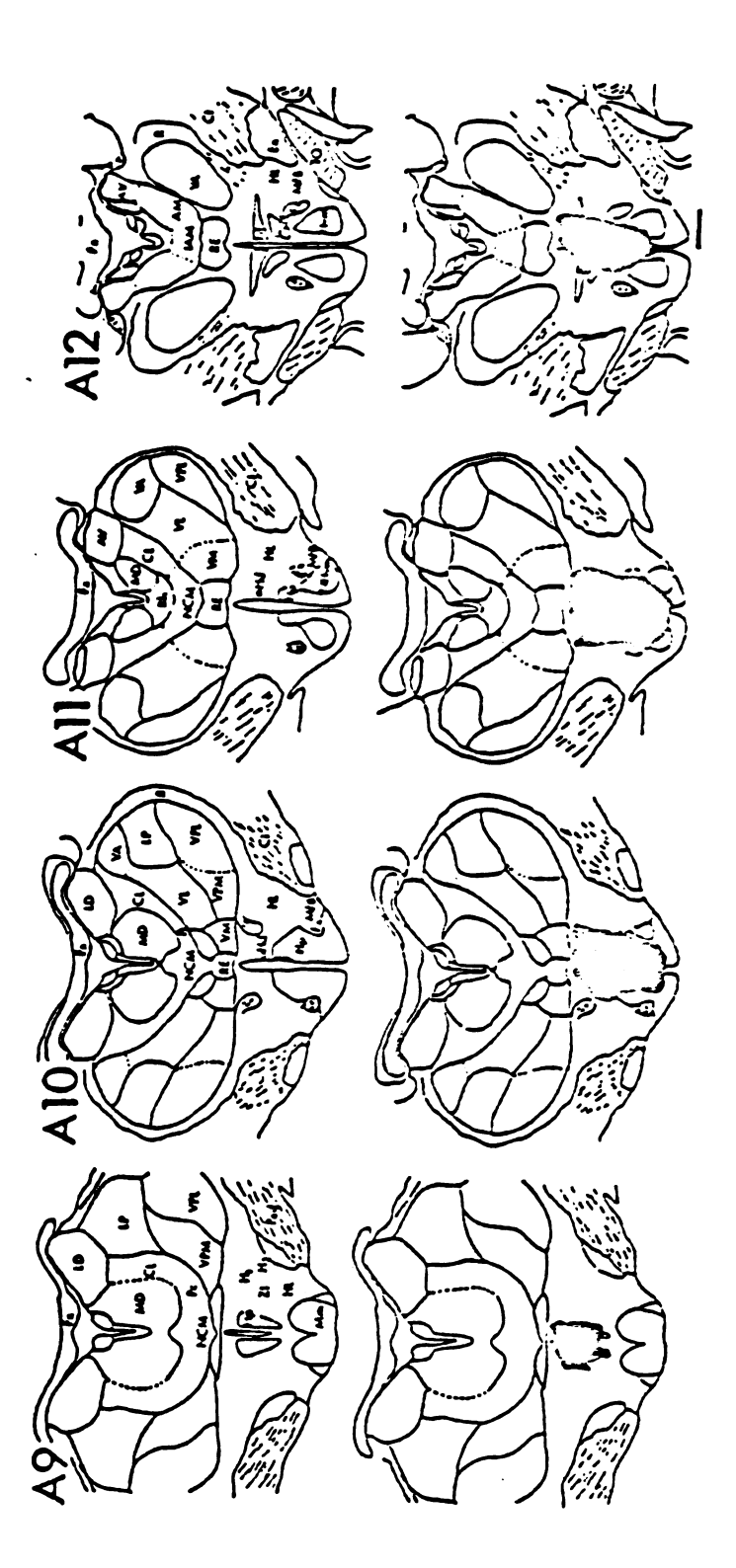


Figure 6

levels. Large medial hypothalamic lesions did not extend into the thalamus nor did they involve the medial forebrain bundle (MFB).

D. Lateral hypothalamic lesions

Lesions placed in the lateral hypothalamic region between stereotaxic planes A9 and A11 attenuated the decreases in inferior cardiac SND and blood pressure produced by midbrain transection. As shown in Figure 7, the reduction in SND was significantly less in these 12 experiments than in nonlesioned cats during the first 15 min after midbrain transection. The decreases in blood pressure were significantly different during the first 10 min after midbrain transection. Mean blood pressure (111±6 mmHg) just prior to midbrain transection in cats with lateral hypothalamic lesions was not different from that of nonlesioned cats.

The extent of the lateral hypothalamic lesion in Figure 8 is typical for this series of experiments. The lesion included portions of the lateral hypothalamic nucleus (HL), H1, H2, ZI and the MFB. The H1, H2 and ZI are considered as part of the hypothalamus rather than the subthalamus in this thesis.

E. Medial thalamic lesions

Lesions of the medial thalamus (0 to 3.5 mm lateral to the midline) between stereotaxic planes A7 and A11 also attenuated the decreases in inferior cardiac SND and blood pressure produced by midbrain transection. As shown in Figure 9, the reduction in SND was significantly less in these seven experiments than in nonlesioned animals during the first 15 min after midbrain transection. The decreases in blood pressure were significantly different only at 2 min after midbrain transection. Mean blood pressure (114+8 mmHg) just prior to midbrain transection in cats with medial thalamic lesions was not different from that in nonlesioned cats.

A typical medial thalamic lesion is shown in Figure 10. The lesion included most of the medial dorsal nucleus (MD), n. rhomboidens (Rh) and the

Figure 7. Comparison of effects of midbrain transection on inferior cardiac sympathetic nerve discharge (SND) and mean blood pressure (BP) in nonlesioned control cats (n=23) with those in cats with lateral hypothalamic lesions (n=12). Same format as in Figure 2. *Denotes a statistically significant difference from corresponding data point on control curve. Values are means + SE.

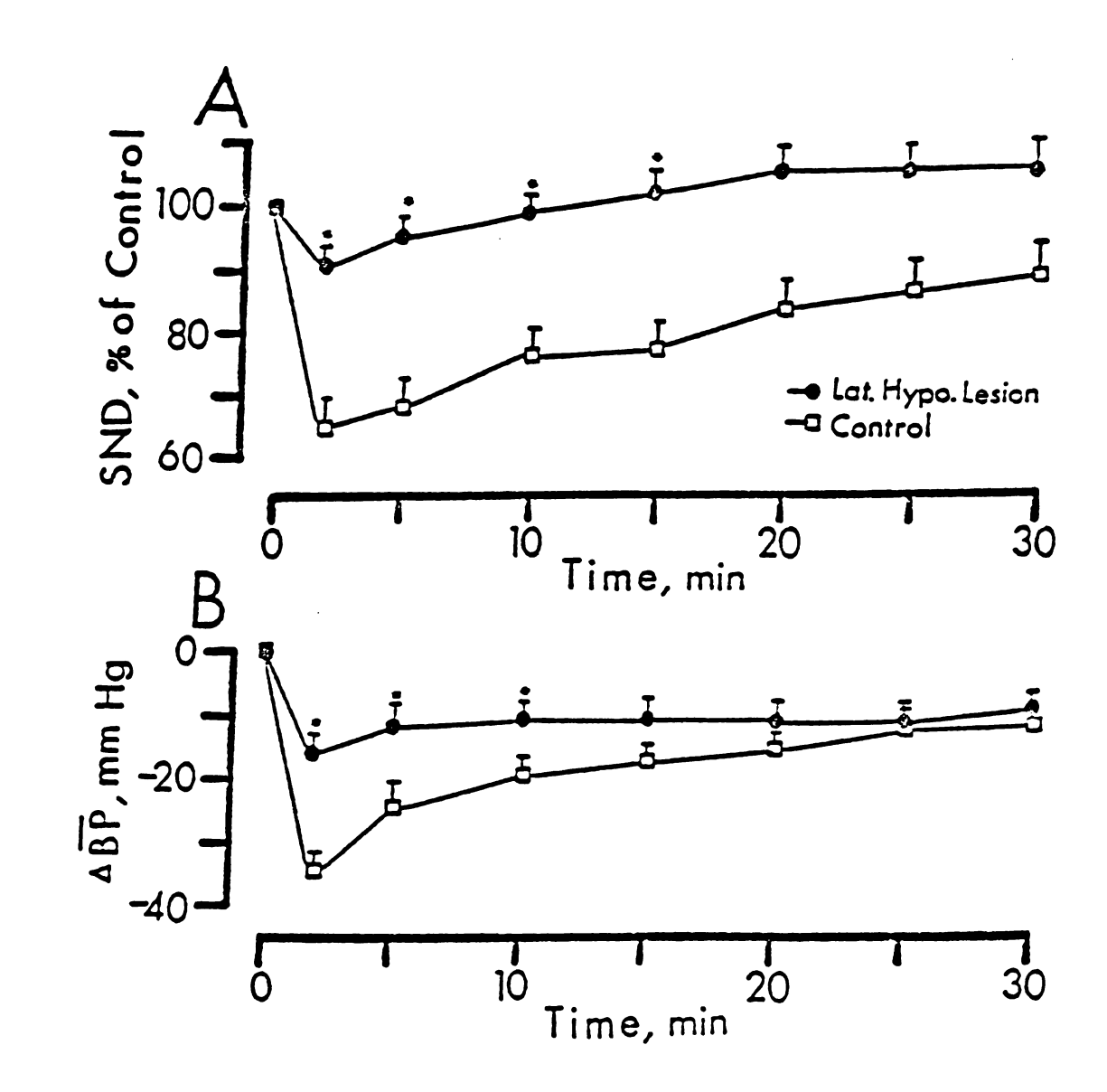


Figure 7

Figure 8. Representative lateral hypothalamic lesion. Abbreviations are as in Figures 5 and 6. Calibration is 2 mm.

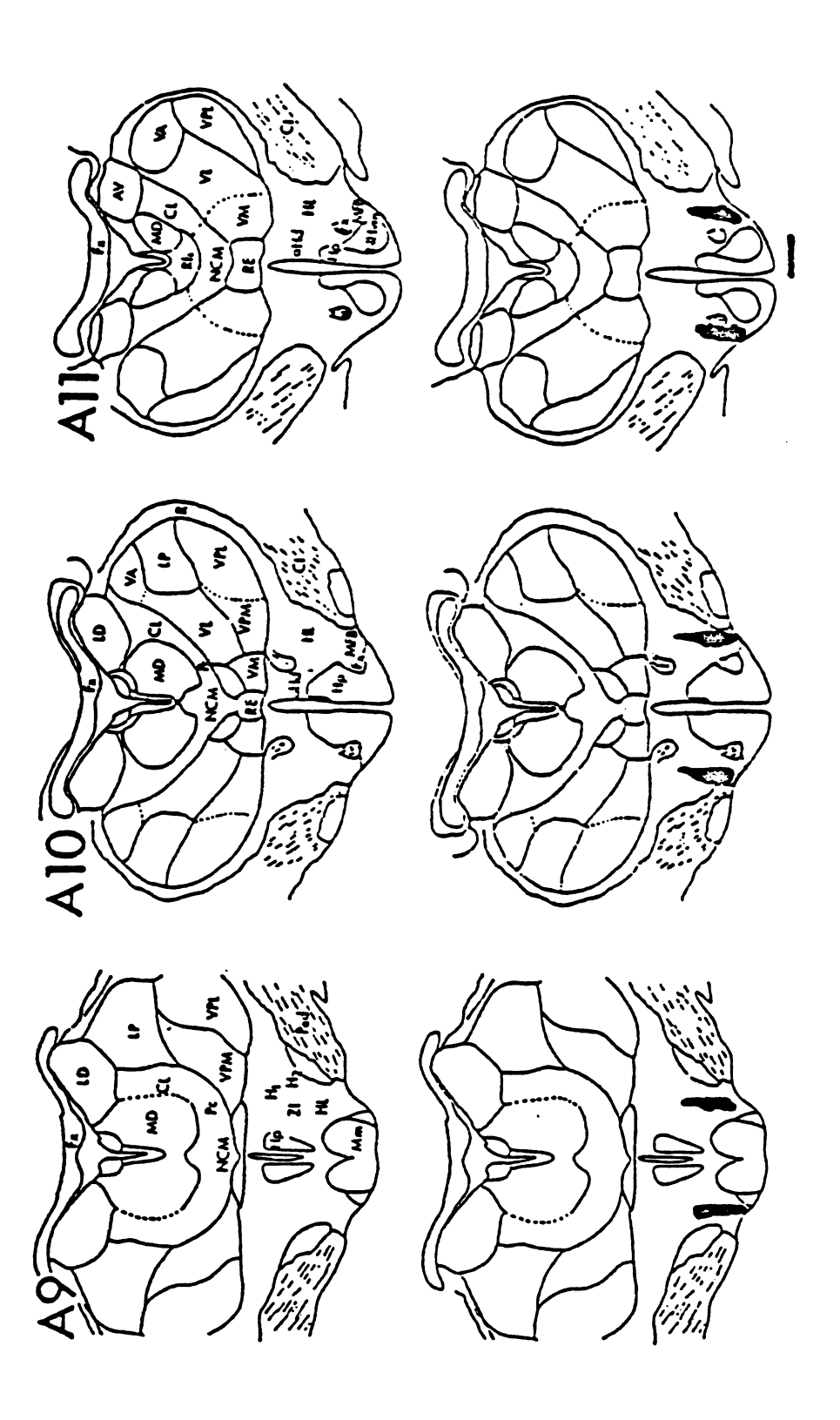


Figure 8

Figure 9. Comparison of effects of midbrain transection on inferior cardiac sympathetic nerve discharge (SND) and mean blood pressure (BP) in nonlesioned control cats (n=23) with those in cats with medial thalamic lesions (n=7). Same format as in Figure 2. *Denotes a statistically significant difference from corresponding data point on control curve. Values are means \pm SE.

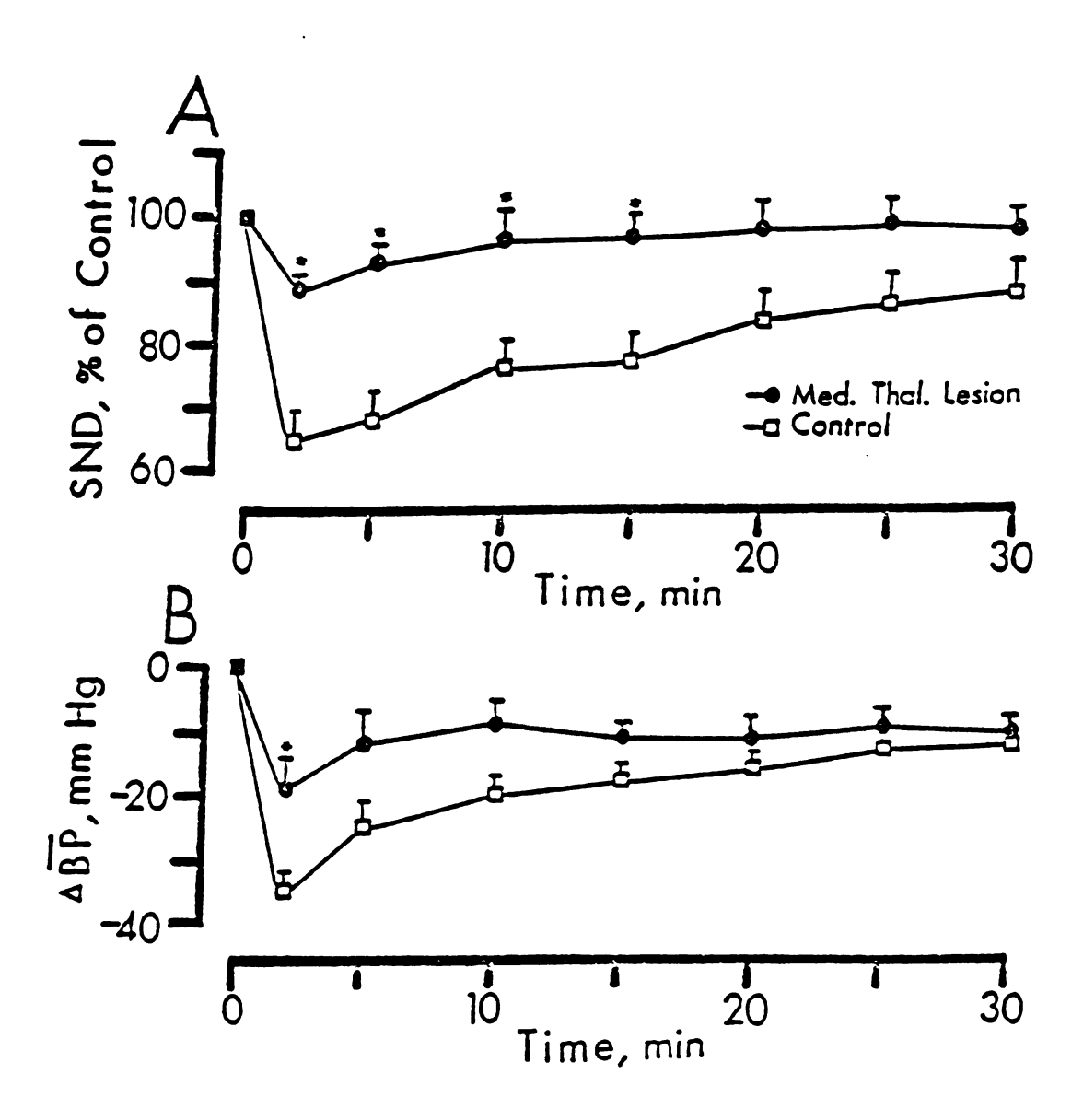


Figure 9

Figure 10. Representative medial thalamic lesion. Abbreviations are as in Figures 5 and 6 with the addition of; CM, N. centrum medianum; HbL, N. habenularis lateralis; NR, N. ruber; Pf, N. parafascularis. Calibration is 2 mm.

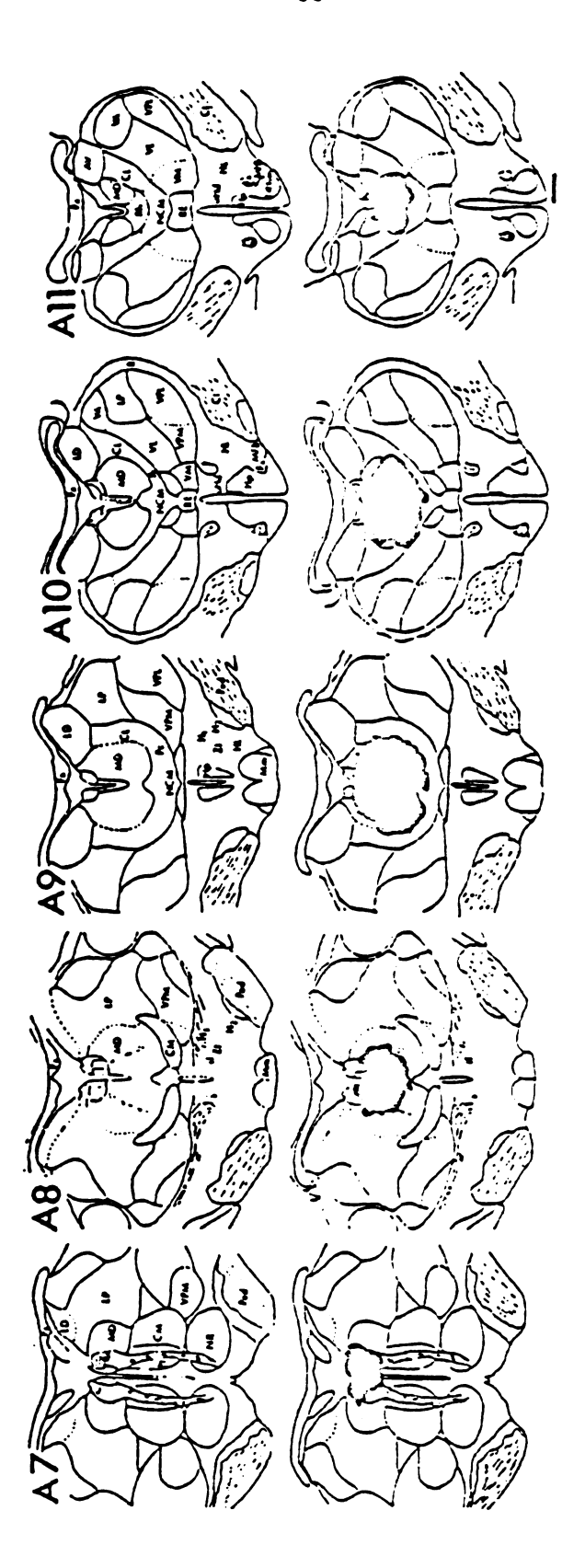


Figure 10

lateral habenula (HbL). In addition, portions of the following intralaminar nuclei were destroyed: centralis lateralis (CL), centralis medialis (NCM), and paracentralis (Pc). Although extensive, medial thalamic lesions did not extend into the hypothalamus or the thalamic sensory relay and association nuclei.

II. Synchronization of SND to diencephalic multiunit activity

A. Multiunit recordings of diencephalic activity

Diencephalic activity was recorded between stereotaxic planes A7 and A11 in 17 baroreceptor-denervated and six baroreceptor-innervated cats. The region from 0 to 3.5 mm lateral to the midline is referred to as the medial thalamus. Recordings in this region were made from sites in the following intralaminar, medial and midline thalamic nuclei: CL, MD, Pc, centrum medianum (CM), reuniens (RE) and ventralis medialis (VM). Recordings in the lateral thalamus were made from the following association and sensory relay nuclei: lateralis dorsalis (LD), lateralis posterior (LP), ventralis posterolateralis (VPL) and ventralis posteromedialis (VPM); and from nuclei ventralis anterior (VA) and ventralis lateralis (VL) which project to motor regions of the neocortex (Jones, 1985). Recordings were made from the following hypothalamic nuclei: aHd, HL, Hp, H1, H2 and ZL

Representative recordings of diencephalic activity and inferior cardiac SND in a baroreceptor-denervated cat are shown in Figure 11. As is the case for cortical activity in chloralose-anesthetized animals (Camerer et al., 1977; Barman and Gebber, 1980), diencephalic slow waves occurred primarily at frequencies between 2 and 6 Hz. The frequency of sympathetic nerve slow wave occurrence was also in the 2- to 6-Hz range. These points are illustrated by the oscillographic traces in Figure 11A and the power spectra in Figure 12A. As reported by others (Andersen and Andersson, 1968; Andersson and Manson, 1971), the patterns

activity denote negativity in this and subsequent figures. Vertical calibration is 100 µV for SND and 50 µV for MD and VPL activity. B: post-R wave averages of arterial pulse wave, SND, MD activity, and VPL activity. Horizontal calibration is 100 ms. Vertical calibration is 10 µV for SND and 5 µV for MD and VPL activity. C: s/division), inferior cardiac SND, medial and lateral thalamic activity recorded from sites in nuclei medialis dorsalis (MD) and ventralis posterolateralis (VPL), respectively. Upward deflections in traces of SND and thalamic frontal section through diencephalon containing recording sites (marked by arrows) in medial and lateral thalamus. Thalamic activity and sympathetic nerve discharge (SND) in a baroreceptor-denervated cat anesthetized with chloralose. A: Traces are from top to bottom blood pressure (BP, mmHg), time base (1 Horizontal calibration is 2 mm.

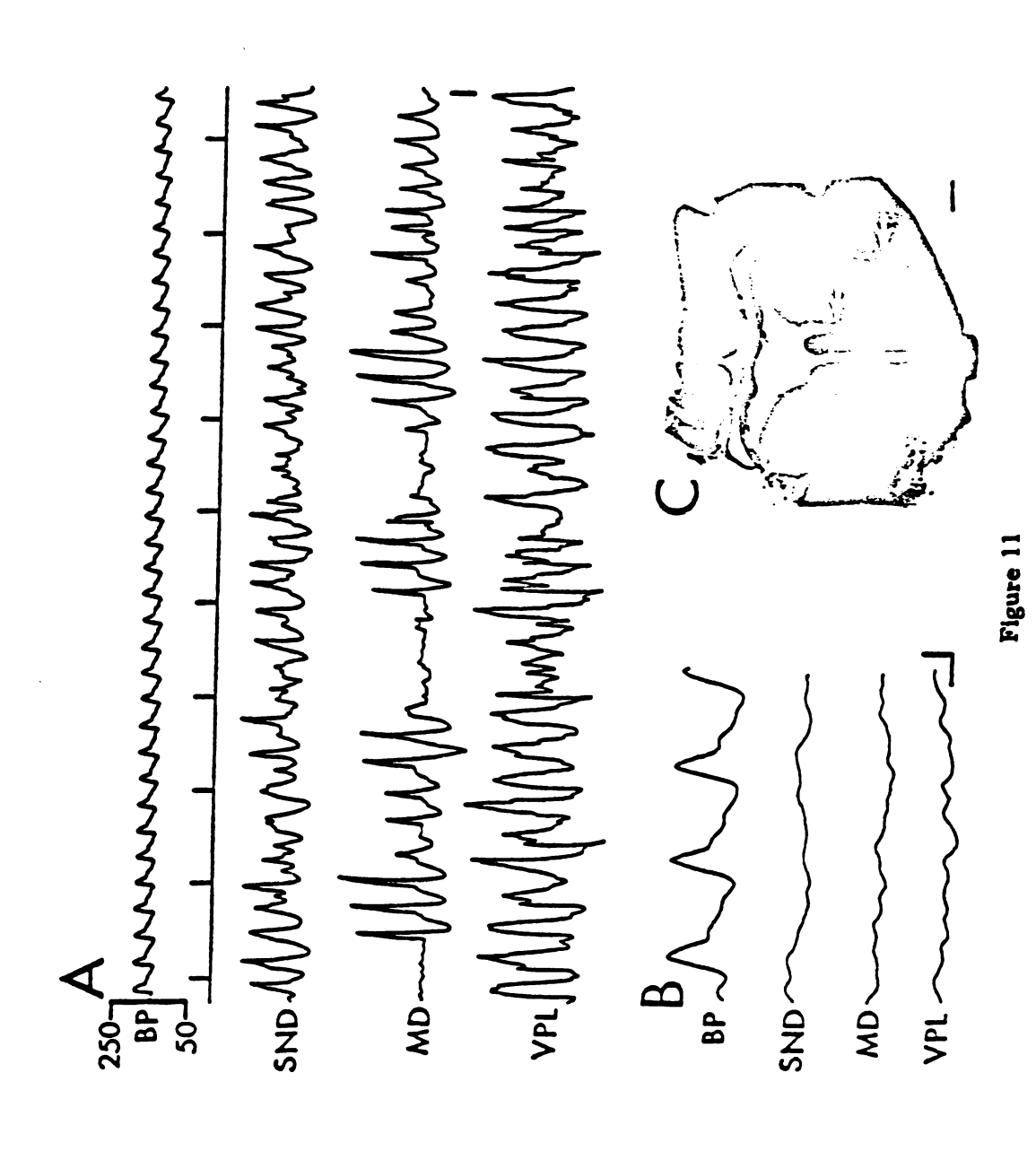


Figure 12. Power spectra of arterial pulse wave (AP), sympathetic nerve discharge (SND) and thalamic activity in two experiments. Records in A are from experiment illustrated in Figure 11. Medial and lateral thalamic activity in A were recorded simultaneously from sites in the nuclei medialis dorsalis (MD) and ventralis posterolateralis (VPL), respectively. Medial and lateral thalamic activity were recorded simultaneously from nuclei paracentralis (Pc) and ventralis posteromedialis (VPM), respectively, in experiment B. Each spectrum is the average of eight 15-s data blocks. Frequency resolution is 0.06 Hz. Vertical range of power (voltage squared) is the same in all traces.

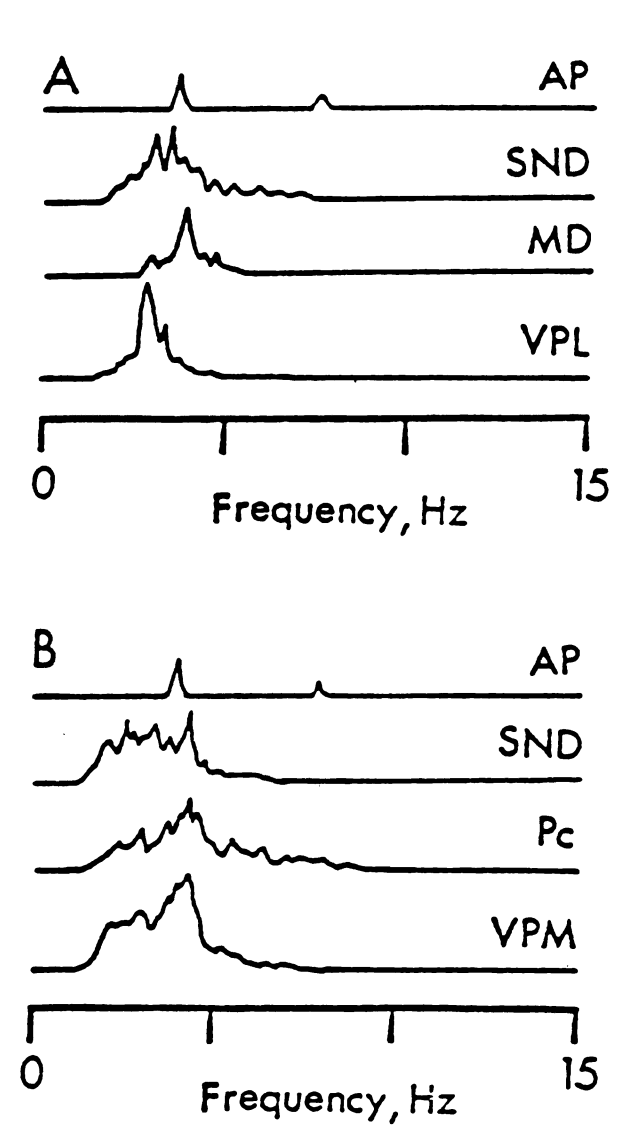


Figure 12

of activity simultaneously recorded from medial and lateral thalamic and from hypothalamic sites could be quite different. In the example shown in Figure 11A, the predominant frequency of slow wave occurrence in the 2- to 6-Hz range was higher in MD than in VPL (also see power spectra in Figure 12A). Neither SND nor thalamic activity contained a cardiac-related component in baroreceptor-denervated cats. This is indicated by the essentially flat post-R wave (ECG) averages of SND and thalamic activity in Figure 11B. Although not shown SND contained a cardiac-related component in baroreceptor-innervated cats (Barman and Gebber, 1980; Gebber, 1980), however, thalamic activity did not.

B. Patterns of relationship between SND and diencephalic activity

1. SND related only to medial thalamic activity

Crosscorrelation analysis was used to determine whether SND and thalamic activity were temporally related. Inferior cardiac SND was temporally related to medial but not to lateral thalamic activity in five baroreceptor-denervated and two baroreceptor-innervated cats. Two of the baroreceptor-denervated cats were decorticate. Figure 13 shows an example of this pattern of relationship in a baroreceptor-denervated cat with an intact neuraxis. The CM -> SND crosscorrelogram (Figure 13B) shows inferior cardiac SND that preceded (left of zero lag) and followed (right of zero lag) medial thalamic activity. Note that the crosscorrelogram contains a sharp peak near zero lag. This peak indicates that a component of SND and medial thalamic (CM) activity were temporally related. The crosscorrelation function (rho value) at the peak was 0.2. A value of 1.0 signifies a perfect relationship. A rhythm with a period of approximately 240 ms appears in both the autocorrelogram of CM activity (Figure 13A) and the CM -> SND crosscorrelogram. Thus, the component common to SND and medial thalamic activity was in the 2- to 6-Hz range. In contrast, the VA -> SND crosscorrelogram (Figure 13B) was flat, indicating that

Figure 13. Selective realtionship between medial thalamic activity and sympathetic nerve discharge (SND). A: autocorrelograms of SND and of activity recorded from nuclei centrum medianum (CM) and ventralis anterior (VA) of medial and lateral thalamus, respectively. B: crosscorrelograms. CM -> SND crosscorrelogram shows SND relative to CM activity at zero lag. VA -> SND crosscorrelogram shows SND relative to VA activity at zero lag. CM -> VA crosscorrelogram shows relationship between activity at both thalamic sites. Analysis time for correlograms was 40 s. Bin width was 10 ms.

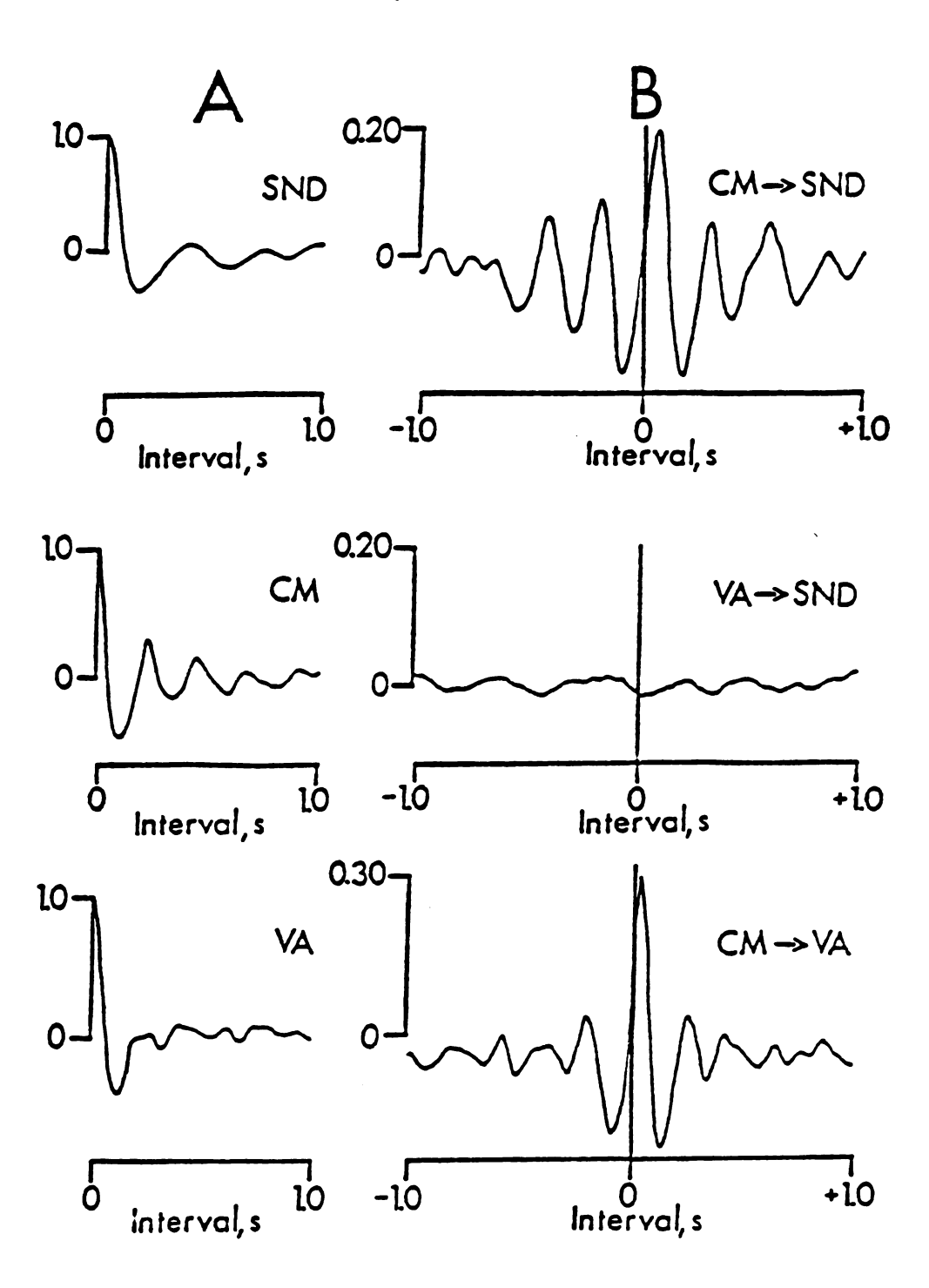


Figure 13

SND was unrelated to activity recorded from this lateral thalamic site. The CM -> VA crosscorrelogram in Figure 13B shows a sharp peak near zero lag indicating that medial and lateral thalamic activity contained a common component. This component apparently was not responsible for the relationship between medial thalamic activity and SND.

As was the case in CNS-intact cats, 2- to 6-Hz slow waves appeared in SND and thalamic activity of decorticate cats. Figure 14A shows representative recordings of SND and medial (VM) and lateral (VPL) thalamic activity in a decorticate cat. The crosscorrelograms in Figure 14B, C demonstrate that SND was temporally related to VM but not to VPL activity.

Recordings were made from 53 medial thalamic and 40 lateral thalamic sites in the seven experiments in which SND was temporally related only to medial thalamic activity. The distribution of thalamic recording sites in these experiments is shown in Figure 15. Twenty-one of the medial thalamic sites had activity related to SND. The mean interval between zero lag and the first peak to the right of zero lag in the medial thalamic -> SND crosscorrelograms for these 21 sites (3) was 73±10 ms. SND was related to thalamic activity recorded in CL (2 of 7 cases), CM (4 of 8 cases), MD (8 of 21 cases), Pc (4 of 8 cases) and VM (3 of 6 cases). No relationship (3) was observed between SND and RE activity (3 cases).

2. SND related to medial and lateral thalamic activity

SND was related to both medial and lateral thalamic activity in seven baroreceptor-denervated and three baroreceptor-innervated cats. Sites with sympathetic nerve-related activity were distributed, without apparent concentration, throughout the medial and lateral thalamus. The mean interval between zero lag and the first peak to the right of zero lag in the medial thalamic -> SND crosscorrelograms was 77±10 ms. The corresponding value for lateral thalamic -> SND crosscorrelograms was 61+11 ms. In the representative example

medialis (VM) and ventralis posterolateralis (VPL), respectively. Vertical calibration is 50 µV for SND and 20 µV for VM and VPL. B: Vm -> SND crosscorrelogram. C, VPL -> SND crosscorrelogram. Analysis time for crosscor-Figure 14. Relationship between medial thalamic activity and sympathetic nerve discharge (SND) in a decorticate and baroreceptor-denervated cat. A: traces are from top to bottom blood pressure (BP, mmHg), time base (1 s/division), inferior cardiac SND, medial and lateral thalamic activity recorded from sites in the nuclei ventralis relograins was 40 s. Bin width was 10 ms.

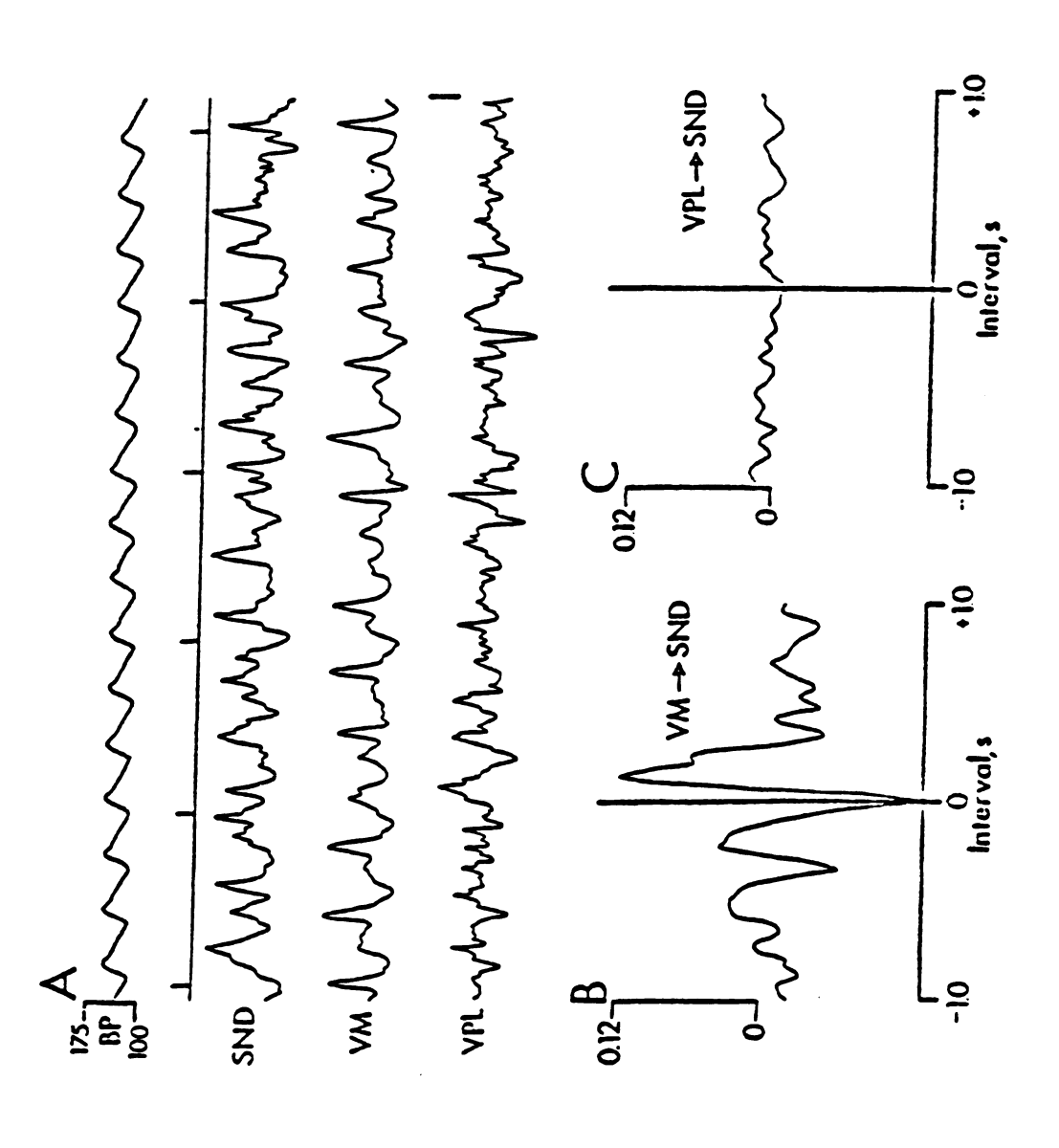
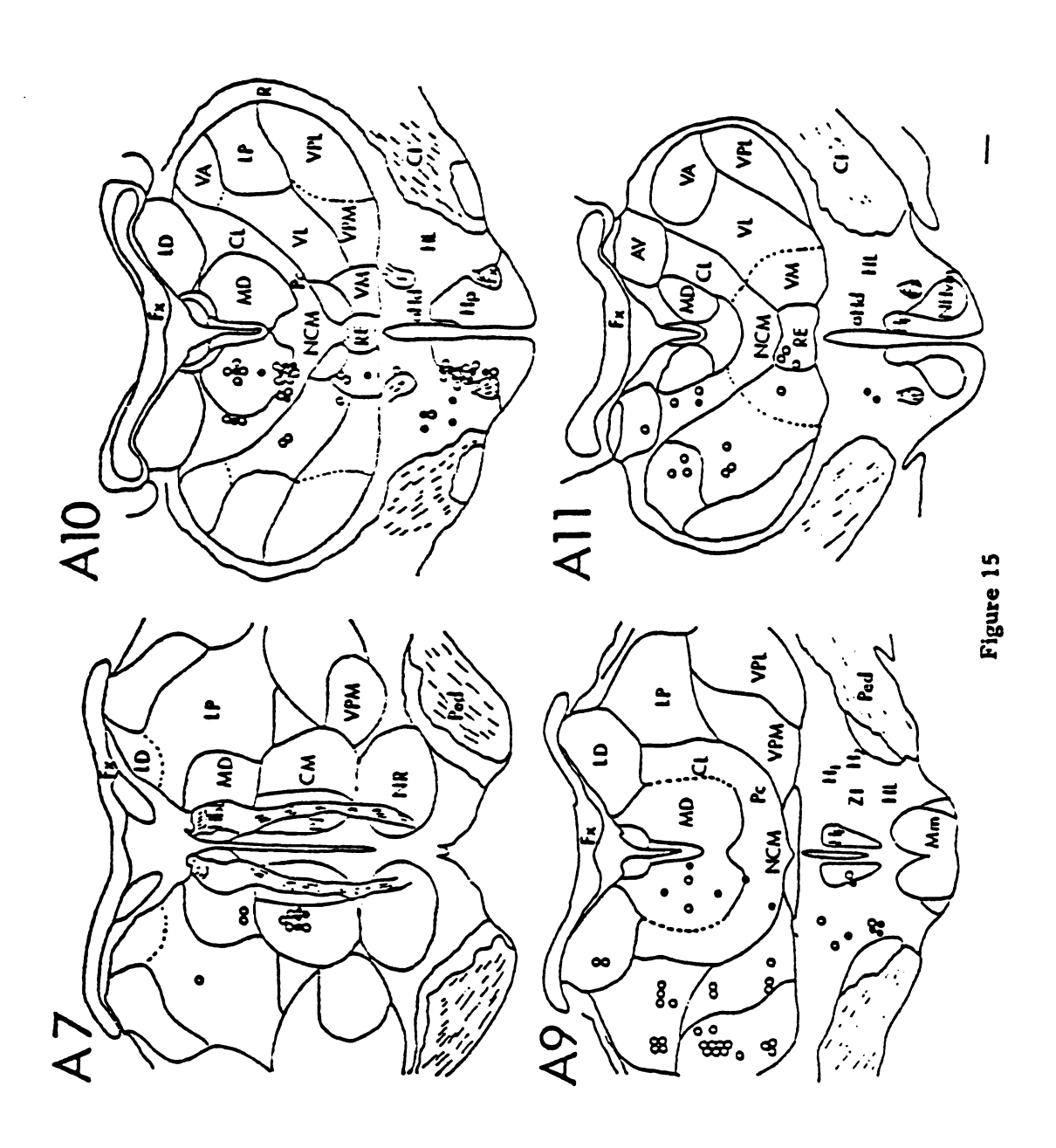


Figure 14

Figure 15. Distribution of diencephalic recording sties in experiments in which sympathetic nerve discharge (SND) was related to activity in medial thalamic and hypothalamic but not in lateral thalamic nuclei. Closed circles show diencephalic sites with activity related to SND, as demonstrated with crosscorrelation analysis. Open circles show diencephalic sites with activity unrelated to SND. Calibration is 1 mm. Abbreviations on frontal sections are as in Figures 5, 6 and 10.



shown in Figure 16, SND was as strongly related to lateral thalamic (LP) activity as to medial thalamic (CL) activity (see peak rho values in crosscorrelograms; panel B). The predominant frequencies of medial and lateral thalamic slow wave occurrence were essentially the same in these experiments (see autocorrelograms of CL and LP activity in Figure 16A). Twenty-nine of 45 medial thalamic sites and 27 of 43 lateral thalamic sites had activity related to SND in these experiments.

3. SND related to hypothalamic activity

The relationship between SND and hypothalamic activity was examined in 19 cats. SND was related to hypothalamic activity as well as to thalamic activity in 13 cats. SND was related to medial thalamic but not to lateral thalamic activity in five of these experiments. An example of the relationship between SND and hypothalamic activity from one of five experiments in which SND was temporally related to medial but not to lateral thalamic activity is illustrated in Figure 17. The mean interval between zero lag and the first peak to the right of zero lag in the hypothalamic -> SND crosscorrelograms was 59±13 ms (19 of 31 sites had activity correlated to SND. The distribution of these sites is shown in Figure 15. Sites with sympathetic nerve-related activity (②) were located in both the lateral and posterior hypothalamic nuclei. In the remaining eight cats, hypothalamic and medial- and lateral thalamic activity was related to SND. In an additional two cats SND was related to hypothalamic but not to thalamic activity.

4. SND unrelated to diencephalic activity

SND was unrelated to hypothalamic and medial- and lateral thalamic activity in one decorticate and three CNS-intact cats with severed baroreceptor nerves. Activity was recorded from a minimum of 20 diencephalic sites in each of these experiments.

Figure 16. Nonselective relationship between thalamic activity and sympathetic nerve discharge (SND). A: autocorrelograms of SND and of activity recorded from nuclei centralis lateralis (CL) and lateralis posterior (LP) of medial and lateral thalamus, respectively. B: crosscorrelograms. CL -> SND crosscorrelogram shows SND relative to CL activity at zero lag. LP -> SND crosscorrelogram shows SND relative to LP activity at zero lag. CL -> LP crosscorrelogram shows relationship between activity at both thalamic sites. Analysis time for correlograms was 40 s. Bin width was 10 ms.

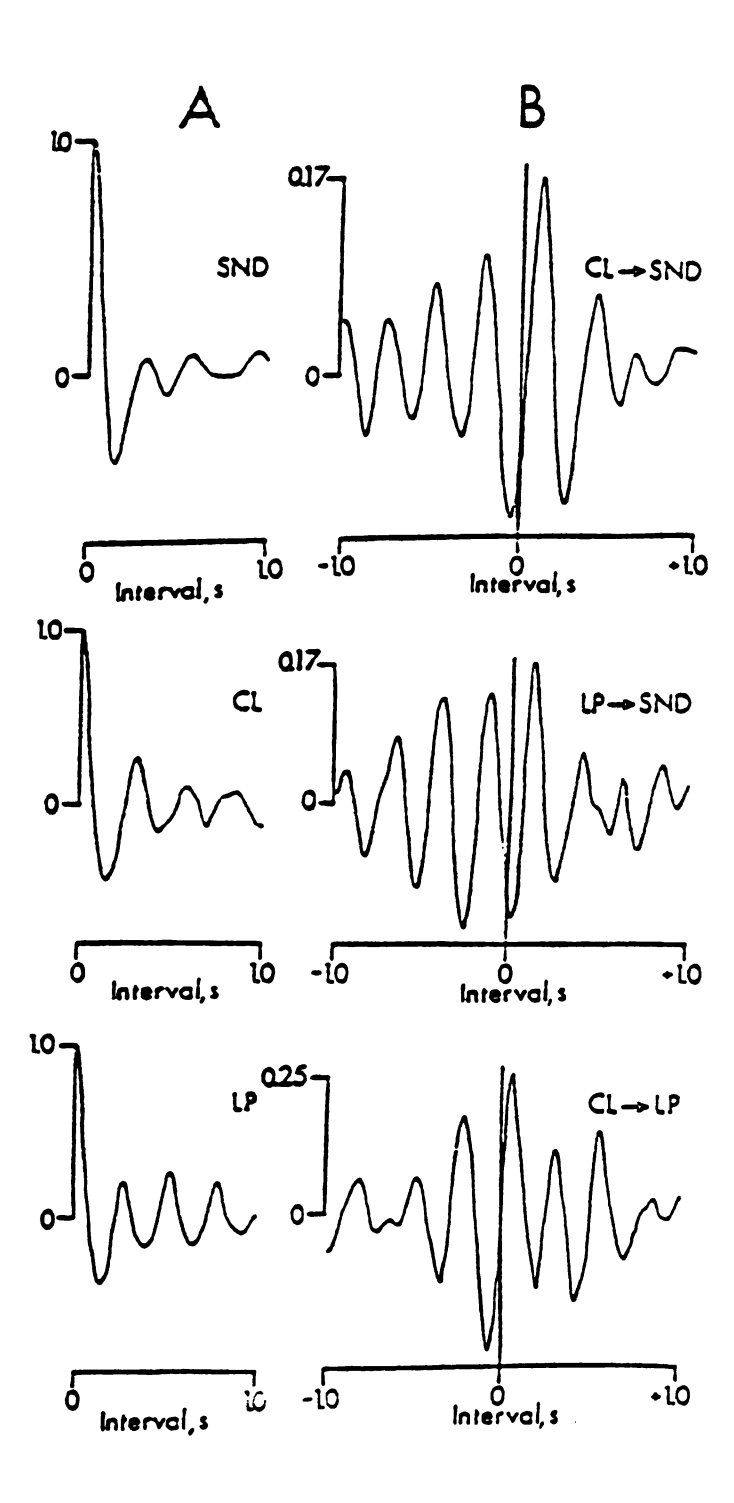


Figure 16

Figure 17. Crosscorrelograms showing relationships of sympathetic nerve discharge (SND) and activity recorded from thalamus and hypothalamus. Diencephalic activity in this baroreceptor-denervated cat was recorded from sites in N. medialis dorsalis (MD) of medial thalamus, the lateral hypothalamus (HL) and N. lateralis posterior (LP) of lateral thalamus. Analysis time for crosscorrelograms was 40 s. Bin width was 10 ms.

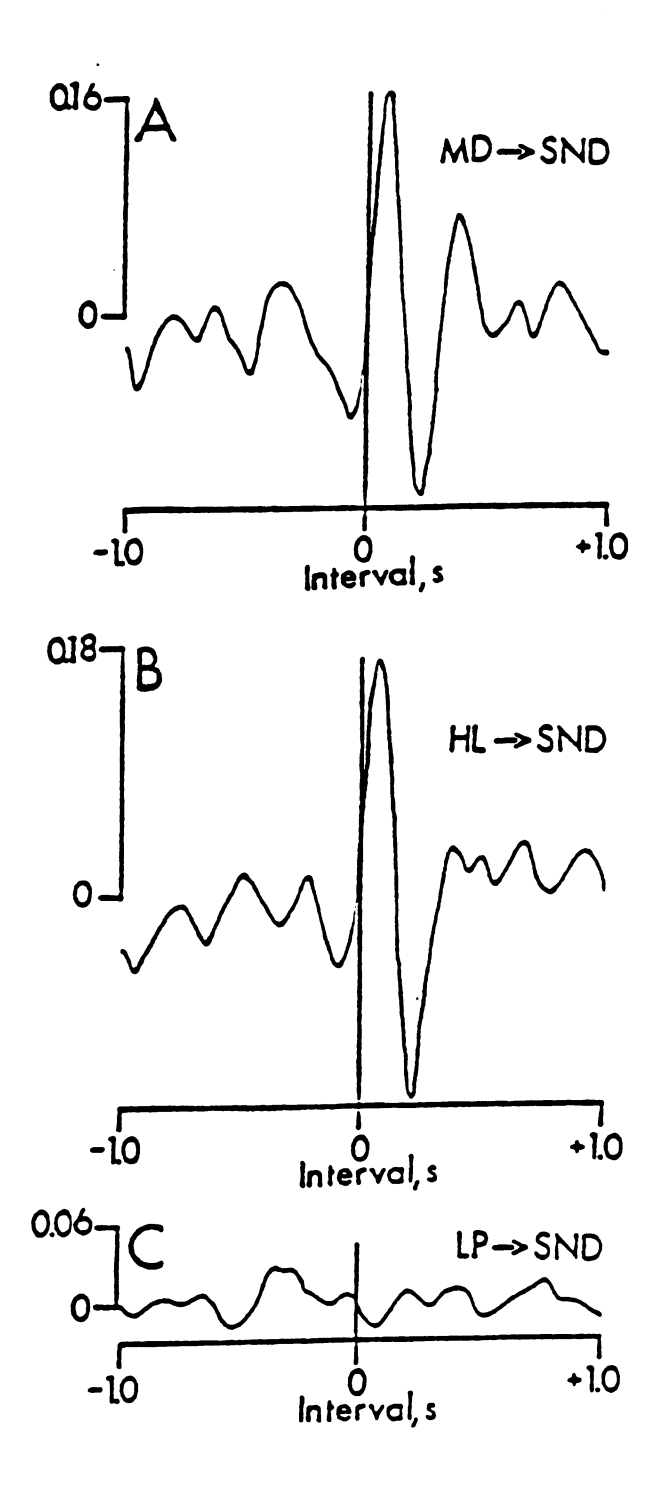


Figure 17

C. Electrical and chemical stimulation of the diencephalon

An important issue raised by the previous series of experiments is whether the temporal relationships between diencephalic and sympathetic nerve activity revealed by crosscorrelation analysis are indicative of a functional connection between the diencephalon and the sympathetic nerves. Alternatively, brain stem networks controlling SND and diencephalic circuits controlling other functions may not be directly connected, but may receive input from a common 2to 6-Hz generator. Assuming that a functional connection exists, a second question which arises is whether the diencephalon contains the cell bodies of neurons capable of influencing SND. These questions were approached in two stages. First, electrical stimulation was used to test for a functional connection between the diencephalon and the sympathetic nerves. Second, chemical stimulation was used to determine whether the thalamus contains the cell bodies of neurons capable of influencing SND. In this study, the hypothalamus was not chemically stimulated. In contrast to the thalamus, numerous studies using chemical stimulation have shown that the posterior hypothalamus (Gellhorn and Redgate, 1955; Redgate and Gellhorn, 1956a; 1956b; Lee et al., 1972; Finch and Hicks, 1977) lateral hypothalamus (Lee et al., 1972; Sun and Guyenet, 1986) and the PVH (Rockhold et al., 1987) contain the cell bodies of neurons capable of influencing blood pressure and heart rate.

1. Sympathetic nerve responses elicited by electrical stimulation

Increases in SND were elicited by 10-ms trains of three pulses applied once every 2 s to sites in the diencephalon of 17 cats, three of which were decorticate. Stimuli were applied to CL, CM, MD, Pc and VM of the medial thalamus, VA, VL and VPL of the lateral thalamus and to sites in the lateral and posterior hypothalamus. Increases in SND could be elicited by stimulation of sites in each of these nuclei. The onset latencies of the sympathetic nerve responses

elicited from different medial and lateral thalamic nuclei were statistically indistinguishable. However, the mean onset latencies of the responses produced by medial or lateral thalamic stimulation were significantly longer than that for the responses elicited by hypothalamic stimulation (Table 1). This was the case even when stimuli of supramaximal intensity (1 mA) were used. Typical examples of averaged sympathetic nerve responses (32 trials) elicited by thalamic and hypothalamic stimulation in a CNS-intact and in a decorticate cat are shown in Figure 18.

In five cats the diencephalon was explored to locate those sites from which sympathetic nerve responses could be elicited with the lowest stimulus current (<30 µA in some cases). The concentric bipolar stimulating electrode was moved vertically in 1 mm steps. Threshold current for eliciting a sympathetic nerve response and the depth of the electrode were recorded for each site of stimulation. Eleven depth-threshold curves were constructed from these data. Representative examples are shown in Figure 19. Electrode tracks passing through the posterior portion of the medial thalamus and underlying midbrain yielded the type of depth-threshold curve shown in Figure 19A. Note that the site requiring the least stimulus current (60 µA) for eliciting an increase in SND was located in CM of the medial thalamus. Thus these responses were most likely not due to current spread to more ventral structures. Electrode tracks passing more anteriorly through the medial thalamus and underlying hypothalamus yielded depth-threshold curves that were broader in contour. In the case shown in Figure 19B, the electrode track extended through MD and Pc of the medial thalamus and the HL. Note that sympathetic nerve response could be elicited with stimulus currents below 100 uA applied to widely separated sites in the medial thalamus and lateral hypothalamus. Sympathetic nerve responses also were routinely

TABLE 1. Mean onset latencies of inferior cardiac sympathetic nerve excitation produced by diencephalic stimulation with 10-ms trains of three pulses of supramaximal intensity (1 mA).

A. Cats with intact neuraxis (n=14)

	No. of Sites	Mean Onset + S.E.
мть	78	69 <u>+</u> 1 ms*
LTh	30	67 <u>+</u> 2 ms*
HTh	27	69 ± 1 ms* 67 ± 2 ms* 60 ± 2 ms

B. Decorticate cats (n=3)

	No. of Sites	Mean Onset + S.E.
MTh	7	64 + 3 ms*
LTh	3	64 <u>+</u> 3 ms* 64 <u>+</u> 4 ms*
HTh	5	52 ± 2 ms

MTh, LTh and HTh are medial thalamus, lateral thalamus and hypothalamus, respectively. * indicates that mean onset latencies of responses elicited by MTh and LTh stimulation were significantly (P < 0.05) longer than that of the responses evoked by HTh stimulation.

Figure 18. Sympathetic nerve responses elicited by diencephalic stimulation (10-ms trains of three 1-mA pulses applied once every 2 s) in a CNS-intact (A) and a decorticate (B) cat. Diencephalic nuclei are labeled as in Figures 5, 6 and 10. Calibration is 1 mm. Post-stimulus averages (32 trials) of inferior cardiac sympathetic nerve responses. Responses are numbered to correspond with the site of stimulation. Bin width was 1 ms. Vertical calibration is 100 uV and horizontal calibration is 100 ms.

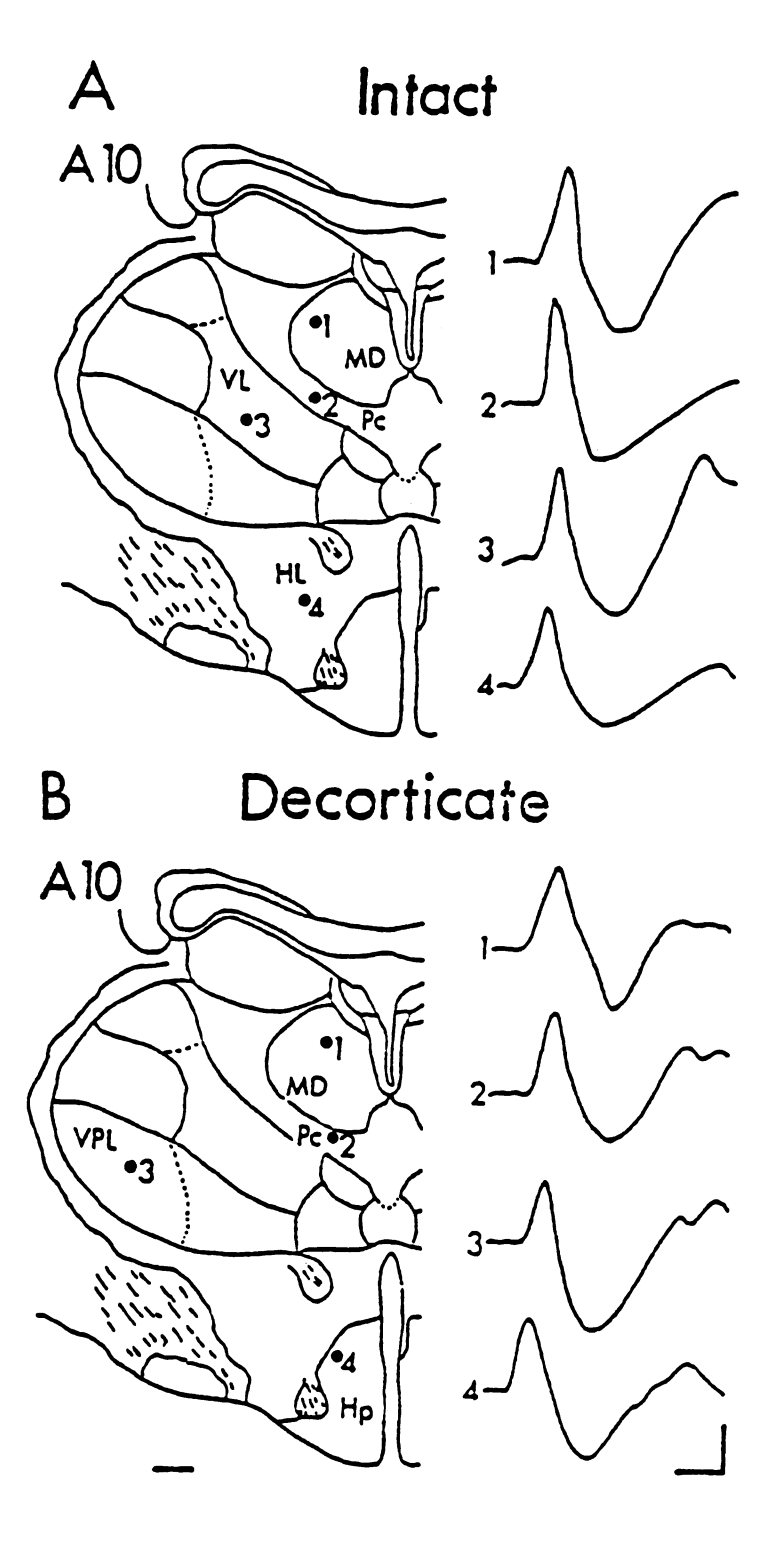


Figure 18

Figure 19. Depth-threshold curves for sympathetic nerve responses elicited by medial thalamic, hypothalamic and midbrain stimulation with 10-ms trains of three pulses. Stereotaxic horizontal plane (H) is plotted against threshold current (μA) for eliciting a response. Nuclei are labelled as in Figures 5, 6 and 10. Data in A and B are from different experiments.

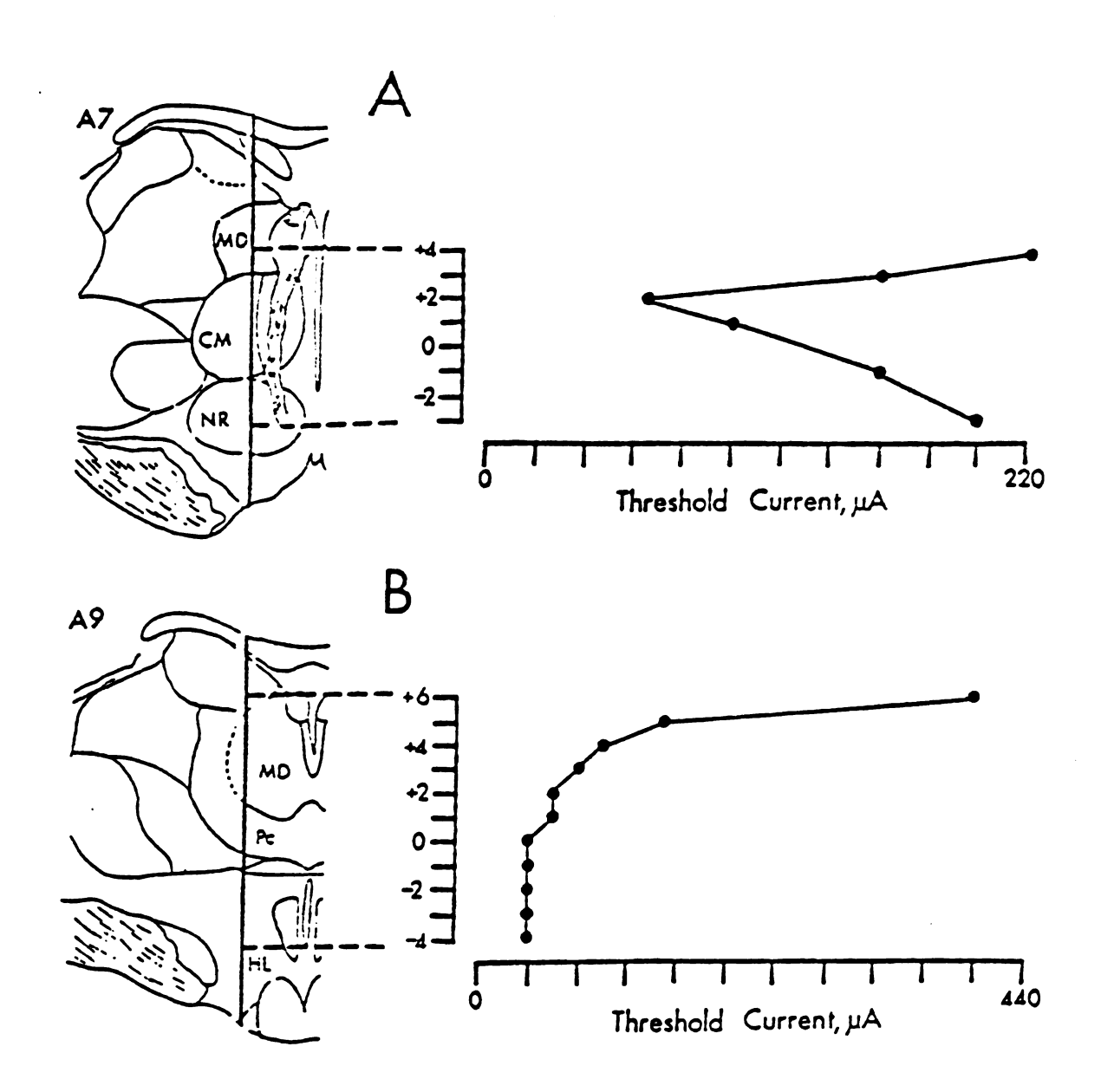


Figure 19

elicited when the stimulus current applied to lateral thalamic sites was less than 100 uA.

2. Intrathalamic injection of picrotoxin

Picrotoxin, a CNS stimulant with GABA antagonistic properties is believed to exert its action on synaptic networks rather than on fibers of passage (Johnston, 1976). SND was monitored before and after this drug was injected into the medial thalamus of five baroreceptor-denervated cats. One or two series of bilateral injections (5 µg picrotoxin in 0.5 µl) were made between stereotaxic planes A9 and A11, 0.5 to 1.5 mm lateral to the midline at H+1 or H+2. Fast green FCF dye injected at these sites at the end of each experiment spread to portions of CL, Pc, MD, NCM and RE of the medial thalamus. No dye was observed in the ventricular system, lateral thalamus (>3 mm lateral to the midline) or the hypothalamus.

Figure 20 illustrates the changes in SND observed in 4 of 5 cats approximately 10 min after picrotoxin was injected into the medial thalamus. The intrathalamic injection of picrotoxin led to an increase in the amplitude of the 2-to 6-Hz sympathetic nerve slow waves and a decrease in the variability of interslow wave intervals (Figure 20IIA). The latter effect indicates that SND became more rhythmic. The reduction in the variability of interslow wave intervals after picrotoxin administration is reflected by the sharp peak between 1 and 2.5 Hz in the power spectra of SND in Figure 20IIB. The changes in SND produced by the injection of picrotoxin into the medial thalamus were accompanied by a rise in blood pressure (20 and 40 mmHg) in 2 of the 4 experiments. The failure of intrathalamic picrotoxin to raise blood pressure in 2 of 4 animals suggests that although picrotoxin altered the rhythm in SND in these animals, it did not sufficiently increase total sympathetic nerve activity to produce a pressor response. No quantitation of total SND was made in these experiments.

Figure 20. Changes in sympathetic nerve discharge (SND) produced by injection of picrotoxin into the medial thalamus. It control. It: 10 min after bilateral injection of picrotoxin (total dose, 10 ug) into the medial thalamus at stereotaxic plane A10. Traces in IA and IIA are from top to bottom blood pressure (BP, mmHg), SND and frontal-parietal cortical activity (EEG). Vertical calibration is 100 μ V for SND and EEG. Horizontal calibration is 500 ms. Traces in IB and IIB power spectra of SND. Traces in IC and IIC are power spectra of EEG. Total power in IIB was 387% of that in IB. Total power in IIC was 128% of that in IC. Each spectrum is the average of 20 6-s data blocks. Frequency resolution is 0.1 Hz.

constitute a rostral extension of the generalized reticular activating system proposed by Magoun and Ranson in 1949. They proposed that the pacemaker activity of the medial thalamic nuclei is relayed to the cortex via n. reticularis and n. ventrais anterior where this activity "acts upon the cortex, controlling the form and rhythm of the background of cortical activity upon which afferent impulses must act, and regulating the generalized excitatory states of the cortex as a whole" (Jasper, 1949). This theory had to be discounted when it became clear that the n. reticularis does not project to the cortex (Scheibel and Scheibel, 1966; Jones, 1985).

2. Mechanisms for the generation of alpha spindle activity

Purpura and coworkers (Purpura and Cohen, 1962; Purpura and Shofer, 1963; Purpura et al., 1965) proposed that the nonspecific medial thalamic nuclei are the major source of synchronizing input to the thalamus. These authors examined the synaptic events occurring in thalamic neurons during the recruiting response elicited by stimulation of the nonspecific medial thalamic nuclei. Intracellular recordings from thalamic neurons during the recruiting response revealed that the synchronization of neuronal firing is produced by a recurring sequence of a short-latency (4-15 ms) excitatory postsynaptic potential (EPSP), followed by a long-latency (15-40 ms), prolonged (80-200 ms) inhibitory postsynaptic potential (IPSP). The prolonged IPSP is thought to be the major feature of the synchronization process since neither spontaneous nor evoked neuronal discharges of the thalamocortical neuron occur during the IPSP. Rather, the discharges of thalamocortical neurons are restricted to the short periods between IPSPs. This EPSP-IPSP sequence is observed in over 70% of the neurons recorded in widely separated regions of the n. ventralis anterior, n. ventralis medialis, n. ventralis lateralis and from the intralaminar and midline thalamic nuclei. Thalamic focal potentials recorded during the recruiting response reveal long-latency (15-40 ms),

long-duration (40-80 ms) positive waves presumably reflecting the summation of EPSP-IPSP sequences throughout the thalamus. These positive thalamic waves are temporally related to the negative waves in the cortical recruiting response. Similar EPSP-IPSP sequences are recorded in cells in the ventrobasal complex during spontaneous alpha spindle activity in the sensory cortex (Maekawa and Purpura, 1967). High frequency (20 Hz) stimulation of the medial thalamic nuclei which blocks the recruiting response in the cortex also prevents the development of prolonged IPSPs in thalamic cells (Purpura and Shofer, 1963). Instead, an increase in neuronal discharge associated with a steady depolarization or no change in membrane potential is observed.

Like Purpura and coworkers, Andersen and Eccles (1962) observed that the rhythmic bursting discharge of thalamic neurons is associated with a recurring sequence of EPSPs and IPSPs. Andersen and Eccles also demonstrated that rhythmic burst discharges in thalamic relay cells occurs during stimulation of peripheral afferents or the antidromic activation of thalamocortical neurons, suggesting that the generation of rhythmic activity is an inherent property of all thalamic neurons. From these data Andersen and Eccles proposed the facultative pacemaker theory for the generation of rhythmic burst discharges in thalamic neurons. This model was later expanded upon by Andersen and Andersson in 1968. Briefly, this model proposes that the thalamocortical cells excited by afferent inputs emit excitatory recurrent axon collaterals onto local interneurons. The interneurons in turn inhibit the thalamocortical neuron. Furthermore, it is proposed that during the declining phase of the interneuron-induced inhibition, the thalamocortical neuron becomes hyperexcitable (post anodal exaltation) and discharges again, thus initiating a repeating cycle of excitation and inhibition. The post anodal exaltation is thought to be an intrinsic property of the membrane, thus endowing the neuron with pacemaker properties. The possibility that

excitatory interneurons help to trigger subsequent neuronal discharges and recruit other relay neurons is also proposed.

Andersen and Sears (1964) demonstrated that spindle bursts and 8- to 12-Hz focal waves can be recorded in midline and relay thalamic nuclei in acute and chronically decorticate cats. Spindle activity is also present in relay nuclei after section of all connections with the nonspecific medial thalamic nuclei. On this basis, it is concluded that all regions of the thalamus are inherently capable of generating rhythmic spindle activity via facultative pacemaker circuits. In contrast to Purpura and coworkers, the medial thalamic nuclei are not believed to be the major source of spindling activity in the thalamus, although these regions may exert control over these rhythms. Andersson and Manson (1971) later demonstrated that rhythmic activity occurring simultaneously from different thalamic regions in unanesthetized decorticate cats can be quite different. These data further suggest that the rhythmic activity in the cortex and thalamus is not generated by or in one specific thalamic region.

Although attractive, the faculatative pacemaker theory is seriously flawed. For example Purpura and colleagues pointed out that the long latency and duration of the IPSP in the thalamocortical cells is hard to reconcile on the basis of a simple feedback inhibitory synapse. These authors also pointed out that brief periods of stimulation (7 Hz) of the midline thalamic nuclei elicits EPSP-IPSP sequences in thalamic neurons and spindle waves in the cortex which persist (in the absence of neuronal spikes) following termination of the stimulus (Purpura et al., 1966). According to the facultative pacemaker model, the thalamocortical neuron must discharge in order to observe the IPSPs in thalamic neurons. Perhaps the strongest evidence against this model comes from anatomical studies of thalamic nuclei using the Golgi method. These studies failed to support the facultative pacemaker theory since only 15-20% of thalamocortical

neurons have recurrent axon collaterals (Scheibel et al., 1973). In Scheibel's words the small number of collaterals was deemed to be "an insignificant substrate for the powerful recursive effects ascribed to them."

3. The thalamic reticular nucleus as a generator of thalamic spindle sequences

The n. reticularis thalami is a sheet-like structure encompassing the rostral and lateral borders of the thalamus. The structure and connections of this nucleus have been well characterized (see Scheibel and Scheibel, 1966; Steriade et al., 1984; Jones, 1985). The axons of most thalamocortical neurons emit collaterals in the n. reticularis in a topographical fashion. The axons of these thalamic reticular neurons project back to those thalamic regions from which the collateral input arises. Corticothalamic neurons also collateralize in the reticular nucleus; however, the reticular nucleus does not have cortical projections.

The early development of the hypothesis that the n. reticularis is involved in the generation of the 8- to 12-Hz spindle rhythms is reviewed by Steriade and Hobson (1976). On the basis of mostly anatomical data, the Scheibels proposed that the rhythmic bursting discharge of the thalamic relay cells is due to direct feedback inhibition from n. reticularis. Physiological evidence in support of this hypothesis was provided by Schlag and Waszak who showed that a reciprocal relationship exists between the burst discharges of n. reticularis and thalamocortical neurons. During episodes of EEG spindling or high amplitude cortical slow waves, the discharge rates of neurons in n. reticularis increase while those of thalamocortical neurons decrease. Moreover, the burst discharges of the reticularis neurons often spanned the spindle sequence and are thus thought to be responsible for the spindle-related hyperpolarization (IPSP) of the thalamocortical neurons. During EEG desynchronization elicited by stimulating the mesencephalic reticular formation, the discharge rates of neurons in n. reticularis decrease while

those of thalamocortical neurons increase. Additional support for this proposal comes from the work of Houser et al. (1980) who demonstrated that many of the projections from n. reticularis to thalamic relay nuclei are GABAergic.

Further evidence that the n. reticularis is involved in generating the alpha spindles is provided by the observation that neurons in the anterior thalamic nuclei (anterior ventral, anterior medial and anterior dorsal) which do not receive afferents from n. reticularis do not display spontaneous or evoked spindle-like discharges (Mulle et al., 1985). This is the case even though these neurons have intrinsic membrane properties similar to those of thalamic neurons displaying spindling activity. Furthermore, EEG recorded from the parasplenial projection cortex of these nuclei also fails to display spindle activity.

Although it is generally accepted that the n. reticularis is involved in generating the alpha rhythm, Steriade and colleagues (Steriade and Deschenes, 1984; Steriade et al., 1985; 1986; 1987) have questioned whether the regulation of activity in thalamocortical neurons is due solely to a direct feedback inhibition from n. reticularis. That a more complex mechanism is involved is suggested by Steriade et al. (1986) who recorded the activity of neurons in thalamic relay nuclei and n. reticularis during various sleep and awake states in cats. As in earlier studies, during EEG synchronization n. reticularis neurons fire in long bursts (increasing then decreasing interspike intervals) which often span the spindle sequence of the thalamocortical cells. In contrast, during arousal and awake states (EEG desynchronized) n. reticularis and thalamocortical neurons both cease spindling and significantly increase their firing rates in parallel. Such parallelism is not consistent with a direct inhibitory action of reticularis neurons on thalamocortical neurons.

To account for the state-dependent relationships between the activity of thalamocortical and n. reticularis neurons, Steriade and colleagues

(Steriade et al., 1985; 1986; 1987) proposed a model whereby n. reticularis controls the activity in thalamocortical circuits. Moreover, these authors propose that the n. reticularis functions as a pacemaker to generate alpha spindling. In this model, neurons in n. reticularis have direct GABAergic projections to thalamocortical neurons and to GABAergic interneurons located near the thalamocortical neurons. These inhibitory interneurons in turn contact the thalamocortical neurons. The presence of GABAergic interneurons was reported by Montero and Singer (1985). A central feature of this model is the notion that the projections from n. reticularis exert differential inhibitory effects on the thalamocortical and GABAergic interneurons, with the more powerful inhibitory effects being exerted on the interneurons. Thus state-dependent changes in the amount of GABA released by the n. reticularis neurons changes the activity pattern in thalamocortical circuits by changing the ratio of inhibition of the interneurons and thalamocortical neurons. For example during EEG-desynchronization, the n. reticularis cells cease bursting and fire tonically as single spikes at an increased rate. The GABA released by the n. reticularis neurons inhibits the more sensitive interneurons. As a consequence, the thalamocortical neurons become more excitable due to the disinhibition and fire at a higher frequency. This proposal is supported by the observation that reticularis-disconnected thalamocortical neurons have a lower average firing rate than do their counterparts in reticularis-intact cats during EEG-desynchronization. Conversely, during EEGsynchronized states, the n. reticularis neurons begin to discharge in prolonged bursts. During these bursts the intraburst frequencies are higher than the fastest tonic discharge rates occurring during desynchronized states and as a consequence, more GABA is released. The increased in GABA release via direct reticularis inputs is now sufficient to hyperpolarize the thalamocortical neurons. The hyperpolarization of the thalamocortical neuron triggers the deinactivation of

a calcium (Ca⁺⁺) conductance, eventually leading to the spindle burst discharge of the neuron. At the same time an overabundance of GABA released by the bursting n. reticularis neuron saturates the more GABA-sensitive interneurons, completely inhibiting their firing.

Evidence in support of this model is presented by Steriade et al. (1985) who examined the discharges of thalamocortical neurons after removing inputs from the n. reticularis by using either knife cuts or kainic acid lesions. Removing inputs from the n. reticularis abolished spindle-related rhythms (sequences of 7-12 Hz waves recurring at 0.1-0.2 Hz) in the thalamus and ipsilateral EEG. In addition, n. reticularis-disconnected thalamocortical neurons no longer display spindle-related sequences of prolonged IPSPs. Instead short duration IPSPs are recorded. Thalamocortical cells exhibit high frequency spike bursts whose parameters (number of spikes, intraburst frequency, duration of consecutive intervals) are the same as those in relay and intralaminar cells having intact reticularis connections. However, the characteristic pattern of spindle-related sequences of spike bursts and irregularly occurring single-spike discharges during non-spindling periods is replaced by solitary bursts occurring with remarkable regularity at 1- to 2-Hz. This regular 1- to 2-Hz burst pattern is thought to be mediated by the GABAergic interneurons which are disinhibited by removing inputs from n. reticularis. The increased activity in the interneurons produces a series of short duration IPSPs in the thalamocortical neurons. The rapidly occurring IPSPs summate and hyperpolarize the thalamocortical neuron deinactivating a low threshold, long duration Ca⁺⁺ conductance whose activation leads to the burst response. This conclusion is based on the finding that a subconvulsive dose of bicuculline administered intravenously changes the discharge pattern of reticularis-disconnected thalamocortical neurons from rhythmic bursting to irregularly occurring single spikes.

Evidence that the n. reticularis functions as a pacemaker in the generation of spindle rhythmicity during EEG-synchronization is provided by Steriade et al. (1987). In this study extracellular recordings of unit discharges and focal potentials were made in the rostral pole of n. reticularis after surgically disconnecting it from all other thalamic nuclei. As previously discussed disconnection of n. reticularis abolishes spindle activity in the ipsilateral cortex and thalamic nuclei (Steriade et al., 1986). However, neurons in the disconnected n. reticularis discharge in the biphasic (acceleration-deceleration) pattern of spike bursts characteristic of neurons in the intact n. reticularis during EEG synchronization. The spike bursts were of long duration (50 ms-1.5 s) and recurred with a frequency of 0.1- to 0.3-Hz. Simultaneous recordings of focal potentials through the recording microelectrode reveal spindle sequences (grouped 7-16 Hz slow waves recurring at 0.1-0.3 Hz) temporally related to the spike bursts of the n. reticularis neurons. The authors suggest that the synchronization of the burst discharge of the reticularis neurons involves dendrodendritic interactions between the GABAergic reticularis neurons. The presence of dendrodendritic connections between reticularis neurons has been demonstrated with the electron microscope (Deschenes et al., 1985). In addition, the intravenous administration of bicuculline greatly reduces spike bursts in the deafferentated n. reticularis.

4. Origin of the cortical delta and theta rhythms

Although it is fairly well established that the cortical alpharhythm (8-12 Hz) is generated in the thalamus there is some controversy as to whether the slower delta and theta rhythms in the EEG are generated in the thalamus.

Villablanca (1974) examined sleep and behavioral patterns in chronic athalamic and decorticate cats. During the first 10 days after removing the thalamus, irregular high voltage slow waves occurring at frequencies of 2- to

4-Hz dominate the EEG. Initially, the synchronized EEG pattern is unchanged during behavioral arousal, however, after 15 to 25 days, periods of desynchronized-like EEG activity accompany arousal. At no time after thalamic ablation are 8- to 12-Hz alpha spindles observed in the EEG, nor can they be induced by administering pentothal. In acute (3-5 days postoperative) decorticate cats, rhythmic 8- to 12-Hz waves which wax and wane in amplitude are recorded in the electrothalamogram (EThG). After six postoperative days, the spindle-like rhythms diminish. During waking irregular, low voltage waves occurring at frequencies of over 10 Hz are recorded in the EThG. During nonREM sleep the irregular waves in the EThG increase in voltage and became slower (2- to 6-Hz). Thus it was suggested that the thalamus is capable of generating at least some of the slow wave activity in the EEG.

Steriade et al. (1987) confirmed Villablanca's (1974) observation that slow wave activity in the EEG persists after removing thalamic influences. Knife cuts of the corona radiata, which severed corticothalamic connections, abolish cortical spindle bursts; however, synchronous 0.5- to 4-Hz slow waves persist in the EEG.

Andersson and Manson (1971) identified three patterns of synchronized thalamic slow wave activity in acute unanesthetized decorticate and decerebrate cats. The first pattern of activity recorded primarily from the ventrobasal complex, is characterized by 10- to 14-Hz spindles. The second pattern is characterized by long lasting irregular slow waves occurring at a frequency of 4- to 8-Hz. This pattern of activity is recorded primarily in the dorsolateral thalamus. The third pattern is most often recorded from the medial thalamic nuclei and consists of 8- to 12-Hz spindle bursts separated by periods of slower frequency (4- to 6-Hz) slow waves. These findings indicate that the

thalamus is capable of generating spindles as well as synchronized slow wave activity.

Jahnsen and Llinas (1984), by using a guinea-pig thalamic slice preparation, demonstrated that most thalamic neurons are endowed with intrinsic membrane properties which allow them to oscillate at frequencies of 9- to 10-Hz or 5- to 6-Hz. Thus each thalamic neuron is capable of operating as a single cell oscillator. The central feature of the proposed mechanism for the 5- to 6-Hz rhythmic discharge is the prolonged afterhyperpolarization following the spike burst. Increasing the level of hyperpolarization by synaptically generated IPSPs or by current injection de-inactivates a transient potassium (K⁺) current and a Ca⁺⁺-dependent K⁺ conductance, thus increasing the duration of the afterhyperpolarization. This in turn de-inactivates a low threshold Ca⁺⁺ conductance triggering a rebound low threshold spike burst which begins the cycle again. The time course (170 ms) of these events is responsible for the 5- to 6-Hz frequency oscillations.

METHODS AND PROCEDURES

A. General Procedures

Cats of either sex, weighing between 2.0 and 4.5 kg were used in these studies. The animals were initially anesthetized with ketamine hydrochloride (10 mg/kg, im) followed by intravenous alpha-chloralose (40 mg/kg, initial dose). The animals were paralyzed with gallamine triethiodide (4 mg/kg, iv) and artificially ventilated. The rate (12-20 strokes/min) and stroke volume (50-75 ml/stroke) of the respirator (Harvard model 607) were adjusted to mimic natural respiration. A bilateral pneumothoracotomy reduced respirator pump-related movements. Supplemental doses of chloralose and neuromuscular blocking agent were administered as required. Rectal temperature was maintained at 37+1°C by using a heat lamp. Blood pressure was monitored from either the femoral or brachial artery with a Statham transducer (Model P23AC) and displayed on a Grass polygraph (model 7D). Standard techniques were used to record lead II of the electrocardiogram (ECG). Drugs were administered through a cannula inserted in the femoral vein. In approximately 60% of the experiments, a solution of dextran (6% in saline) and norepinephrine (20 µg/ml) was infused through a femoral vein cannula to maintain mean arterial blood pressure at or above 100 mmHg. The cats were placed in a David Kopf Instruments stereotaxic apparatus and spinal investigation unit.

1. Baroreceptor denervation

In some experiments the baroreceptor nerves (carotid sinus, aortic depressor and cervical vagus nerves) were sectioned bilaterally. These nerves

were isolated from a ventral approach after reflecting the trachea and esophagus. The carotid sinus nerve was identified on both sides at its junction with the hypoglossal nerve. The cervical, vagus and aortic depressor nerves were isolated at a midcervical level. Denervation was deemed complete if 1) a sudden rise in blood pressure failed to inhibit reflexly inferior cardiac SND and 2) sympathetic slow wave activity was no longer locked in a 1:1 fashion to the cardiac cycle.

2. Nerve recordings

The left postganglionic inferior cardiac sympathetic nerve was isolated retropleurally at its exit from the stellate ganglion after removing the head of the first rib. The nerve was tied distal to the ganglion with saline-soaked silk thread. A loop was then tied in the thread and the nerve cut distal to the tie. Nerve activity was recorded monophasically after placing the silk loop on the indifferent pole and the proximal portion of the nerve on the central pole of a bipolar platinum electrode. To prevent drying, the nerve and ganglion were covered with an emulsion of silicone release agent (Dow Corning 7 Compound) and paraffin oil (Fischer Scientific Co.).

The left postganglionic renal sympathetic nerve was isolated retroperitoneally through an incision in the left flank. One of the branches was tied
with saline-soaked silk thread and cut between the tie and the nerve's junction
with the renal artery. A loop was then tied in the thread. Monophasic recordings
were made as just described. The abdominal skin flaps were secured to a frame in
order to form a pool which was filled with warm paraffin oil to cover the nerve.

Nerve activity was amplified by using a capacity-coupled preamplifier at a band pass of 1 to 1,000 Hz. This allowed the synchronous discharges of the sympathetic nerves to be viewed as slow waves (i.e. envelopes of spikes) on the polygraph and oscilloscope (see RESULTS; Figure 11).

Electrical cortical activity (electroencephalogram, EEG) was recorded monophasically between a gold plated electrode (Grass Instruments, Model E4G) affixed to the frontal bone and a indifferent electrode (an alligator clip) attached to reflected scalp muscle. Cortical activity was preamplified using a band pass of 1 to 1,000 Hz and displayed on a polygraph and oscilloscope.

3. Electrical stimulation of the diencephalon and cortex

Square wave pulses (10-ms trains of three pulses or single shocks) were delivered to selected sites in the diencephalon and frontal-parietal cortex by using a Grass S88 stimulator connected to a Grass PSIU-6 constant current unit. Stimuli were passed through either concentric bipolar electrodes, 0.25 mm exposed tip (Rhodes Medical Instruments, Model NE-100) or etched monopolar tungsten microelectrodes (10-30 kilo ohm tip impedance). In the latter case, the anode (an alligator clip) was attached to reflected scalp muscle. Stimulus current was measured by monitoring the voltage drop across a 100 ohm resistor in series with the anode. Potentials evoked on sympathetic nerves by stimulation of the diencephalon and cortex were computer averaged (Nicolet, Model 1070; see section B.4), displayed on an oscilloscope and photographed.

4. Histology

The diencephalon and in some cases the brain stem were removed and placed in 10% buffered formalin for a period of at least 7 days. In decerebration studies the completeness and level of midbrain transection was verified by gross inspection of the brain stem and microscopic evaluation of frontal sections of 30
µm thickness stained with cresyl violet. Transection at stereotaxic plane A3 was at a level approximately midway between the rostral and caudal borders of the superior colliculus. Transection at stereotaxic plane A0 was near the midcollicular level. Only those experiments in which the transections were complete and the planes of transection were within +0.5 mm of the A3 and APO planes of Jasper

and Ajmone-Marsan (1954) are included in the RESULTS. To identify unit (or multiunit) recording sites and stimulation sties, frontal sections (30-µm thickness) of the diencephalon were cut on a cryostat microtome and stained with cresyl violet. Diencephalic lesions were reconstructed by projecting serially arranged frontal sections onto the stereotaxic planes of Jasper and Ajmone-Marsan (1954). Sites of stimulation and unit recording in the diencephalon were also reconstructed from stained frontal sections. Since I recorded the depth of all stimulation and recording sites for each electrode penetration, these sites were reconstructed using the end of the tracks as reference points. Shrinkage during fixing was taken into account.

B. Data Analysis

Data were analyzed either on- or off-line. On-line analysis used a Nicolet MED-80 computer. Off-line analysis from magnetic tape was performed by using either a Nicolet MED-80 computer or an RC Electronics Computerscope System. For this purpose arterial pressure, neural activity and pulses derived from the R wave of the ECG or stimuli applied to the neuraxis were stored on magnetic tape. The data from tape were analyzed after passing SND, EEG and diencephalic multiunit activity through an A.P. Circuit Corp. variable filter with the low pass cut-off frequency set at 50 Hz. The following methods of analysis were used.

1. Quantification of SND and blood pressure

In Projects A and D, after preamplification the sympathetic nerve signal was led to a Grass 7P10 cumulative integrator. Raw and integrated SND were displayed on a polygraph (see RESULTS; Figure 4). Changes in integrated SND were quantified by comparing mean epoch length (integrated records). Corrections were made for the integration of noise. The noise level was measured following ganglionic blockade with hexamethonium chloride (5 mg/kg, iv). Mean

blood pressure was calculated from pulsatile records of blood pressure recorded on the polygraph. The mean blood pressure (BP) was calculated using the formula:

$$BP = Pd + 1/3 (Ps - Pd)$$

where Pd is the diastolic pressure and Ps is the systolic pressure.

2. Crosscorrelation and autocorrelation analysis

Autocorrelation was used to extract the rhythmic components in inferior cardiac SND, EEG, and thalamic and hypothalamic multiunit activity. Forty seconds of data were analyzed. Crosscorrelation analysis was used to determine whether SND, multiunit diencephalic activity and the EEG contained common components that were temporally correlated. Normalized crosscorrelation functions [Rxy(T)] N were calculated by using the formula:

$$[Rxy(T)]N = \frac{Rxy(T)}{\{Rxx(O)Ryy(O)\}}$$
 {} = square root

where Rxy(T) is the nonnormalized crosscorrelation function in watts (voltage squared); x and y are the input signals; T is the lag in the crosscorrelation function; Rxx(0) and Ryy(0) are values (in watts) at zero lag in the nonnormalized autocorrelograms. The resolution was 20 ms and 10 ms for the crosscorrelation and autocorrelation analysis.

3. Post-R wave interval analysis

Trigger pulses coincident with the R wave of the ECG were used to construct normalized averages (minimum of 500 trials) of the arterial pulse wave, inferior cardiac SND, EEG and diencephalic multiunit activity. Post-R wave interval histograms of unit discharge were also constructed. These analyses revealed whether SND, EEG, multiunit diencephalic activity and diencephalic unit discharges were temporally related to the cardiac cycle.

4. Post-stimulus analysis

Trigger pulses coincident with stimuli delivered through metal electrodes in the diencephalon or cortex were used to construct normalized averages of evoked responses in the inferior cardiac nerve and histograms of unit responses. From these averages the modal onset latency of synaptic activation or inhibition of the neuron and onset latency and time to peak of the evoked sympathetic nerve response were calculated.

5. Power spectral density analysis

This analysis, performed by fast Fourier transform (Bendat and Piersol, 1971), was used to examine the frequency components and relative power (in watts) of each frequency band in SND, EEG and diencephalic activity. Power is plotted against frequency. Aliasing of high frequency components into the 0- to 15-Hz frequency bands was prevented by filtering the signals (15 Hz low pass cutoff) prior to analysis. Spectra were constructed by averaging six 20-s data blocks. The resolution of the analysis was 0.1 Hz.

6. Peri-spike-trigger averaging

Normalized averages (minimum of 500 trials) of SND and EEG activity were acquired before and after the spike trigger (a naturally occurring unit spike). For this purpose, the unit discharge was passed through a window discriminator. A standardized pulse coincident with unit spike occurrence was used to trigger computer sweeps. The portion of the average to the left of time zero was computed from data that preceded the spike trigger, while the second half (right 0 lag) represents data that followed the spike. Thus it was possible to determine whether the activity of the neuron was temporally related to changes in SND or EEG which preceded or followed its discharge. A random pulse train with about the same frequency as the neuronal spike train was used to trigger a "dummy" average of SND and EEG. Neurons were considered to have sympathetic nerve-

related and/or EEG-related activity if the amplitude of the first peak to the right of time zero in the spike-triggered averages of SND and EEG exceeded by at least a factor of three that of the largest deflection in the "dummy" averages.

7. Interspike interval analysis

This routine constructs a histogram of the distribution of the intervals between consecutive spontaneously occurring neuronal spikes. A minimum of 500 spikes are used. This method was used to calculate the mean frequency of discharge of the individual diencephalic units as well as to gain information on the periodic components in the spike train.

8. Statistical analysis

Data are expressed as mean \pm S.E. The Student's t-test was used to compare changes in mean blood pressure between lesioned and nonlesioned groups. Changes in mean SND between lesioned and nonlesioned groups were compared using the Students's t-test after transforming the data using arcsin square root transformation. A random block design analysis of variance (ANOVA) was used to analyze the effect of time on mean blood pressure after midbrain transection. The least significant difference test (LSD) was used for individual comparisons. Regression analysis was used to compare the intervals between the spontaneous unit spike to peak SND and stimulus to peak SND intervals in the spike-triggered averages of diencephalic neurons with activity related to SND. In all cases, a 95% confidence level was used as a criteria for significance.

C. <u>Project A:</u> Experiments Involving Midbrain Transection and Radio-frequency Lesions

1. Decerebration procedures

Following removal of the appropriate portions of the parietal bone and dura mater, serial transections at stereotaxic planes A3 and AP0 were made with spatulas constructed so that their diameters and contours corresponded with those

of the left and right halves of the midbrain. The spatulas were held in a stereotaxic electrode manipulator. Left and right hemisections were performed sequentially at each stereotaxic plane. The two-stage transection was completed within 90 s without excessive bleeding or subsequent swelling of the brain stem. The experiment was terminated on those rare occasions when transection caused excessive bleeding or swelling of the brain.

2. Radio-frequency diencephalic lesions

Diencephalic lesions were made bilaterally with a radio-frequency generator (Radionics Inc., Model RFG-4). An unmodulated sine wave (500 Hz) was passed through an electrode (0.7 mm tip diam; 1.5 mm uninsulated tip length) stereotaxically placed into the diencephalon. Current was adjusted to maintain the temperature of the tissue contacting the thermal sensing electrode tip at 75°C for 1 min. A lesion of 1-2 mm in diameter was produced at each site of current application.

3. Data analysis

Changes in SND and blood pressure were quantified as described in section B.1. The level of activity during the 5-min period before midbrain transection was compared with that during the first 2-min period, the following 3-min period and then during subsequent 5-min periods after midbrain transection. Either mean blood pressure or change in mean blood pressure was plotted at these specified intervals following midbrain transection.

4. Histology

The completeness and level of transection were verified and lesions reconstructed as described in section A.4.

D. Project B: Multiunit Diencephalic Activity

CNS-intact or decorticate cats with intact or sectioned baroreceptor nerves were used in this study. Portions of the parietal bone and underlying dura were removed bilaterally providing access to the diencephalon. The exposed neural tissue was covered with paraffin oil to prevent drying. In those instances in which decortication was performed, the skull was removed from the coronal suture to the lambdoidal suture in a rostral caudal direction and bilaterally as close to the squamosal suture as possible. Decortication was performed in two steps. First, a bilateral frontal lobotomy was performed 1 mm caudal to the ansate sulcus. Second, the cortex, hippocampus, corpus callosum and fornix surrounding the diencephalon and basal ganglia were removed by suction under visual observation with 6X magnification. The completeness of decortication was evaluated by gross inspection and subsequent examination of histological sections. In two cases there was damage to the anterior portions of the caudate and in all cases a small portion of the pyriform cortex remained connected to the diencephalon.

1. Multiunit diencephalic recordings

Multiunit activity in the thalamus and hypothalamus was recorded (capacity-coupled preamplifier band pass, 1 to 1,000 Hz) by using concentric bipolar stainless steel electrodes (Rhodes Medical Instruments, Model NE-100) with exposed leads (0.5 mm) separated by 0.5 mm. The electrodes were placed stereotaxically into the diencephalon according to the coordinates of Jasper and Amjone-Marsan (1954). The multiunit thalamic and hypothalamic activity was displayed on the polygraph and oscilloscope.

2. Electrical and chemical stimulation of the diencephalon

The diencephalon was electrically stimulated and sympathetic potentials averaged as described in section B.4. In a series of experiments, chemical stimulation was accomplished by microinjecting the GABA antagonist picrotoxin

(5 µg in 0.5 µl saline) bilaterally over a 2 minute period into selected thalamic sites by using a 26 gauge needle attached to a 10 µl Hamilton syringe. The needle was placed stereotaxically according to the coordinates of Jasper and Amjone-Marsan (1954).

3. Data analysis

The following methods of computer analysis were used: 1) crosscorrelation and autocorrelation analysis. 2) Post-R wave interval averaging. 3) Power spectral density analysis. 4) Post-stimulus averaging. The methodology and application of these analyses are described in section B.

E. <u>Project C</u>: Characterization of Diencephalic Neurons with Sympathetic Nerve-related Activity

1. Diencephalic unit recordings

Metal microelectrodes (Frederick Haer, 2-µm tip diam, 2-3 mega ohm tip impedance, 0.5 mm exposed tip length) were used to record extracellularly the action potentials of thalamic and hypothalamic neurons from the left side of the diencephalon in baroreceptor-innervated cats. The indifferent electrode was a gold-plated disc affixed to the frontal bone. Capacity coupled preamplification with a band pass of 0.3-3 KHz was used. The position of the recording electrode was controlled by using a David Kopf Instruments stepping hydraulic microdrive. Stereotaxic placement of the electrodes was made according to the coordinates of Jasper and Ajmone-Marsan (1954). The unitary nature of the recordings was judged on the basis of the constancy of action potential shape, amplitude and duration. For units which discharged as high frequency bursts, the comparison was made for the first spike in successive bursts. The majority (60%) of unit recordings were from the soma-dendritic region of the neurons. This was indicated by the presence of an inflection on the rising phase of the action

potential (see RESULTS; Figure 22B2, C2). These inflections likely reflect separation of the action potentials of the axon hillock and the soma dendritic region (Coombs et al., 1957).

2. Electrical stimulation

A Grass S88 stimulator and a PSTD-6 stimulus isolation unit were used to deliver square wave pulses (90-800 µA, 1.0 ms duration) to selected recording sites in the thalamus and hypothalamus. Stimuli were passed through the recording microelectrode. The strength of the stimulus was measured as described in section A.3.

3. Effect of baroreceptor reflex activation

Baroreceptor reflex activation was produced by either the bolus injection of norepinephrine bitartrate (1-2 µg/kg, iv) or by inflating the ballcontipped end of a catheter (Fogerty embolectomy catheter, Model 12 A-100-4F) placed into the abdominal acrta via the femoral artery. The firing rate of selected thalamic and hypothalamic neurons was assessed during baroreceptor-induced reflex inhibition of SND. These procedures do not affect unit activity or SND in baroreceptor-denervated cats (Barman and Gebber, 1987).

4. Data analysis

The following methods of computer analysis were used: 1) Peri-spike-triggered averaging. 2) Interspike interval analysis. 3) Post-R wave interval analysis. 4) Post-stimulus averaging and histogram construction. 5) Autocorrelation analysis. The methodology and applications of these analyses are discussed in section B.

F. Project D: Sympathetic Responses Elicited by Cortical Stimulation

Experiments were performed on baroreceptor-intact and -denervated cats.

Baroreceptor denervation was performed as described in section A.1. In four

animals the meninges on the left cerebral hemisphere were deafferentated by sectioning the left trigeminal nerve at a point between the medulla and the sensory ganglion. The trigeminal nerve was exposed by removing portions of the occipital and basisphenoid bones and the tympanic bulla. EEG activity was recorded using either a plate electrode (as described in section A.3) or a wick electrode. Wick electrodes consisted of a small (2x6 mm) piece of cotton wrapped with silver wire. The electrode was then soaked in saline and placed directly on the cortical surface. The indifferent lead was an alligator clip placed on crushed scalp muscle.

1. Electrical stimulation of the cortex

The prefrontal and sensorimotor cortex was exposed bilaterally by removing the appropriate portions of the frontal and parietal bones and dura mater as described in section C.1. The exposed cortex was covered with warm paraffin oil. Electrical stimuli were applied to the cortex using procedures described in section A.3.

2. Diencephalic unit recordings

In some experiments the action potentials of medial thalamic neurons with sympathetic nerve-related activity were recorded. The responses of these neurons to cortical stimulation were recorded on magnetic tape for later off-line construction of post-stimulus histograms (see section B.4).

3. Data analysis

Computer-aided analyses and changes in blood pressure and inferior cardiac SND before and after lobotomy and A3 transection were quantified as described in sections B and C.3.

G. Drugs Used

The following drugs were used in this study. alpha-chloralose (Sigma), gallamine triethiodide (Lederle), hexamethonium chloride (Mann Research Laboratories), atenolol (Sigma) and picrotoxin (Sigma).

RESULTS

L Identification of diencephalic regions contributing to SND

Huang et al. (1987) reported that decerebration in the anesthetized cat produces transient (<30 min) decreases in inferior cardiac postganglionic SND (reduced to 62±7% of control) and blood pressure (33±4 mmHg). Three observations led Huang et al. to conclude that the transient effects of midbrain transection (i.e., decerebration) reflect the loss of a forebrain-dependent component of SND in the anesthetized cat rather than a nonspecific phenomenon such as generalized trauma or the mechanical stimulation of a descending sympathoinhibitory system. First, following recovery from the effects of decerebration, a second transection more caudally in the midbrain (APO) fails to affect SND and blood pressure. Second, crosscorrelation analysis revealed that a component of SND is synchronized to frontal-parietal cortical activity only in those experiments in which subsequent midbrain transection reduces SND > 30%. Third, the effects of the initial transection are prevented by prior removal of the hypothalamus and those medial thalamic nuclei located 0 to 4 mm lateral to the midline.

The diencephalic lesions made by Huang et al. were extensive. Thus, the purpose of my first set of experiments was to localize those regions of the hypothalamus and/or medial thalamus responsible for the forebrain-dependent component of SND. For this purpose, the effects of midbrain transection on SND and blood pressure in nonlesioned control cats were compared with those in cats in which selective diencephalic lesions were made with radio-frequency current.

Figure 1 shows examples of histological sections used to reconstruct the diencephalic lesions made in these experiments. The lesions in panels A, B, and C were in the lateral hypothalamic region, the posterior hypothalamic region and the medial thalamus, respectively.

A. Midbrain transection in nonlesioned cats

The effects of midbrain transection on inferior cardiac SND and mean blood pressure in 23 nonlesioned baroreceptor-denervated cats are summarized in Figure 2A and B, respectively. SND was reduced to 65±5% of control and mean blood pressure was reduced 35±3 mmHg in the first 2 min after midbrain transection at A3. These changes were statistically significant. There was a tendency for recovery toward control levels, however, in contrast to the results of Huang et al. (1987) SND and blood pressure were still significantly reduced at the end of the 30 min observation period.

In six of the 23 nonlesioned cats, renal as well as inferior cardiac SND were recorded. As shown in Figure 3, A3 midbrain transection produced parallel changes in renal and inferior cardiac SND. Figure 4 shows the polygraph records of raw and integrated SND and blood pressure from one of the six experiments in this series. The reductions in SND and blood pressure produced by A3 transection are shown in panel A. Subsequently, hexamethonium (5 mg/kg, iv) was used to produce ganglionic blockade (panel B).

B. Anterior medial hypothalamic lesions

Lesions placed in the anterior medial hypothalamus failed to attenuate significantly the decreases in inferior cardiac SND and blood pressure produced by midbrain transection (Figure 2). A3 transection was performed one hour after completion of the lesions. Mean blood pressure (111±4 mmHg) just prior to midbrain transection in these six experiments was not different from that (109±4 mmHg) in the 23 nonlesioned control cats.

Figure 1. Representative histological sections showing lesions of lateral hypothalamus (A), posterior hypothalamus (B) and medial thalamus (C). Each section is from a different cat. Calibration is 2 mm.

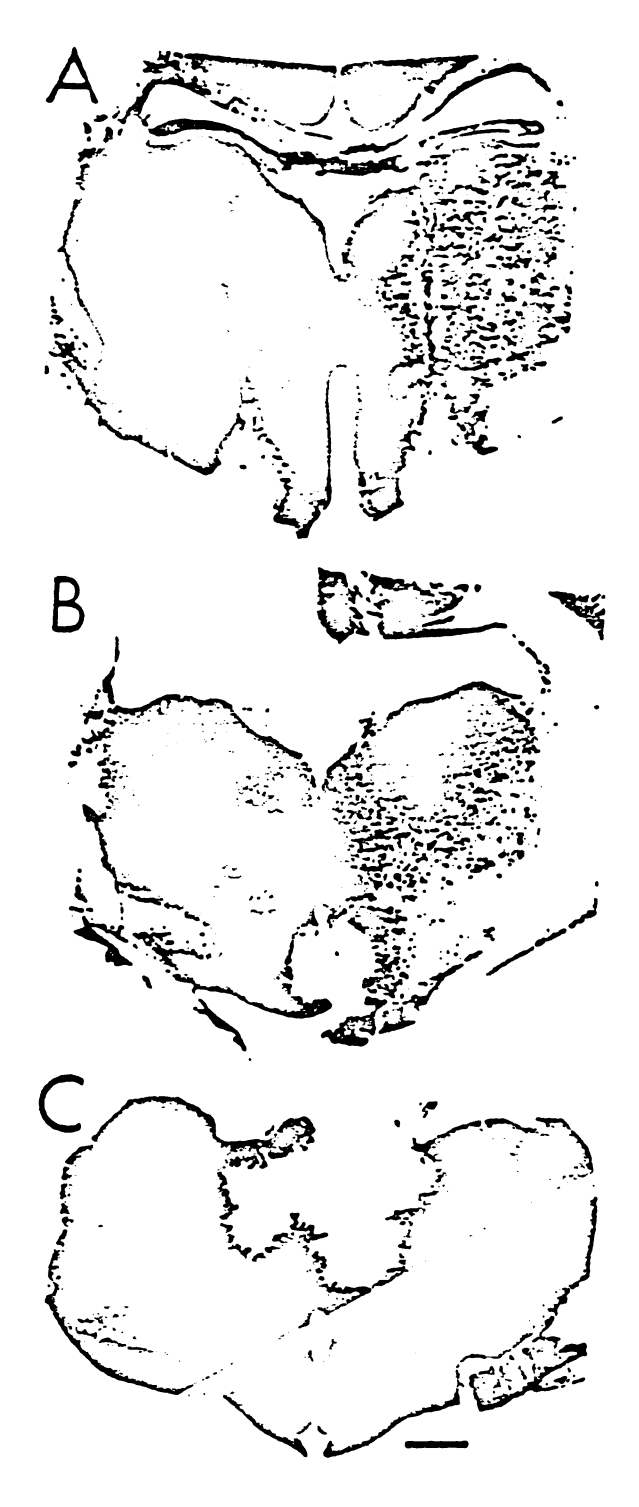


Figure 1

Figure 2. Comparison of effects of midbrain transection on inferior cardiac sympathetic nerve discharge (SND) and mean blood pressure (BP) in nonlesioned control cats (n=23) with those in cats with anterior medial hypothalamic (n=6) or large medial hypothalamic (n=7) lesions. All cats were baroreceptor-denervated and anesthetized with alphachloralose. Changes in SND (% of control) in panel A were quantified by comparing mean epoch length (integrated records) during 5-min period before transection with that during the first 2-min period, the following 3-min period, and then during subsequent 5-min periods after midbrain transection. Change in BP (mmHg) is shown. *Denotes a statistically significant difference from corresponding data point on control curve. Values are means ± SE.

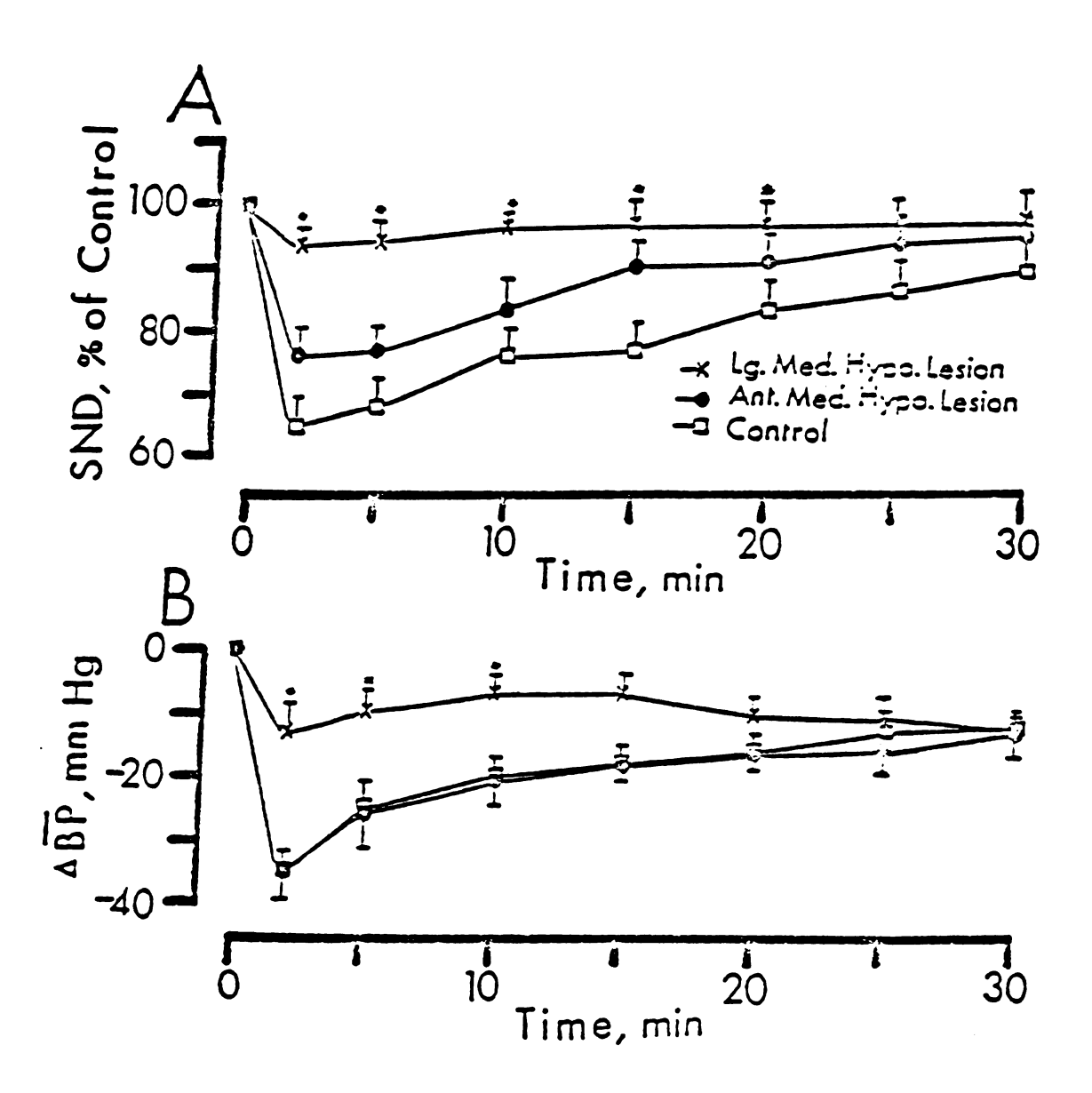


Figure 2

Figure 3. Effect of midbrain transection on inferior cardiac (ICN) and renal (RN) sympathetic nerve discharge (SND), and mean blood pressure (BP) in 6 nonlesioned baroreceptor-denervated cats anesthetized with chloralose. SND was quantified as described for Figure 2. BP (mmHg) is plotted against time after transection (panel B). Values are means + SE. *Denotes a statistically significant difference from pretransection level.

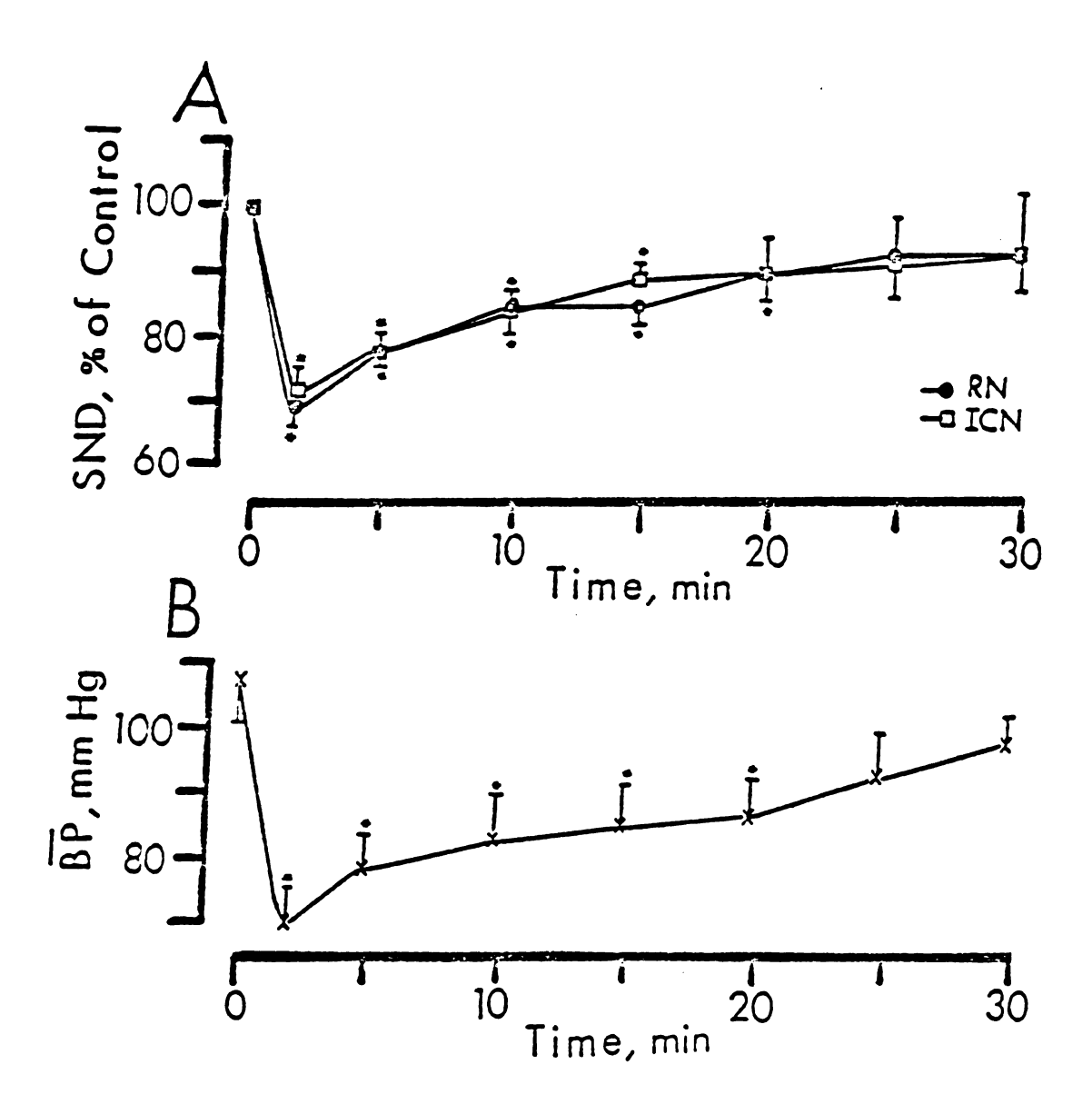
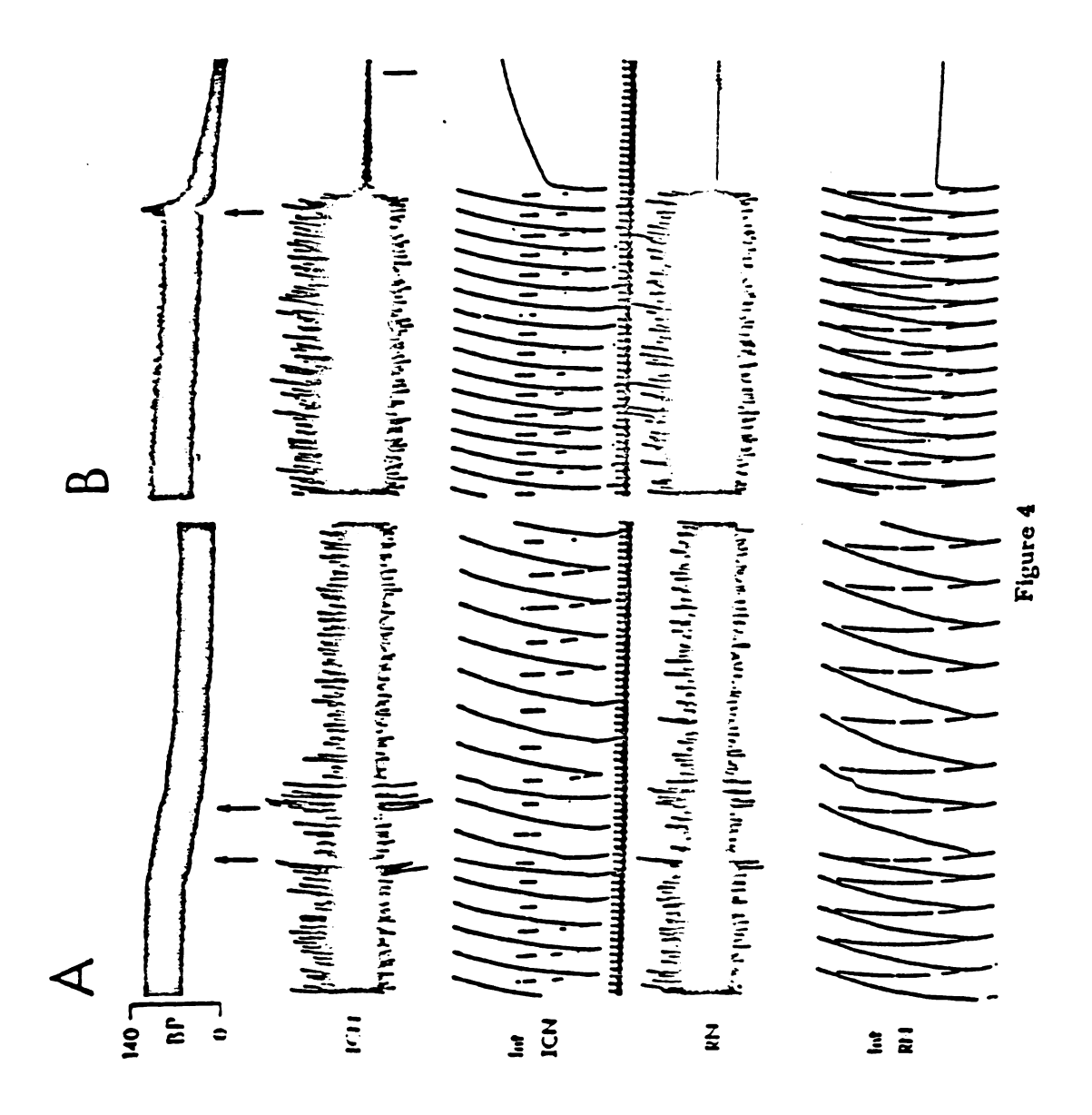


Figure 3

cat ancethetized with chloralose. Raw and integrated records of sympathetic nerve activity are shown. Arrows in panel A mark left then right hemisection. Arrow in B marks injection of hexamethonium chloride (5 mg/kg, iv) 1 hr after midbrain transection. Vertical calibration is 75 µV for ICN and 125 µV for RN. Time base is 5 s per division. Figure 4. Effects of midbrain transection at stereotaxic plane A3 (A) and ganglionic blockade (B) on blood pressure (BP), inferior cardiac (ICN) and renal (RN) sympathetic nerve discharge in a nonlesioned baroreceptor-denervated



The extent of the anterior medial hypothalamic lesion shown in Figure 5 is typical for this series of experiments. This lesion destroyed most of the paraventricular hypothalamic nucleus (PVH) and n. filiformis (Fil), and a small portion of the dorsal hypothalamic area (aHd) between stereotaxic planes All and Al3. There was minimal involvement of the posterior hypothalamic (Hp) and anterior hypothalamic (Ha) nuclei. A small portion of the fornix (Fx) on the right side was destroyed in this particular experiment.

C. Large medial hypothalamic lesions

More extensive lesions of the medial hypothalamus attenuated the decreases in inferior cardiac SND and blood pressure produced by midbrain transection. Thus large medial hypothalamic lesions attenuated the forebrain-dependent component of SND. The reductions in SND and blood pressure were significantly smaller in these seven experiments than in nonlesioned animals during the first 20 min and 10 min, respectively, after midbrain transection (Figure 2). The absence of significant differences beyond 20 min reflects the rapid, although partial recovery of SND and blood pressure towards control levels following midbrain transection in nonlesioned cats. Mean blood pressure (107±5 mmHg) just prior to midbrain transection in this series of experiments was not different from that in nonlesioned cats. Thus, it appears that between 30 and 60 min were required for complete recovery from the loss of the forebrain-dependent component of SND produced by either midbrain transection or diencephalic lesions.

The extent of the large medial hypothalamic lesion shown in Figure 6 is typical for this series of experiments. In addition to PVH and Fil in the anterior medial hypothalamus, large portions of aHd, posterior hypothalamic (Hp) and the ventromedial hypothalamic (NHvm) nuclei were destroyed at more posterior

traces. Stereotaxic planes and abbreviations (top) are as defined by Jasper and Ajmone-Marsan (1954). aHd, area hypothalamica dorsalis; AM, N. anterior medialis; AV, N. anterior ventralis; CC, corpus callosum; Cd. N. caudatus; Cl, capsula interna; CL, N. centralis lateralis; En, N. entopeduncularis; Fil., N. filiformis; Fx, fornix; Ha, hypothalamus anterior; HL, hypothalamus lateralis; Hp, hypothalamus posterior; Hvm, hypothalamus ventromediaventromedialis; PVII, N. paraventricularis hypothalami; R, N. reticularis; RE, N. remiens; Rh, N. rhomboidens; Figure 5. Representative lesion in anterior medial hypothalamus. Extent of lesion is shown in black on bottom lis; IAM, N. interanteriormedialis; MD, N. medialis dorsalis; MFB, medial forebrain bundle; NHvm, N. hypothalami TO, tractus opticus; VA, N. ventralis anterior; VL, N. ventralis lateralis; VM, N. ventralis medialis; VPL, N. ventralis posterolateralis. Calibration is 2 mm.

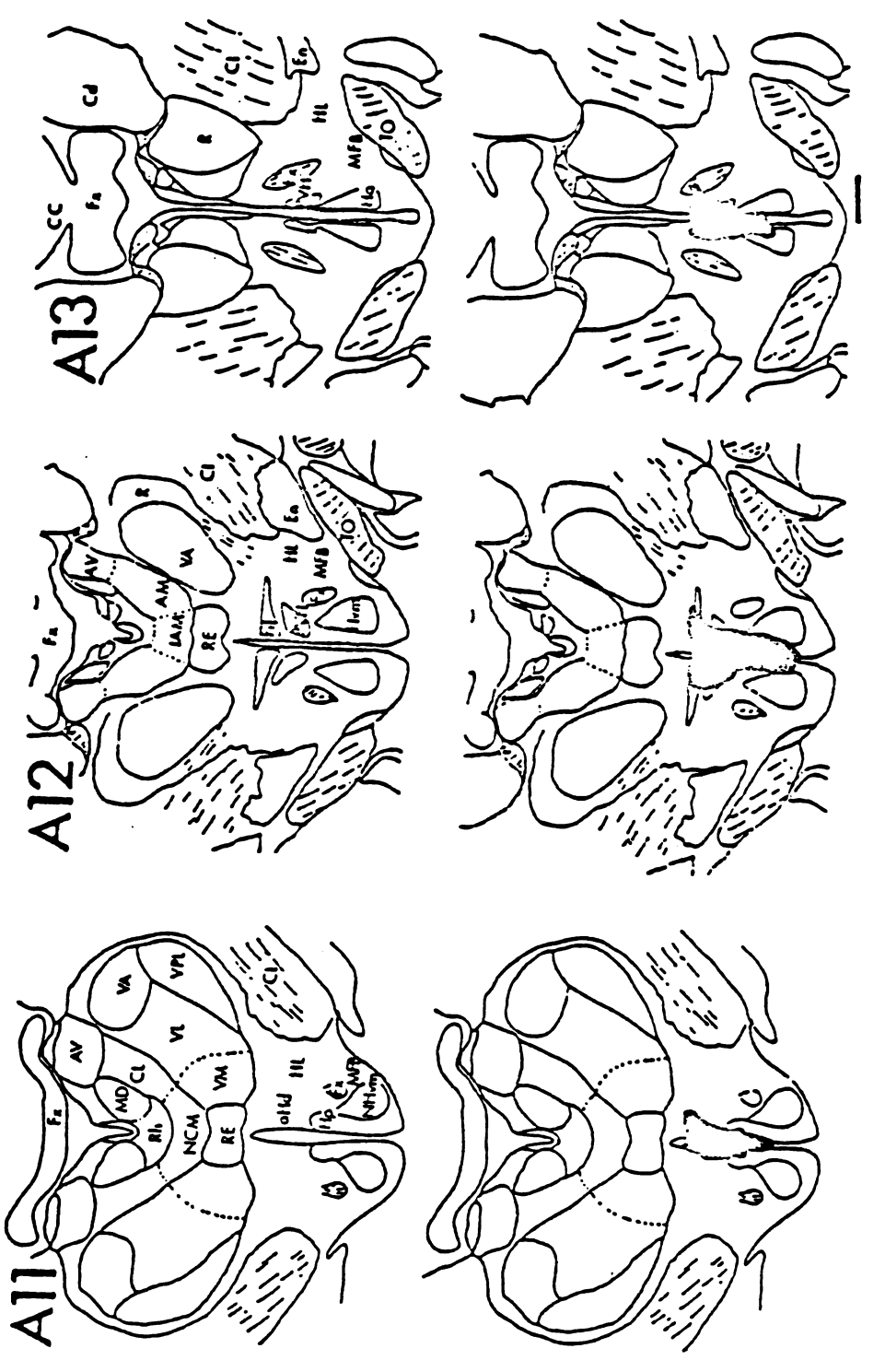


Figure 5

Figure 6. Representative large lesion in medial hypothalamus. Abbreviations are as in Figure 5 with the addition of III, H2, Forel's fields; LD, N. lateralis LP, N. lateralis posterior; Mm, Corpus mammillare; NCM, N. centralis medialis, Pc paracentralis; Ped, Pedunculus cerebralis; VPM, N. ventralis posteromedialis; ZI, zona incerta. Calibration is 2 mm.

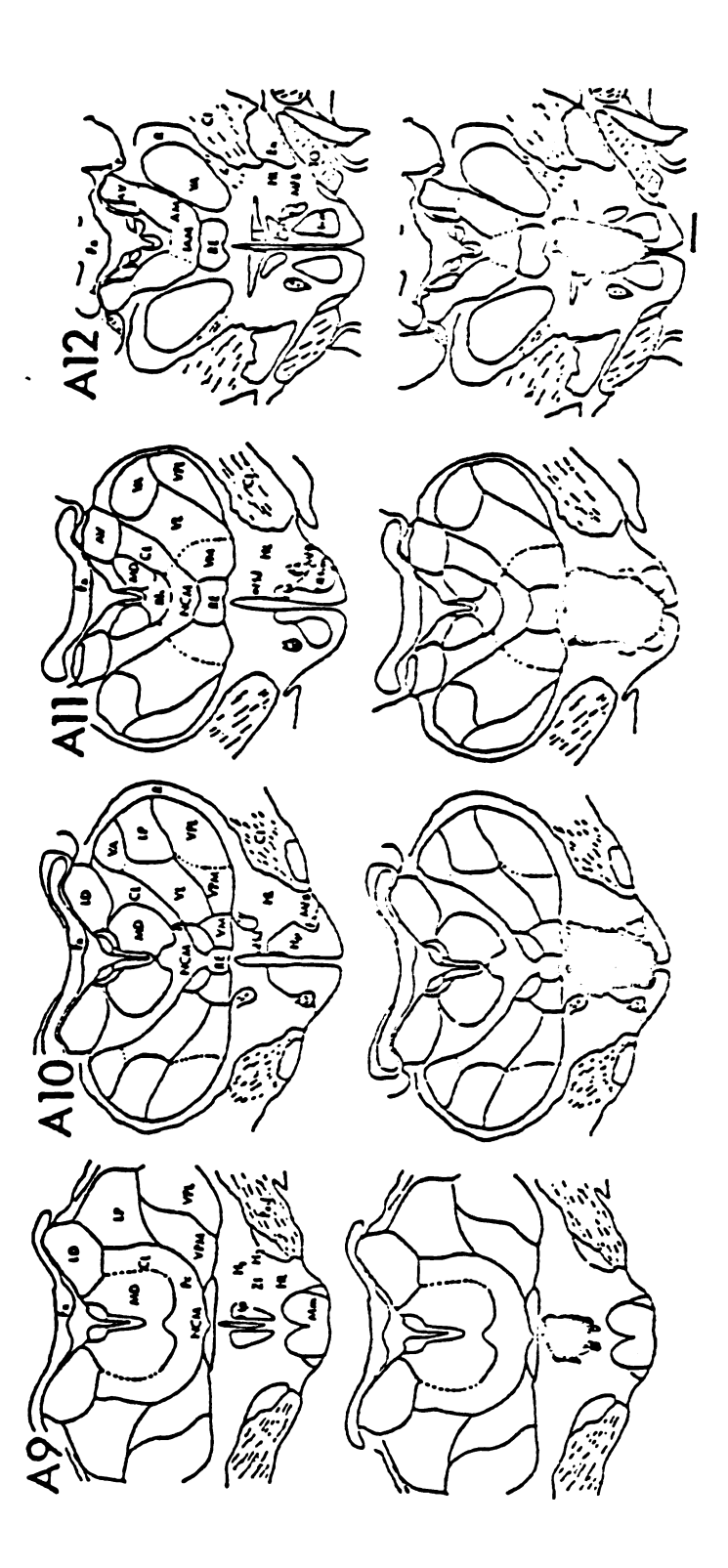


Figure 6

levels. Large medial hypothalamic lesions did not extend into the thalamus nor did they involve the medial forebrain bundle (MFB).

D. Lateral hypothalamic lesions

Lesions placed in the lateral hypothalamic region between stereotaxic planes A9 and A11 attenuated the decreases in inferior cardiac SND and blood pressure produced by midbrain transection. As shown in Figure 7, the reduction in SND was significantly less in these 12 experiments than in nonlesioned cats during the first 15 min after midbrain transection. The decreases in blood pressure were significantly different during the first 10 min after midbrain transection. Mean blood pressure (111±6 mmHg) just prior to midbrain transection in cats with lateral hypothalamic lesions was not different from that of nonlesioned cats.

The extent of the lateral hypothalamic lesion in Figure 8 is typical for this series of experiments. The lesion included portions of the lateral hypothalamic nucleus (HL), H1, H2, ZI and the MFB. The H1, H2 and ZI are considered as part of the hypothalamus rather than the subthalamus in this thesis.

E. Medial thalamic lesions

Lesions of the medial thalamus (0 to 3.5 mm lateral to the midline) between stereotaxic planes A7 and A11 also attenuated the decreases in inferior cardiac SND and blood pressure produced by midbrain transection. As shown in Figure 9, the reduction in SND was significantly less in these seven experiments than in nonlesioned animals during the first 15 min after midbrain transection. The decreases in blood pressure were significantly different only at 2 min after midbrain transection. Mean blood pressure (114+8 mmHg) just prior to midbrain transection in cats with medial thalamic lesions was not different from that in nonlesioned cats.

A typical medial thalamic lesion is shown in Figure 10. The lesion included most of the medial dorsal nucleus (MD), n. rhomboidens (Rh) and the

Figure 7. Comparison of effects of midbrain transection on inferior cardiac sympathetic nerve discharge (SND) and mean blood pressure (BP) in nonlesioned control cats (n=23) with those in cats with lateral hypothalamic lesions (n=12). Same format as in Figure 2. *Denotes a statistically significant difference from corresponding data point on control curve. Values are means \pm SE.

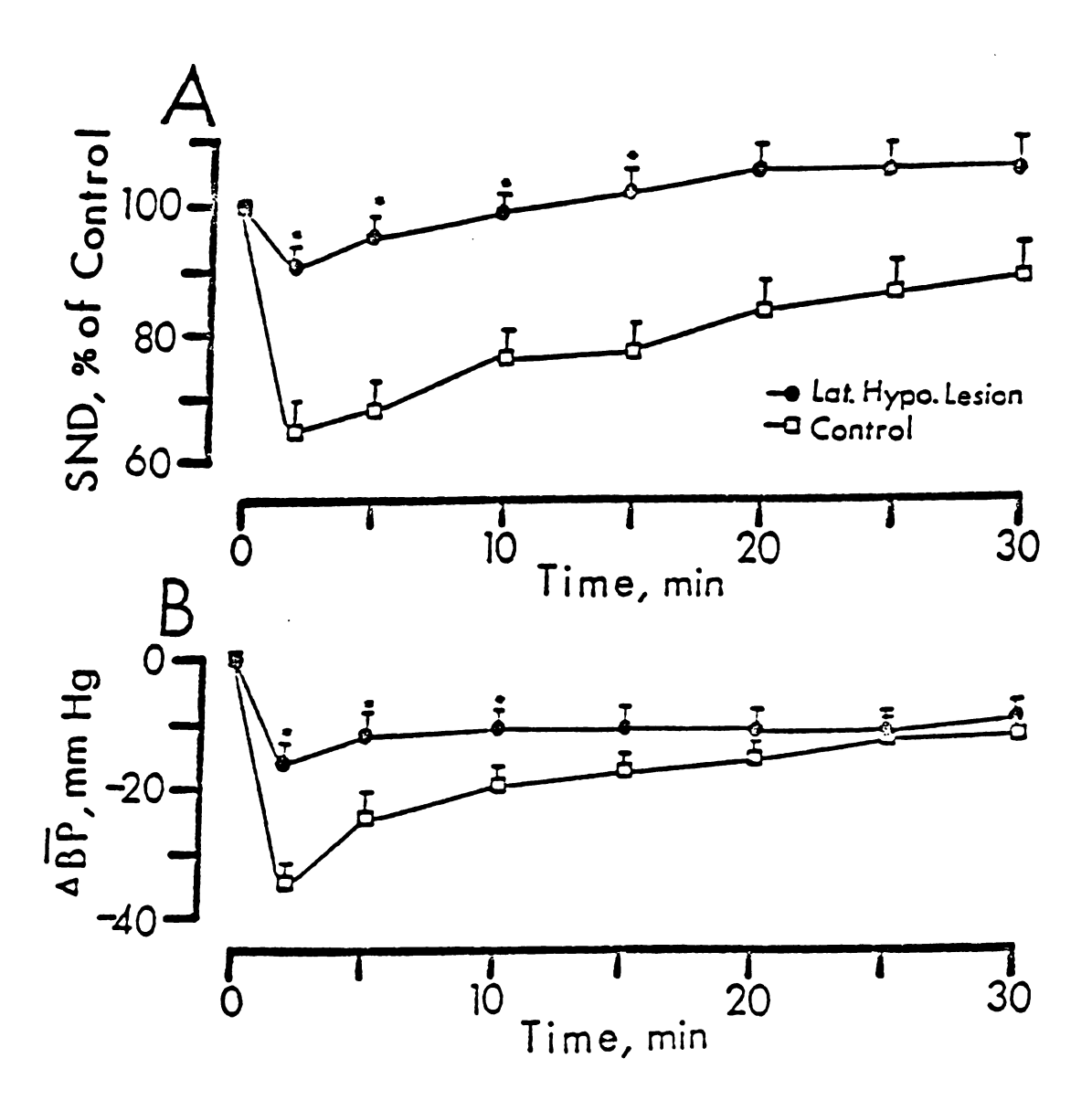


Figure 7

Figure 8. Representative lateral hypothalamic lesion. Abbreviations are as in Figures 5 and 6. Calibration is 2 mm.

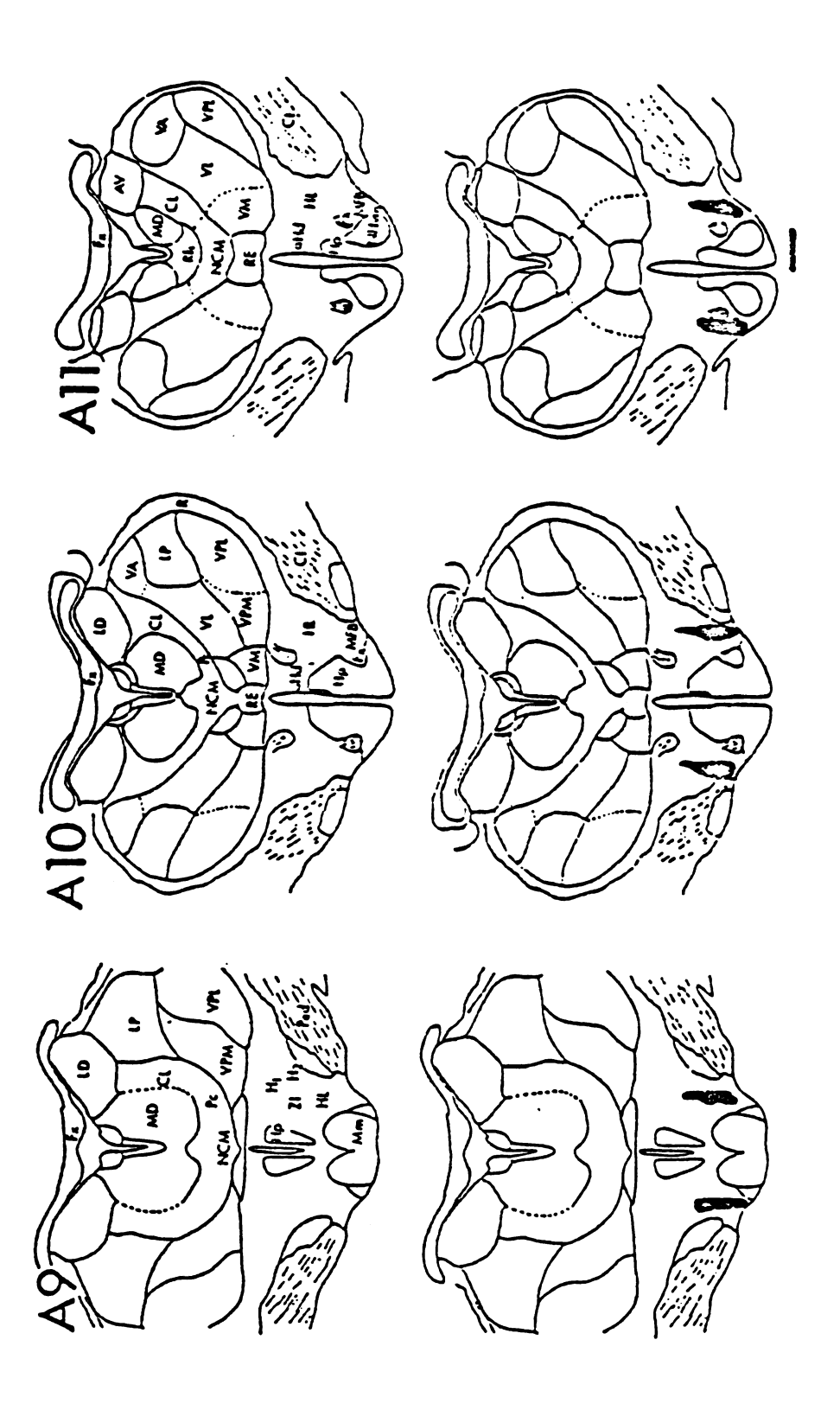


Figure 8

Figure 9. Comparison of effects of midbrain transection on inferior cardiac sympathetic nerve discharge (SND) and mean blood pressure (BP) in nonlesioned control cats (n=23) with those in cats with medial thalamic lesions (n=7). Same format as in Figure 2. *Denotes a statistically significant difference from corresponding data point on control curve. Values are means \pm SE.

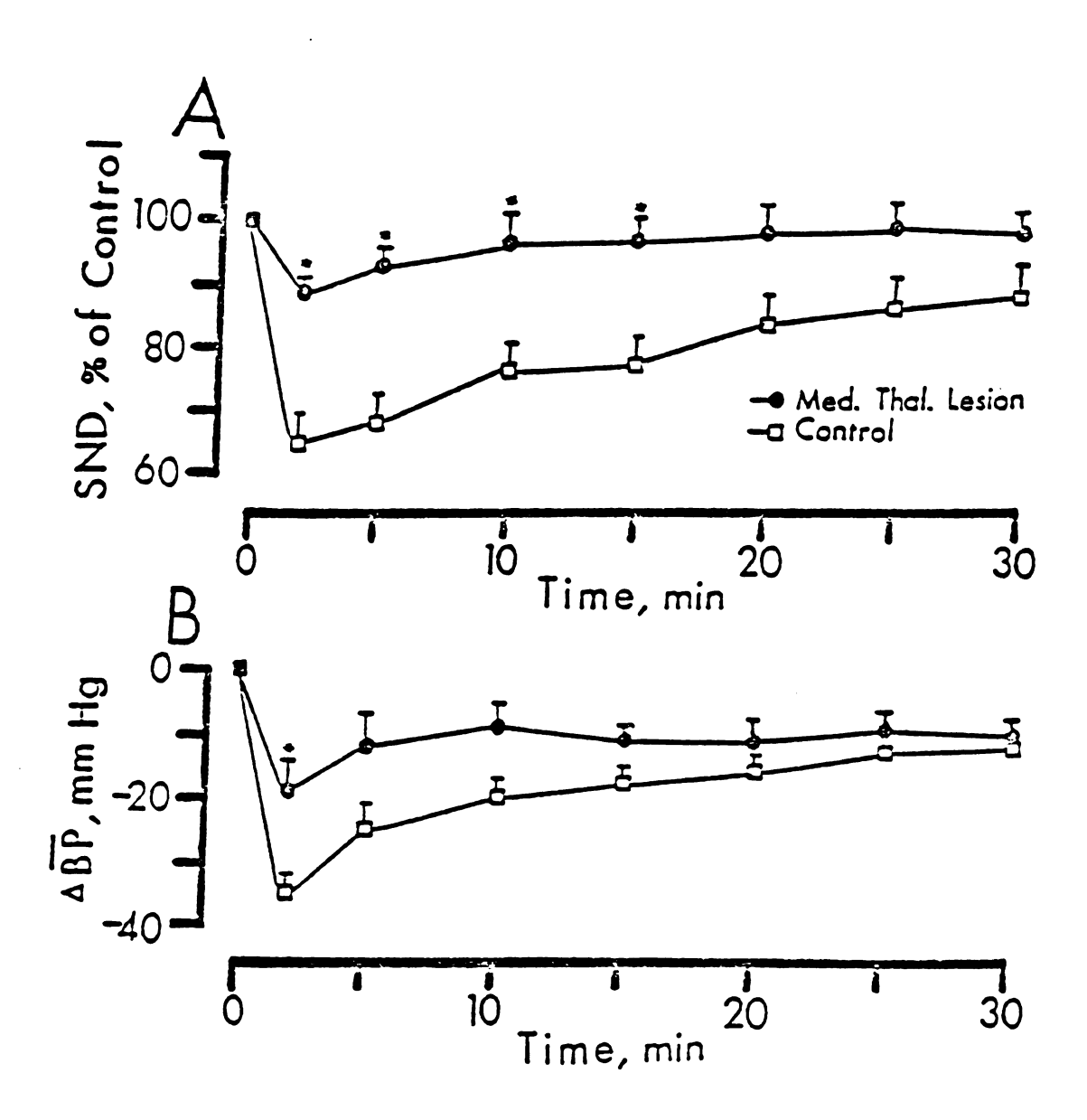


Figure 9

Figure 10. Representative medial thalamic lesion. Abbreviations are as in Figures 5 and 6 with the addition of; CM, N. centrum medianum; HbL, N. habenularis lateralis; NR, N. ruber; Pf, N. parafascularis. Calibration is 2 mm.

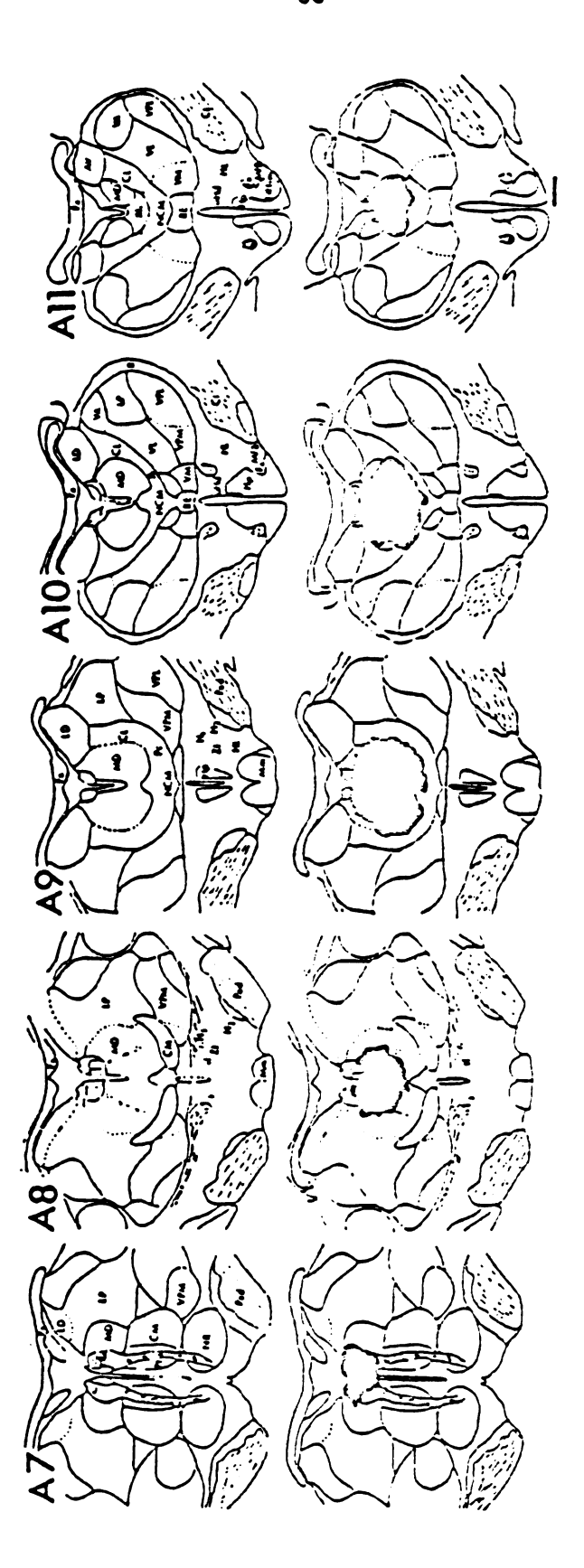


Figure 10

lateral habenula (HbL). In addition, portions of the following intralaminar nuclei were destroyed: centralis lateralis (CL), centralis medialis (NCM), and paracentralis (Pc). Although extensive, medial thalamic lesions did not extend into the hypothalamus or the thalamic sensory relay and association nuclei.

II. Synchronization of SND to diencephalic multiunit activity

A. Multiunit recordings of diencephalic activity

Diencephalic activity was recorded between stereotaxic planes A7 and A11 in 17 baroreceptor-denervated and six baroreceptor-innervated cats. The region from 0 to 3.5 mm lateral to the midline is referred to as the medial thalamus. Recordings in this region were made from sites in the following intralaminar, medial and midline thalamic nuclei: CL, MD, Pc, centrum medianum (CM), reuniens (RE) and ventralis medialis (VM). Recordings in the lateral thalamus were made from the following association and sensory relay nuclei: lateralis dorsalis (LD), lateralis posterior (LP), ventralis posterolateralis (VPL) and ventralis posteromedialis (VPM); and from nuclei ventralis anterior (VA) and ventralis lateralis (VL) which project to motor regions of the neocortex (Jones, 1985). Recordings were made from the following hypothalamic nuclei: aHd, HL, Hp, H1, H2 and ZL

Representative recordings of diencephalic activity and inferior cardiac SND in a baroreceptor-denervated cat are shown in Figure 11. As is the case for cortical activity in chloralose-anesthetized animals (Camerer et al., 1977; Barman and Gebber, 1980), diencephalic slow waves occurred primarily at frequencies between 2 and 6 Hz. The frequency of sympathetic nerve slow wave occurrence was also in the 2- to 6-Hz range. These points are illustrated by the oscillographic traces in Figure 11A and the power spectra in Figure 12A. As reported by others (Andersen and Andersson, 1968; Andersson and Manson, 1971), the patterns

and VPL activity. B: post-R wave averages of arterial pulse wave, SND, MD activity, and VPL activity. Horizontal calibration is 100 ms. Vertical calibration is 10 µV for SND and 5 µV for MD and VPL activity. C: s/division), inferior cardiac SND, medial and lateral thalamic activity recorded from sites in nuclei medialis activity denote negativity in this and subsequent figures. Vertical calibration is 100 µV for SND and 50 µV for MD frontal section through diencephalon containing recording sites (marked by arrows) in medial and lateral thalamus. dorsalis (MD) and ventralis posterolateralis (VPL), respectively. Upward deflections in traces of SND and thalamic A: Traces are from top to bottom blood pressure (BP, mmHg), time base (1 Thalamic activity and sympathetic nerve discharge (SND) in a baroreceptor-denervated cat anesthetized with chloralose. Horizontal calibration is 2 mm.

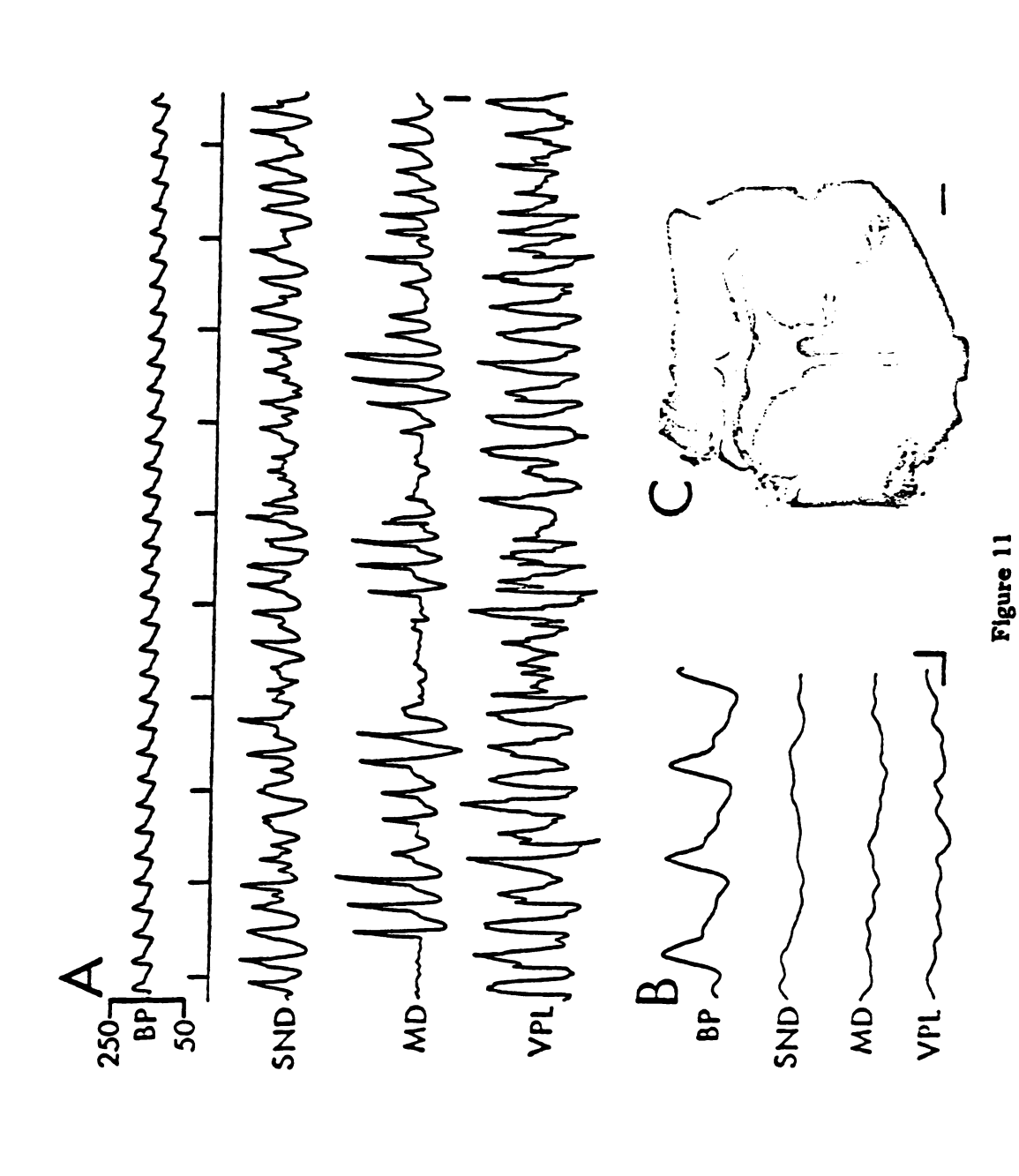


Figure 12. Power spectra of arterial pulse wave (AP), sympathetic nerve discharge (SND) and thalamic activity in two experiments. Records in A are from experiment illustrated in Figure 11. Medial and lateral thalamic activity in A were recorded simultaneously from sites in the nuclei medialis dorsalis (MD) and ventralis posterolateralis (VPL), respectively. Medial and lateral thalamic activity were recorded simultaneously from nuclei paracentralis (Pc) and ventralis posteromedialis (VPM), respectively, in experiment B. Each spectrum is the average of eight 15-s data blocks. Frequency resolution is 0.06 Hz. Vertical range of power (voltage squared) is the same in all traces.

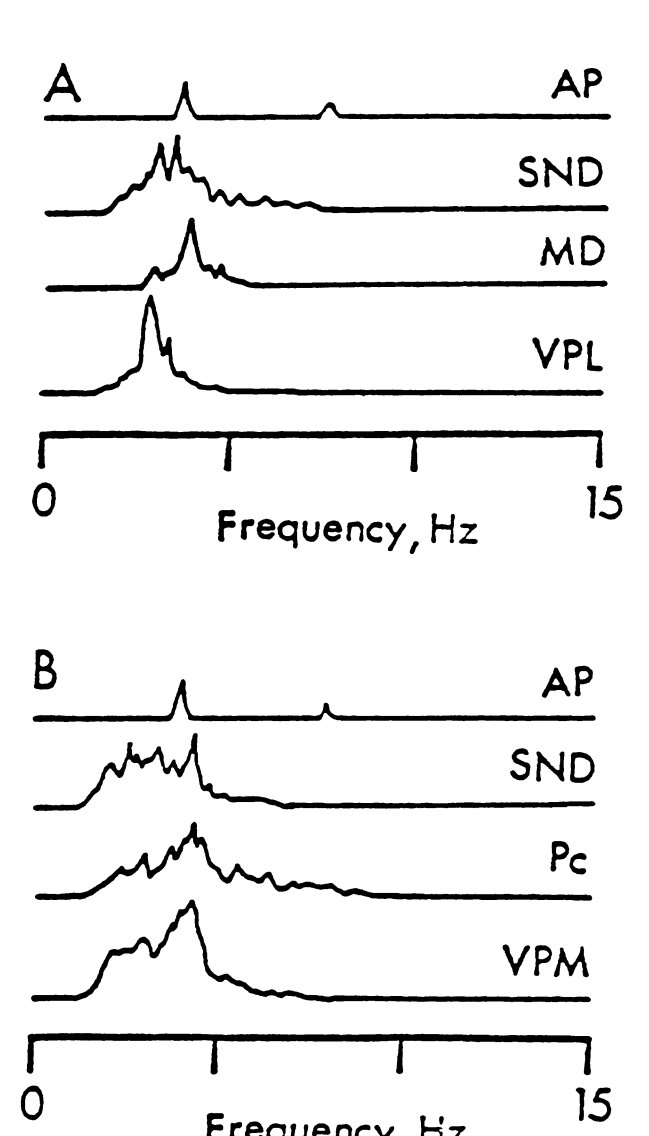


Figure 12

Frequency, Hz

of activity simultaneously recorded from medial and lateral thalamic and from hypothalamic sites could be quite different. In the example shown in Figure 11A, the predominant frequency of slow wave occurrence in the 2- to 6-Hz range was higher in MD than in VPL (also see power spectra in Figure 12A). Neither SND nor thalamic activity contained a cardiac-related component in baroreceptor-denervated cats. This is indicated by the essentially flat post-R wave (ECG) averages of SND and thalamic activity in Figure 11B. Although not shown SND contained a cardiac-related component in baroreceptor-innervated cats (Barman and Gebber, 1980; Gebber, 1980), however, thalamic activity did not.

B. Patterns of relationship between SND and diencephalic activity

1. SND related only to medial thalamic activity

Crosscorrelation analysis was used to determine whether SND and thalamic activity were temporally related. Inferior cardiac SND was temporally related to medial but not to lateral thalamic activity in five baroreceptor-denervated and two baroreceptor-innervated cats. Two of the baroreceptor-denervated cats were decorticate. Figure 13 shows an example of this pattern of relationship in a baroreceptor-denervated cat with an intact neuraxis. The CM -> SND crosscorrelogram (Figure 13B) shows inferior cardiac SND that preceded (left of zero lag) and followed (right of zero lag) medial thalamic activity. Note that the crosscorrelogram contains a sharp peak near zero lag. This peak indicates that a component of SND and medial thalamic (CM) activity were temporally related. The crosscorrelation function (rho value) at the peak was 0.2. A value of 1.0 signifies a perfect relationship. A rhythm with a period of approximately 240 ms appears in both the autocorrelogram of CM activity (Figure 13A) and the CM -> SND crosscorrelogram. Thus, the component common to SND and medial thalamic activity was in the 2- to 6-Hz range. In contrast, the VA -> SND crosscorrelogram (Figure 13B) was flat, indicating that

Figure 13. Selective realtionship between medial thalamic activity and sympathetic nerve discharge (SND). A: autocorrelograms of SND and of activity recorded from nuclei centrum medianum (CM) and ventralis anterior (VA) of medial and lateral thalamus, respectively. B: crosscorrelograms. CM -> SND crosscorrelogram shows SND relative to CM activity at zero lag. VA -> SND crosscorrelogram shows SND relative to VA activity at zero lag. CM -> VA crosscorrelogram shows relationship between activity at both thalamic sites. Analysis time for correlograms was 40 s. Bin width was 10 ms.

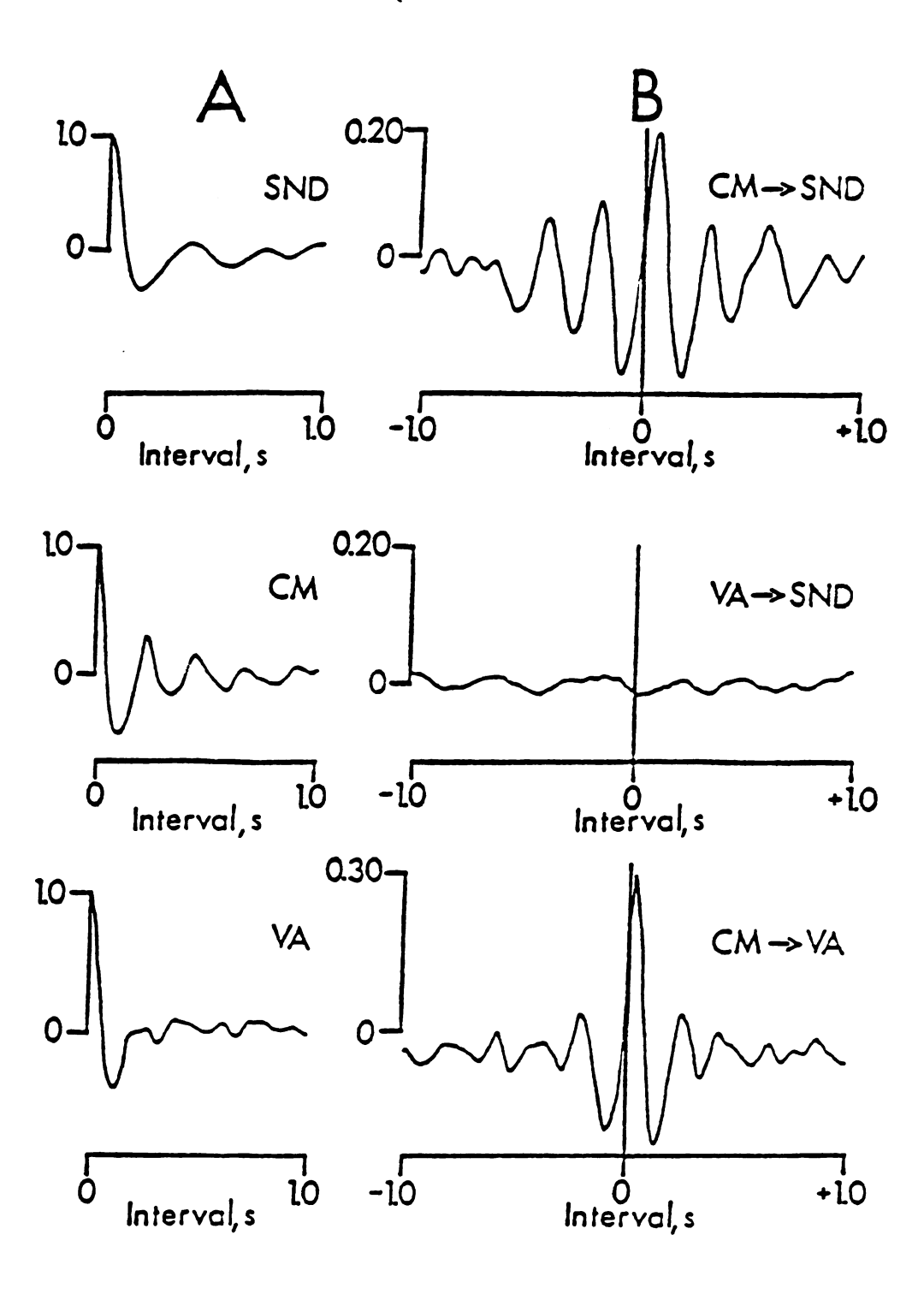


Figure 13

SND was unrelated to activity recorded from this lateral thalamic site. The CM -> VA crosscorrelogram in Figure 13B shows a sharp peak near zero lag indicating that medial and lateral thalamic activity contained a common component. This component apparently was not responsible for the relationship between medial thalamic activity and SND.

As was the case in CNS-intact cats, 2- to 6-Hz slow waves appeared in SND and thalamic activity of decorticate cats. Figure 14A shows representative recordings of SND and medial (VM) and lateral (VPL) thalamic activity in a decorticate cat. The crosscorrelograms in Figure 14B, C demonstrate that SND was temporally related to VM but not to VPL activity.

Recordings were made from 53 medial thalamic and 40 lateral thalamic sites in the seven experiments in which SND was temporally related only to medial thalamic activity. The distribution of thalamic recording sites in these experiments is shown in Figure 15. Twenty-one of the medial thalamic sites had activity related to SND. The mean interval between zero lag and the first peak to the right of zero lag in the medial thalamic -> SND crosscorrelograms for these 21 sites (()) was 73±10 ms. SND was related to thalamic activity recorded in CL (2 of 7 cases), CM (4 of 8 cases), MD (8 of 21 cases), Pc (4 of 8 cases) and VM (3 of 6 cases). No relationship (()) was observed between SND and RE activity (3 cases).

2. SND related to medial and lateral thalamic activity

SND was related to both medial and lateral thalamic activity in seven baroreceptor-denervated and three baroreceptor-innervated cats. Sites with sympathetic nerve-related activity were distributed, without apparent concentration, throughout the medial and lateral thalamus. The mean interval between zero lag and the first peak to the right of zero lag in the medial thalamic -> SND crosscorrelograms was 77±10 ms. The corresponding value for lateral thalamic -> SND crosscorrelograms was 61+11 ms. In the representative example

and baroreceptor-denervated cat. A: traces are from top to bottom blood pressure (BP, mmHg), time base (1 s/division), inferior cardiac SND, medial and lateral thalamic activity recorded from sites in the nuclei ventralis medialis (VM) and ventralis posterolateralis (VPL), respectively. Vertical calibration is 50 µV for SND and 20 µV for VM and VPL. B: Vm -> SND crosscorrelogram. C, VPL -> SND crosscorrelogram. Analysis time for crosscor-Figure 14. Relationship between medial thalamic activity and sympathetic nerve discharge (SND) in a decorticate relograms was 40 s. Bin width was 10 ms.

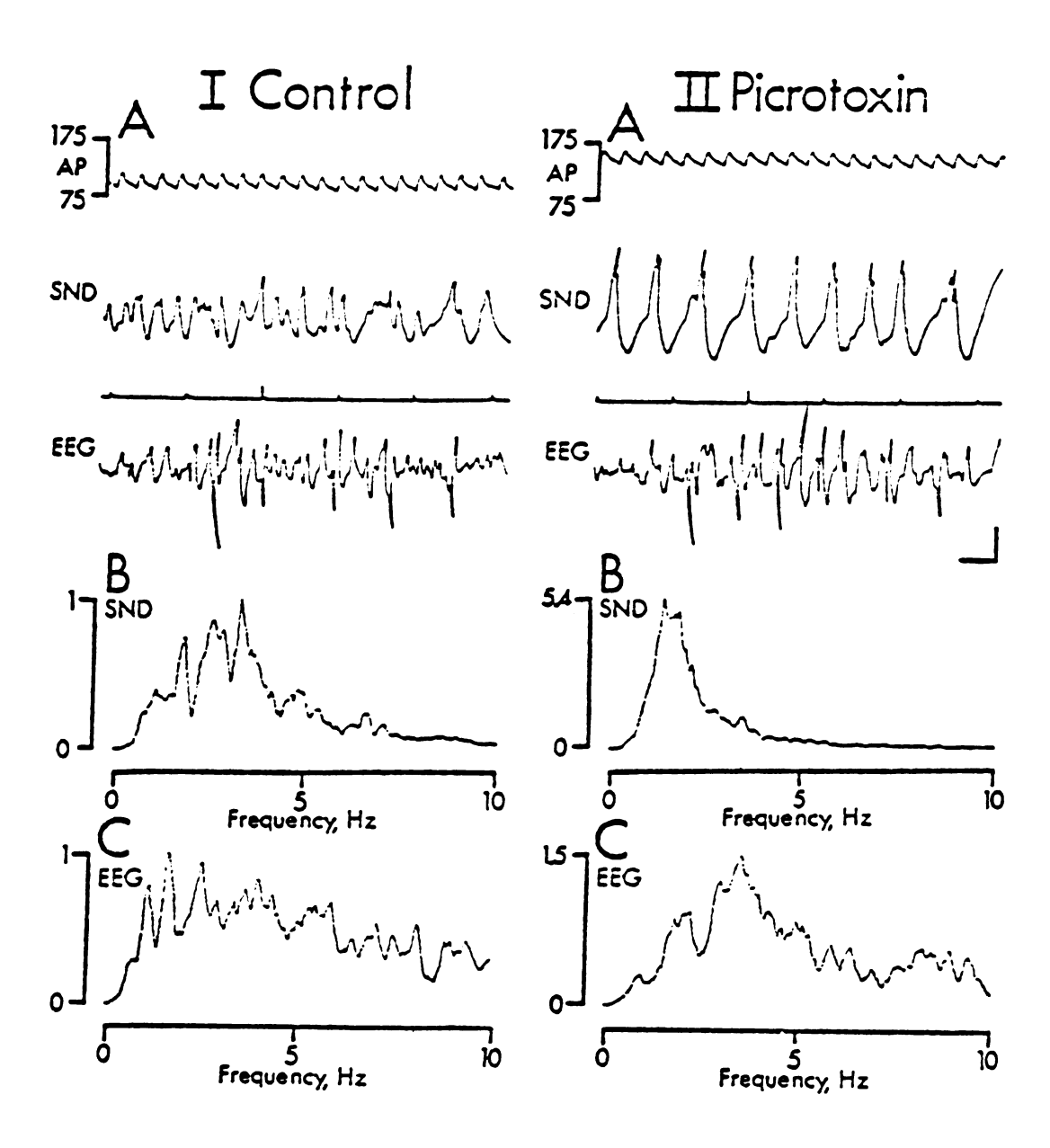


Figure 20

Recovery of SND and blood pressure to near control levels occurred between 1 and 1 1/2 hr after picrotoxin injection (not shown). After recovery, the same pattern of results could be obtained following a second series of picrotoxin injections into the medial thalamus (not shown). In one cat intrathalamic picrotoxin (110 ug total dose) failed to alter SND.

As seen in the raw records (Figure 20IA, IIA) and power spectra (Figure 20IC, IIC) of EEG activity, the intrathalamic injection of picrotoxin increased the amplitude and frequency of the EEG (4 of 5 cats). However, these effects were not as dramatic as the effects on the SND as indicated by the smaller increase in power and the broad peak in the power spectrum of the EEG (Figure 20IIC). In two cats larger doses of picrotoxin (60 and 90 µg total dose) changed the synchronous 1- to 2-Hz rhythm in SND into a less synchronous pattern dominated by periods of spike-like activity. The spikes in SND were locked to spikes in the EEG in a 1:1 fashion. The degree to which these larger injections volumes spread was not assessed in these experiments. The periods of synchronized sympathetic and cortical spikes resembled those seen after intravenous administration of convulsive doses of picrotoxin (0.5-1.0 mg/kg). The polygraphic records of EEG and SND in Figure 21 are representative of the patterns of activity observed during picrotoxin-induced (1 mg/kg, iv) seizures in eight cats. Note the wide variety of activity patterns and the strong 1:1 synchronization of EEG and SND (panels B, C and D). The changes in blood pressure (increases and decreases) of 10-35 mmHg shown in the example in Figure 21 are typical of those accompanying picrotoxin-induced seizure activity in all eight cats.

In contrast to the changes produced by injection of picrotoxin into the medial thalamus, multiple injections of normal saline (0.5 µl) into the same regions failed to affect SND (3 experiments). SND also was unaffected when bilateral injections of picrotoxin (10-20 µg total dose) were made into VL,

Figure 21. Changes in sympathetic nerve discharge (SND) and frontal parietal cortical activity (EEG) produced by the intravenous (iv) administration of a convulsive dose of picrotoxin. A: control. B, C and D, are 3, 5 and 7 min, respectively, after iv injection of 1 mg/kg picrotoxin. Traces in A, B, C and D are from top to bottom blood pressure (BP, mmHg), SND and EEG. Vertical calibration for SND is 100 μV and EEG is 80 μV . Time base is 1 s/division.

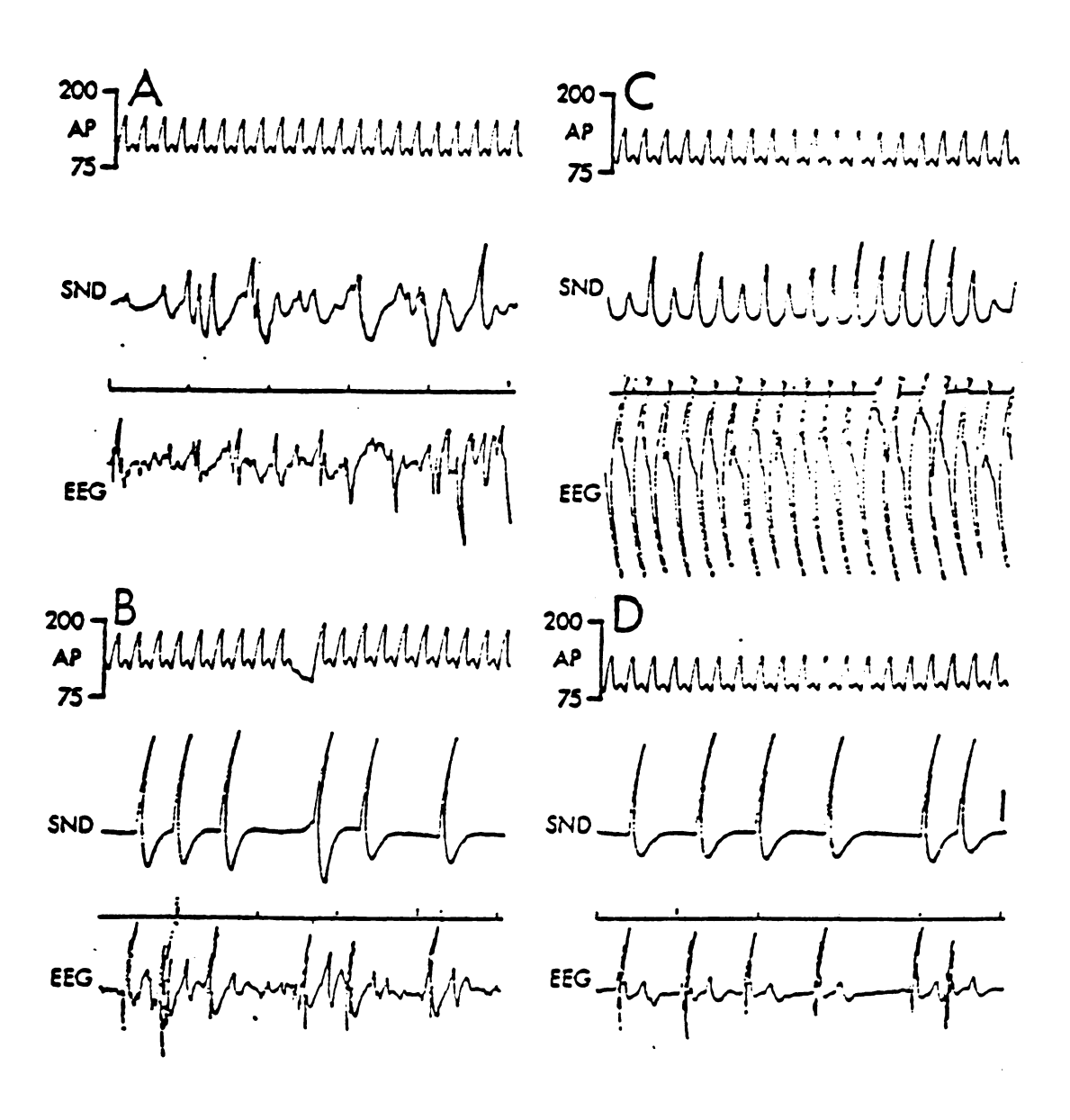


Figure 21

VPL and LP of the lateral thalamus (4 experiments) or when the drug was injected intravenously in a dose of 250 μ g/kg (2 experiments).

III. Identification of diencephalic neurons with sympathetic nerve-related activity

The experiments with chemical stimulation in this and other studies suggest that the medial thalamus and hypothalamus contain the cell bodies of neurons capable of influencing SND. However, the question of whether these cells are tonically active thus accounting for the temporal relationship between SND and multiunit diencephalic activity required further investigation. To test this I recorded from individual neurons in the medial thalamus and hypothalamus.

Whereas the experiments with radio-frequency lesions were performed on baroreceptor-denervated cats, single neurons were studied in cats with intact baroreceptor nerves. This allowed me to characterize baroreceptor reflex influences on diencephalic neurons with sympathetic nerve-related activity. Although the decreases in SND and blood pressure produced by decerebration are most pronounced in nonlesioned baroreceptor-denervated cats, qualitatively similar effects are observed in baroreceptor-innervated cats (Huang et al., 1987).

A. Identification of diencephalic neurons with sympathetic nerve-related activity

In 30 cats, the hypothalamus was explored from 8.5 to 14 mm rostral to the interaural line and between 0.5 and 3.5 mm lateral to the midline for neurons whose spontaneous discharges were temporally related to postganglionic inferior cardiac SND. In another 23 cats, the medial thalamus was searched from 7.0 to 11.0 mm rostral to the interaural line and from 0 to 3.0 mm lateral to the midline for neurons with sympathetic nerve-related activity.

1. Diencephalic unit discharge patterns

The unit discharge patterns illustrated in Figure 22 are typical of those of diencephalic neurons with sympathetic nerve-related activity. Most medial thalamic neurons fired in bursts of three or more spikes. Interspike intervals (ISI) within a burst usually were < 10 ms. This was reflected by a large number of counts in the first bin of the IS' histograms (Figures 26D, 27D, 29D and 30D). A second sharp peak corresponding to a frequency between 2 and 6 Hz appeared in the ISI histograms for thalamic neurons with regularly spaced bursts (Figures 27D, 29D and 30D). This peak was absent when the bursts were irregularly spaced (Figure 26D). Raw records of the regularly spaced bursts of a medial thalamic neuron are shown in Figure 22A1, whereas the irregularly spaced bursts of another thalamic neuron appear in Figure 22B1. Hypothalamic neurons rarely discharged in a burst. These neurons were most apt to generate single spikes or doublets (ISIs < 50 ms; Figure 22C1) that were usually irregularly spaced (Figure 28D). Representative recordings of inferior cardiac SND and frontalparietal cortical activity are shown in Figure 22D.

2. Synchronization of diencephalic unit activity to inferior cardiac SND

Peri-spike-triggered averaging was used to identify diencephalic neurons with naturally occurring (i.e., spontaneous) activity temporally related to inferior cardiac SND. Sixty of 310 hypothalamic neurons (including those in the ZI and H1, H2 Forel's Fields) and 47 of 196 medial thalamic neurons tested had activity related to SND. Neurons with sympathetic nerve-related activity were intermingled with those whose discharges were unrelated to SND. Recordings were made from the vicinity of the cell body in most cases. This was indicated by the appearance of an inflection on the rising phase of the spikes of 60% of the neurons with sympathetic nerve-related activity. These inflections are believed

Figure 22. Representative recordings of action potentials of diencephalic neurons with sympathetic nerve-related activity. A, B: two thalamic neurons located in nucleus medialis dorsalis. C: hypothalamic neuron located in paraventricular nucleus. Horizontal calibration is 200 ms for A1, B1 and C1, 1 ms for A2, C2, and 2 ms for B2. Vertical calibration is 200 μV for A and 100 μV for B and C. Note inflection on rising phase of action potential when spike amplitude decremented during the burst in B2. Five successive spikes of hypothalamic neuron were superimposed in C2. Note separation of action potential into two components. This occurred for the second spike of a doublet. Arrows in A3-C3 mark locations of neurons. Calibration for histological sections is 2 mm. D: representative recordings of arterial pressure (AP; mmHg), inferior cardiac sympathetic nerve discharge (SND), and frontal-parietal cortical activity (EEG). Horizontal calibration is 1 s. Vertical calibration is 200 μV for SND and 100 μV for EEG.

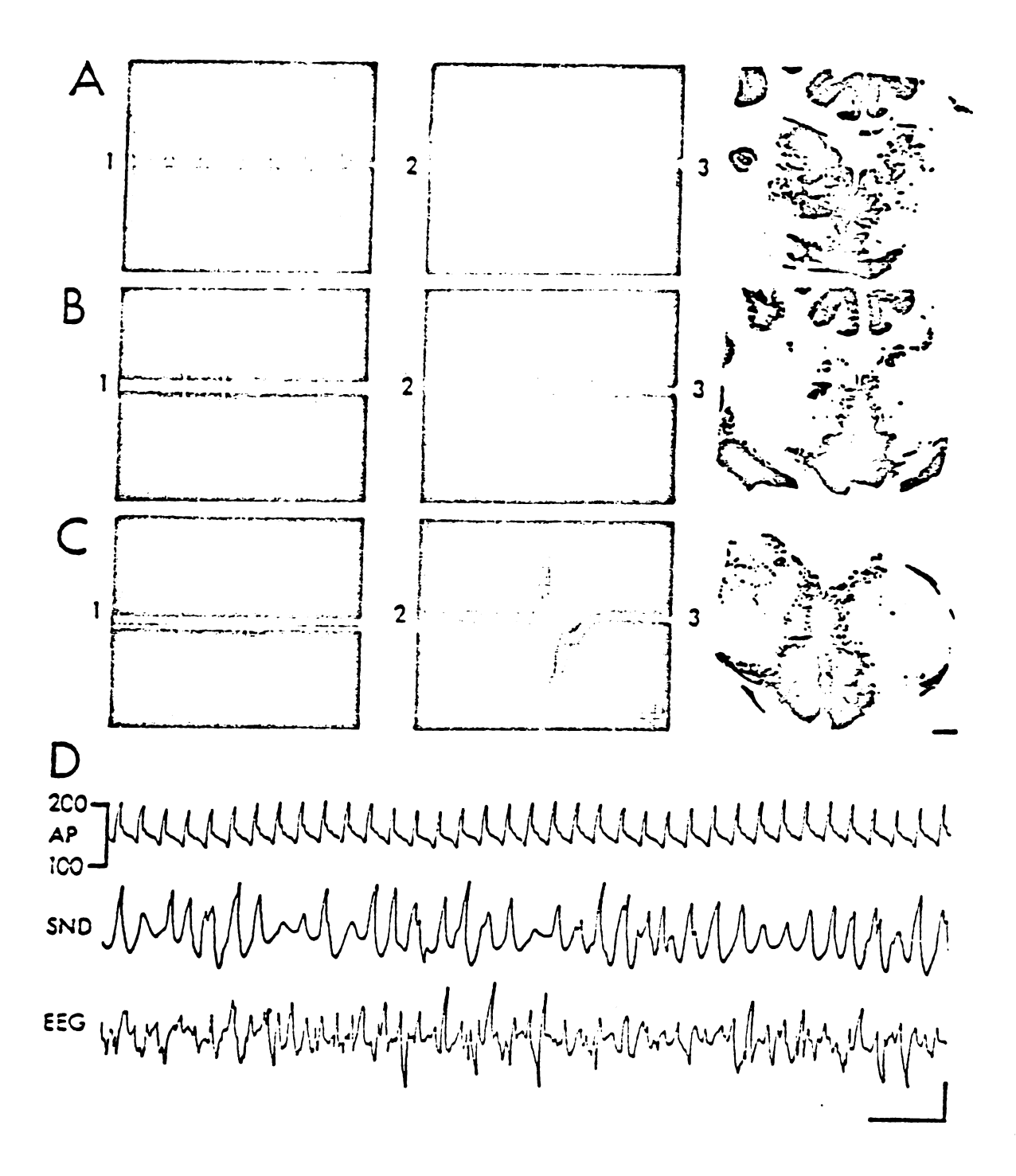


Figure 22

to reflect separation of the action potentials of the initial segment and somadendritic regions (Coombs et al., 1957). Examples are shown in Figure 22B2 and C2. The inflections were particularly evident when spike amplitude decremented during a burst or doublet.

Peri-spike-triggered averaging revealed two patterns of relationship between diencephalic unit activity and SND, both of which often occurred in the same experiment. These patterns are illustrated in Figure 23. The first pattern was characterized by synchronization of unit activity to an aperiodic spike-like event in SND. The aperiodic component could be detected in raw records of inferior cardiac nerve activity (Figure 23A). Neurons with activity synchronized to the aperiodic component are referred to as type 1 units. A typical example of the spike-triggered average (based on 729 spikes) of SND for one of these neurons is shown in Figure 23B1. The trace shows the average of inferior cardiac SND that preceded (left of zero lag) and followed (right of zero lag) the action potential of the hypothalamic neuron. Unit discharge was followed by a sharp spike-like increase (upward negative deflection) in SND that was succeeded by a positive wave and then by a second smaller negative wave. The portion of the average to the left of zero lag was flat. Thus, type I unit discharges were unrelated to preceding activity in the inferior cardiac nerve. Diencephalic neurons were considered to have activity synchronized to SND when the amplitude of the peak closest to zero lag in the spike-triggered average was at least three times as great as the largest deflection in the "dummy" average of SND (Figure 23B2). "Dummy" averages of SND were constructed by using a random pulse train whose mean frequency approximated that of the unit spike train. Fortyfour type 1 neurons were located in the hypothalamus and 34 type 1 neurons were found in the medial thalamus.

Figure 23. Peri-spike-triggered averages of inferior cardiac sympathetic nerve discharge (SND) for a type 1 hypothalamic and a type 2 hypothalamic neuron in the same cat. A: oscillographic record of SND showing 2- to 6-Hz slow waves and aperiodic spike-like events (marked by dots). Horizontal calibration is 0.5 s. Vertical calibration is 200 μ V. B1: normalized peri-spike-triggered average (729 trials) of SND for type 1 neuron. Unit spike occurrence is at zero lag. B2: "dummy" pulse-triggered average (729 trials) of SND. C1: peri-spike-triggered (500 trials) of SND for type 2 neuron. C2: "dummy" pulse-triggered average (500 trials). Vertical calibration is 20 μ V. Bin width for averages is 4 ms.

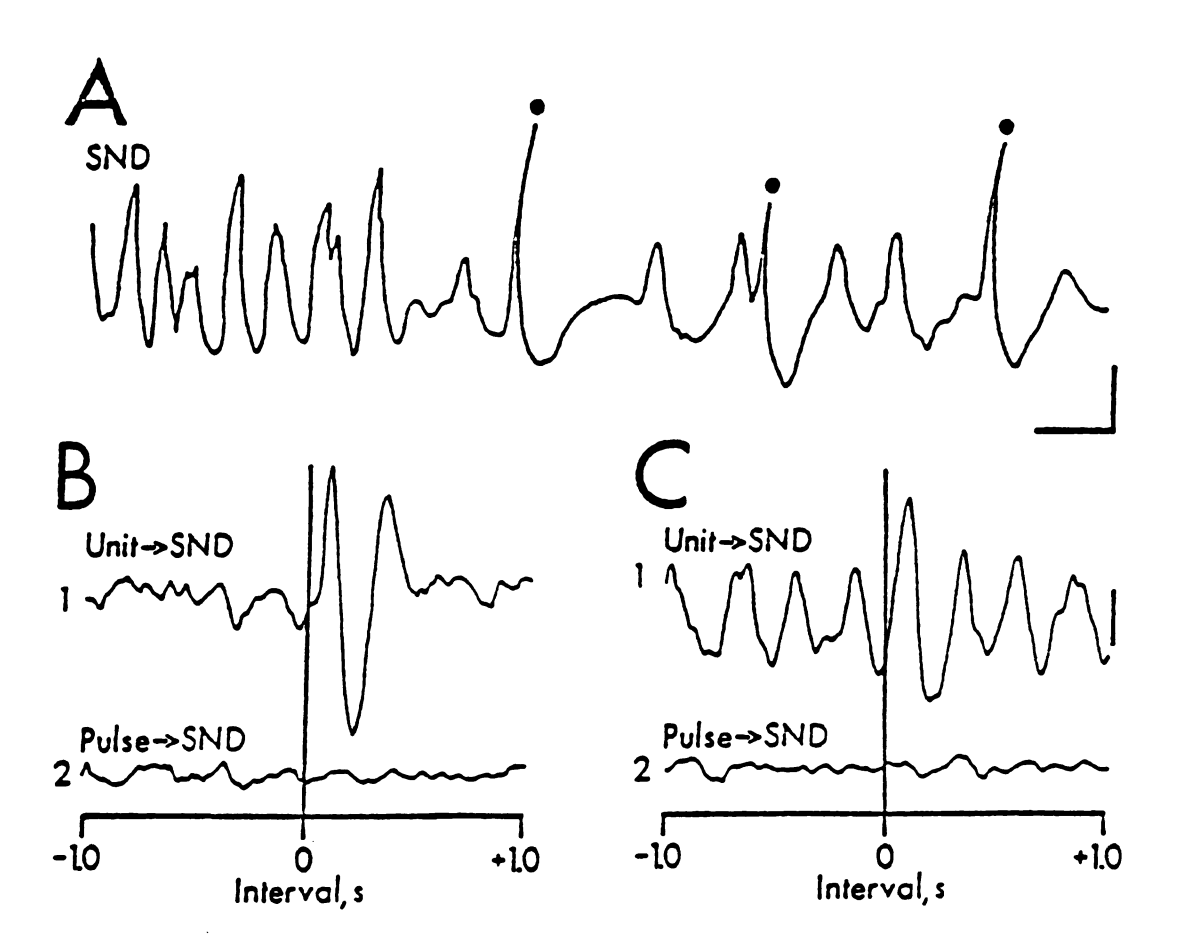


Figure 23

This pattern was characterized by synchronization of unit activity to a 2- to 6-Hz rhythmic component in inferior cardiac SND. Neurons of this kind are referred to as type 2 units. Their spike-triggered averages of SND contained a 2- to 6-Hz rhythmic component both to the left and right of zero lag. This rhythm was clearly discernible in raw records of SND (Figure 23A). Type 2 neurons were located in the hypothalamus (n=16) and in the medial thalamus (n=13).

The distributions of type 1 (left side of coronal sections) and type 2 (right side) neurons in the hypothalamus and medial thalamus are shown in Figure 24. The two neuronal types generally were intermingled. The hypothalamic regions containing these neurons included: Fil, H1, H2, HL, Hp, PVH and the ZL In addition, three type 1 neurons were located in the preoptic region (RPO) of the hypothalamus. Medial thalamic nuclei containing type 1 and type 2 neurons included: CL, CM, MD, Pc, RE and VM. CL, CM and Pc are part of the intralaminar complex.

3. Comparison of unit firing times

The firing times of type 1 and type 2 neurons relative to the spike-like event and 2- to 6-Hz rhythmic components in inferior cardiac SND, respectively, were assessed from spike-triggered averages. I measured the interval between unit spike occurrence and the first peak to the right of zero lag in the average of SND. The distributions of the intervals for type 1 and type 2 neurons are shown in Figure 25. The mean intervals for corresponding unit types in the hypothalamus and medial thalamus were not significantly different. Further analysis (not shown) failed to reveal differences in unit firing times on the basis of location in a particular nucleus.

Figure 24. Anatomical distribution of diencephalic neurons with sympathetic nerve-related activity. Type 1 (②) neurons are shown on left of coronal sections: type 2 neurons (△) are shown on right. Calibration is 1 mm. Stereotaxic planes and abbreviations are the same as those in Figures 5, 6 and 10 with the addition of: CA, commissura anterior; Ch, chiasma opticum; RPO, Regio preoptica.

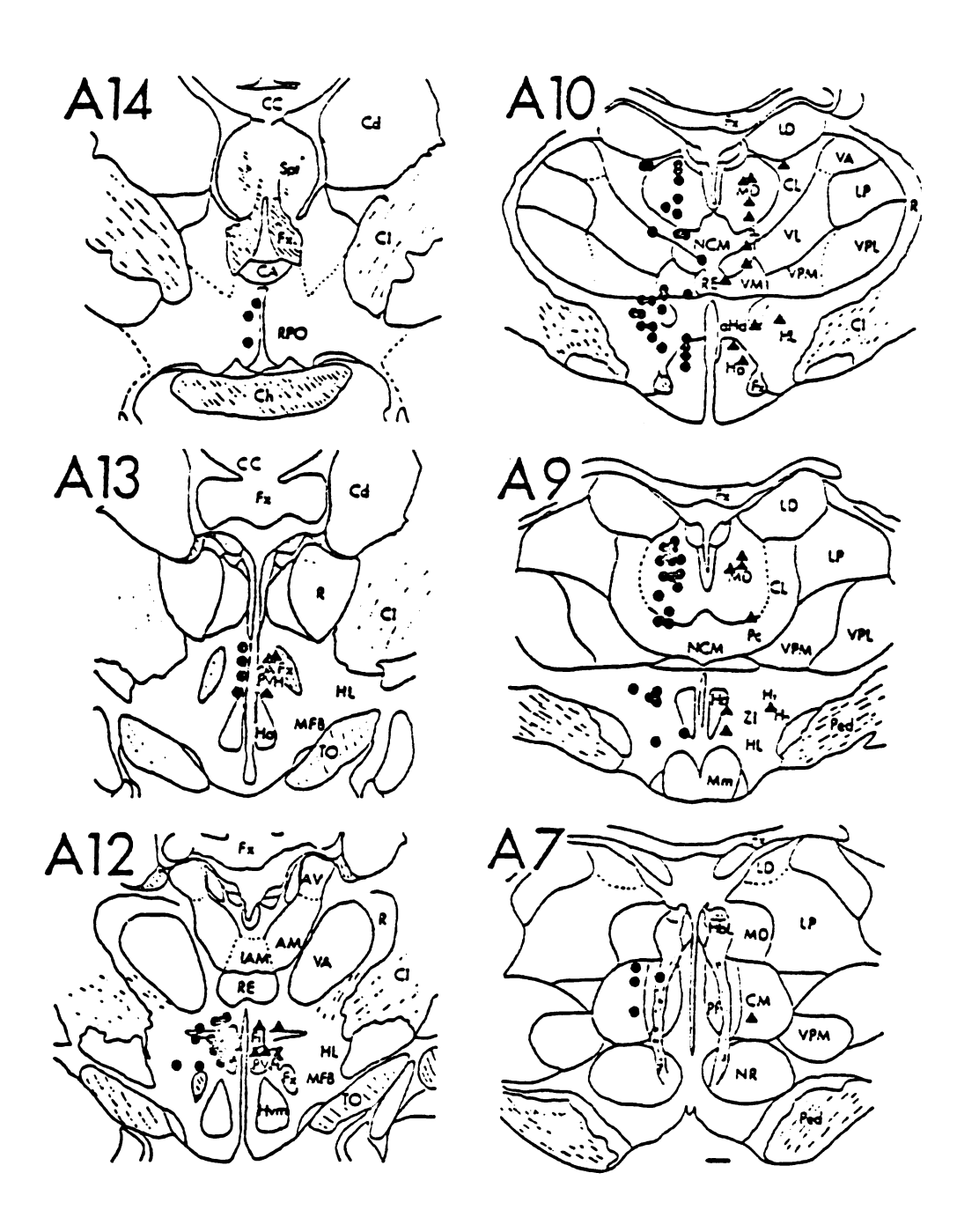


Figure 24

Figure 25. Firing times of type 1 (A,B) and type 2 (C,D) hypothalamic and medial thalamic neurons relative to inferior cardiac sympathetic nerve discharge (SND). Number of neurons is plotted against interval between unit spike occurrence and the first peak to the right of zero lag in the spike-triggered average of SND. Values are means \pm SE.

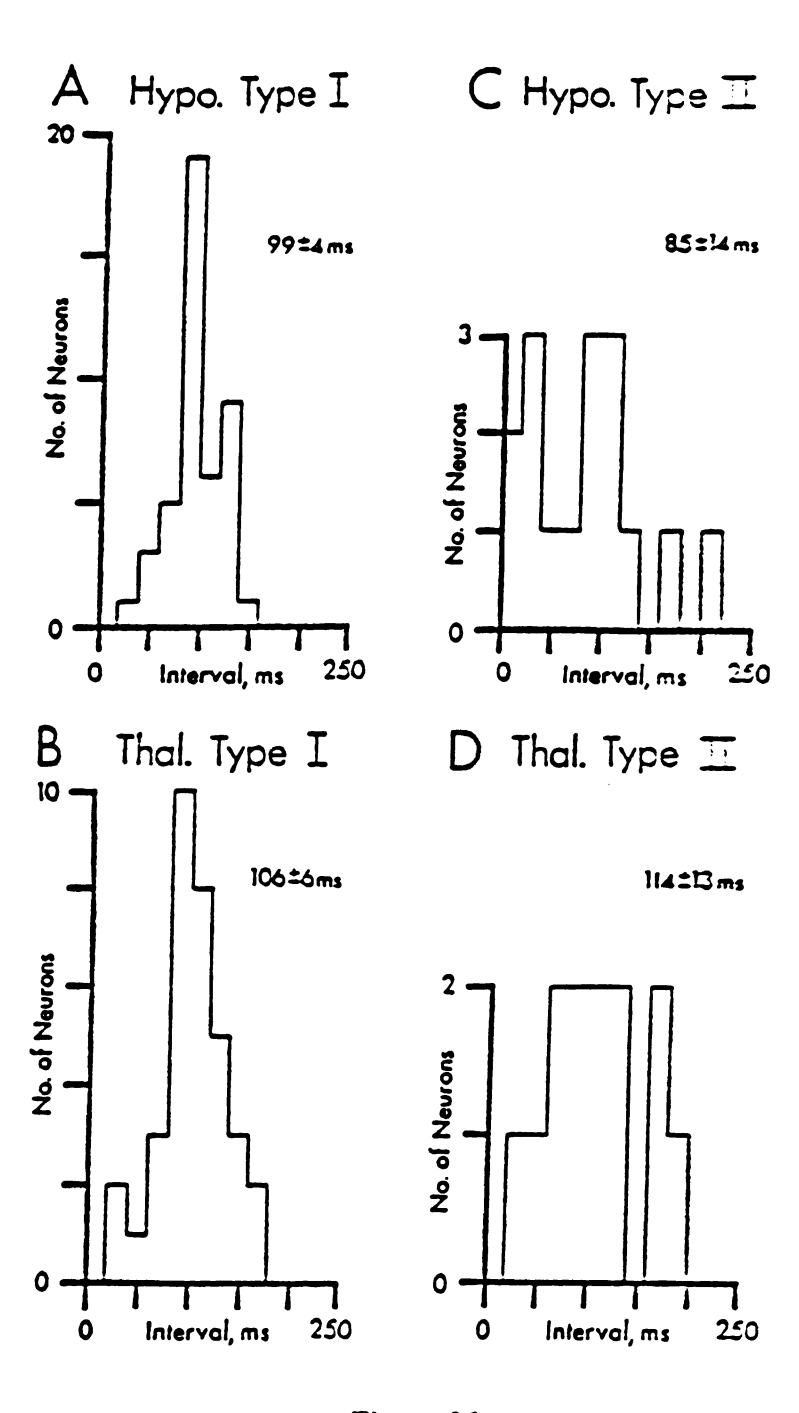


Figure 25

B. Detailed analysis of diencephalic neurons with sympathetic nerverelated activity

1. Detailed analysis of type 1 neurons

Post-R wave analysis was performed off-line for 12 type 1 hypothalamic and 11 type 1 medial thalamic neurons. The relationships between unit activity, SND, cortical activity and the cardiac cycle were similar for these 23 neurons. A typical example is shown in Figure 26. The discharges of this medial thalamic neuron were synchronized to spike-like events in SND (Figure 26A) and cortical activity (Figure 26B). While the sharp increase in SND followed the action potential of the neuron (i.e., zero lag in the average), the onset of the spike-like event in cortical activity preceded the unit action potential. This was the case for 20 of the 23 type 1 neurons. The discharges of the other three type 1 neurons preceded the casets of the spike-like events in cortical activity and SND. As evidenced by the flat post-R wave histograms of unit discharges, type 1 neurons did not have cardiac-related activity (Figure 26C). Type 1 neurons had irregular firing patterns as indicated by the absence of sharp peaks beyond the first bin in their ISI histograms (Figure 26D). The mean firing rates of the 12 type 1 hypothalamic and 11 type 1 medial thalamic neurons were 1.8±0.8 and 3.0±0.3 spikes/s, respectively.

2. Detailed analysis of type 2 neurons

Post-R wave analysis was performed for seven type 2 hypothalamic and seven type 2 medial thalamic neurons. The mean firing rates of these hypothalamic and medial thalamic neurons were 2.9±7 and 4.9±1.5 spikes/s, respectively. Five of the hypothalamic and three of the medial thalamic neurons had cardiac-related activity. Figures 27C and 28C show the post-R wave histograms (1118 and 1630 R wave triggers, respectively) of the discharges of two of these neurons. As might be expected, the rhythm (3.6±0.2 Hz) in the spiketriggered averages of SND for the eight type 2 neurons with cardiac-related

Figure 26. Type 1 medial thalamic neuron. A: normalized peri-spike-triggered (trace 1) and "dummy" pulse-triggered (trace 2) averages (565 trials) of inferior cardiac sympathetic nerve discharge (SND). Unit spike occurrence and "dummy" pulse were at zero lag. Bin width is 4 ms. B: same for frontal-parietal cortical activity (EEG). Vertical calibration is 10 μ V for SND and EEG. C: normalized post-R wave averages (2595 trials) of arterial pulse (AP), SND and EEG, and histogram of thalamic unit spike occurrences. Bin width is 1 ms for averages and 10 ms for histogram. Vertical calibration is 20 μ V for SND and EEG. D: interspike interval histogram based on 2700 spikes. Bin width is 32 ms.

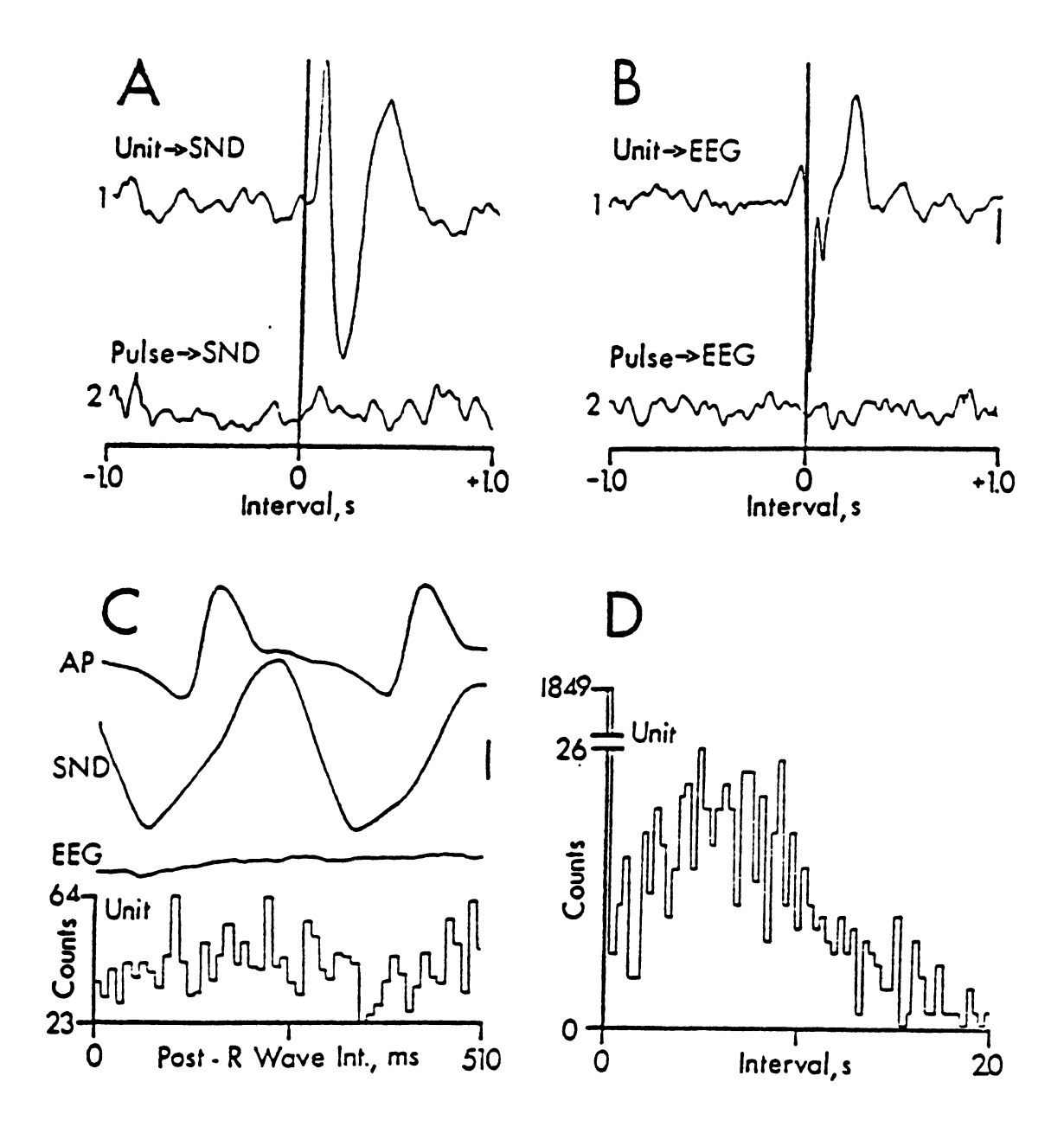


Figure 26

Figure 27. Type 2 medial thalamic neuron with cardiac-related activity. Same format and abbreviations as in Figure 23 except that "dummy" pulse-triggered averages are not shown. A, B: peri-spike-triggered averages based on 3011 trials. Bin width is 4 ms. Vertical calibration is 10 μ V. C: based on 1118 R wave triggers. Bin width is 1.1 ms for averages and 11 ms for histogram. Vertical calibration is 20 μ V. D: interspike interval histogram based on 2732 spikes. Bin width is 16 ms.

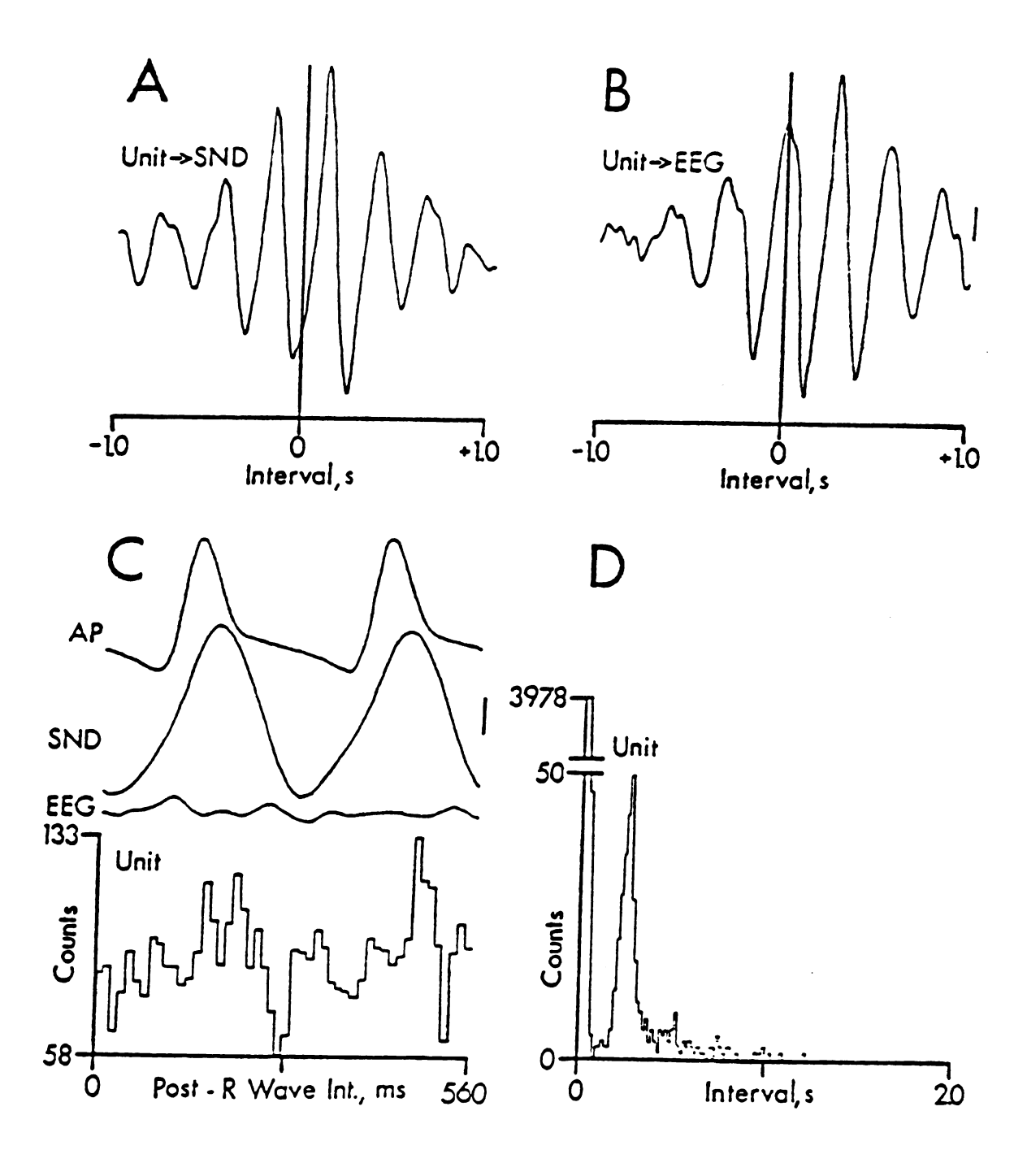


Figure 27

Figure 28. Type 2 hypothalamic neuron with cardiac-related activity. Same format and abbreviations as in Figure 23 except that "dummy" pulse-triggered averages are not shown. A, B: peri-spike-triggered averages based on 3070 R wave triggers. Vertical calibration is $10 \, \mu V$. C: based on 1630 R wave triggers. Bin width is 1.4 ms for averages and 14 ms for histogram. Vertical calibration is $20 \, \mu V$. D: interspike interval histogram based on 3149 spikes. Bin width is 32 ms.

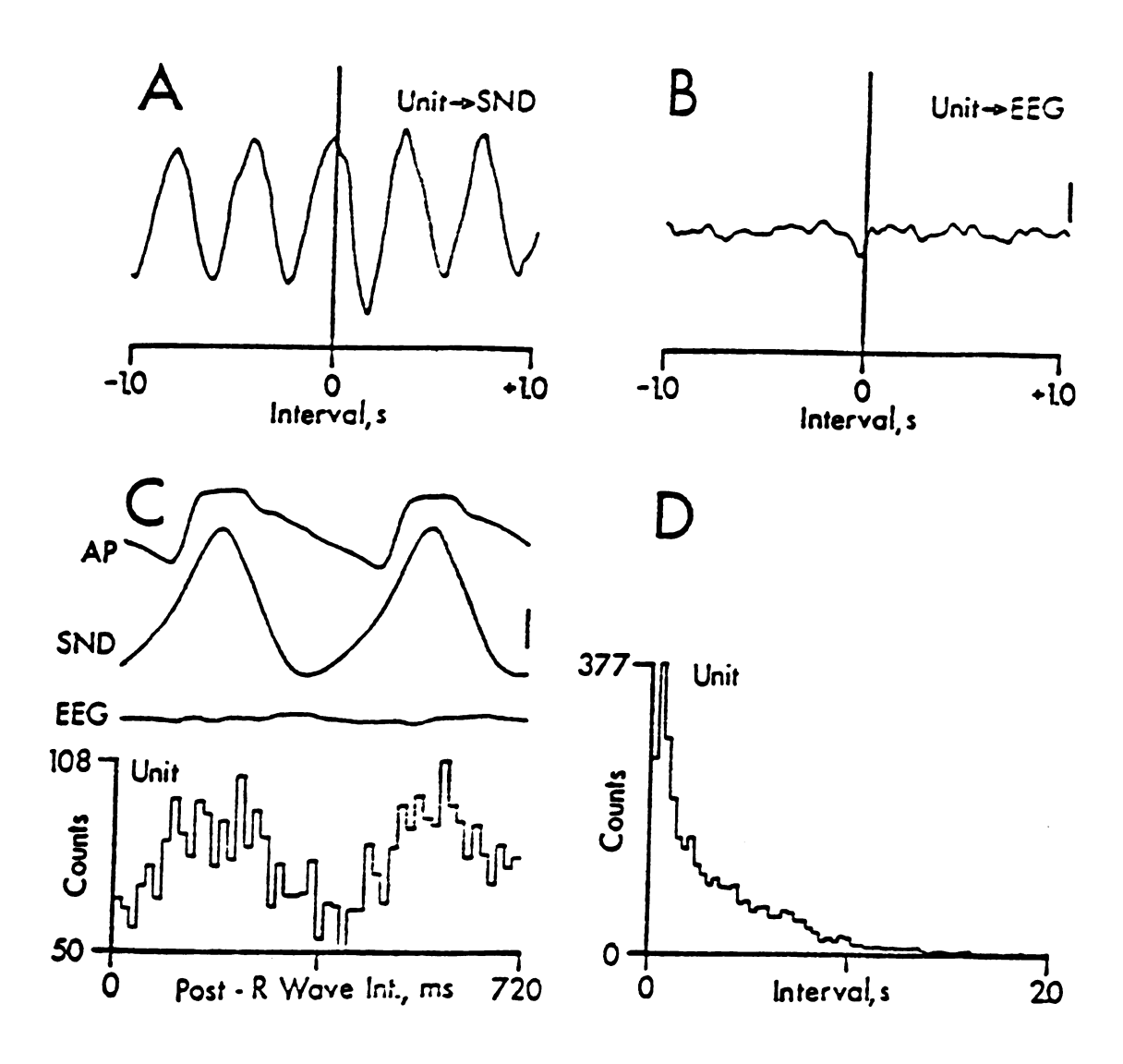


Figure 28

activity was the same as that (3.6-0.2 Hz) appearing in the post-R wave averages of SND (see examples in Figures 27A, C and 28A, C). The frequency of the rhythm in the spike-triggered average of SND was taken as the reciprocal of the interval between the two peaks closest to zero lag x 1000. Cortical activity did not contain a cardiac-related rhythm (Figures 26C-30C). Nevertheless, the discharges of 6 of the 8 type 2 neurons with cardiac-related activity were synchronized to a rhythm in cortical activity whose frequency (3.9+0.2 Hz) was close to that of the cardiac-related sympathetic nerve rhythm. The spiketriggered average (based on 3011 spikes) of cortical activity for one of these neurons is shown in Figure 27B. The peak at 240-256 ms in the ISI histogram (2732 spikes) for this medial thalamic neuron corresponded to a frequency higher than that of the rhythms in the spike-triggered averages of SND and cortical activity. This was not surprising since first order ISI analysis reflects the mean interval between the last spike in a burst and the first spike in the next burst rather than that between the first spikes in successive bursts. The discharges of two type 2 hypothalamic neurons with cardiac-related activity were not synchronized to cortical activity (Figure 28B).

The remaining two type 2 hypothalamic and four type 2 thalamic neurons did not have cardiac-related activity even though SND contained a prominent cardiac-related rhythm. Examples are shown in Figures 29 and 30. The spike-triggered averages of SND for these neurons contained a rhythm (3.4±0.3 Hz) that was the same as that (3.4±0.3 Hz) appearing in their spike-triggered averages of cortical activity. The cardiac-related sympathetic nerve rhythm was 3.1±0.4 Hz in these experiments. Figure 30 shows an example in which there was a marked difference in the frequencies of the rhythm in the spiketriggered average (2.8 Hz) and the cardiac period (2.2 Hz). This neuron was located in a cat

Figure 29. Type 2 medial thalamic neuron without cardiac-related activity. Same format and abbreviations as in Figure 23 except that "dummy" pulse-triggered averages are not shown. A, B: peri-spike-triggered averages based on 732 trials. Bin width is 4 ms. Vertical calibration is 10 μ V. C: based on 2360 R wave triggers. Bin width is 1.1 ms for averages and 11 ms for histogram. Vertical calibration is 20 μ V. D: interspike interval histograms based on 2732 spikes. Bin width is 32 ms.

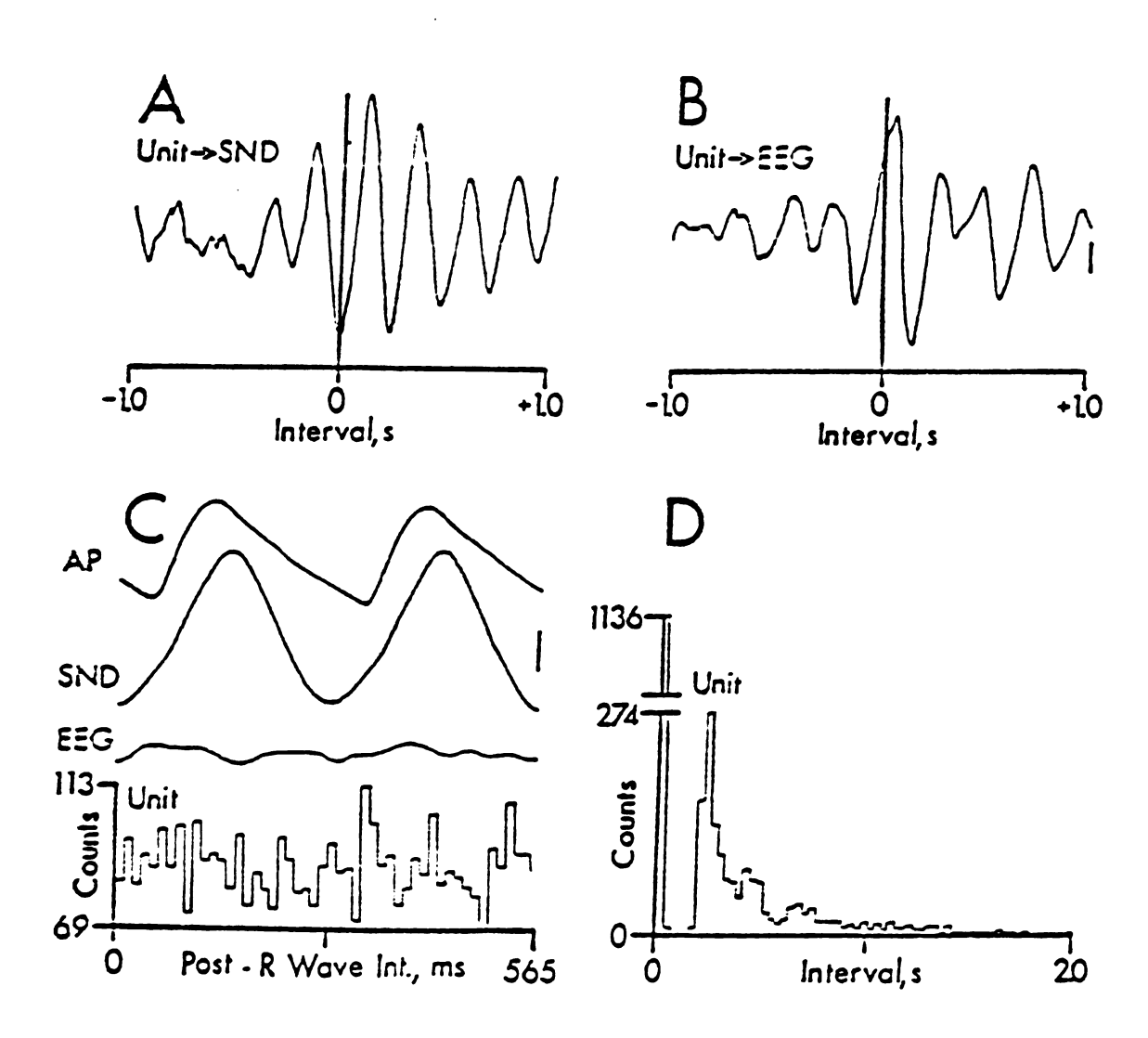


Figure 29

Figure 30. Activity of a type 2 medial thalamic neuron synchronized to a noncardiac-related component in sympathetic nerve discharge (SND). Cardiac period was lengthened by administration of atenolol (0.5 mg/kg, iv). Same format and abbreviations as in Figure 23 except that "dummy" pulse-triggered averages are not shown. A, B: peri-spike-triggered averages based on 1100 trials. Bin width is 4 ms. Vertical calibration is 12 μ V for SND and 10 μ V for EEG. C: based on 618 R wave triggers. Bin width is 1.7 ms for averages and 17.5 ms for histogram. Vertical calibration is 18 μ V. D: interspike interval histograms based on 1112 spikes. Bin width is 32 ms.

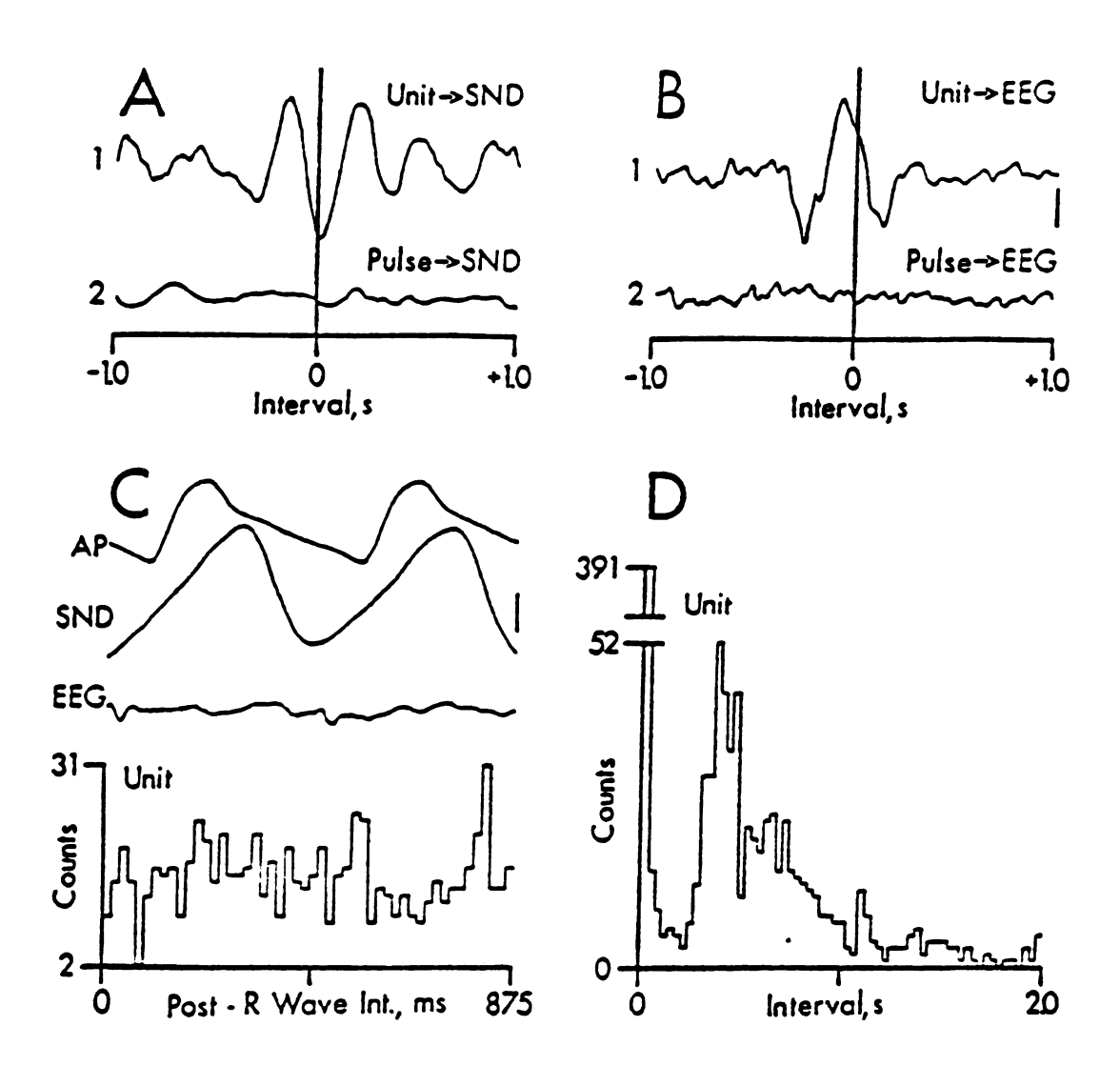


Figure 30

in which the cardiac period had been slowed by administering the beta-adrenergic antagonist atenolol (0.5 mg/kg, iv).

3. Electrical stimulation

A square wave pulse (0.5 ms duration) was applied once every 2.5 s at 32 type 1 and nine type 2 diencephalic unit recording sites. Sixty-four trials were averaged. In each case, stimulation increased SND. The minimum current needed to increase SND ranged from 18-140 µA. Using two to three times threshold current, I measured the interval between the stimulus and the peak increase in inferior cardiac nerve activity from the post-stimulus average of SND. This interval was compared with that between unit spike occurrence and the first peak to the right of zero lag in the peri-spike-triggered average of SND. The data points for type 1 unit recording sites in the hypothalamus and medial thalamus are shown in Figure 31A. The diagonal line is the identity line. By definition, the slope (i.e., regression coefficient) of the identity line is one and the y-intercept is zero. The slope (1.11±0.25) and y-intercept (-27±30 ms) of the regression line were not significantly different from those of the identity line. The mean interval between unit spike occurrence and the first peak to the right of zero lag in the averages of SND for the 32 type 1 neurons was 104+6 ms. The interval between the stimulus applied to type 1 unit recording sites and the peak increase in SND was 118+3 ms. Figure 32 shows an example of close correlation of the intervals in the spike-triggered and stimulus-triggered averages of SND. Note that the contour of the sympathetic nerve potential synchronized to the discharges of this type 1 hypothalamic neuron (panel A) was similar to that of the sympathetic nerve response evoked by electrical stimulation at the site of unit recording (panel B).

The slope (2.85±1.08) and y-intercept (-266±127 ms) of the regression line for the data from type 2 unit recording sites were not significantly

Figure 31. Comparison of changes in inferior cardiac sympathetic nerve discharge (SND) accompanying diencephalic unit spike occurrence and an electrical stimulus applied at site of unit recording. The interval between unit spike occurrence and the first peak to the right of zero lag in the peri-spike-triggered average of SND is plotted against that between the stimulus and the peak increase in SND (as measured from peri-stimulus average). A: data points for type 1 unit recording sites. B: data points for type 2 unit recording sites. hypothalamic site, thalamic site. The diagonal line in each plot is the identity line. See text for slopes and y-intercepts of regression lines.

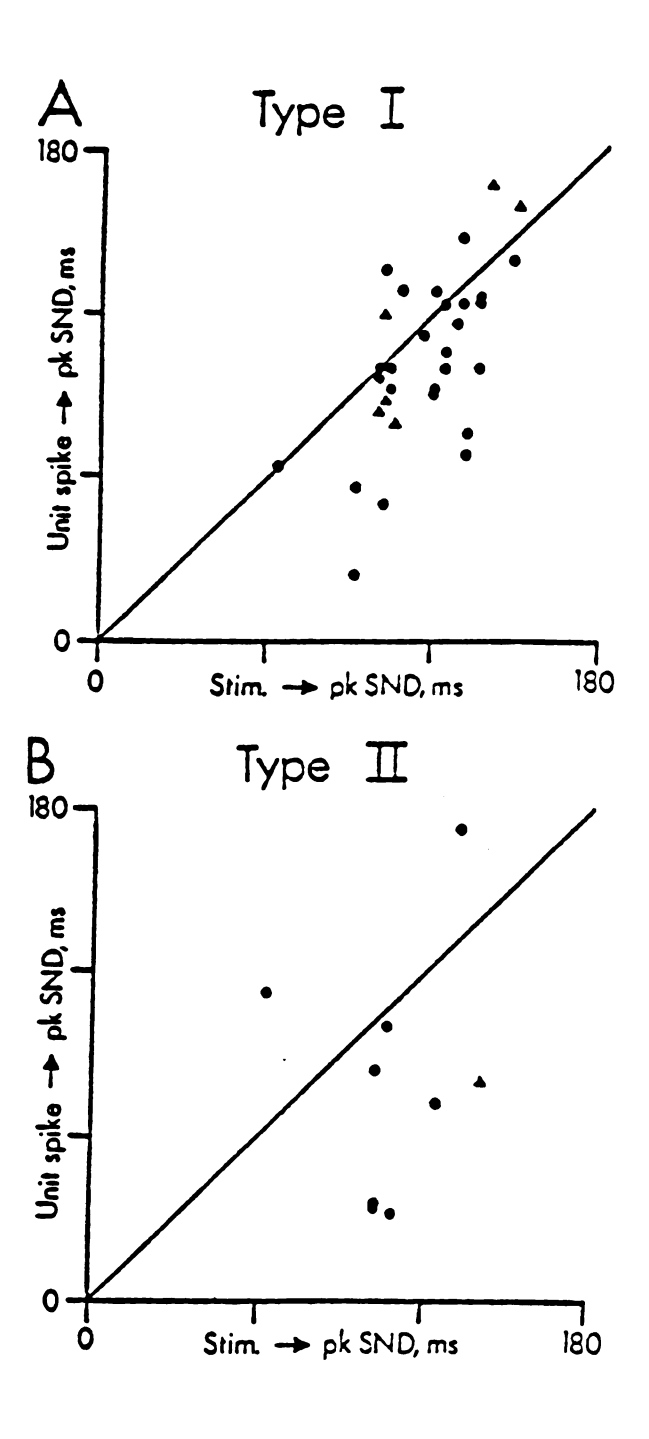


Figure 31

Figure 32. Peri-spike-triggered and peri-stimulus averages of inferior cardiac sympathetic nerve discharge (SND). A: spike-triggered average (519 trials) of SND for a type 1 hypothalamic neuron. Unit spike occurrence is at zero lag. B: peri-stimulus average (64 trials). Stimulus at zero lag (50 μ A, 0.5 ms) was applied once every 2.5 s at site of unit recording. Bin width is 1 ms. Vertical calibration is 10 μ V in A and 40 μ V in B.

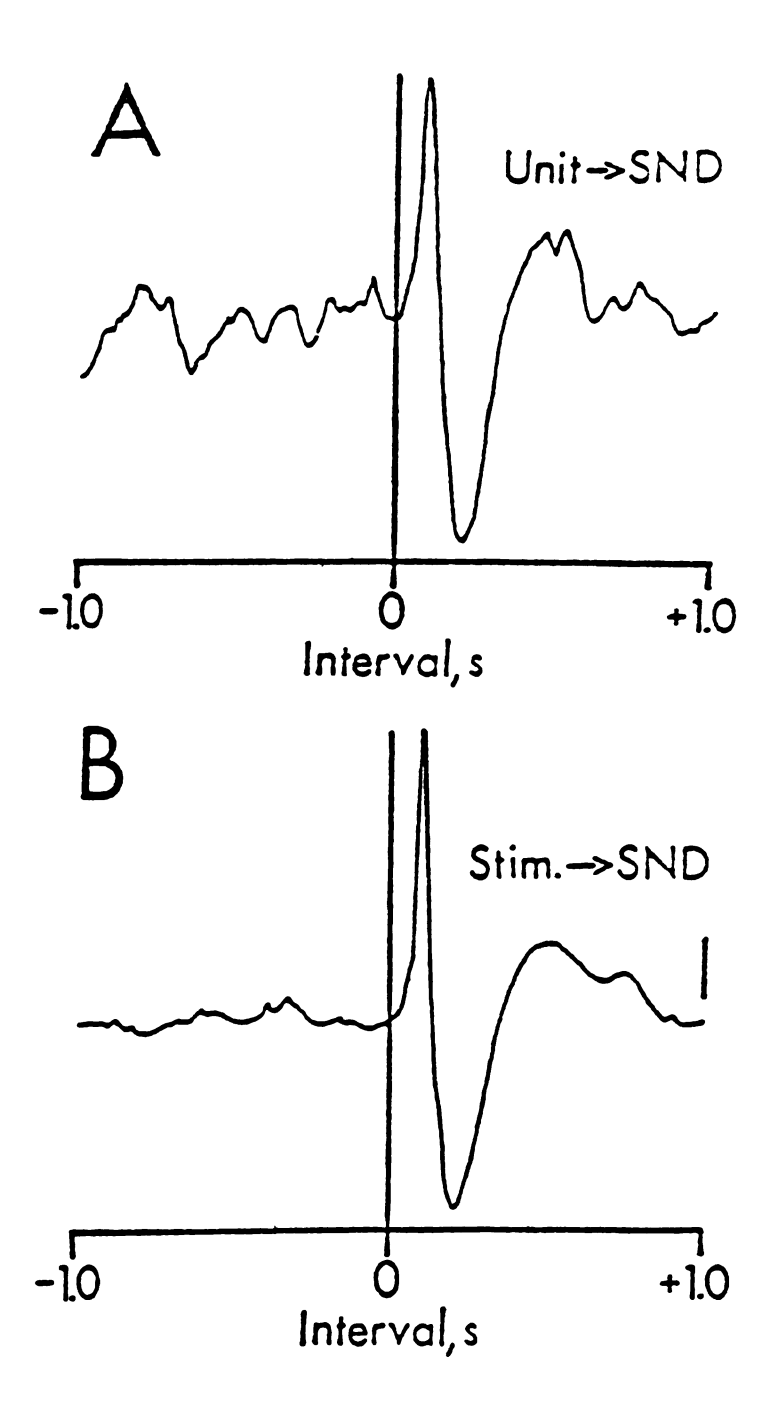


Figure 32

data points fell far from the identity line. Thus, it was not surprising that the mean interval (68±17 ms) between type 2 unit spike occurrence and the peak of the accompanying 2- to 6-Hz sympathetic nerve slow wave differed considerably from that (117±5 ms) between the electrical stimulus applied to the unit recording site and the peak increase in SND.

4. Baroreceptor reflex activation

I monitored the effect of baroreceptor reflex activation on the firing rate of 25 diencephalic neurons with sympathetic nerve-related activity in 18 cats with intact carotid sinus, aortic depressor and vagus nerves. Arterial pressure proximal to the point of aortic obstruction was raised to a level needed to inhibit maximally SND (Figure 33). Baroreceptor reflex activation was considered to affect unit firing rate when a change (increase or decrease) of > 20% was observed during the reflex inhibition of SND. Six of 13 type 1 hypothalamic neurons were affected by baroreceptor reflex activation even though they did not have cardiac-related activity. Three of these neurons were inhibited (1.5±0.4 to 0.4±0.4 spikes/s) while the other three cells were excited (5.2+4.1 to 8.1±4.9 spikes/s). Two of four type 2 hypothalamic neurons were inhibited (2.3±0.3 to 0.5+0.2 spikes/s) during baroreceptor reflex activation. Both of these neurons had cardiac-related activity. The baroreceptor reflex-induced response of one of these cells is shown in Figure 33L. Note that the undershoot of brachial arterial pressure following the release of aortic obstruction was accompanied by a rebound increase in unit discharge rate. This response is consistent with a reduced level of baroreceptor nerve activity during the fall in arterial pressure. The type 2 hypothalamic neurons unaffected by baroreceptor reflex activation did not have cardiac-related activity. The failure of baroreceptor reflex activation to affect the firing rate of one of these neurons is shown in Figure 33II.

Figure 33. Effect of baroreceptor reflex activation produced by aortic obstruction on firing rate of two type 2 hypothalamic neurons (I, II). IA, IIA: traces from top to bottom are brachial arterial pressure (AP: mmHg), standardized pulses derived from unit action potentials, inferior cardiac sympathetic nerve discharge (SND) and time base (1 s/division). Vertical calibration for SND is 100 µV. IB, IIB: histograms of unit firing rate based on 4 episodes of baroreceptor reflex activation for each neuron.

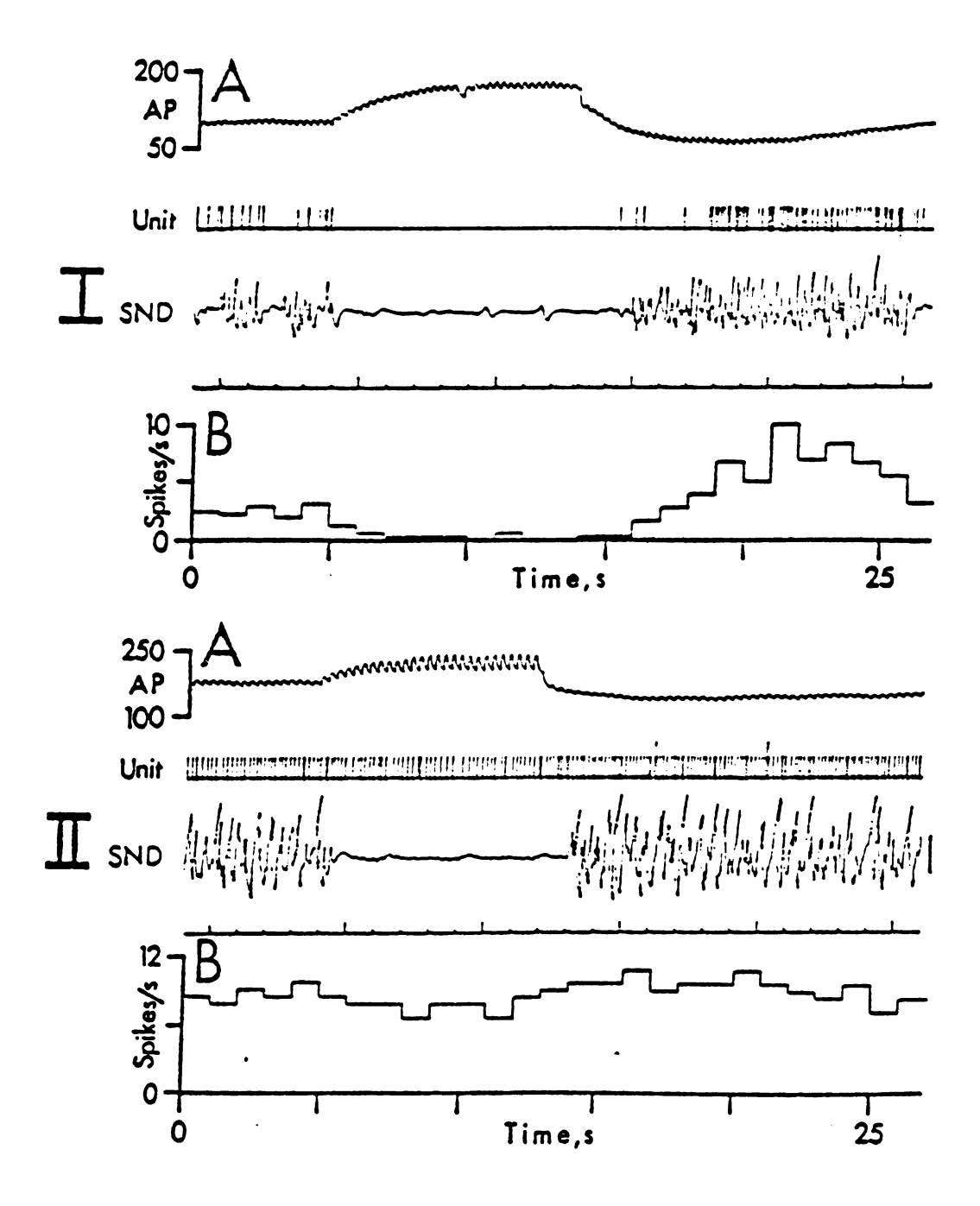


Figure 33

Baroreceptor reflex activation failed to affect the firing rate of medial thalamic neurons with sympathetic nerve-related activity. Six type 1 and three type 2 neurons were studied. None of these cells had cardiac-related activity.

IV. Sympathetic nerve responses elicited by cortical stimulation

The locking of type 1 diencephalic unit activity to a preceding spike-like event in frontal-parietal cortical activity raised the possibility that this region of the cortex provides input to sympathetic neurons in the diencephalon. To determine whether these cortical regions had sympathetic representation I examined the responses of the inferior cardiac nerve and diencephalic neurons with sympathetic nerve-related activity to electrical stimulation of the frontal-parietal cortex.

A. Sympathetic nerve responses elicited by cortical stimulation

This series of experiments was performed in 24 cats, 10 of which were baroreceptor-denervated. In these animals, sites of stimulation in the frontal-parietal cortex were along electrode penetrations through the gray matter located both on the convexities of the gyri and hidden in the depths of the sulci. On occasion stimulation also included portions of the underlying white matter. In most cases, cortical stimulation (10-ms trains of three 1-mA pulses) elicited increases in SND. Occasionally, increases in SND were also elicited by single shocks of 1-ms duration. The post-stimulus average of SND in Figure 34A1 is typical of an excitatory sympathetic nerve response. In all cases, the increase (upward negative deflection) in SND was followed by a downward positive deflection. Such positive wave forms are indicative of a decrease in background SND time-locked to the stimulus. In some cases, the negative and positive wave forms could be differentiated by lowering the stimulus current (Figure 34A). In

Figure 34. Increases and decreases in inferior cardiac sympathetic nerve discharge (SND) elicited by stimulation (10-ms trains of three pulses applied once every two s) of the motor cortex. A1-3: post-stimulus averages (64 trials) of SND elicited using stimulus currents of 1 mA, 200 μ A and 50 μ A, respectively. B1,B2: Post-stimulus averages (128 trials) of increase and decrease, respectively, in SND elicited by supramaximal (1-mA) stimulation. Sites of stimulation in the motor cortex in B1 and B2 were separated by 2 mm. Ein width was 1 ms for all averages. Vertical calibration is 100 μ V for A and 200 μ V for B. Horizontal calibration is 125 ms for A and 500 ms for B.

the example shown in Figure 34A, the ratio of the amplitudes of the negative to the positive wave forms decreased as the stimulus current was lowered, until at 50 µA (A3) only the positive wave form remained. These results suggest that the decrease in SND following an excitatory response is, at least in part, due to active inhibition. In 13 instances (in seven cats), stimulation using supramaximal (1 mA) currents elicited inhibitory sympathetic nerve responses (Figure 34B2). In these seven cats, stimulation of other cortical sites elicited increases in SND. Figure 34B1, B2 compares an excitatory and an inhibitory sympathetic nerve response elicited by stimulation (1 mA) of the motor cortex in the same cat. The mechanism responsible for producing the sympathetic nerve responses was not studied.

As shown in Figure 35, increases in SND could be elicited from widely separated regions of the frontal-parietal and infralimbic cortex. These regions included the primary motor (MI, sites 1 and 2), primary sensory (SI, sites 3, 4, 5 and 6), secondary sensory (SII, site 7) and infralimbic (IL, sites 1-4 in panel B) cortex. Although not shown, increases in SND were also elicited from the orbital gyrus (O.G.) and the parietal association cortex (ASC). The ASC cortex included the anterior marginal (M.G.) and suprasylvian (S.S.G.) gyri. Sites from which inhibitory responses were elicited with supramaximal stimulus currents (1 mA) were dispersed throughout the MI, SI, ASC and O.G. Inhibitory responses were not elicited from the SII or IL cortex. Sympathetic nerve responses could be evoked in the left inferior cardiac nerve by stimulation of either the left or right cerebral hemisphere (not shown).

The mean onset latencies of the sympathetic nerve responses evoked by cortical stimulation were calculated for each of the cortical regions listed above. These values are listed in Table 2. The mean onset latencies of responses elicited from the different cortical regions were not significantly different from Figure 35. Sympathetic nerve responses elicited by stimulation (10 ms trains of three 1-mA pulses applied once every 2 s) of prefrontal, frontal (A) and infralimbic (B) cortex. A,B: Dorsal and sagital (approximately 0.5 mm from midline) views, respectively, of the cat brain and post-stimulus averages (64 trials) of inferior cardiac sympathetic nerve responses. Responses are numbered to correspond with the site of stimulation. Sites of stimulation in A were 1 to 3 mm deep in gray matter. Bin width was 1 ms in A and B. Vertical calibration is 100 μ V for A and 50 μ V for B. Horizontal calibration is 500 ms in A and B. Cortical structures are labeled as defined by Crouch (1969) and include: A.S., ansate sulcus; CC, corpus callosum; C.G., coronal gyrus; Co.S., coronal sulcus; Cr.S., cruciate sulcus, E.S.G., ectosylvian gyrus; F.G., fornicatus gyrus; M.G., marginal gyrus; O.B., olfactory bulb; O.G., orbital gyrus; S.G. sigmoid gyrus and S.S.G., suprasylvian gyrus.

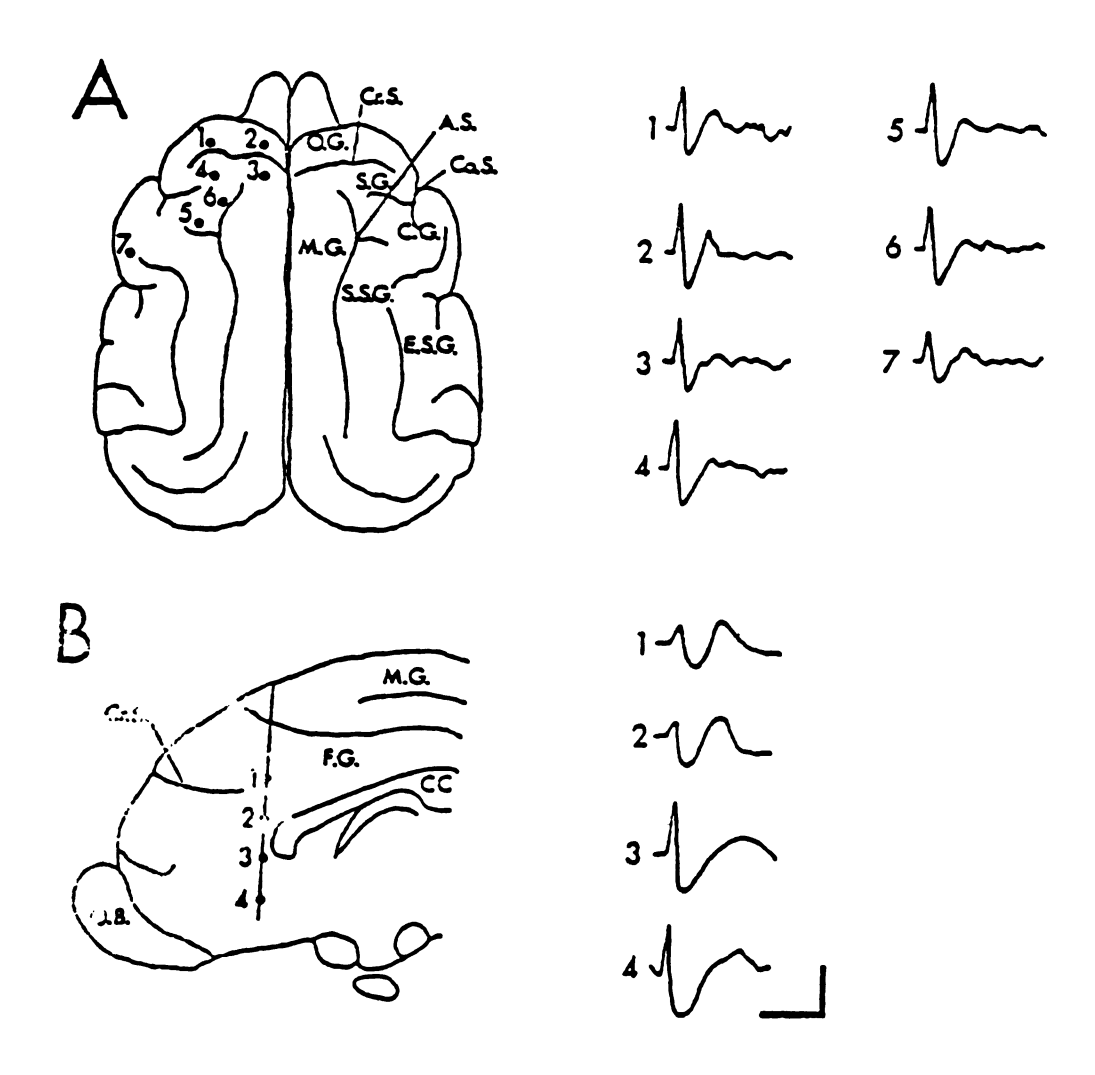


Figure 35

TABLE 2. Mean conset latencies of inferior cardiac sympathetic nerve responses produced by cortical stimulation with 10-ms trains of three pulses or 1-ms single shocks of supramaminal intensity (1-mA).

A. Cortically evoked increases in SND

	No. of Sites	Mean Onset + S.E.
ASC	5	66 <u>+</u> 2 ms
IL.	30	$72 \pm 1 \text{ ms}$
IL O.G.	7	66 - 7 ms
MI	52	64 + 2 ms
SI	15	65 + 2 ms
SII	3	60 + 1 ms

B. Cortically evoked decreases in SND

	No. of Sites	Mean Onset + S.E.
combined	13	104 <u>+</u> 2 ms

Cortical regions are abbreviated and defined as follows: ASC, association cortex area 5 (anterior marginal and suprasylvian gyri); II, infralimbic area (anterior fornicatus gyrus and subcallesal cortex); O.G., orbital gyrus; MI, primary motor area (anterior sigmoid gyrus including the hidden cortex on the banks of the cruciate sulcus); SI, primary sensory area (posterior sigmoid and coronal gyri); SII, secondary sensory area (anterior ectosylvian gyrus).

each other. In determining the onset latency for a given cortical site, measurements were made for the potential elicited with 1-mA pulses that had the greatest amplitude along each electrode penetration.

In view of the suggestion by Wall and Pribram (1950) that sympathetic responses elicited by cortical stimulation result from the activation of meningeal afferents, I compared the sympathetic nerve responses elicited by stimulation of the frontal-parietal cortex in cats having intact or sectioned meningeal afferents. In three cats, two of which were baroreceptor-denervated, the left trigeminal nerve was sectioned. Both increases (n=20) and decreases (n=4) in SND were elicited by stimulation of the left O.G., M1, S1 and ASC cortex in these animals. No attempt was made to elicit responses from the S2 or IL cortex in these animals. The shape and mean onset latencies of the excitatory and inhibitory responses evoked from the deafferentated frontal-parietal cortex were similar to those of the corresponding responses elicited from these same regions in cats having intact meningeal afferents. For this reason the responses elicited in meningeally deafferentated and intact cats were pooled for statistical analysis of onset latencies in Table 2.

B. Synaptic activation of type 1 and type 2 neurons by cortical stimula-

The possibility that cortically—evoked increases in SND are mediated via a relay in the medial diencephalon was tested by determining whether medial diencephalic neurons with sympathetic nerverelated activity could be activated synaptically by cortical stimulation.

Stimulation (10-ms trains of three 1-mA pulses) of the sensorimotor cortex in seven cats synaptically activated 4 of 4 type 1 hypothalamic and 2 of 4 type 1 medial thalamic neurons. The other 2 type 1 medial thalamic neurons tested were inhibited by cortical stimulation for 165 and 210 ms. All type 1 neurons tested were related to a spike-like event in the EEG preceding their

discharge. In response to cortical stimulation hypothalamic neurons discharged as a single or a pair of spikes with variable onset latencies. Thalamic neurons discharged as a burst of 3 to 6 spikes also with variable onset latencies. The modal onset latencies of synaptic activation were calculated from the poststimulus histograms of the units (Figure 36B). The modal onset latencies of synaptic activation ranged from 22 to 26 ms for the type 1 hypothalamic neurons, while those of the type 1 thalamic neurons were 90 and 105 ms. For those type 1 neurons activated by cortical stimulation a comparison was made to determine whether the modal onset latency of synaptic activation, plus the time to peak in the peri-spike-triggered average of SND for the unit was similar to the interval between the cortical stimulus and the peak of the increase in SND in the poststimulus average. If the cortically evoked sympathetic nerve responses involved the diencephalic neurons, these values should be similar. For three of the type 1 hypothalamic neurons the modal onset latency, plus the time to peak in the spiketriggered average was similar (within 10 ms) to the time to the peak of the cortically evoked increase in SND. The example in Figure 36 is representative of the results obtained for these three hypothalamic units. In this example the modal onset latency (26 ms) plus the time to peak SND in the peri-spike-triggered average (116 ms) was similar to the time to the peak of the increase in SND (144 ms) evoked by cortical stimulation. The comparison of times to peak and onset latencies for type 1 medial thalamic neurons showed that the latency of the cortically-induced activation of the thalamic neurons was more than 50 ms less than that of the accompanying increase in SND.

Stimulation of the sensorimotor cortex in three cats synaptically activated 2 of 2 type 2 medial thalamic neurons with modal onset latencies of 45 and 105 ms. Cortical stimulation inhibited the two type 2 hypothalamic neurons tested for 172 and 72 ms. The discharge patterns of the type 2 neurons in

Figure 36. Synaptic activation of a type 1 hypothalamic neuron by stimulation (10-ms trains of three 1-mA pulses delivered once every 2.5 s) of the motor cortex. A: normalized peri-spike-triggered average (873 trials) of inferior cardiac sympathetic nerve discharge (SND). Unit spike occurrence is at zero lag. Bin width is 4 ms. Vertical calibration is 30 μ V for SND. B: post-stimulus histogram (513 trails) of synaptic activation of the unit. Modal onset latency of synaptic activation of the unit is 27 ms. Bin width is 2 ms. C: normalized post-stimulus average (513 trials) of inferior cardiac SND elicited by cortical stimulation. Vertical calibration is 80 μ V.

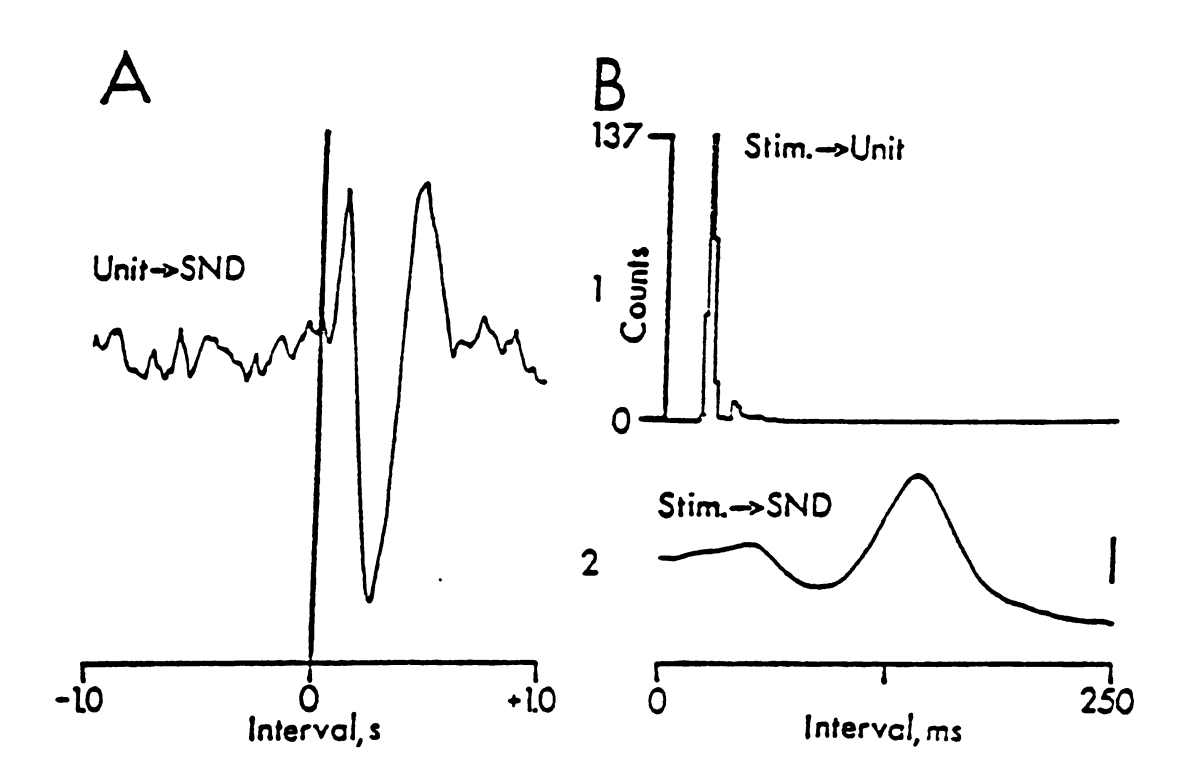


Figure 36

response to cortical stimulation were similar to those described for the type 1 neurons. All of the type two neurons were related to a rhythmic component in the EEG. For the type 2 thalamic neurons the sum of the modal onset latency and the time to peak in the spike-triggered average of SND was at least 40 ms less than the interval between the cortical stimulus and the peak increase in SND.

C. Effects of frontal lobotomy on the forebrain-dependent component of SND

Although diencephalic neurons with sympathetic nerve-related activity can be activated synaptically by stimulation of the frontal-parietal cortex, the question still remained as to whether these cortical regions contribute to basal SND in the anesthetized cat. This possibility was tested by first examining the effects of bilateral frontal lobotomy on blood pressure and inferior cardiac SND. Subsequently, an A3 transection was performed and the changes in SND and blood pressure compared with those produced by A3 transection in a group of control cats.

The results obtained in seven baroreceptor-denervated cats anesthetized with chloralose are summarized in Figure 37. Frontal lobotomy was performed bilaterally 1-2 mm behind the apex of the ansate sulcus. In five cats, the plane of transection passed immediately anterior to the genu of the corpus callosum. In the remaining three cats the transection removed 1 to 2 mm of the anterior corpus callosum. Frontal lobotomy failed to significantly reduce SND or mean blood pressure (Figure 37A, B). One hour after lobotomy, midbrain transection at A3 reduced SND initially (i.e., 2 min reading) to 72% of control and mean blood pressure by 44 mmHg (Figure 37C, D). These changes were statistically significant. Mean blood pressure before A3 transection (116±3 mmHg) was not significantly different than that (123±7 mmHg) before lobotomy. The level and time course of the reductions in SND and blood pressure produced by A3 transection in the lobotomized animals were not significantly different

inferior cardiac sympathetic nerve discharge (SND) and mean blood pressure (BP) in 7 baroreceptor-denervated cats anesthetized with chloralose. SND was quantified as described for Figure 2. Change in BP (mmHg) is shown. Panels C and D compare effects of mildbrain transection on SND and BP in 23 control cats with those in the 7 Figure 37. Effect of bilateral frontal lobotomy (panels A and B) and midbrain transection (panels C and D) on lobotomized cats. Values are means + SE.

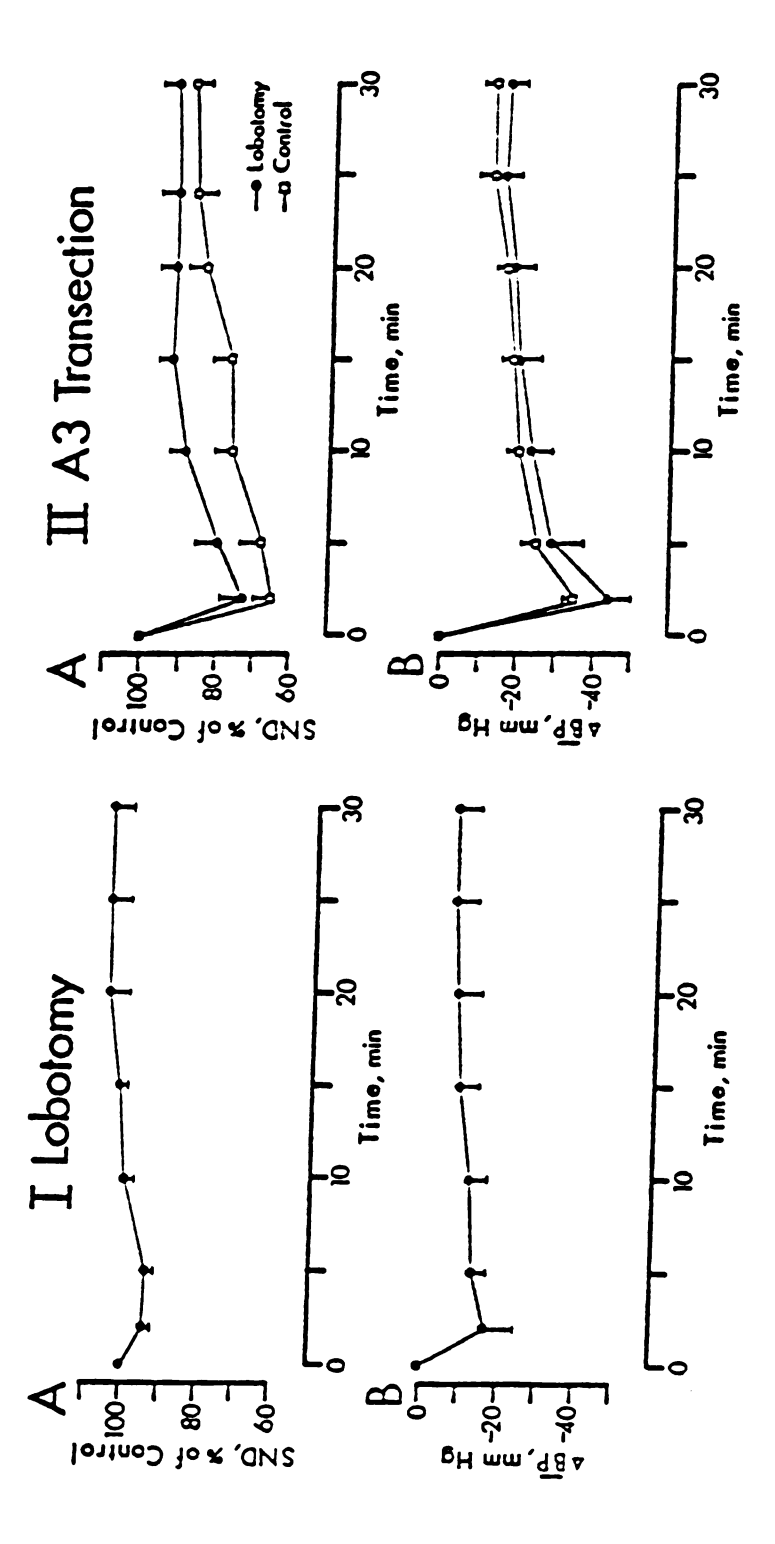


Figure 3

from those in 23 control animals (Figure 37C, D). These data suggest that the frontal-parietal cortex did not contribute to the forebrain-dependent component of SND in the anesthetized cat.

DISCUSSION

The purpose of this thesis was to determine whether the diencephalon is responsible for a component of basal SND in the anesthetized cat. Several lines of evidence from this study support this hypothesis. First, radio-frequency lesions of the hypothalamus or the medial thalamus significantly attenuated the reductions in SND and blood pressure produced by midbrain transection.

The reductions in SND and blood pressure produced by midbrain transection were attenuated similarly by either lateral hypothalamic, large medial hypothalamic or medial thalamic lesions. Whether these lesions were made at different points in the same pathway is not known. It is also possible that the forebrain-dependent component of SND was manifested only when two or more independent systems were simultaneously active. It is doubtful that attenuation of the effect of midbrain transection resulted from a nonspecific effect of the diencephalic lesions. Regarding this point the effectiveness of a lesion was related to the region rather than the amount of tissue destroyed. For example, small lateral hypothalamic lesions including a major output pathway to the brain stem [MFB (Nauta and Haymaker, 1969)] significantly attenuated the effects of midbrain transection on SND and blood pressure whereas larger lesions in the anterior medial hypothalamus did not.

Anterior portions of the medial hypothalamus participate in the expression of several forms of experimental hypertension (see INTRODUCTION, ILLD). For instance, destruction of either the AV3V region (Brody et al., 1984) or the PVH (Zhang and Ciriello, 1985a, 1985b) prevents or reverses the hypertension

produced by sinoaortic or aortic baroreceptor denervation in unanesthetized rats. In the present study, anterior medial hypothalamic lesions including the PVH failed to affect significantly the decreases in SND and blood pressure produced by midbrain transection. Medial hypothalamic lesions attenuated the effects of midbrain transection only when large portions of aHd, Hp and NHvm were destroyed. Whereas species differences as well as the use of an anesthetic might explain why anterior hypothalamic lesions failed to attenuate the effects of midbrain transection in my experiments, it should also be recognized that the basic phenomenon studied was different from that in unanesthetized rats. I examined the consequences of diencephalic lesions on the acute reductions in SND and blood pressure produced by midbrain transection. These acute changes were short lived (<1 hour). Moreover, although most pronounced in baroreceptordenervated cats, the effects of midbrain transection are qualitatively the same in cats with intact baroreceptor nerves (Huang et al., 1987). Thus the present study examined the effects of diencephalic lesions on a forebrain system that contributes to SND in both baroreceptor-innervated and -denervated cats, and whose loss is rapidly compensated for presumably by heightened activity in neural circuits located in the brain stem or spinal cord. The mechanism(s) responsible for the compensatory increase in neural activity remain to be determined. In contrast, the studies (Brody et al., 1984; Zhang and Ciriello, 1985a; 1985b) in unanesthetized rats focused on the effects of hypothalamic lesions on the chronic elevation of blood pressure observed in hypertensive models.

Diencephalic lesions were more effective in attenuating the reduction in SND produced by midbrain transection than the reduction in blood pressure. This is indicated by the fact that the changes in SND produced by midbrain transection in lesioned and nonlesioned cats deviated significantly from each other for a

longer period of time than did the changes in blood pressure. This was most evident for the series of experiments with medial thalamic lesions.

Currently, it is unclear why diencephalic lesions were more effective in attenuating the effects of midbrain transection on SND than on blood pressure. Inferior cardiac and renal SND were similarly affected by midbrain transection in nonlesioned cats (see Figures 3 and 4). Thus, the changes in inferior cardiac SND in these preparations were representative of those occurring in at least one sympathetic nerve controlling the vasculature. Whether such is also the case in cats with diencephalic lesions was not tested. Consequently, the possibility remains that the diencephalic regions lesioned exerted greater control over cardiac sympathetic nerves than vascular sympathetic nerves.

Humoral substances may have played a role in determining the degree to which blood pressure was reduced by midbrain transection. If so, differential attenuation of the effects of midbrain transection on SND and blood pressure may indicate that the lesions destroyed diencephalic regions that were more involved in controlling SND than the release of these substances. In this regard, although some of the hypothalamic lesions destroyed the PVH, none of the lesions in this study destroyed both the PVH and the supraoptic nuclei. Both of these nuclei are known to be involved in the humpral control of the circulation through the release of vasopresssin (Blessing et al., 1982; Johnson, 1985; Page, 1987).

The second line of evidence supporting the view that the medial diencephalon contributes to SND in the anesthetized cat was obtained in experiments in which multiumit activity was recorded in the hypothalamus and thalamus. SND was coupled to ongoing diencephalic activity in both CNS-intact and decorticate cats. In some experiments, SND was temporally related to medial thalamic and hypothalamic multiunit activity but not to lateral thalamic activity. In other cases, SND was coupled to lateral thalamic as well as to medial thalamic and

hypothalamic activity. The potential significance of this observation will be discussed subsequently.

Radio-frequency lesions undoubtedly destroyed diencephalic neurons and axons of passage. Moreover, multiunit diencephalic activity synchronized to SND may have been recorded from axons of passage rather than synaptic networks. Thus, other approaches were required to determine whether the hypothalamus and/or medial thalamus contain the cell bodies of neurons that contribute to SND in the anesthetized cat. Evidence that the medial thalamus contains synaptic networks capable of influencing SND was provided by the results of chemical stimulation studies. While other investigators (Powell and Buchannan, 1985: Rockhold et al., 1985) reported that the injection of CNS stimulants into the medial thalamus increases blood pressure and heart rate, the present study was the first to demonstrate directly changes in SND upon chemical stimulation of the medial thalamus. The intrathalamic injection of picrotoxin increased the amplitude and decreased the variability of the interslow wave intervals (i.e. synchronized) in inferior cardiac SND (see Figure 20). The changes in SND were accompanied by an increase in blood pressure in 40% of the experiments. This CNS stimulant with GABA antagonistic properties was chosen in view of the large GABAergic innervation of the medial thalamus (Houser et al., 1980; Steriade et al., 1985). The microinjection of equal volumes of saline into the medial thalamus or of picrotoxin into the lateral thalamus failed to elicit sympathetic responses. Although intrathalamic injections of fast green dye did not spread to the hypothalamus or the ventricular system, I cannot be completely certain that the extent of dye spread was representative of that of picrotoxin. qualification, it appears that the medial thalamus contains synaptic networks capable of generating sympathetic rhythms. This also seems to be the case for the hypothalamus. Regarding this point, numerous investigators (Gellhorn and

Redgate, 1955; Redgate and Gellhorn, 1956a,b; Lee et al., 1972; Finch and Hicks, 1977; Williford et al., 1980; Schmidt and Dimicco, 1984; Dimicco and Abshire, 1987; Rockhold et al., 1987) have reported that blood pressure and heart rate changes are elicited by the injection of neurotoxins and excitatory amino acids into the hypothalamus of rats and cats.

While the results of chemical stimulation indicate that synaptic networks in the medial diencephalon can influence SND, these experiments did not answer the question of whether these networks are the same as those responsible for the tonic forebrain-dependent component of SND in the anesthetized cat. Thus experiments were initiated to locate individual diencephalic neurons with naturally occurring (i.e., spontaneous) discharges temporally related to SND. Barman and Gebber (1982) identified hypothalamic neurons with sympathetic nerve-related activity. The current study confirmed this finding and, in addition, demonstrated for the first time that such neurons are also contained in the medial thalamus. Two types of neurons with sympathetic nerve-related activity were located in both the hypothalamus and medial thalamus. Type 1 unit activity was synchronized to an aperiodic spike-like event in SND while type 2 neuronal activity was synchronized to a 2- to 6-Hz rhythm in SND (see Figure 23). Neurons with these patterns of relationship to SND are also located in the cat medulla (Barman and Gebber, 1981; 1985; 1987; Gebber and Barman, 1981; Morrison and Gebber, 1985).

The major issue raised by these results is whether the temporal relationships between diencephalic unit activity and SND reflect the existence of functional connections between these neurons and sympathetic nerves. That is, were type 1 and/or type 2 diencephalic neurons contained in networks contributing to SND in the anesthetized cat? Two lines of evidence support this possibility. First, as demonstrated by the lesion studies, ablation of either hypothalamic or medial thalamic regions containing type 1 and type 2 neurons attenuated the reduction in

SND produced by decerebration. The distribution of neurons with sympathetic nerve-related activity in widely separated diencephalic nuclei (see Figure 24) presumably explains why large lesions were required to attenuate the effect of decerebration on SND. Small diencephalic lesions significantly attenuated the reduction in SND produced by decerebration only when they destroyed the MFB, a major output pathway to the brain stem (Nauta and Haymaker, 1969; Conrad and Pfaff, 1976).

The second line of evidence supporting the view that at least some of the diencephalic neurons studied contributed to SND was obtained with electrical stimulation. SND was increased by low current stimuli applied through the microelectrode used to record from hypothalamic and medial thalamic neurons with sympathetic nerve-related activity. The interval between the stimulus and the peak increase in SND often was close to that between unit spike occurrence and the peak of the accompanying change in SND. This was most evident from type 1 unit recording sites. These data suggest that at least some diencephalic neurons with sympathetic nerve-related activity were involved in mediating the increases in SND produced by electrical stimulation of the diencephalic recording sites.

An important issue in these studies concerns the sources of the sympathetic nerve-related activity of diencephalic neurons. Is such activity inherent to diencephalic circuits or is it imposed on these neurons by inputs from other sources? The second alternative likely holds for type 1 diencephalic neurons. The discharges of these cells were also synchronized to a spike-like event in frontal-parietal cortical activity. The onset of the spike-like event in cortical activity in most cases preceded the discharge of the type 1 diencephalic neuron. This observation suggests that the spike-like event in SND was not generated in the diencephalon. Nevertheless, type 1 diencephalic neurons may have been in the

pathway transmitting this activity pattern to sympathetic nerves. As already discussed, this possibility is supported by the results obtained with microstimulation at type 1 diencephalic unit recording sites. There are at least two ways to explain why spike-like cortical activity preceded type 1 diencephalic unit activity. First, the frontal-parietal cortex may have provided an important driving input to type 1 diencephalic neurons. This possibility seems remote, however, since frontal lobotomy failed to attenuate the effects of midbrain transection on SND. This observation indicates that the sympathetic nerve-related activity of these neurons did not arise in the frontal cortex. However, these observations do not rule out the possibility that the frontal-parietal cortex contributes to SND under other conditions. For example, Skinner and Reed (1931) demonstrated that cryogenic blockade of a frontocortico-hypothalamo-brain stem pathway prevents ventricular fibrillation in the ischemic heart of emotionally stressed conscious pigs.

The second possible explanation for the relationship of type 1 units to a spike-like cortical event preceding their discharge is that the cortex and the diencephalon share input from a common source. In this case, conduction time from the source to the cortex would have been shorter than from the source to the diencephalon.

Choosing between these possibilities is complicated by the fact that the origin of the spike-like activity in the EEG of chloralose-anesthetized animals is unknown. Under chloralose anesthesia, the EEG is characterized by a pattern of 2- to 6-Hz slow waves and spikes (Winters and Spooner, 1966). A similar EEG pattern is observed during natural or experimentally-induced global epileptic seizures (Gloor and Testa, 1974). At this time, neither the origin nor the mechanism responsible for this epileptic pattern of cortical slow waves and spikes is known. Studies have implicated the cortex (Fischer and Prince, 1977; Gloor et

al., 1977), the medial and intralaminar thalamic nuclei (Quesney et al., 1977; Kostopoulos et al., 1981) and the reticular formation (Velasco et al., 1975; Faingold, 1980) as being involved in the genesis of this EEG pattern.

The origin of the sympathetic nerve-related discharges of type 2 diencephalic neurons is also unknown. SND contains 2- to 6-Hz rhythmic components in decerebrate, baroreceptor-denervated cats (Barman and Gebber, 1980). This activity pattern is abolished by acute high spinal cord transection (McCall and Gebber, 1975). These observations led to the proposal that brain stem circuits are inherently capable of generating a 2- to 6-Hz component in SND (Barman and Gebber, 1980; Gebber, 1980). Forebrain circuits can also generate 2- to 6-Hz rhythms since this rhythm appears in thalamic (Andersson and Manson, 1971; Villablanca, 1974) and cortical (Barman and Gebber, 1980; Steriade et al., 1987) activity in decerebrate cats and in guinea-pig thalamic slice preparations, in vitro (Jahnsen and Llinas, 1984). Thus there are at least three ways to explain synchronization of type 2 diencephalic unit activity to 2- to 6-Hz SND. First, the diencephalic neurons may comprise a generator of 2- to 6-Hz SND subsidiary to that located in the brain stem. Second, type 2 diencephalic neurons may receive input from a 2- to 6-Hz generator of SND located in the brain stem. In this case, the temporal relationship between type 2 diencephalic unit activity and SND might not reflect a sympathetic nerve controlling function of these neurons. Regarding this possibility there are numerous pathways from the VLM, medullary LTF and raphe nuclei to the diencephalon. These medullary regions contain neurons with activity locked to the 2- to 6-Hz activity pattern in SND. Neurons in the VLM have been shown both anatomically and electrophysiologically to project to the RPO, Ha, PVH, HL and supraoptic nuclei in the hypothalamus (Loewy et al., 1981; Kaba et al., 1986). Although a direct projection from the medullary LTF to the hypothalamus has not been reported, the medullary LTF

may influence the hypothalamus via a relay in the VLM (Barman and Gebber, 1987). Alternatively, inputs from the medullary LTF may reach the hypothalamus via a polysynaptic route through the reticular core (Scheibel and Scheibel, 1958). A similar pathway may exist whereby LTF influences are transmitted through the mesencephalic reticular formation and then to the medial thalamus (Scheibel and Scheibel, 1958). Neither the VLM nor the medullary LTF project directly to the medial thalamus; however, their influences may reach the thalamus via a relay in the HL, ZI or aHd (Velayos, 1982; Irle, 1984; Ono and Niimi, 1985). Direct projections from raphe magnus and obscurus to most nuclei in the medial, lateral and dorsal hypothalamus in rats and cats have been identified (Bobillier et al., 1976; Takagi et al., 1980; Bowker, 1986). In addition, Bobillier et al. (1976) reported direct projections from raphe magnus to CM, CL, Pf and Pc, but not to MD in the cat.

A third possibility which might account for the synchronization of type 2 diencephalic neurons to 2- to 6-Hz SND is that these neurons receive input from a 2- to 6-Hz generator located elsewhere in the forebrain such as in the medial septum. Wilson et al. (1976) demonstrated that the septum of the anesthetized cat contains pacemaker neurons which discharge in rhythmic bursts at frequencies of 2- to 6-Hz. These neurons are presumed to generate the hippocampal theta rhythm. The septum projects to the lateral and medial hypothalamus (Szentagothai, 1968; Palkovits and Zaborszky, 1979) and medial thalamus (Gullery, 1952; Irle et al., 1984) of the cat.

The relationships between the discharges of type 2 units and the inferior cardiac nerve suggest that the 2- to 6-Hz rhythmic components in SND arise from more than one central source. Regarding this point, the peri-spike-triggered averages of SND for type 2 neurons contained a 2- to 6-Hz rhythm independent of whether the unit had cardiac-related activity. Although close in frequency, one

can presume that the rhythm in the spike-triggered average of SND for type 2 neurons without cardiac-related activity is distinct from the cardiac-related rhythm. Indeed, the period of the 2- to 6-Hz rhythm in the peri-spike-triggered average of SND for a thalamic unit without cardiac-related activity was clearly different from that of the cardiac rhythm when the heart rate was slowed by atenolol (see Figure 30). Thus, I propose that SND contains both cardiac- and noncardiac-related 2- to 6-Hz rhythmic components. This hypothesis is indirectly supported by other observations. The activity of most type 2 neurons was synchronized to a noncardiac-related 2- to 6-Hz rhythm in cortical activity. The frequency of the cortical rhythm was the same as that of the rhythm in the spike-triggered averages of SND for type 2 neurons without cardiac-related activity. These data may explain why crosscorrelation analysis in some cats reveals a common 2- to 6-Hz rhythm in SND and cortical activity (Camerer et al., 1977; Barman and Gebber, 1980; Gebber and Barman, 1981; Huang et al., 1987).

Descending connections from the hypothalamus to autonomic regions of the brain stem and spinal cord have been studied extensively. The VLM receives projections from aHd, HL and Hp (Lovick, 1985). In addition, the axons of neurons in the PVH, HL and aHd pass through the VLM on their way to the IML of the spinal cord in rats and cats (Kuypers and Maisky, 1975; Saper et al., 1976; Tucker and Saper, 1985). Whether the axons of these hypothalamic neurons emit collaterals in the VLM has not been determined. Hilton and coworkers (1983) by using electrical stimulation traced a functional pathway from the midbrain defense regions to the VLM. They speculated that the pathway controls sympathetic tone even in the anesthetized animal. Hilton and Smith (1984) and Lovick et al. (1984) showed that medullospinal VLM neurons are synaptically activated by stimulation of the midbrain and/or hypothalamic defense regions.

The raphe nuclei (magnus, pallidus and obscurus) receive direct afferent projections from HL, HP and H1, H2 in the cat (Abolos and Basbaum, 1981) and from HL, aHd, PVH, Hp in the rat (Conrad and Pfaff, 1976; Hosoya, 1985; ter Horst and Luiten, 1986).

In contrast to the hypothalamus, relatively little attention has been paid to descending connections emanating from medial and intralaminar thalamic nuclei. There are at least four routes from the medial thalamus that might be involved in the control of SND. First, a projection from the medial thalamus to the lateral hypothalamus has been anatomically (Seigel et al., 1973) and functionally mapped by using the 2-deoxyglucose technique (Brutus et al., 1984). Such a pathway might explain why type 1 and type 2 hypothalamic neurons fired at about the same time as their counterparts in the medial thalamus (see Figure 25). Alternatively, these data may indicate that hypothalamic and medial thalamic neurons with sympathetic nerve-related activity received input from a common source. It is also possible that the thalamic neurons were influenced by their hypothalamic counterparts. Indeed, projections from hypothalamic regions containing type 1 and type 2 neurons to the medial thalamus have been demonstrated (Velayos, 1982; Irle, 1984; Ono and Niimi, 1985).

Two other routes over which medial thalamic neurons might influence SND include projections to the midbrain. One route includes a monosynaptic connection from the intralaminar thalamic nuclei to the midbrain tegmentum. This pathway was defined in rats, mice and cats by using the Golgi technique (Scheibel and Scheibel, 1967). The second route includes a disynaptic pathway from the intralaminar and medial thalamic nuclei to the periaqueductal gray (PAG) of the midbrain tegmentum and the superior colliculus via the n. reticularis thalami (Scheibel and Scheibel, 1966; Grofova et al., 1978; Parent and Steriade, 1984). Regarding these potential pathways for the control of SND, the microinjection of

excitatory amino acids into the midbrain tegmentum or PAG increases blood pressure (Hilton, 1982; Tan et al., 1983; McDougall et al., 1985). Thus these midbrain regions are believed to contain the cell bodies of neurons that control SND. Hypothalamic influences on SND may also involve a relay in the PAG since Ha, aHd, PVH, HL, ZI are known to project to this region (Saper et al., 1976; 1978; ter Horst and Luiten, 1986).

A fourth route over which medial thalamic neurons might influence SND includes a loop through the prefrontal and infralimbic cortex. CL, MD and Pc contain neurons projecting to these cortical regions (Scheibel and Scheibel, 1967; Jones, 1985). Moreover, changes in blood pressure and heart rate can be elicited by electrical stimulation of these cortical regions (Hoff and Green, 1936; Green and Hoff, 1937; Hsu et al., 1942; Kaada, 1951; Eliasson et al., 1952; Hoff et al., 1959; 1963; Delagado, 1960; Lofving, 1961; Clarke et al., 1968). It should be noted, however, that the integrity of thalamocortical projections is not mandatory for eliciting increases in SND by electrical stimulation of the medial thalamus. Regarding this point, sympathetic nerve responses elicited by low current stimuli applied to sites in the medial thalamus were similar in intact and decorticate cats (see Figure 18).

Although some hypothalamic neurons respond to natural or electrical activation of baroreceptor afferents (Hilton and Syper, 1971; Calaresu et al., 1975) or have cardiac-related activity (Barman and Gebber, 1982), this is the first study to describe the effects of baroreceptor reflex activation on diencephalic neurons with sympathetic nerve-related activity. These results further reflect the heterogeneity of such neurons. Perhaps the most interesting finding was that some of the hypothalamic neurons and all of the medial thalamic neurons with sympathetic nerve-related activity did not respond to baroreceptor reflex activation. This was the case even when the reflex inhibition of inferior cardiac SND

was complete (see Figure 33IB, IIB). Some of these neurons may have exerted sympathoexcitatory actions. If so, their influences on SND would have been intercepted at a lower level of the neuraxis.

Although it is generally accepted that cardiovascular responses can be elicited by stimulation of the prefrontal, sensorimotor and infralimbic cortex in an variety of species (Hoff and Green, 1936; Green and Hoff, 1937; Hsu et al., 1942; Kaada, 1951; Eliasson et al., 1952; Hoff et al., 1959; 1963; Delgado, 1960; Lofving, 1961; Clarke et al., 1963), this is the first study to demonstrate directly that sympathetic nerve responses can be elicited by electrical stimulation of these cortical regions. Evidence is presented suggesting that both sympathoexcitatory and -inhibitory systems are represented in these cortical regions.

In view of the preceding discussion of diencephalic involvement in the control of SND in the anesthetized cat, a major issue is whether sympathetic nerve responses elicited by electrical stimulation of the frontal-parietal cortex involve a synaptic relay in the diencephalon. That is, are diencephalic neurons with sympathetic nerve-related activity part of a corticosympathetic pathway? If the diencephalic neurons were contained within pathways mediating cortical influences to the sympathetic nerves, one would expect that these neurons could be synaptically activated by stimulation of those cortical areas from which sympathetic nerve responses were elicited. Furthermore, the sum of the modal onset latency of synaptic activation of the diencephalic neuron and the interval between its spontaneous discharge and the peak increase in SND (as measured from its peri-spike-triggered average) should be close to the interval between the cortical stimulus and the peak of the increase in SND in the post-stimulus average. This was the case for 3 of 4 type 1 hypothalamic neurons activated by stimulation of the cortex, suggesting that these neurons were part of a corticosympathetic pathway. However, such was not the case for the type 1 nor the type

2 medial thalamic neurons activated by cortical stimulation, since the intervals were not similar. Thus, the results are consistent with the possibility that hypothalamic but not thalamic neurons with sympathetic nerve-related activity are contained in a pathway responsible for the sympathetic nerve responses elicited by stimulation of the frontal-parietal cortex. The functional significance of those type 2 hypothalamic and type 1 medial thalamic neurons inhibited by stimulation of the cortex remains to be determined.

While the results of my study suggest that cortically-evoked sympathetic nerve responses are, at least in part, mediated through the hypothalamus, anatomical studies have failed to demonstrate a direct connection from the frontal cortex to the hypothalamus in the cat (Szentagothai, 1968; Palkovitz and Zaborszky, 1969). However, a direct frontocortico-hypothalamic connection has recently been demonstrated in the rat (Beakstead, 1979; Van der Kooy et al., 1984). In the cat, influences from the frontal cortex may reach the hypothalamus via a multisynaptic pathway through the septum or amygdala (cf. Brodal, 1981; Kuypers, 1981).

The possibility that the sympathetic nerve responses elicited by cortical stimulation involved extra-diencephalic as well as diencephalic pathways must also be considered. Indeed this is believed to be the case in the monkey (Wall and Davis, 1951). There are at least two extra-diencephalic pathways by which cortical sympathetic responses may reach sympathetic nerves. First, these responses may have involved the activation of a direct cortical projection to the medullary tegmental field or the PAG (Brodal, 1981; Kuypers, 1981). Second, some of the responses may have been mediated via a monosynaptic pathway from the medial frontal cortex to the IML. Such a pathway was recently identified in the task by Hurley-Guis et al., (1986).

The possibility that the cortically-evoked sympathetic responses did not involve the activation of cortical neurons must also be considered. These responses may have resulted from the antidromic activation of thalamic or hypothalamic neurons connected via collaterals to caudally projecting sympathetic neurons. In this case, the synaptic activation of diencephalic neurons with sympathetic nerve-related activity may have been due to collateral input to these neurons from the antidromically activated thalamocortical or hypothalamocortical neurons. Both the thalamus (Jones, 1985) and the hypothalamus (Conrad and Pfaff, 1976) contain neurons with cortically projecting axons.

There are no studies implicating the relay and association nuclei of the lateral thalamus in the control of SND and blood pressure. Thus, the finding that multiunit lateral thalamic activity was temporally related to SND in some experiments was unexpected. There are at least three possible explanations to account for the synchronization of SND to lateral thalamic activity. First, the sympathetic nerve-related activity in the lateral thalamus may have resulted from the hypersynchronization of activity in different thalamic nuclei rather than simply a role of the lateral thalamus in the control of SND. Regarding this possibility, the predominant frequency of slow wave activity at medial and lateral thalamic sites was essentially the same in these experiments. Such occurrences may reflect the level of cateleptic anesthesia produced by chloralose, since this agent is known to be capable of hypersynchronizing activity in different thalamic nuclei and cortical regions (Winters and Spooner, 1966). Direct pathways from the medial to the lateral thalamus which might account for the synchronization of activity in these two regions have been demonstrated (Purpura et al., 1966; Purpura, 1970).

A second explanation of sympathetic nerve-related activity in the lateral thalamus is that this activity was recorded from the axons of medial thalamic

neurons passing through the lateral thalamus. Evidence against this possibility comes from the finding that in some experiments activity recorded from medial, but not lateral thalamic nuclei was related to SND. In these experiments the lateral thalamus was extensively searched, suggesting that the lack of sympathetic nerve-related activity in the lateral thalamus was not due simply to the failure to locate the axons of medial thalamic neurons with activity related to SND.

A third possibility is that lateral thalamic neurons are involved in controlling SND. This possibility is supported by the fact that electrical stimulation of
the lateral thalamus increased SND. Whether these responses involved the
activation of lateral thalamic neurons or fibers of passage is not known. The fact
that picrotoxin injected into the lateral thalamus failed to affect SND does not
distinguish between these alternatives. Lateral thalamic "sympathetic" neurons
may be picrotoxin-insensitive. If such neurons exist, there are at least two routes
by which they may influence SND. First, their influences may be relayed through
the cortex which is a major target of lateral thalamic neurons (Scheibel and
Scheibel, 1967; Jones, 1985). Second, they may control SND via the n. reticularis
thalami or medial and intralaminar thalamic nuclei. These nuclei project to the
midbrain and hypothalamus (Scheibel and Scheibel, 1966; 1967; Seigel et al., 1973;
Grofova et al., 1978; Brutus et al., 1984; Parent and Steriade, 1984) and receive
input from the lateral thalamic nuclei (Jones, 1985). None of these potential roles
of the lateral thalamic nuclei in the control of SND were tested in this thesis.

SUMMARY

My thesis involved studies on the role of the diencephalon in the control of sympathetic nerve discharge (SND) in the anesthetized cat. The thesis is comprised of four main projects. The findings and conclusions of each of these projects are summarized below.

A. Localization of diencephalic regions contributing to SND in the baroreceptor-denervated cat anesthetized with chloralose.

The results of this project are:

- 1. Midbrain transection at stereotaxic plane A3 produced significant decreases in blood pressure (38±6 mmHg) and SND in the inferior cardiac (34+4%) and renal (35+3%) sympathetic nerves.
- 2. Radio-frequency lesions of the lateral hypothalamus (including the MFB), posterior medial hypothalamus or medial thalamus significantly attenuated the decreases in SND and blood pressure produced by midbrain transection.
- 3. Lesions of the anterior medial hypothalamus (including the PVH) failed to attenuate the effects of midbrain transection.

The conclusions of this project are:

1. As previously suggested by Huang et al. (1987), the forebrain makes a significant contribution to SND in this preparation.

- The medial hypothalamus and medial thalamus are, at least in part, responsible for the forebrain-dependent component of basal SND in this preparation.
- B. Synchronization of SND to diencephalic multiunit activity and sympathetic nerve responses to electrical and chemical stimulation of the diencephalon.
 - Multiunit activity recorded from the thalamus and hypothalamus was temporally related to a 2- to 6-Hz component of SND in the majority of baroreceptor-denervated and -intact cats anesthetized with chloralose.
 - 2. In some CNS-intact and decorticate cats, activity recorded from the medial thalamus and hypothalamus, but not from the lateral thalamus was related to SND. In other cats, lateral as well as medial thalamic and hypothalamic activity was synchronized to SND.
 - Electrical stimulation of the medial and lateral thalamus and hypothalamus elicited increases in inferior cardiac SND in decorticate and CNS-intact cats.
 - 4. The injection of the GABA antagonist picrotoxin into the medial, but not the lateral thalamus increased the amplitude of the 2- to 6-Hz sympathetic slow wave activity and decreased the variability of the interslow wave intervals.

The conclusions of this project are:

The results of this project are:

1. A component of basal SND in the 2- to 6-Hz range can be coupled to thalamic and hypothalamic activity in both CNS-intact and decorticate cate cats anesthetized with chloralose.

- 2. A functional connection exists between the diencephalon and the sympathetic nerves.
- The medial thalamus contains the cell bodies of neurons capable of influencing SND.
- C. Identification of diencephalic neurons with sympathetic nerve-related activity.

The results of this project are:

- 1. Peri-spike-triggered averaging showed that some diencephalic neurons (type 1 neurons) were related to a spike-like event in SND following their discharge but were not related to SND preceding their discharge.

 All type 1 neurons were also related to a cortical event which most often preceded the discharge of the neuron.
- Peri-spike-triggered averaging showed that some diencephalic neurons
 (type 2 neurons) were related to a 2- to 6-Hz rhythm in SND. All type
 medial thalamic and most type 2 hypothalamic neurons were also related to a 2- to 6-Hz rhythm in frontal-parietal cortical activity.
- 3. Stimulation through the recording microelectrode at type 1 and type 2 recording sites elicited increases in inferior cardiac SND. In some instances, the interval between the stimulus and the peak increase in SND was close to that between unit spike occurrence and the peak of the accompanying increase in SND.
- 4. Post-R wave averaging in combination with spike-triggered averaging revealed that the discharges of some type 2 diencephalic neurons were synchronized to a cardiac-related component in SND while those of other type 2 neurons were locked to a noncardiac-related 2- to 6-Hz component.

5. Baroreceptor reflex activation altered (increased or decreased) the firing rate of some type 1 and type 2 hypothalamic neurons. Reflex activation did not affect the firing of medial thalamic neurons with sympathetic nerve-related activity.

The conclusions of this project are:

- 1. The medial thalamus and hypothalamus in the chloralose-anesthetized cat contains two types of neurons with sympathetic-nerve related activity.
- 2. At least some diencephalic neurons with sympathetic nerve-related activity are contained in pathways mediating the increases in SND produced by electrical stimulation of the diencephalon.
- 3. Some hypothalamic but none of the medial thalamic neurons with sympathetic nerve-related activity receive inputs from baroreceptor afferents.
- 4. There is more than one central source of basal 2- to 6-Hz SND in the chloralose-anesthetized cat.
- D. Sympathetic nerve responses elicited by cortical stimulation.

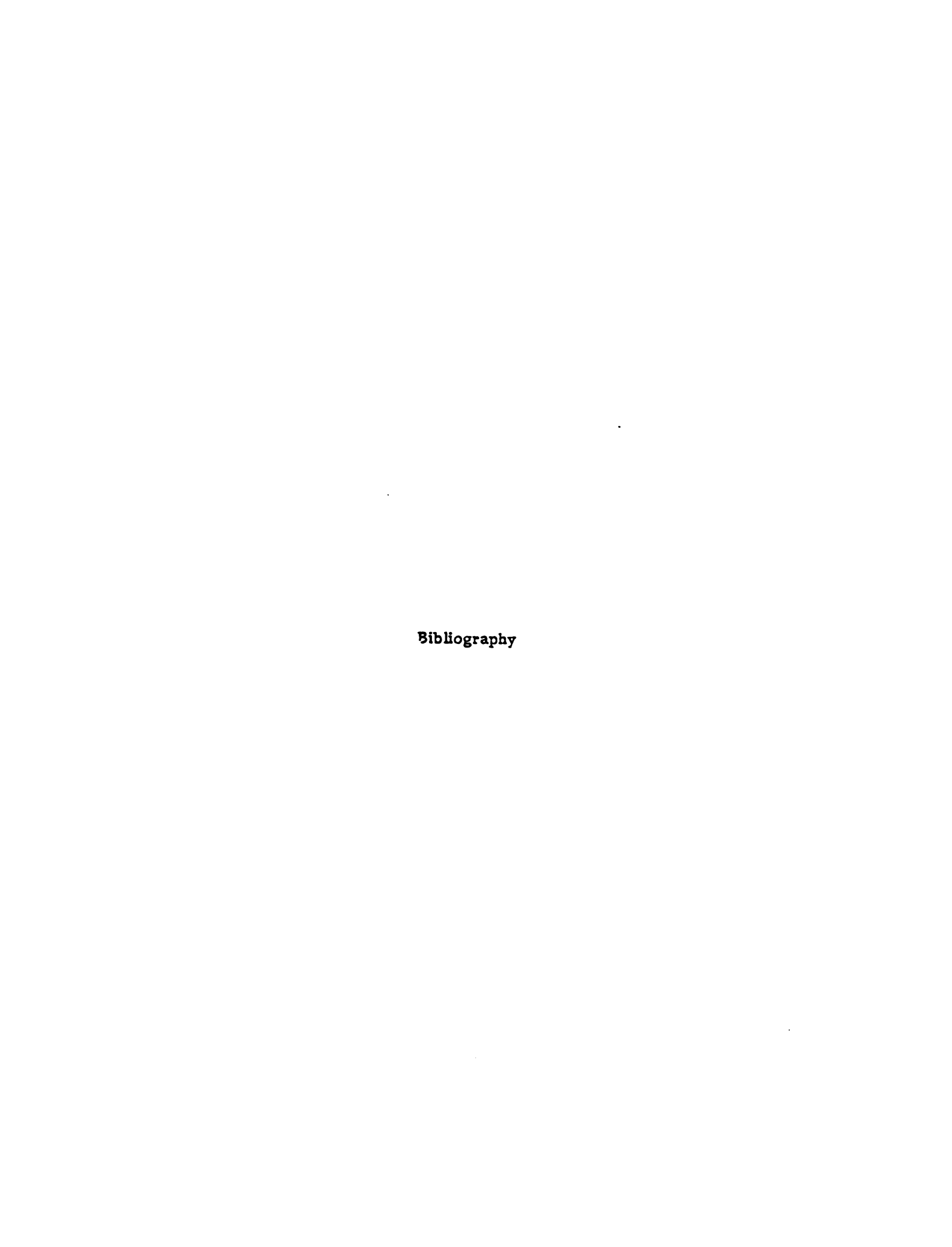
The results of this project are:

- Both increases and decreases in inferior cardiac SND can be elicited
 by stimulation of the frontal-parietal and infralimbic cortex.
- 2. Stimulation of the frontal (sensorimotor) cortex synaptically activated medial thalamic and hypothalamic type 1 and medial thalamic type 2 neurons.
- 3. For some of the hypothalamic type 1 neurons, the sum of the modal onset latency of synaptic activation plus the time to peak in the spiketriggered average of SND was similar to the interval between the

- cortical stimulus and the peak of the evoked increase in inferior cardiac SND.
- 4. Bilateral frontal lobotomy failed to attenuate the decreases in SND and blood pressure produced by midbrain transection at stereotaxic plane A3 in baroreceptor-denervated cats anesthetized with chloralose.

The conclusions of this project are:

- The prefrontal, frontal and infralimbic cortex have sympathetic representation. Both sympathoexcitatory and -inhibitory systems are represented.
- 2. Some type 1 hypothalamic neurons may be contained in pathways mediating sympathetic responses to cortical stimulation.
- 3. The prefrontal and frontal cortex is not involved in providing the forebrain-dependent component of SND under the conditions of my experiments.



BIBLIOGRAPHY

- Abolis, LA. and Basbaum, A.L.: Afferent connections of the rostral medulla of the cat: A neural substrate for midbrain-medullary interactions in the modulation of pain. J. Comp. Neurol. 201: 285-297, 1981.
- Abrahams, V.C., Hilton, S.M. and Zbrozyna, A.: Active muscle vasodilatation produced by stimulation of the brain stem: its significance in the defense reaction. J. Physiol. (London) 154: 491-513, 1960.
- Adair, J.R., Hamilton, B.L., Scappaticci, K.A., Helke, C.J. and Gillis, R.A.: Cardiovascular responses to electrical stimulation of the medullary raphe area of the cat. Brain Res. 128: 141-145, 1977.
- Adrian, E.D., Bronk, D.W. and Phillips, G.: Discharges in mammalian sympathetic nerves. J. Physiol. (London) 74: 115-133. 1932.
- Alexander, N. and Morris, M.: Elevated plasma vasopressin in the sinoaortic denervated (SAD) rat. Fed. Proc. 41: 1094, 1982.
- Alexander, R.S.: Tonic and reflex functions of medullary sympathetic cardiovascular centers. J. Neurophysiol. 9: 205-217, 1946.
- Anand, B.K. and Dua, S.: Circulatory and respiratory changes induced by electrical stimulation of limbic system (visceral brain). J. Neurophysiol. 19: 391-400. 1956.
- Andersen, P. and Eccles, J.C.: Inhibitory phasing of neuronal discharge. Nature 196: 645-647, 1962.
- Andersen, P., Eccles, J.C. and Sears, T.A.: The ventrobasal complex of the thalamus: Types of cells, their responses and their functional organization. J. Physiol. (London) 174: 370-399, 1964.
- Andersen, P. and Andersson, S.A.: In Physiological basis of the alpha rhythm, ed. by A. Towe, Appleton-Century-Crafts, New York, 1968.
- Andersson, S.A. and Manson, J.R.: Rhythmic activity in the thalamus of the decorticate cat. Electroenceph. clin. Neurophysiol. 31: 2134, 1971.
- Angyan, L.: Cardiovascular effects of septal, thalamic, hypothalamic and midbrain self-stimulation. Physiol. Behav. 20: 217-226, 1978.
- Bachoo, M. and Polosa, C.: Properties of the inspiration-related activity of sympathetic preganguionic neurons of the cervical trunk in the cat. J. Physiol. 385: 545-564, 1987.

- Barman, S.M. and Gebber, G.L.: Basis for synchronization of sympathetic and phrenic nerve discharges. Am. J. Physiol. 231(5): 1601-1607, 1976.
- Barman, S.M. and Gebber, G.L.: Tonic sympathoinhibition in the baroreceptor-denervated cat. Proc. Soc. Exp. Biol. Med. 157: 648655, 1978.
- Barman, S.M. and Gebber, G.L.: Sympathetic nerve rhythm of brain stem origin. Am. J. Physiol. 239: R42-R47, 1980.
- Barman, S.M. and Gebber, G.L.: Brain stem neuronal types with activity patterns related to sympathetic nerve discharge. Am. J. Physiol. 240 (Regulatory Integrative Comp. Physiol. 9): R335-R347, 1981.
- Barman, S.M. and Gebber, G.L.: Hypothalamic neurons with activity patterns related to sympathetic nerve discharge. Am. J. Physiol. 242 (Regulatory Integrative Comp. Physiol. 11): R34-R43, 1982.
- Barman, S.M. and Gebber, G.L.: Sequence of activation of ventrolateral and dorsal medullary sympathetic neurons. Am. J. Physiol. 245 (Regulatory Integrative Comp. Physiol. 14): R438-R447, 1983.
- Barman, S.M. and Gebber, G.L.: Axonal projection patterns of ventrolateral medullospinal sympathoexcitatory neurons. J. Neurophysiol. 53(6): 1551-1566, 1985.
- Barman, S.M. and Gebber, G.L.: Lateral tegmental field neurons of cat medulla: a source of basal activity of ventrolateral medullospinal sympathoexcitatory neurons. J. Neurophysiol. 57(5): 1410-1424, 1987.
- Barman, S.M., Gebber, G.L. and Calaresu, F.R.: Differential control of sympathetic nerve discharge by the brain stem. Am. J. Physiol. 247 (Regulatory Integrative Comp. Physiol. 16): R513-R519, 1984.
- Beckstead, R.M.: An autoradiographic examination of corticocortical and subcortical projections of the mediodorsal-projection (prefrontal) cortex in rat. J. Comp. Neurol. 184: 43-62, 1979.
- Bendat, J.S. and Piersol, A.G.: Random Data: Analysis and Measurement Procedures, Wiley, New York, 1971.
- Berecek, K.H., Barron, K.W., Webb, R.L. and Brody, M.J.: Vasopressin-central nervous system interactions in the development of DOCA hypertension. Hypertension 4(suppl. II): II-131-II-137, 1982.
- Bernard, C: Lecons sur la Physiologie et la Pathologie du systeme Nerveux, vol. 1, Bailliere, Paris, 1863.
- Bing, R.J., Thomas, C.B. and Waples, E.C.: The circulation in experimental neurogenic hypertension. J. Clin. Invest. 24: 513522, 1945.
- Blessing, W.W., Sved, A.F. and Reis, D.J.: Destruction of noradrenergic neurons in rabbit brain stem elevates plasma vasopressin, causing hypertension. Science 217: 661-663, 1982.

- Bobillier, P., Seguin, S., Petitjean, F., Salvert, D., Touret, M. and Jouvet, M.: The raphe nuclei of the cat brain stem: A topographical atlas of their efferent projections as revealed by autoradiography. Brain Res. 113: 449-486, 1976.
- Bowker, R.M.: The relationship between descending serotonin projections and ascending projections in the nucleus raphe magnus: a double labeling study. Neurosci. Lett. 70: 348-353, 1986.
- Brodal, A.: Neurological Anatomy in Relation to Clinical Medicine, Oxford Univ. Press, New York, 1981.
- Brody, M.J., Faber, J.E., Mangiapane, M.L. and Porter, J.P.: The central nervous system and prevention of hypertension. In Handbook of Hypertension 4 Experimental and Genetic Models of Hypertension, ed. by W. de Jong, pp. 474-494, Elsevier, New York, 1984.
- Bronk, D.W., Ferguson, L.K., Margaria, R. and Solandt, D.Y.: The activity of the cardiac sympathetic centers. Am.J. Physiol. 117: 237-249, 1936.
- Brutus, M. Watson, Jr., R. E., Shakh, M.B., Siegel, H.E., Weiner, S. and Siegel, A.: A [C]2-deoxyglucose analysis of the functional neuronal pathways of the limbic forebrain in the rat. IV. A pathway from the prefrontal cortical-medial thalamic system to the hypothalamus. Brain Res. 310: 279-293, 1984.
- Buchanan, S.C. and Powell, D.A.: Cardiovascular adjustments elicited by electrical stimulation of dorsomedial and anteriomedial nuclei of the thalamus. Physiol. Psych. (in press), 1987.
- Buggy, J., Fink, G.D., Johnson, A.K. and Brody, M.J.: Prevention of the development of renal hypertension by anteroventral third ventricular tissue lesion. Circ. Res. 40(suppl. 1): 110-117, 1977.
- Buggy, J., Fink, G.D., Haywood, J.R., Johnson, A.K. and Brody, M.J.: Interruption of the maintenance phase of established hypertension by abation of the anteroventral third ventricle (AV3V) in rats. Clin. Exp. Hyperten. 1(3): 337-353, 1978.
- Bumpus, F.M., Sen, S., Smeby, R.R, Sweet, C., Ferrario, C.M. and Khosla, M.C.: Use of angiotensin II antagonists in exper hypertension. Circ. Res. 32-33(suppl. 1): 150-158, 1973.
- Bunag, R.D. and Eferakeya, A.E.: Immediate hypotensize after-effects of posterior hypothalamic lesions in awake rats with spentaneous, renal or DOCA hypertension. Cardiovasc. Res. 10: 663-671, 1975.
- Calaresu, F.R., Faiers, A.A. and Mogenson, G.J.: Central neural regulation of heart and blood vessels in mammals. Prog. Neurobiol. 5: 1-35, 1975.
- Camerer, H., Stroh-Werz, M., Kreinke, B. and Langhorst, P.: Postganglionic sympathetic activity with correlation to heart rhythm and central cortical rhythms. Pfluegers Arch. 370: 221-225, 1977.

- Clarke, N.P., Smith, O.A. and Shearn, W.D.: Topographical representation of vascular smooth muscle of limbs in primate motor cortex. Am. J. Physiol. 214(1): 122-129, 196 8.
- Cohen, M.L and Gootman, P.M.: Spontaneous and evoked oscillations in respiratory and sympathetic discharge. Brain Res. 15: 265-268, 1969.
- Cohen, M.L and Gootman, P.M.: Periodicities in efferent discharge of splanchnic nerve of the cat. Am. J. Physiol. 218: 1092-1101, 1970.
- Conrad, L.C.A., and Pfaff, D.W.: Efferents from medial basal forebrain and hypothalamus in the rat. IL An autoradiographic study of the anterior hypothalamus. J. Comp. Neurol. 169: 221-262, 1976.
- Coombs, J.S., Curtis, D.R. and Eccles.: The interpretation of spike potentials of motoneurons. J. Physiol. (London) 139: 198-231, 1957.
- Coote, J.H., Hilton, S.M. and Zbrozyna, A.W.: The ponto-medullary area integrating the defense reaction in the cat and its influence on muscle blood flow. J. Physiol. (London) 229: 257-274, 1973.
- Coote, J.H.: Repiratory and circulatory control during sleep. J. Exp. Biol. 100: 223-244, 1982.
- Crouch, J.E.: Text-Atlas of Cat Anatomy. Lea and Ferbiger, Philadelphia, 1969.
- Dampney, R.A.L. and Moon, E.A.: Role of the ventrolateral medulla in vasomotor response to cerebral ischemia. Am. J. Physiol. 239 (Heart Circ. Physiol. 8): H349-H353, 1930.
- Delgado, J.M.: Circulatory effects of cortical stimulation. Physiol. Rev. 40(suppl. 4): 145-171, 1960.
- Dempsey, E.W. and Morison, R.S.: The production of rhythmically recurrent cortical potentials after localized thalamic stimulation. Am. J. Physiol. 135: 293-300, 1942a.
- Dempsey, E.W. and Morison, R.S.: The interaction of certain spontaneous and induced cortical potentials. Am. J. Physiol. 135: 301-308, 1942b.
- Deschenes, M., Madariaga-Domich, A. and Steriade, M.: Dendrodendritic synapses in the cat reticularis thalami nucleus: A structural basis for thalamic spindle synchronization. Brain Res. 334: 165-168, 1985.
- Dimicco, J.A. and Abshire, V.M.: Evidence for GABAergic inhibition of a hypothalamic sympathoexcitatory mechanism in anesthetized rats. Brain Res. 402: 1-10, 1987.
- Dittmar, C.: Uber die Laga des songenannten Gefasscentrums der medulla oblongata. Ber. Vehr. Saechs. Wiss. Leipzig Math. Phys. Kl. 25: 449-479, 1873.
- Doba, N. and Reis, D.J.: Acute fulminating neurogenic hypertension produced by brain stem lesions in the rat. Circ. Res. 32: 534-593, 1973.

- Dusser de Barenne, J.G. and McColloch, W.S.: The direct functional interrelation of sensory cortex and optic thalamus. J. Neurophysiol. 1: 176-186, 1938a.
- Dusser de Barenne, J.G. and McColloch, W.S.: Sensorimotor cortex, nucleus caudatus and thalamus opticus. J. Neurophysiol. 1: 364377, 1938b.
- Eliasson, S., Lindgren, P. and Uvnas, B.: Representation in the hypothalamus and the motor cortex in the dog of the sympathetic vasodilator outflow to the skeletal muscles. Acta. Physiol. Scand. 27: 13-37, 1952.
- Faingold, C.L.: Enhancement of mesencephalic reticular neruonal responses to sensory stimuli with pentylenetetrazol. Neuropharmacol. 19: 53-62, 1980.
- Finch, L. and Hicks, P.E.: Involvement of hypothalamic histamine-receptors in the central cardiovascular actions of histamine. Neuropharmacol. 16: 211-218, 1977.
- Fink, G.D., Haywood, J.A., Bryan, W.J., Packwood, W. and Brody, M.J.: Central site for pressor action of blood-borne angiotensin in rat. Am. J. Physiol. 239 (Regulatory Integrative Comp. 8): R353-R351, 1980.
- Fischer, R.S. and Prince, D.A.: Spike-wave rhythms in cat cortex induced by parenteral penicillin. L. Electroencephalographic features. Electroenceph. clin. Neurophysiol. 42: 608-624, 1977.
- Folkow, B., Johansson, B. and Oberg, B.: A hypothalamic structure with a marked inhibitory effect on tonic sympathetic activity. Acta Physiol. Scand. 462-270, 1959.
- Galeno, T.M., Van Hoesen, G.W., Maixner, W., Johnson, A.K. and Brody, M.J.: Contribution of the amygdala to the development of spontaneous hypertension. Brain Res. 246: 1-6, 1982.
- Galeno, T.M., Van Hoesen, G.W. and Brody, M.J.: Central amygdaloid nucleus lesion attenuates exaggerated hemodynamic responses to noise stress in spontaneously hypertensive rat. Brain Res. 291: 249-259, 1984.
- Gebber, G.L.: Basis for phase relations between baroreceptor and sympathetic nervous discharge. Am. J. Physiol. 230(2): 263-270, 1976.
- Gebber, G.L. and Barman, S.M.: Basis for 2-6 cycle/s rhythm in sympathetic nerve discharge. Am. J. Physiol. (Regulatory Integrative Comp. Physiol. 8): R48-R56, 1980.
- Gebber, G.L. and Barman, S.M.: Sympathetic-related activity of brain stem neurons in baroreceptor-denervated cats. Am. J. Physiol. 240 (Regulatory Integrative Comp. Physiol. 9): R348-R355, 1981.
- Gebber, G.L.: Brain stem mechanisms and substrates involved in generation of sympathetic nerve discarge. In Exciation and Neural Control of the Heart, ed. by M.N. Levy and M. Vassalle, pp. 203-226, Am. Physiol. Soc., Williams and Wilkins, Baltimore, 1982.

- Gebber, G.L.: Brain stem systems involved in cardiovascular regulation. In Nervous Control of Cardiovascular Function, ed. by W.C. Randall, pp. 374-350, Oxford Univ. Press, New York, 1984.
- Gebber, G.L. and Barman, S.M.: Lateral tegmental field neurons of cat medulla: A potential source of basal sympathetic nerve discharge. J. Neurophysiol. 54(6): 1498-1512, 1985.
- Gellhorn, E. and Redgate, E.S.: Hypotensive drugs [Acetylcholine, mecholyl, histamine] as indicators of the hypothalamic excitability of the intact organism. Int. Pharmacodyn. 102: 162-178, 1955.
- Gellhorn, E.: The significance of the state of the central autonomic nervous system for quantitative and qualitative aspects of some cardiovascular reactions. Am. Heart J. 67(1): 106-120, 1964.
- Gloor, P. and Testa, G.: Generalized penicillin epilepsy in the cat: effects of intracarotid and intravertebral pentylenetetrazol and amobarbital injections. Electroenceph. clin. Neurophysiol. 36: 499-515, 1974.
- Gloor, P., Quesney, L.F. and Zumstein, H.: Pathophysiology of generalized penicillin epilepsy in the cat: the role of cortical and subcortical structures. Il topical application of penicillin to the cerebral cortex and to subcortical structures. Electroenceph. clin. Neurophysiol. 43: 19-94, 1977.
- Goodchild, A.K. and Dampney, R.A.L.: A vasopressor cell group in the rostral dorsomedial medulla of the rabbit. Brain Res. 360: 24-32, 1985.
- Gordon, F.J., Haywood, J.R., Brody, M.J. and Johnson, A.K.: Effect of lesions of the anteroventral third ventricle (AV3V) on the development of hypertension in spontaneously hypertensive rats. Hypertension 4: 387-393, 1982.
- Green, J.H. and Heffron, P.F.: Observations on the origin and genesis of a rapid sympathetic rhythm. Arch. Int. Pharmacodyn. 169: 403-411, 1967.
- Green, H.D. and Hoff, E.C.: Effects of fardic stimulation of the cerebral cortex on limb and renal volumes in the cat and monkey. Am. J. Physiol. 118: 641-658, 1937.
- Grofova, L, Ottersen, O.P. and Rinvik, E.: Mesencephalic and diencephalic afferents to the superior colliculus and periaqueductal gray substance demonstrated by retrograde axonal transport of horseradish peroxidase in the cat. Brain Res. 146: 205-220, 1978.
- Guertzenstein, P.G., Hilton, S.M., Marshall, J.M. and Timms, R.J.: Experiments on the origin of vasomotor tone. J. Physiol. (London) 275: 78P-79P, 1978.
- Gullery, R.W.: Afferent fibers to the dorso-medial thalamic nucleus in the cat. J. Anat. 93: 403-419, 1959.
- Hallback, M. and Folkow, B.: Cardiovascular responses to acute mental "stress" in spontaneously hypertensive rats. Acta. Physiol. Scand. 90: 684-698, 1974.

- Hartle, D.K. and Brody, M.J.: Hypothalamic vasomotor pathways mediating the development of hypertension in the rat. Hypertension 4(suppl. III): III-68-III-71, 1982.
- Hartle, D.K., Lind, R.W., Johnson, A.K. and Brody, M.J.: Localization of the anterior hypothalamic angiotensin II pressor system. Hypertension 4(suppl. 165, 1982.
- Haywood, J.R., Fink, G.D., Buggy, J., Boutelle, S., Johnson, A.K. and Brody, M.J.: Prevention of two-kidney, one clip renal hypertension in rat by ablation of AV3V tissue. Am. J. Physiol. 245 (Heart Circ. Physiol. 14): H683-H689, 1983.
- Hilton, S.M. and Spyer, K.M.: Participation of the anterior hypothalamus in the baroreceptor reflex. J. Physiol (London) 218: 271-293, 1971.
- Hilton, S.M., Spyer, K.M. and Timms, R.J.: The origin of the hind limb vasodilation evoked by stimulation of the tex in the cat. J. Physiol. (London) 287: 545-557, 1979.
- Hilton, S.M.: The defense-arousal system and its relevance for circulatory and respiratory control. J. Exp. Biol. 100: 159-174, 1982.
- Hilton, S.M., Marshall, J.M. and Timms, R.J.: Ventral medullary relay neurons in the pathway from the defense areas of the cat and their effect on blood pressure. J. Physiol. (London), 345: 149-16.
- Hilton, S.M. and Smith, P.R.: Ventral medullary neurons excited from the hypothalamic and mid-brain defense areas. J. Autonom. Nerv. Sys. 11: 35-42, 1984.
- Hilton, S.M. and Redfern, W.S.: A search for brain stem cell groups integrating the defense reaction in the rat. J. Physiol. (London) 378: 213-228, 1986.
- Hoff, E.C. and Green, H.D.: Cardiovascular reactions induced by electrical stimulation of the cerebral cortex. Am. J. Physiol. 117: 411-422, 1936.
- Hoff, E.C., Kell, Jr., J.F., Bourne, J.M. and Velo, A.: Pressor responses to cortical stimulation in unanesthetized cats and dogs. Fed. Proc. 18: 69-76, 1959.
- Hoff, E.C., Kell, J.F. and Carroll, M.N.: Effects of cortical stimulation and lesions on cardiovascular function. Physiol. Rev. 43: 68-114, 1963.
- Hosya, Y.: Hypothalamic projections to the ventral med oblongata in the rat, with special reference to the nucleus raphe pallidus: A study using autoradiographic and HRP. Brain Res. 344: 338-350, 1985.
- Houser, C.R., Vaughn, J.E., Barber, R.P. and Roberts, E.: GABA neurons are the major cell type of the nucleus reticularis thalams. Brain Res. 200: 341-354, 1980.

- Hsu, S.-H., Hwang, K. and Chu, H.-N.: A study of the cardiovascular changes induced by stimulation of the motor cortex in dogs. Am. J. Physiol. 137: 468-472, 1942.
- Huang, Z.S., Gebber, G.L., Barman, S.M. and Varner, K.J.: Forebrain contribution to sympathetic nerve discharge in anesthetized cats. Am J. Physiol. 252 (Regulatory Integrative Comp. Physiol. 21): R645-R652, 1987.
- Hurley-Gius, K.M., Cechetto, D.F. and Saper, C.B.: Spinal connections of the infralimbic autonomic cortex. Soc. Neurosci. Abstr. Part 1, 145.4: 538, 1986.
- Irle, E., Markowitsch, H.J. and Streicher, M.: Cortical and subcortical, including sensory-related, afferents to the thalamic mediodorsal nucleus of the cat. J. Hirnforsch. 25: 29-51, 1984.
- Jahnsen, H. and Llinas, R.: Ionic basis for the electroresponsiveness and oscillatory properties of guinea-pig thalamic neurons in vitro. J. Physiol. (London) 349: 227-247, 1984.
- Jasper, H.: Diffuse projection systems: the integrative action of the thalamic reticular system. Electroenceph. clin. Neurophysiol. 1: 405-420, 1949.
- Jasper, H.H. and Ajmone-Marsan, C.: A Stereotaxic Atlas of the Diencephalon of the Cat. Natl. Res. Council Canada, Ottawa, 1954.
- Johnson, A.K.: Role of periventricular tissue surrounding the anteroventral thaird ventricle (AV3V). In The Regulation of Body Fluid Homeostasis, ed. by R.W. Schrier, pp. 319-331, Raven Press, New York, 1985.
- Johnston, G.A.R.: Physiologic pharmacology of GABA and its antagonists in the vertebrate nervous system. In GABA in Nervous System Function, ed. by E. Roberts, T.N. Chase and D.B. Tower, pp. 395411, Raven Press, New York, 1976.
- Jones, E.G.: The Thalamus. Plenum, New York, 1985.
- Judy, W.V., Watanabe, A.M., Henry, D.P., Besch, H.R., Murphy, W.R. and Hochel, G.M.: Sympathetic nerve activity: role in regulation of blood pressure in the spontaneously hypertensive rat. Circ. Res. 38 (suppl. 2): II-21-II-34, 1976.
- Jurf, A.N. and Blake, W.D.: Renal response to electrical stimulation in the septum and diencephalon of rabbits. Circ. Res. 30: 322-331, 1972.
- Kaada, B.R.: Somato-motor, autonomic and electrocorticographic responses to electrical stimulation of rhinencephalic and other structures in primates, cat and dog. Acta Physiol. Scand. 24(suppl. 33): 285 p., 1951.
- Kaada, B.R.: Cingulate, posterior orbital, anterior insular and temporal pole cortex. In Handbook of Physiology, Sec 1.2, Part 2, pp. 1345-1372, Am Physiol. Soc., Williams and Wilkins, Baltimore, 1960.

- Kaba, H., Saito, H., Otsuka, K. and Seto, K.: Ventrolateral medullary neurons projecting to the medial preoptic/anterior hypothalamic area through the medial forebrain bundle: an electrophysiological study in rats. Exp. Brain Res. 63: 369-374, 1986.
- Kabat, H., Magoun, W.H. and Ranson, S.W.: Electrical stimulation of points in the forebrain and midbrain. Arch. Neurol. and Psychiat. 34(5): 931-955, 1935.
- Katholi, R.E., Winternitz, S.R. and Oparil, S.: Role of the renal nerves in the pathogenesis of one-kidney renal hypertension in the rat. Hypertension 3: 404-409, 1981.
- Keim, K.L. and Sigg, E.B.: Activation of central sympathetic neurons by angiotensin II. Life Sci. 10(1): 565-574, 1971.
- Koepchen, H.P. and Thurau, K.: Uber die Entstehungsbedingungen der atemsynchronen Schwankungen des Vagustonous (Respiratorische Arrhythmie). Pfluegers Arch. 269: 10-18, 1959.
- Kortweg, G.C.J., Boeles, J.Th.F. and Ten Cate, J.: Influences of stimulation of some subcortical areas on electorcardiogram. J. Neurophysiol. 20: 100-107, 1957.
- Kostopoulos, G., Gloor, P., Pellegrias, A. and Siatitsas, I.: A study of the transition from spindles to spike and wave discharge in feline generalized penicillin epilepsy: EEG features. Exp. Neurol. 73: 43-54, 1981.
- Kumada, M., Dampney, R.A.L. and Reis, D.J.: Profound hypotension and abolition of the vasomotor component of the cerebral ischemic response produced by restricted lesions of medulla oblongata in rabbit. Circ. Res. 44: 63-70, 1979.
- Kuypers, H.G.J.M. and Miasky, V.A.: Retrograde axonal transport of horseradish peroxidase from spinal cord to brain stem cell groups in the cat. Neurosci. Lett. 1: 9-124, 1975.
- Kuypers, H.G.J.M.: Anatomy of the descending pathways. In Handbook of Physiology, Sec. 1, Part 1., pp. 597-666, Am. Physiol. Soc., 1981.
- Langhorst, P., Stroh-Wertz, M., Dittmar, K. and Camerer, H.L: Faculatative coupling of reticular neuronal activity with peripheral cardiovascular and central cortical rhythms. Brain Res. 87: 407-418, 1975.
- Langhorst, P., Schultz, B., Lambertz, M., Schultz, G. and Camerer, H.: Dynamic characteristics of the "Unspecific" brain stem system. In Central Interaction Between Respiratory and Cardiovascular Control Systems, ed. by H.P. Koepchen, S.M. Hilton and A Trzebski, pp. 30-41, Springer-Verlag, Berlin, 1980.
- Langhorst, P., Schultz, G. and Lambertz, M.: Oscillating neuronal network of the "common brain stem" system. In Mechanisms of Blood Pressure Waves, ed. by K. Miyakawa, pp. 257-275, Japan Sci. Soc. Press, Tokyo/Springer-Verlag, Berlin, 1984.

- Lappe, R.W. and Brody, M.J.: Mechanisms of the central pressor action of angiotensin II in conscious rats. Am. J. Physiol. 246 (Regulatory Intergrative Comp. Physiol. 15): R56-R62, 1984.
- Lee, T.M., Yang, K.L., Kou, J.S. and Chai, C.Y.: Importance of sympathetic mechanisms on cardiac arrhythmias induced by picrotoxin. Expt. Neurol. 36: 389-398, 1972.
- Loewy, A.D., Wallach, J.H. and McKellar, S.: Efferent connections of the ventral medula oblongata in the rat. Brain Res. Rev. 3: 63-80, 1981.
- Lofving, B.: Cardiovascular adjustments induced from the rostral cingulate gyrus.

 Acta. Physiol. Scand. 53(suppl. 184): 1-83, 1961.
- Lovick, T.A., Smith, P.R. and Hilton, S.M.: Spinally projecting neurones near the ventral surface of the medulla in the cat. J. Autonom. Nerv. Sys. 11: 27-33, 1984.
- Lovick, T.A.: Projections from the diencephalon and mesencephalon to the nucleus paragigantocellularis lateralis in the cat. Neurosci. 14(3): 853-861, 1985.
- Maekawa, K. and Purpura, D.P.: Intracellular study of lemniscal and non-specific synaptic interactions in thalalmic ventrobasal neurons. Brain Res. 4: 308-323, 1967.
- Mancia, G., Baccelli, G., Adams, D.B. and Zanchetti, A.: Vasomotor regulation during sleep in the cat. Am. J. Physiol. 220: 1086-1093, 1970.
- Manning, Jr., J.W. and Peiss, C.N.: Cardiovascular responses to electrical stimulation in the diencephalon. Am. J. Physiol. 198(2): 366-370, 1960.
- Masserman, J.H.: Effects of sodium amytal and other drugs on the reactivity of the hypothalamus of the cat. Arch. Neurol. Psychiat. 387: 617-628, 1937.
- McAllen, R.M., Neil, J.J. and Loewy, A.D.: Effects of kaini applied to the ventral surface of the medulla oblongata on vasomotor tone, the baroreceptor reflex and hypothalamic autonomic responses. Brain Res. 238: 65-76, 1982.
- McCall, R.B. and Gebber, G.L.: Brain stem and spinal synchronization of sympathetic nervous discharge. Brain Res. 89: 139-143, 1975.
- McCall, R.B. and Humphrey, S.J.: Evidence for GABA mediation of sympathetic inhibition evoked from midline medullary depressor sites. Brain Res. 339: 356-360, 1985.
- McDougal, A., Dampney, R. and Bandler, R.: Cardiovascular components of the defense reaction evoked by excitation of neuronal cell bodies in the midbrain periaqueductal gray of the cat. Neurosci. Lett. 60: 69-75, 1985.
- Montero, V.M. and Singer, W.: Ultrastructural identification of soma and neural processes immunoreactive to antibodies against glutamic acid decarboxylase (GAD) in the dorsal lateral geniculate nucleus of the cat. Exp. Brain Res. 59: 151-165, 1985.

- Morison, R.S. and Rioch, D.McK.: The influence of the forebrain on an autonomic reflex. Am. J. Physiol. 120: 257-276, 1937.
- Morison, R. and Dempsey, E.W.: A study of thalamo-cortical relations. Am. J. Physiol. 135: 281-292, 1942.
- Morrison, S.F. and Gebber, G.L.: Classification of raphe neurons with cardiac-related activity. Am. J. Physiol. 243 (Regulatory Integrative Comp. Physiol. 12): R49-R59, 1982.
- Morrison, S.F. and Gebber, G.L.: Raphe neurons with sympathetic-related activity: Baroreceptor responses and spinal connections. Am. J. Physiol. 246 (Regulatorve Comp. Physiol. 15): R338-R34, 1984.
- Morrison, S.F. and Gebber, G.L.: Axonal branching patterns and axonal trajectories of raphespinal sympathoinhibitory neurons. J. Neurophysiol. 53(3): 759-772, 1985.
- Mulle, C., Steriade, M. and Deschenes, M.: Absence of spindle oscillations in the cat anterior thalamic nuclei. Brain Res. 334: 169-171, 1985.
- Nauta, W.J.H. and Haymaker, W.: Hypothalamic nuclei and fiber connections. In The Hypothalamus, ed. by W. Haymaker, E. Anderson and W.J.H. Natua, pp. 136-209, Springfield, C. Thomas, 1969.
- Ono, K. and Niimi, K.: Direct projections of the hypothalamic nuclei to the thalamic mediodorsal nucleus in the cat. Neurosci. Lett. 57: 283-287, 1985.
- Owsjannikow, P.: Die tonischen und reflectorischen Centren der Gefassnerven. Ber. Vehr. Saechs. Wiss. Leipzig Math. Phys. Kl 23: 135-147, 1971.
- Page, LH.: Hypertension Mechanisms. Grune and Stratton, Orlando, FL, 1987.
- Palkovits, M. and Zaborszky, L.: Neural connections of the hypothalamus. In Anatomy of the Hypothalamus, ed. by P.J. Moragne and J. Pankesepp, pp. 379-510, Marcel Decker Inc., New York, 1979.
- Parent, A. and Steriade, M.: Midbrain tegmental projections of nucleus reticularis thalami of cat and monkey: A retrograde transport and antidromic invasion study. J. Comp. Neurol. 229: 548-558, 1984.
- Peiss, C.N.: Concepts of cardiovascular regulation: past, present and future. In Nervous Control of the Heart, ed. by W.C. Randall, pp. 154-197, Williams and Wilkins, Baltimore, 1965.
- Powell, D.A. and Buchanan, S.: Autonomic changes elicited by chemical stimulation of the mediodorsal nucleus of the thalamus. Pharmacol., Biochem, Behav. 25(2): 423-430, 1986.
- Preiss, G., Kirchner, F. and Polosa, C.: Patterns of sympathetic preganglionic neuron firing by the central respiratory drive. Brain Res. 87: 363-374. 1975.
- Purpura, D.P. and Cohen, B.: Intracellular recording from thalamic neurons during recruiting responses. J. Neurophysiol. 25: 621-635, 1962.

- Purpura, D.P. and Shofer, R.J.: Intracellular recording from thalamic neurons during reticulo-cortical activation. J. Neurophysiol. 26: 496-505, 1963.
- Purpura, D.P., Scarff, T. and McMurtry, J.G.: Intracellular study of intranuclear inhibition in ventrolateral thalamic neurons. J. Neurophysiol. 28: 487-496, 1965.
- Purpura, D.P., Frigyesi, T.L., McMurtry, J.G. and Scarff, T.: Synaptic mechanisms in thalamic regulation of cerebello-cortical projection activity. In The Thalamus, ed. by D.P. Purpura and M.D. Yahr, pp. 153-170, New York, 1966.
- Purpura, D.P.: Operations and processes in thalamic and synaptically related neural subsystems. In The Neurosciences, ed. by F.O. Schmitt, pp. 453-470, Rockefellar Univ. Press, New York, 1970.
- Quesney, L.F., Gloor, P., Kratzenberg, E. and Zumstein, H.: Pathophysiology of generalized penicillin epilepsy in the cat: the role of cortical and subcortical structures. I. Systemic application of penicillin. Electroenceph. clin. Neurophysiol. 42: 640-655, 1977.
- Ranson, S.W., Kabat, H. and Magoun, H.W.: Autonomic responses to electrical stimulation of hypothalamus, preoptic region and septum. Arch. Neurol. Psychiat. 33: 467-474, 1935.
- Redgate, E.S. and Gellhorn, E.: The tonic effects of the posterior hypothalamus on blood pressure and pulse rate as disclosed by the action of intrahypothalamically injected drugs. Arch. Int. Pharmacodyn. 105: 193-198, 1956a.
- Redgate, E.S. and Gellhorn, E.: The alteration of anterior hypothalamic excitability through intrahypothalamic injections of drugs and its significance for the measurement of parasympathetic hypothalamic excitability in the intact organism. Arch. Int. Pharmacodyn. 105: 199-208, 1965b.
- Reis, D.J. and Cuenod, M.: Tonic influences of rostral brain structures on pressure regulating mechanisms in the cat. Science Wash. D.C. 145: 64-65, 1964.
- Reis, D.J. and Nathan, M.A.: Hypertension and pulmonary edema in rats after hypothalamic lesions. Circulation 44(suppl. 4): 44, 1973.
- Rockhold, R.W., Jin, C.-B., Huang, C. and Farley, J.M.: Excitatory neurotoxin stimulated cardiovascular responses following diencephalic microinjecitons. Soc. Neurosci. Abstr. Part 2, 242.1: 825, 1985.
- Rockhold, R.W., Jin, C.-B., Huang, C. and Farley, J.M.: Acute tachycardia and pressor effects following injections of kainic acid into the antero-dorsal medial hypothalamus. Neuropharm. 26(6): 567-573, 1987.
- Ross, C.A., Ruggerio, D.A., Park, D.H., Joh, T.H., Sved, A.F., Fernandez-Parda, J., Saaverda, F.M. and D.J. Reis.: Tonic vasomotor control by the rostral ventrolateral medulla: effect of electrical or chemical stimulation of the area containing C1 adrenaline neurons on arterial pressure, heart rate, and plasma catecholamines and vasopressin. J. Neurosci. 4: 474-494, 1984.

- Saper, C.B., Loewy, A.D., Swanson, L.W. and Cowan, W.M.: Direct hypothalamoautonomic connections. Brain Res. 117: 305-312, 1976.
- Saper, C.B., Swanson, L.W. and Cowan, W.M.: The efferent connections of the anterior hypothalamic area of the rat, cat and monkey. J. Comp. Neurol. 182: 575-600, 1978.
- Scheibel, M.E. and Scheibel, A.B.: Structural substrates for integrative patterns in the brain stem reticular core. In Reticular Formation of the Brain, ed. by H.H. Jasper and Associates, pp. 31-55, Little, Brown, Boston, 1958.
- Scheibel, M.E. and Scheibel, A.B.: The organization of the nucleus reticularis thalami: a Golgi study. Brain Res. 1: 43-62, 1966.
- Scheibel, M.E. and Scheibel, A.B.: Structural organization of nonspecific thalamic nuclei and their projection toward the cortex. Brain Res. 6: 60-94, 1967.
- Scheibel, M.E., Davies, T.L. and Scheibel, A.B.: On thalamic substrates of cortical synchrony. Neurol. 23(3): 300-304, 1973.
- Schmidt, B. and Dimicco, J.A.: Blockade of GABA receptors in periventricular forebrain of anesthetized cats: effects on heart rate, arterial pressure and hind limb vascular resistance. Brain Res. 301: 111-119, 1984.
- Seigel, A., Edinger, H. and Troiano, R.: A pathway from the mediodorsal nucleus of thalamus to the hypothalamus in the cat. Expt. Neurol. 38: 201-217, 1973.
- Skinner, J.E. and Reed, J.C.: Blockade of a frontocortical-brain stem pathway prevents ventricular fibrillation of ischemic heart. Am. J. Physiol. 240 (Heart Circ. Physiol. 9): H156-H163, 1781.
- Smith, W.K.: The functional significance of the rostral cingular cortex as revealed by its responses to electrical excitation. J. Neurophysiol. 8: 241-255, 1945.
- Steriade, M. and Hobson, J.A.: Neuronal activity during the sleep-wake cycle. Prog. Neurobiol. 6: 155-376, 1976.
- Steriade, M. and Deschenes, M.: The thalamus as a neuronal oscillator. Brain Res. Rev. 8: 1-63, 1984.
- Steriade, M., Parent, A. and Hada, J.: Thalamic projections of nucleus reticularis thalami of cat: a study using retrograde transport of horseradish peroxidase and flourescent tracers. J. Comp. Neurol. 229: 531-547, 1984.
- Steriade, M., Deschenes, M., Domich, L. and Mulle, C.: Abolition of spindle oscillations in thalamic neurons disconnected from nucleus reticularis thalami. J. Neurophysiol. 54(6): 1473-1497, 1985.
- Steriade, M., Domich, L. and Oakson, G.: Reticularis thalamic neurons revisited: activity changes during shifts in states of vigilance. J. Neurosci. 6(1): 63-81, 1986.

- Steriade, M., Domich, L, Oakson, G. and Deschenes, M.: The deafferentated reticular thalamic nucleus generates spindle rhythmicity. J. Neurophysiol. 57(1); 260-273, 1987.
- Sun, M.-K. and Guyenet, P.G.: Hypothalamic glutamatergic input to medullary sympathoexcitatory neurons in rats. Am. J. Physiol. 251 (Regulatory Intergrative Comp. Physiol. 20): R798-R810, 1986.
- Szentagothai, J., Flerko, B., Mess, B. and Halasz, B.: Hypothalamic Control of the Anterior Pituitary, Akademiai Kiado, Budapest, 1768.
- Takagi, H., Shiosaka, S., Tohyama, M., Senba, E. and Sakanaka, M.: Ascending components of the medial forebrain bundle from the lower brain stem in the rat, with special reference of raphe and catecholamine cell groups. A study by the HRP method. Brain Res. 139: 315-337, 1980.
- Takeda, K. and Bunag, R.D.: Augmented sympathetic nerve activity and pressor responsiveness in DOCA hypertensive rats. Hypertension 2: 97-101, 1980.
- Takeuchi, J., Yagi, S., Nakayama, S., Ikeda, S., Uchida, E., Inoue, G., Shintani, F. and Ueda, H.: Experimental studies on the nervous control of the renal circulation-effect of electrical stimulation of the diencephalon on the renal circulation. Jap. Heart J. 1(3): 288-299, 1960.
- Takeuchi, J., Yagi, S., Takeda, T., Uchida, E., Inoue, G. and Ueda, H.: Experimental studies on the nervous control of the renal circulation-changes in renal circulation induced by electrical stimulation of the diencephalon and effect of several drugs on the circulatory response. Jap. Heart J. 3(1): 57-72, 1962.
- Tan, E., Goodchild, A.K. and Dampney, R.A.L.: Intense vasoconstriction and bradycardia evoked by stimulation of neurones within the midbrain ventral tegmentum of the rabbit. Clin. Exp. Pharmacol. Physiol. 10: 305-309, 1983.
- Taylor, D.G. and Gebber, G.L.: Baroreceptor mechanisms controlling sympathetic nervous rhythms of central origin. Am. J. Physiol. 228: 1002-1013, 1975.
- ter Horst, G.J. and Luiten, P.G.M.: The projections of the dorsomedial hypothalamic nucleus in the rat. Brain Res. Bull. 16: 231-248, 1986.
- Tobey, J.C., Fry, H.K., Mizejewski, C.S., Fink, G.D. and Weaver, L.C.: Differential sympathetic responses iniated by angiotensin and sodium chloride. Am. J. Physiol. 245 (Regulatory Integrative Comp. Physiol. 14): R60-R68, 1983.
- Touw, K.B., Haywood, J.R., Shaffer, R.A. and Brody, M.J.: Contribution of the sympathetic nervous system to vascular resistance in conscious young and adult spontaneously hypertensive rats. Hypertension 2: 408-418, 1980.
- Tucker, D.C. and Saper, C.B.: Specificity of spinal projections from hypothalamic and brain stem areas which innervate sympathetic preganglionic neurons. Brain Res. 360: 159-164, 1985.

- Van der Kooy, D., Koda, L.Y., McGinty, J.F., Gerfen, C.R. and Bloom F.E.: The organization of projections from the cortex, amygdala and hypothalamus to the nucleus of the solitary tract in rat. J. Comp. Neurol. 224: 1-24, 1984.
- Velayos, J.L.: Topographical organization of the prosencephalic afferents to the mediodorsal thalamic nucleus. Neurosci. Lett. Suppl. 10: S502, 1982
- Velasco, F., Velasco, M., Estrada-Villanueva, F. and Machado, J.P.: Specific and nonspecific multiple unit activities during the onset of pentylenetetrazol seizures. L Intact animals. Epilepsia 16: 207-214, 1975.
- Villablanca, J.: Role of the thalamus in sleep control: Sleep-wakefulness studies in chronic diencephalic and athalamic cats. In Basic Sleep Mechanisms, ed. by O. Petre-Quadens and J.D. Schlag, pp. 51-81, Academic Press, New Yok, 1974.
- Wall, P.D. and Pribram, K.H.: Trigeminal neuroanatomy and blood pressure responses from stimulation of lateral cerebral cortex of macaca mulatta. J. Neurophysiol. 13: 409-412, 1950.
- Wang, S.C. and Ranson, S.W.: Autonomic responses to electrical stimulation of the lower brain stem. J. Comp. Neurol. 71: 437455, 1939.
- Wang, S.C. and Ranson, S.W.: The role of the hypothalamus and preoptic region in the regulation of heart rate. Am. J. Physiol. 132: 5-8, 1941.
- Wang, S.C. and Chai, C.Y.: Central control of sympathetic cardioacceleration in medulla oblongata of the cat. Am. J. Physiol. 202: 31-34, 1962.
- Williford, D.J., Dimicco, J.A. and Gillis, R.A.: Evidence for the presence of a tonically active forebrain GABA system influencing central sympathetic outflow in the cat. Neuropharmacol. 9: 245-250, 1980.
- Wilson, C.L., Motter, B.C. and Lindsley, D.B.: Influences of hypothalamic stimulation upon septal and hippocampal electrical activity in the cat. Brain Res. 107: 55-68, 1976.
- Winters, W.D. and Spooner, C.E.: A neurophysiological comparison of alphachloralose with gamma-hydroxybutyrate in cats. Electroenceph. clin. Neurophysiol. 20: 83-90, 1966.
- Zhang, T.-X. and Ciriello, J.: Effect of paraventricular nucleus lesions on arterial pressure and heart rate after aortic baroreceptor denervation in rat. Brain Res. 341: 101-109, 1985a.
- Zhang, T.-X. and Cireillo, J.: Kainic acid lesions of paraventricular nucleus neurons reverse the elevated arterial pressure after aortic baroreceptor denervation in the rat. Brain Res. 358: 334-338, 1985b.